A Computer Code for Calculating Subcooled Boiling Pressure Drop in Forced Convective Tube Flows

By

Christopher Fong Wong
B.S. (University of California, Davis) 1984

UCRL--21165

DE89 015709

THESIS

Submitted in partial satisfaction of the requirements for the degree of

MASTER OF SCIENCE

in

Mechanical Engineering

in the

GRADUATE DIVISION

of the

UNIVERISITY OF CALIFORNIA

DAVIS

Approved:

Committee in Charge

1988

Table of Contents

Abstract

A calculation procedure, embodied in a computer code, was developed to calculate the convective subcooled boiling (SCB) pressure drop of water flowing in small diameter vertical or horizontal tubes under the condition of high heat fluxes. The present investigation is an extension of previous work performed by C.T. Kline in 1985. The computer code, presented then and now, numerically integrates the single-phase and separated-flow-model pressure drop equations from the inlet to the outlet of a heated tube.

Efforts in this study were concentrated on identifying weaknesses in Kline's best code version and investigating his recommendations for future work. The calculation procedures for each flow regime in the tube were modified to give better overall results. New work focused primarily on the partially-developed boiling(PDB) and fully-developed boiling(FDB) regimes. The pressure drop predictions from each code version were compared to the experimental pressure drop results from the experimental investigations of Dormer/Bergles, Owens/Schrock, and Reynolds.

Because flow properties in SCB usually change so rapidly along the tube length, only a computer code which numerically integrates the governing flow equations can hope to yield accurate SCB pressure drop predictions.

The final computer code version was validated against experimental pressure drop data for water over the ranges of pressures from 2 x 10^5 to 28 x 10^5 Pa (29 to 406 psia), inner wall surface heat fluxes from 0 to 12.2 MW/m^2 (0 to 3.87 x 10^6 Btu/hrft^2), inlet mass velocities from 2500 to 10,000 kg/m^2s (512 to 2048 lb/ft^2s), inlet subcoolings from approximately 10 to 200 °C (18 °F to 360 °F), tube diameters from 1.5 to 4.6 mm (0.0591 to 0.1811 in), length-to-diameter ratios 49 to 127, and for vertical and horizontal tube orientations.

While there was variation in the degree of accuracy from run to run, the final code version provided generally good agreement with the experimental pressure drop data at a better success rate than Kline. We estimate the predicted pressure drop uncertainty range of Kline's best code version to be around -30% to +45%, excluding a few pathological cases. Our new code version will generally provide designers with accurate solutions with maximum uncertainties of about ±20% for the SCB pressure drop calculation of water in small diameter tubes.

Objective(Preface)

The aim of this research was to produce a subcooled boiling computer code which will be useful for design engineers in the power plant and process industries. Although this code was developed on a Digital VAX-780, the code is primarily intended to be run on an IBM PC/AT or compatible microcomputer. Simplicity, user-friendliness, and wide applicability make this code an important tool in the today's engineering design process.

Acknowledgements

I would like to gratefully thank Professor Hoffman for his guidance, assistance, and instruction during the research and writing stages of this thesis.

I would also like to show my appreciation to Professor Baughn and to Professor Kennedy for their review of this work and many helpful suggestions.

Funding for this study was provided by Mechanical Engineering Research, Lawrence Livermore National Laboratory (Livermore, California) under Intramural Purchase Order No. 9222705.

List of Tables

List of Figures

Notation(From Ref. [3])

Acronyms :

OFDB	**onset of fully developed boiling**
ONB	**onset of nucleate boiling**
OBB	**onset of bulk boiling**
PDB	**partially developed boiling**
SCB	**subcooled nucleate boiling**
OSNVG	onset of significant net vapor generation
SPL	**single phase liquid**

Symbols :

A	**cross-sectional flow area**
A_g	vapor cross-sectional flow area
A_f	liquid cross-sectional flow area
C_o	distribution parameter equal to

$$= \left[\frac{\dfrac{\int_A j\alpha \, dA}{\int_A dA}}{\dfrac{\int_A j \, dA}{\int_A dA} * \dfrac{\int_A \alpha \, dA}{\int_A dA}} \right]$$

where j=local volumetric flux density or superficial velocity

by definition $j = j_g + j_f$

$$j_g = \alpha u_g \qquad j_f = (1-\alpha) u_f$$

C_{pf} isobaric liquid specific heat

D inner diameter

D_d mean bubble diameter at the instant of departure from the heating surface

D_e equivalent diameter

D_h hydraulic diameter

dz differential element of axial tube length

e equivalent surface roughness

f_{fo} Fanning friction factor for total liquid flow modified for viscosity variations

f_{iso} Fanning friction factor for smooth ducts

f_{tp} two-phase friction factor

G mass velocity

g gravitational acceleration

h_{fo} convective heat transfer coefficient for total liquid flow

i enthalpy

i_{fg}	latent heat of vaporization
$i_{f,sat}$	enthalpy of saturated liquid
K	thermal conductivity
P	pressure
p_h	heated perimeter
Q'' or q''	heat flux
R_d	average radius of vapor bubble at instant of departure from the heating surface
S	slip or slip ratio (u_g / u_f)
T_b	bulk fluid temperature
T_{sat}	saturation temperature
T_w	wall temperature
ΔT_{flim}	film temperature difference; temperature difference between wall and bulk fluid
ΔT_{sat}	superheat; temperature difference in excess of saturation temperature ($T - T_{sat}$)
ΔT_{sub}	subcooling; temperature difference below saturation temperature ($T_{sat} - T$)
u_g	vapor velocity
$\bar{u}_{gj}$	drift flux velocity
u_f	liquid velocity
v	specific volume
T_g	liquid vapor temperature

w	mass flow rate	
X'	flow quality	
X	thermodynamic equilibrium quality	
z	axial tube length from the inlet	

Dimensionless Numbers :

B_o	local boiling number	$B_o = \frac{q''}{G i_{fg}}$
Nu	local Nusselt number *	$Nu = \frac{Q D_h}{K_f (T_{sat} - T_{sub})}$
Pe	local Peclet number *	$Pe = q D_h C_{pf} / K_f$
Pr	Prandtl number	$Pr = C_{pf} \mu / K_f$
Re	Reynolds number	$Re = \frac{qD}{\mu}$
$\widetilde{St}$	local Stanton number * (subcool)	$St = \frac{Q}{G C_{pf} (T_{sat} - T_{sub})}$

* in accordance with Reference 15

Greek :

α	void fraction $\left[\frac{A_g}{A_g + A_f} \right]$
α_{w} or α_{wall}	void attached to heating surface
δ	bubble boundary layer thickness
θ	angle to horizontal plane
$\bar{\mu}$	mean two-phase viscosity
μ_b	bulk fluid viscosity
μ_w	viscosity at the wall

ρ density

σ surface tension at the liquid-vapor interface

ϕ^2_{fo} two-phase friction multiplier $\left[\dfrac{\left.\dfrac{dP}{dz}\right|_{fric,tp}}{\left.\dfrac{dP}{dz}\right|_{fric,fo}} \right]$

Subscripts :

acc	acceleration
b	bulk
eff	effective
f	liquid
fo	total liquid flow
fric	friction
g	vapor
geom	geometry
grav	gravity
sat	saturation condition
tp	two-phase
w	wall
1	upstream location
2	downstream location

Superscripts :

$\overline{\quad}$	average value
$'$	non-equilibrium condition
$\sim$	special definition

1. Introduction

The phenomenon of convective subcooled (nucleate) boiling, abbreviated SCB, is often utilized in the design of high heat flux cooling systems. Subcooled nucleate boiling occurs when the cooling fluid at or in the near-wall(heating surface) region exceeds the local saturation temperature while the bulk temperature of the fluid remains below the saturation point. In SCB, vapor bubbles generated at the heated surface are in a non-equilibrium state, either recondensing as they enter the bulk of the fluid or remaining as vapor in the near-wall region. In the case of forced convective flows through tubes, the heat transfer coefficient in SCB is commonly many times that of the single-phase liquid coefficient. Because of this and the fact that the cooling fluid never fully vaporizes, designers are able to transfer the same amount of heat with smaller pumping systems than would be required using only single-phase liquid cooling. Three common applications of SCB heat transfer are high-field electromagnets, high temperature pressure transducers, and particle accelerators.

The design of SCB cooling systems is complicated due to the techniques needed for accurate estimation of system pressure drops. Because of non-equilibrium thermal and hydraulic conditions of the flow, the full analytical solutions are not yet available. This approach would require solution of local instantaneous equations for the vapor and liquid phases of the flow and associated interface conditions. In light of these

facts, researchers have made substantial efforts to quantify the actual SCB physics by constructing purely empirical equations based on experimental results. However, strictly empirical approaches are often too restrictive for general design use and can give the user a false sense of accuracy. Hewitt[1] demonstrates the typical accuracy of one such purely empirical pressure drop correlation in his figure number 2, reproduced in this paper as figure 1.1.

In his paper, Hewitt suggests that a phenomenological approach to formulating a solution has advantages over purely empirical approaches, in that one gains a better understanding of the physical occurrences, and that a model developed under such conditions can have a wider range of applicability. The application of this approach is best manifested in a computer code which integrates of the basic flow equations using verified empirical equations to describe needed flow quantities. Such a computer code was developed by Hoffman et. al.[2] in 1975. Hoffman's code was one of the first efforts to calculate the pressure drop while taking into account large pressure drop gradients and changing flow properties. The current investigation is a third generation improvement of that early code version with emphasis on improved accuracy over a wider range of flow conditions and more flexibility for the designer.

The specific focus of the present research is to calculate the SCB pressure drop in small diameter tubes, under the conditions of fully-turbulent forced convection, at relatively

high heat fluxes, and at relatively high pressures. The final code version is to be validated against experimental data from the open literature. The goal of this research is to formulate a computer code which can return pressure drop predictions which agree with selected experimental data to within a difference of approximately ± 20%.

This new work is a direct extension of C.T. Kline's M.S. Thesis[3] completed in 1985. His most promising code version, SR-2F, is modified to better predict the SCB pressure drop as compared against experimental results. The investigation follows Kline's recommendations for future work, but also identifies weaknesses in his final code version. Sensitivity studies of the major SCB regimes indicated where we(the current investigators) should concentrate our efforts. Comparison of the computer code results with experimental data indicated which SCB models worked the best and which ones had shortcomings. The experimental database, which includes data from the investigations of Dormer and Bergles[4], Owens and Schrock[5], and Reynolds[6], allows for evaluating code modifications with reasonable certainty of the conclusions drawn. However, due to the enormous amount of test data available from just these three investigations, and the time constraint of this research program, a small, representative group of experimental data runs was first selected for comparison; additional data were then compared to the code as time permitted. The major emphasis of this current study is to use as much information from the previous authors, while

including new developments in this field, without turning this investigation into another scoping study of SCB correlations. The degree of success in defining the model and choice of empirical equations will be clear from either the good or poor agreement with the experimental data.

A brief review of the pertinent literature will be presented in chapter 2; the reader should refer to Kline's Thesis[3] for a more complete review. The theoretical formulation and flow model will be presented in chapter 3. The results of modifications to Kline's best SCB pressure drop calculation procedure will be presented in chapter 4. For this investigation, Kline's SR-2F computer code version, and associated correlations and assumptions, will also be referred to simply as Kline's SCB model.

The process of modifying Kline's model can be traced through the listing of the over 53 separate code versions formulated(see appendix I). Listing of the constituent equations for each code version is shown there.

The code version containing the overall best combination of correlations is ASCB53. It will be shown that this version, except for three pathological cases, predicts pressure drops which agree with the selected experimental data to within about $\pm 20\%$.

2. Review of the Pertinent Literature

The review of the pertinent literature for this research consists of two parts: pressure drop correlations, and experimental data for checking the computed pressure drop results.

2.1 Pressure Drop Correlations in the Open Literature

Kline[3] formulated a computer code to step-wise integrate the basic governing equations for SCB flow through small diameter tubes with a uniformly applied outer tube wall heat flux. He investigated various empirical equations from the open literature for the flow parameters needed to completely describe the SCB region(i.e. non-equilibrium void fraction, two-phase friction factor multiplier, and non-equilibrium flow quality). Kline's extensive survey of correlations led to the construction and evaluation of several SCB pressure drop models. The corresponding computer code versions for each model were compared to the experimental data of Reynolds[6], Mendler[7], and Dormer and Bergles[4]. The code version best matching the selected experimental data, designated SR-2F, was recommended; the accuracy was quoted as being $\pm$20% based on a selected set of experimental data but was actually only good to about -30% to +45% for his entire compiled experimental data set, excluding a few pathological cases.

Kline's computer code was designed to predict the SCB pressure drop of water flowing in a heated tube with the following assumptions:

(1.) Forced-convective flows through horizontal and vertical heated small diameter tubes under steady-state conditions.

(2.) Circumferentially and axially uniform applied outer heat flux.

(3.) The working fluid(water) enters in a subcooled state and all fluid properties are well defined.

(4.) Entrance and flow development effects on the velocity and thermal boundary layers are neglected(i.e. fully-developed, turbulent flow is assumed at the inlet).

In addition to the pressure drop, his code also returned the bulk, inner and outer wall temperatures profiles, the transition point between single-phase liquid(SPL) and SCB regimes, the transition between the partially developed boiling(PDB) and fully developed boiling(FDB) regimes, and critical heat flux levels from four different correlations.

Kline found that for vertical tubes, the gravity pressure drop term dominated in both the SPL and SCB flow regimes; the momentum pressure drop term dominated in all horizontal runs. He found the best agreement when using the Kroeger and Zuber[8] flow quality model, the Zuber et. al.[9] void fraction model, and a two-phase friction factor multiplier not equal to one. Kline also found that if the onset of significant net vapor generation(OSNVG) could be accurately predicted, the calculated SCB pressure drop matched the experimental data with reasonable accuracy. Of most importance, Kline showed that most combinations of available

SCB pressure drop equations and correlations did not give accurate pressure drop predictions.

In 1964, Dormer and Bergles[4] developed a graphical SCB pressure drop correlation after extensive experimentation. These investigators measured the pressure drop in heated, small diameter, horizontal tubes under a variety of flow conditions and correlated their final results in a single graph ($\Delta P/\Delta P_{sat}$ vs. q''/q''_{sat}). Smooth tubes of diameters 1.57, 2.39, 3.07, 4.57 mm (0.062, 0.094, 0.121, and 0.180 in) were tested with an electrically heated equivalent applied heat flux ranging from 0 to 17.3 MW/m^2 (0 to 5.5 x 10^6 $Btu/hrft^2$). Length to diameter ratios varied from 25 to 200. Exit pressures were set at 2.068, 3.447, and 5.516 bar (30, 50, and 80 psia); mass velocities varied from 1520 - 19750 kg/m^2s (311 to 4045 lb_m/ft^2s). All runs were operated with inlet and outlet temperatures below the local saturation value and heat fluxes below the estimated critical values. Each curve in their graphical correlation, reproduced here as figure 2.1, represents the correlated pressure drop results for a particular test section over a range of flow conditions. An example is shown in figure 2.2. The final curve representing T.S. 25(a) on figure 2.1 is a best curve fit to all the data on figure 2.2. Based on the data scatter on figure 2.2, it may be estimated that the single curve represented on figure 2.1 has an associated uncertainty band of ±10% to ±15%. This correlation was developed for a specific range of flow conditions; the pressures were quite low being no greater than

about 5 atmospheres. The authors do not state whether the correlation can be extrapolated outside the range of their experiments.

More recently, Jia and Schrock[10] proposed a procedure for calculating the SCB pressure drop in small diameter tubes; their calculation procedure is essentially a modification to Kline's model. In their research, Jia and Schrock surveyed different SCB correlations needed to completely describe the frictional, gravitational, and acceleration pressure gradient terms. These terms were integrated along the tube length to calculate the pressure drop. Their model differs from Kline's in a few ways. Jia and Schrock defined the linear attached wall void profile for the PDB regime using the Levy[20] equation for determining the bubble size and corresponding wall void at OSNVG, in contrast to the Rouhani[21] expression used by Kline. In conjunction with this new wall void value, they also proposed that the attached wall void roughens the flow passage in PDB causing an increase in the friction factor. The Hirata[25] equation was used to model this effect. Jia and Schrock also spent considerable effort in more accurately defining the distribution parameter needed in the void fraction equation for the FDB regime. Their model used the Hancox and Nicoll[11] correlation which relates the distribution parameter to the local void fraction. Finally, the onset of nucleate boiling(ONB) was defined using the Bergles and Rohsenow[12] correlation for the wall superheat at that point. Jia and Schrock compared their predicted results

with the experimental data of Dormer and Bergles[4], Owens and Schrock[5], and Reynolds[6]. Their presented results agree reasonable well with the experimental data.

2.2 Experimental Data in the Open Literature

Because of the practical constraints of this research program, each code modification could only be compared with a select group of experimental data. This group of experimental runs needed to be carefully chosen so that changes in the calculation method could be quickly and directly evaluated, with confidence that the results would be representative of a larger data set. In addition, these test runs needed to cover a wide range of flow conditions in order to assure that the final code version would have a wide range of applicability.

The experimental data selected for comparison to the code results of this investigation appear to meet these conditions. The data selected comes from the testing programs of Dormer and Bergles[4], Owens and Schrock[5], and Reynolds[6]. A careful selection of individual experimental runs was made from each of these programs for comparison to each computer code version developed in the present investigation; those choices will be discussed in section 2.3. The full data sets of each testing program are described next.

(a) Dormer/Bergles Test Data[4]

Perhaps one of the most complete sets of experimental data for the conditions of high heat flux and low pressure comes from the experimental testing program of Dormer and Bergles. These authors performed pressure drop tests for water in

horizontal tube sections under the following geometric conditions:

Tube A:	Type 304 Stainless Steel		
	Heated Lengths:	0.0584 m (2.3 in)	L/D = 25
		0.1249 m (4.9 in)	L/D = 50
	D_i = 2.388 mm (0.094 in)		
	D_o = 3.048 mm (0.120 in)		
Tube B:	Nickel Steel		
	Heated Lengths	0.112 m (4.41 in)	L/D = 25
		0.230 m (9.06 in)	L/D = 50
		0.457 m (18.0 in)	L/D = 100
	D_i = 4.585 mm (0.1805 in)		
	D_o = 5.359 mm (0.2110 in)		
Tube C:	Type 304 Stainless Steel		
	Heated Lengths	0.074 m (2.92 in)	L/D = 25
		0.150 m (5.90 in)	L/D = 50
		0.301 m (11.85 in)	L/D = 100
		0.454 m (17.86 in)	L/D = 150
	D_i = 3.073 mm (0.121 in)		
	D_o = 6.350 mm(0.250 in)		
Tube D:	Type 304 Stainless Steel		
	Heated Lengths	0.151 m (5.94 in)	L/D = 100
		0.229 m (9.00 in)	L/D = 150
		0.306 m (12.06 in)	L/D = 200
	D_i = 1.575 mm (0.062 in)		
	D_o = 3.175 mm (0.125 in)		

Pressure drop measurements were taken over the following range of flow conditions for each test section:

Heat Fluxes:	0 - 17.35 MW/m^2 (0 - 5.5 x 10^6 $Btu/hrft^2$)
Exit Pressures:	2.06 - 5.52 bar (30 - 80 psia)
Inlet Temps:	10 - 62.8 °C (50 - 145 °F)
Inlet Velocities:	1.52 - 18.29 m/s (5 - 65 ft/s)

Dormer and Bergles performed mostly overall pressure drop tests for a wide range of parameters, although a few pressure

drop distribution tests were conducted at the beginning of their testing program. The majority of the test runs were made at 75 °F or 80 °F because they considered this temperature to be representative of most cooling systems operating at a few atmospheres pressure. Their results were presented mostly in the form of total pressure drop vs. heat flux plots, with a few pressure drop vs. tube length curves. Pressure drop data used in this investigation was read from enlarged photocopies of these graphs with an estimated uncertainty of ±1%. Although Dormer and Bergles did not run pressure drop tests for every possible combination of flow conditions, their experimental program is one of the most extensive covering high heat flux, low pressure conditions. A plot of the flow parameter space, along with the full flow conditions for their testing program, is given in appendix D.

(b.) Owens and Schrock[5]

In their experiments for vertical flow in heated tubes, Owens and Schrock produced a substantial amount of pressure drop distribution data over a higher range of pressures, but lower range of heat fluxes than Dormer and Bergles. Tests were conducted for water on two sections fabricated of 347 stainless steel. The geometric conditions were:

Test Section IV: Heated Length: 0.406 m (16 in)
D_i = 4.63 mm (0.1824 in)
D_o = 6.386 mm (0.2514 in)

Test Section VII: Heated Length: 0.381 m (15 in)
D_i = 3.000 mm (0.1181 in)
D_o = 4.684 mm (0.1844 in)

Pressure drop measurements were taken over the following range of flow conditions:

Heat Fluxes:	0.67 - 4.0 MW/m^2 (0.21 - 1.27 x 10^6 $Btu/hrft^2$)
Exit Pressures:	3.4 - 27.9 bar(increments of 3.4 bar) (50 - 400 psia(increments of 50 psia))
Inlet Temps:	93.3 - 194.4 °C (200 - 382 °F)
Inlet Mass Fluxes:	830 - 5322 kg/m^2s (170 - 1090 lb/ft^2s)

Their testing program was constructed to assure maximum coverage of the flow parameters of heat flux, mass flux, pressure, tube diameter and degree of subcooling for the given equipment and time limitations. The pressure drop measurements at each of the eight pressure taps were presented in tabular form. Pressure values between these taps were estimated from a plotted curve fit of the data with an estimated uncertainty of ±2%. This set of experimental data is particularly useful because the range of pressures match those of typical SCB cooling systems, although the heat fluxes values where not as high as those of Dormer and Bergles. Pressure drop distribution data of this testing program was particularly useful in our code validation procedure by helping us to evaluate our predictions of the ONB and OSNVG locations along the tube, and hence, the predicted pressure drop profiles in each of the flow regimes. This was not possible from the overall pressure drop vs. heat flux curves of Dormer and Bergles.

(c.) Reynolds[6]

The final experimental data used in this investigation comes from the testing program of Reynolds. The total pressure gradient for water flowing in a horizontal uniformly heated tube was measured for a limited range of conditions. The Reynolds program was of a smaller magnitude than the previous two, being limited to a single test section with the following dimensions:

Heated length: 1.829 m (6 ft)
D_i = 9.525 mm (0.375 in)
D_o = 12.7 mm (0.50 in)
Material - AISI 347 Stainless Steel

The range of flow conditions were:

Heat Fluxes:	0.41, 0.55, 0.69, 0.82, 0.96 MW/m^2 (0.13, 0.17, 0.22, 0.26, 0.30 x 10^6 $Btu/hrft^2$)
Exit Pressures:	3.07, 4.1, 5.13, 6.86 bar (45, 60, 75, 100 psia)
Inlet Temps:	93.3 - 194.4 °C (200 - 382 °F)
Inlet Mass Fluxes:	2121, 2651, 3181 kg/m^2s (434.4, 543.0, 651.5 lb/ft^2s)

Pressure drop measurements(referenced to the inlet pressure) were measured at seven locations along the length of the tube and presented in tabular form. The seven experimental data points were plotted directly on the predicted pressure drop vs. tube length curves generated in this investigation as a means of comparison because a smooth curve fit of the experimental data was not possible. Accurate interpolation between the experimental data points was not possible. Since

this was one of the earliest published works devoted to quantifying the pressure drop in SCB, it appears that Reynolds and his researchers may have restricted the range of flow parameters for their experiments because of technological limitations of their equipment.

2.3 Choice of Experimental Data to be Used in This Investigation

For the most part, these three sets of experimental data provide a pool of comparison data roughly covering heat fluxes 0 - 17 MW/m^2 (0 - 5.39 x 10^6 $Btu/hrft^2$), pressures 2 - 28 bar (30 - 405 psia), and mass fluxes 830 - 18,250 kg/m^2s (170 - 3740 lb/m^2s). Because of the enormous amount of data presented in these sets(over 1500 individual runs), it was not feasible to compare each computer code modification to every experimental run. It was thus necessary to select a representative set of runs(the basic data set) for use in the code modification procedure and once satisfied with the results, compare the final code version to additional selected experimental data.

(a.) Dormer and Bergles Data Selected

As reviewed earlier, Dormer and Bergles presented their pressure drop results in two formats, pressure vs. length and total pressure drop vs. heat flux. Each pressure vs. length curve represents the results of a single test run under a single set of flow conditions. Each total pressure drop vs. heat flux curve, in contrast, represents a collection of pressure drop results for a single test section over a range

of heat fluxes, but with the same inlet fluid velocity, same inlet temperature and same exit pressure. The selected runs have been given designations based on their D&B figure numbers. Letter suffixes were assigned when more than one curve was taken from a figure.

Basic Data set: Figure 11a, 11b, 11c, 11d, 17, 19, and 28.

Additional Data: Figure 19a, 19b, 24.

D&B figures 17,19, 19a, 19b, 24, and 28 are overall pressure drop results for varying heat fluxes which represent a collection of 115 individual runs; figures 11a thru 11d are pressure drop distribution results for four specific runs.

The selection of these individual experiment runs from this data set was relatively simple. Because Kline chose data from all but one of the figures listed above for his investigation, choosing those runs for this study allowed for direct comparison and evaluation of the new modifications to Kline's best computer code version. The individual runs corresponding to these figures have an inlet temperature of 26.7 °C(80 °F) because most of the D&B test runs were limited to an inlet temperature of 26.7 °C(80 °F). Despite this restriction, the runs chosen do cover most of the range of pressures and mass velocities of the experimental program. The additional experimental runs were purposely chosen as figures where Kline showed poor agreement between his predictions and the experimental data, or figures which had an exceptionally large FDB region as indicated on the overall pressure drop versus heat flux plots.

(b.) Owens and Schrock Data Selected

Basic Data set: Runs 182, 210, 245, 253.

Additional Data: Runs 208, 215, 255.

All of these data runs are pressure distribution results along the tube length.

The first four experimental data runs were selected for use in this investigation primarily because Jia and Schrock[10] chose to compare their pressure drop calculation procedure to these runs. Improvements presented by Jia and Schrock to Kline's model could be evaluated using these common runs. In order to better sample the range of flow conditions of the Owens and Schrock data, especially at high q" and high G, three additional runs were selected. The only flow condition which was not sampled well by these choices was the inlet temperature. The runs selected all had inlet fluid temperatures below 96 °C(204 °F), despite the temperature ranging to 194 °C(317.2 °F) for other data of the Owens and Schrock investigation. However, the choice of lower temperature runs could not be avoided. Higher temperature runs corresponded to only lower heat flux values. Since we were interested mainly in high heat flux conditions, only lower temperature range runs were available for selection. No high heat flux and high temperature runs exist in this experimental program because all runs were required to have a subcooled boiling condition at the exit.

(c.) Reynolds Data Selected

Experimental runs from this testing program were again chosen primarily because Kline used them in his investigation. Since the range of flow conditions of the Reynolds program is covered in the Dormer and Bergles testing program, these data runs are only of limited interest to us. Consequently, this data was not used to evaluate any of the computer code versions produced during the modification process. Only two runs from the Reynolds experimental program were selected for comparison to the final code version ASCB53. They appear in appendix H.

Basic Data set: Runs 115, 129.

Additional data: none

These two runs have mass velocities of greater than 2500 kg/m^2s (512 lb/m^2s) because during the modification procedure, it was discovered that runs with G < 2500 kg/m^2s, the uncertainty in our code predictions in the SPL and PDB regimes was larger than +20%. Consequently, these runs really have no function other than to show if the final code version results of this investigation are any worse than the already adequate results of Kline's best computer code version SR-2F.

2.4 Transformation of the Data Into Usable Forms

The flow conditions of Dormer and Bergles runs selected had to be transformed into parameters which could be entered directly into the code. For each run, Dormer and Bergles specified the inlet velocity, inlet temperature, and exit pressure. The computer code needs the inlet mass velocity,

inlet temperature, and inlet pressure as inputs. The exit pressure was converted to an inlet pressure by adding the experimental pressure drop result quoted for the corresponding heat flux of that run to the exit pressure. The inlet mass velocity was calculated by multiplying the quoted inlet velocity by the inlet density corresponding to the inlet temperature and inlet pressure found from the compressed liquid tables. It is presumed that this density was used by Dormer and Bergles in transforming their measured mass flow rate to an inlet velocity.

All flow parameters, except the inlet temperature, for each run of the Owens and Schrock data were given directly. Values for the fluid temperature were given as a function of a non-dimensional SCB length instead of more straight forward as a function of Z. The subcooled boiling length was defined to be the region where the inner wall temperature remains approximately constant up to the OBB point(see figure 3.2). Since the beginning of this region never coincided with the inlet of the tube, the inlet temperature for each run selected had to be found by linearly extrapolating back from the given temperatures further down the tube.

Since the two Reynolds runs used for comparison of the code were also selected by Kline, all the flow parameters needed at the tube inlet were taken directly from Kline's work.

A complete list of the flow conditions for each of the selected data runs appears in Appendix D.

3. Review of Equations and Procedures Used in the Final Computer Code

Fifty-three computer code versions were constructed in the process of finding the best match to the entire set of selected experimental data runs used in the code validation procedure. The final set of SPL and SCB equations and correlations used in the final code version(ASCB53) will be presented in this chapter. The important candidate expressions examined in the formulation of the final code version will also be briefly discussed in this chapter. Refer to figure 3.1 for a schematic of the code calculation logic and to figures 3.2, 3.3, and 3.4 for the temperature and vapor void profiles assumed in the new model. Major details describing the modification process of Kline's SR-2F code will be presented in chapter four.

3.1 Flow Regimes Possible in the Tube

The computer code models the flow of water through a small diameter, uniformly heated tube. Three different flow regimes are possible in the tube depending on the flow conditions and the applied surface heat flux.

(a.) Single phase liquid (SPL)

In the SPL flow regime, no boiling of the fluid occurs; everywhere, the fluid remains below the saturation temperature. Standard SPL heated flow correlations, of which many exist in the open literature, are applicable for calculation of the pressure drop in this regime.

(b.) Partially Developed Boiling (PDB)

The PDB flow regime is bounded by the onset of nucleate boiling at the start and by the onset of significant net vapor generation at the end. Vapor bubbles generated in a non-equilibrium manner stay attached to or slide along the heating surface. Those bubbles which do try to leave the surface condense in the cooler bulk fluid. Since the non-equilibrium vapor void and non-equilibrium flow quality are so small in this regime, and almost negligible, they can be ignored for most purposes. Only the blockage effect that the bubble layer has on the mass velocity and hydraulic diameter is considered. This regime is often described as the first half of the subcooled boiling region.

(c.) Fully Developed Boiling (FDB)

The second half of the SCB region is known as the fully-developed boiling regime. It is marked by the onset of significant net vapor generation at the start and by the onset of bulk boiling(saturated boiling) at the end. In this region, the non-equilibrium void and non-equilibrium flow quality increase rapidly along the length of the tube. This affects the flow patterns and thus the local pressure drop. The intensity of local boiling is highly dependent on surface conditions, local subcooling and physical properties of the liquid and vapor phases. In the FDB region, the inner wall temperature reaches an approximately stable threshold value necessary to sustain the generation of vapor bubbles from the wall. There is no sharp physical distinction between the end

of the SCB region and the beginning of the bulk boiling flow regimes. The non-equilibrium void fraction and flow quality models fair gradually into the equilibrium void and flow quality models of the saturated boiling regime.

The equations used in the pressure drop and heat transfer calculation procedures are described next.

3.2 Equations for the Single-Phase Liquid Regime

In the SPL flow regime, the pressure drop gradient equations derived from the basic equations under steady flow conditions are given as

$$\left[\frac{dP}{dZ}\right]_{fric} = \frac{[2\ f_{fo}\ G^2\ v_f]}{D}$$

$$\left[\frac{dP}{dZ}\right]_{accel} = G^2\ \frac{d}{dZ}\ [v_{f2} - v_{f1}]$$

$$\left[\frac{dP}{dZ}\right]_{grav} = g\ \sin\theta\ \frac{d}{dZ}\ [\rho_2 - \rho_1]$$

where f_{fo} is the SPL heated friction factor of Fanning definition, θ is in degrees, point 2 is the exit of the differential flow element, point 1 is the entrance of the differential flow element, and all other parameters are in SI units.

These terms are numerically integrated along the tube length using the local water property data to yield the pressure drop.

The equation used to calculated the SPL heated friction factor is

$$\frac{f_{fo}}{f_{iso}} = \left[\frac{\mu_{wall}}{\mu_{bulk}}\right]^{n}$$

where the isothermal friction factor for fully-developed turbulent SPL tube flow is given by the Fanning definition as

$$f_{iso} = 0.046\ Re_b^{-0.2} \qquad \text{for } 2300 \leq Re_b \leq 10^6$$

$$f_{iso} = 0.0246\ Re_b^{-0.155} \qquad \text{for } Re_b > 10^6$$

for smooth tubes only.

Under the conditions of heating, the isothermal friction factor of a liquid must be adjusted for the effect of fluid viscosity variations in the boundary layer. Sieder and Tate[22] introduced an expression of the form $f/f_{iso} = (\mu_w/\mu_b)^n$ where n equals 0.14 for water. The exact value of n for water is of considerable speculation. Dormer and Bergles[4] were able to correlate their test data with n = 0.35. Owens and Schrock's[5] investigation found values of n ranging from 0.3 to 0.6, with the average being 0.4. Owens and Schrock argue that more of the liquid near the wall is affected by the heating than previously believed, resulting in more effect on the viscosity ratio. Thus it was initially decided to use the expression with n = 0.4. In contrast, Kline chose to use the Petukhov[23] equation for the heating adjustment. Both expressions will be examined in this investigation. It will be shown using the final code version that an exponent of 0.3 instead of 0.4 will yield better agreement with the experimental data selected for this investigation. Thus, the equation used in the final code version is

$$\frac{f_{fo}}{f_{iso}} = \left[\frac{\mu_{wall}}{\mu_{bulk}}\right]^{0.3} .$$

Many correlations are known to exist for the SPL heat transfer coefficient. Kline chose a correlation adequate for design from the G.E. Heat Transfer Data Book[29]. The equation for the heat transfer coefficient at any Z location is

$$h = 0.11125\ f_{iso}\ c_{pf}\ G \left[\frac{Re}{10^4}\right]^{0.0685} [Pr]^{-0.53} \left[\frac{\mu_{bulk}}{\mu_{wall}}\right]^{m}$$

where m is a constant given as a function of Re number interpolated between the following:

Re	m
2,100	0.14
12,500	0.02
25,000	0.05
50,000	0.08
1,000,000	0.08

where f_{iso} is the isothermal friction factor for a SPL of the Fanning definition as listed before and all parameters are in SI units.

With the heat transfer coefficient known, the inner wall temperature at any given Z location along the tube can be easily calculated from the definition of the film drop,

$$\Delta T_{film} = (T_{wall} - T_{bulk}) = \frac{q''}{h}$$

where T_{bulk} comes from the steady state energy balance equation at the particular Z location, temperatures are in °K, q" is in W/m^2 and h is in W/m^2 °K.
This calculation procedure is continued along the tube until the ONB point is reached.

3.3 Equations for the Onset of Nucleate Boiling

The onset of nucleate boiling marks the beginning of the subcooled boiling region. There exists sufficient superheating of the wall(heating surface) over the local saturation temperature, to allow the growth of vapor bubbles. This is an inherently non-equilibrium thermodynamic condition which occurs only in the near-wall region. The two correlations considered in this investigation are from Bergles and Rohsenow[12], and Davis and Anderson[13]. Both are based on Hsu's[14] model of formation of a bubble from a surface cavity in a thermal boundary layer. Hsu's model is illustrated in figure 3.5.

The Bergles and Rohsenow correlation is an empirical fit to Hsu's equations governing growth of a bubble on a heated surface. The solution is for the special case where surface cavities of all sizes up to r_{crit}, are assumed to be available for nucleation at the given q". It corresponds to the tangency point of equations 1(the vapor temperature of the liquid at the top of a bubble at the bubble nucleation condition) and 2(the approximated linear expression describing the temperature gradient of the fluid away from the wall) in

figure 3.5, designated r_{crit}. Their correlation gives the wall superheat at ONB as

$$\Delta T_{sat(ONB)} = 0.556\left[\frac{q''}{1082\ p^{1.156}}\right]^{0.463p^{0.0234}}$$

where $\Delta T_{sat(ONB)}$ is in °C, q" is in W/m^2, and p is in bar. The equation is valid only for water over the pressure range 1 to 138 bar.

Davis and Anderson proposed an equation which is an analytical solution to the intersection of the two equations using Hsu's model. Under the assumption that the wall superheat is not too high and using other simplifying assumptions, they were able to express the wall superheat at ONB as

$$\Delta T_{sat(ONB)} = \frac{B}{r_{max\text{-}active}} + \frac{q''\ r_{max\text{-}active}}{k_f}$$

where $B = \left[\frac{2\ \sigma\ T_{sat}\ v_g}{i_{fg}}\right]$, $r_{max\text{-}active} = \left[\frac{B\ k_f}{q''}\right]^{0.5}$ for the special case where $r_{max\ active}$ is different from r_{crit} in fig. 3.5, and all parameters are in SI units.

Davis and Anderson also point out that the use of $r_{max\text{-}active}$ equal to r_{crit} from above may be incorrect if the actual heating surface does not have a sufficiently wide range of active cavity sizes available for nucleation. This would indicate that the formation of bubbles on the surface would not initiate until higher superheat values and consequently higher wall temperatures shown as $(T'_w)_{ONB}$ on figure 3.5. In such cases, an estimate of $r_{max\text{-}active}$ derived from experiments

on the heating surface may inserted into the equation for better prediction of the wall superheat at the ONB condition.

For $r_{max\text{-}active}$ equal to r_{crit}, the Davis/Anderson equation compares well with the Bergles/Rohsenow equation and adequately predicts the ONB point from the experimental data of Bergles and Rohsenow[12]. The Davis/Anderson correlation is used in the final code version because it can easily be modified for fluids other than water and is valid for the conditions of $r_{max\text{-}active}$ different from r_{crit}. Refer to Collier[24] for a more detailed discussion of the phenomenon of ONB.

If the inner wall temperature in the SPL regime remains below that of the value calculated using the Davis and Anderson ONB correlation for wall superheat,

$$T'_{wall(ONB)} = T_{sat} + \frac{B}{r_{max\text{-}active}} + \frac{q'' \, r_{max\text{-}active}}{k_f}$$

then the flow is considered to remain in the SPL state. Once the wall temperature reaches or exceeds $T'_{wall(ONB)}$, the code switches to the PDB calculation procedure.

3.4 Equations for the Partially-Developed Boiling Regime

In the PDB regime, the SPL pressure gradient equations are assumed to be applicable if adjusted to account for the flow blockage resulting from the growth of the vapor bubble layer along the wall. The same frictional and acceleration pressure gradient equations can be used if the hydraulic diameter and effective mass velocity are substituted for the tube diameter and mass velocity, respectively. The modifications are given

for a uniform bubble layer around the inside of a round tube as

$$D_{hydr} = D \left[\frac{4\ A_{eff}}{\pi}\right]^{0.5}$$

$$G_{eff} = \frac{G}{1 - \alpha_{wall}(Z)}$$

where $A_{eff} = A(1 - \alpha_{wall}(Z))$

$$\alpha_{wall}(Z) = \alpha_{wall \text{ at OSNVG}} \left[\frac{Z - Z_{ONB}}{Z_{OSNVG} - Z_{ONB}}\right]$$

The gravity pressure loss gradient is also modified slightly to account for the blockage effect.

$$\left[\frac{dP}{dZ}\right]_{grav} = g \sin\theta \left\{\frac{d}{dZ}\left[\rho_2 - \rho_1\right]\right\}(1 - \alpha_{wall})$$

With these minor changes, the PDB gradient terms are integrated along the tube length to calculate the pressure drop along the tube.

The attached wall void(or bubble layer) in the PDB regime is assumed to grow linearly along the tube, from ONB, under the competing effects of evaporation and condensation. The corresponding wall void fraction profile starts at zero at ONB and grows linearly to a value approximately 67% the size of a bubble at OSNVG as shown in figure 3.4. This bubble size at OSNVG can be given by the Levy[20] equation(which we did not use in our final code version)

$$Y_{OSNVG} = 0.015 \left[\frac{\sigma\ D}{\tau_{wall}}\right]^{0.5}$$

where $\tau_{wall} = \left[\frac{f_{fo}\, G^2\, v_f}{2.0}\right]$, f_{fo} is the SPL heated friction factor given before and the attached wall void is given as

$$\alpha_{w(OSNVG)} = \frac{\pi\, Y_{OSNVG}}{6} D_h$$

if the bubbles are idealized as being packed in a square array with a diameter to pitch ratio of 0.5.

The Levy model is derived from a force balance on a vapor bubble about to depart the heated wall in forced convection. The proposed model is said to compare satisfactorily with the void measurements at OSNVG of Rouhani[21] to within plus or minus 30 percent(Levy[20] p. 956). We have not yet found any models in the open literature for the bubble layer profile in the PDB regime except that of a linear one.

Alternately, the wall void at OSNVG can be given by the Rouhani[21] correlation

$$\alpha_{wall\ at\ OSNVG} = \frac{P_h\, \delta}{A_{geom}} = \frac{4}{D}\left[1.59 \times 10^{-4}\, P^{-0.237}\right]$$

where P is in bar and D is in meters. The Rouhani equation assumes that the average vapor thickness on a heated surface covered with small bubbles can be given as

$$\delta = 0.67\, R_d$$

where the bubble radius is described empirically as

$$R_d = \frac{0.000237}{[P(bar)]^{0.237}} .$$

Kline's model used the Rouhani equation. It will also be used in our final code version with the assumption of linear bubble layer growth in PDB.

It has been proposed by Jia and Schrock[10] that the attached bubble layer in PDB causes a surface roughness greater than the plain wall roughness. It is described by the Hirata[25] equation(using the Fanning friction factor definition)

$$f_{iso} = 0.0275 \left[\frac{68}{Re} + \frac{e(z)}{D}\right]^{0.25}$$

and

$$e(z) = 0.75\ Y(z),$$

$$Y(z) = 0.15[\sigma\ D\ \tau_{wall}]^{0.5} \quad \text{(from Levy)},$$

$$\tau_{wall} = \left[\frac{f_{fo}\ G^2\ v_f}{2.0}\right] \quad \text{(from Levy)},$$

and all parameters are in SI units.

This set of equations was used by Jia and Schrock in conjunction with the Levy model for the bubble size at OSNVG. In contrast, Kline used the SPL friction factor to model the surface friction in the PDB region, so that the friction pressure gradient is only adjusted for the effect of blockage on the flow. The two approaches for defining this friction factor will be studied. Only the SPL friction factor, with the Rouhani model for the bubble size at OSNVG, is used in our final code version.

The inner wall temperature in the PDB regime is assumed to follow a linear profile from ONB to OSNVG for simplicity. It will be shown later that the pressure drop solution is not sensitive to the shape of the inner wall temperature profile. The wall temperatures at the end points can be found from the

Davis and Anderson ONB correlation as discussed earlier and from the Jens and Lottes equation for the wall superheat in the FDB regime. These equations are

$$\Delta T_{sat(ONB)} = \frac{B}{r_{max\text{-}active}} + \frac{q'' \, r_{max\text{-}active}}{k_f}$$

$$\Delta T_{sat(OFDB)} = 25 \left[\frac{q''}{10^6}\right]^{0.25} e^{-\left(\frac{P}{62 \times 10^5}\right)}$$

where $T_{wall} = T_{sat} + \Delta T_{sat}$, ΔT_{sat} and T_{sat} are in °K, P is in Pa, and q" is in W/m^2.

With the inner wall temperatures known at the end points, the inner wall temperature at any location Z in the PDB region is given by a simple linear relationship as

$$T_{wall}(Z) = m(Z - Z_{ONB}) + T_{w(ONB)}$$

$$\text{where } m = \frac{T_{w(OSNVG)} - T_{w(ONB)}}{Z_{OSNVG} - Z_{ONB}} .$$

Once the wall temperature is described, the heat transfer coefficient can be calculated from the definition of the film drop temperature given in the form

$$h = \frac{q''}{\Delta T_{film}} \text{ for any Z location in the PDB region}$$

where q" is in W/m^2 and ΔT_{film} is in °K.

3.5 Equations for the Onset of Significant Net Vapor Generation (OSNVG)

The onset of significant net vapor generation point defines the break between the low and high subcooled boiling regions. The OSNVG is characterized by the significant detachment of vapor bubbles from the heated surface. Bubbles, which were either coalescing or condensing at or near the wall in the PDB

regime, now have sufficient energy to stabilize in the vapor form and drift toward the core of the flow. This rapid increase in void fraction causes a sudden increase in the pressure drop. Two candidate expressions for the OSNVG point are given by Saha and Zuber[15] and Shah[16].

Saha and Zuber formulated a general correlation predicting the subcooling of fluids(water,freon-114,freon-22) at the OSNVG condition as

$$\Delta T_{sub(OSNVG)} = \frac{q'' A D}{455 k_f} \qquad \text{for Pe} < 70{,}000$$

$$\Delta T_{sub(OSNVG)} = \frac{q'' A}{0.0065 G c_{pf}} \qquad \text{for Pe} > 70{,}000$$

where all parameters are in SI units.

It will be shown using the final code version, that agreement with experimental data is improved if the Saha/Zuber correlation is modified for tube diameters less than 7 mm.

$$\Delta T_{sub(OSNVG)} = \frac{q'' A D}{455 k_f} \qquad \text{for Pe} < 70{,}000$$

$$\Delta T_{sub(OSNVG)} = \frac{q'' A}{G c_{pf} \tilde{St}} \qquad \text{for Pe} > 70{,}000$$

where the subcool Stanton number($\tilde{St}$), as defined by Saha and Zuber, is given as a function of the applied heat flux q" and the local Peclet number as

$$\tilde{St} = 0.0065 + m(70{,}000 - Pe)$$

where $m = -3.952 \times 10^{-9} \left[\frac{q''}{30.0 \times 10^6}\right]^{-1.03}$, and all parameters are in SI units.

In addition to the Saha/Zuber correlation, which Kline chose to use in his model, a promising alternate expression for OSNVG given by Shah[16] was examined,

$$\left[\frac{\Delta T_{sub}(Z)}{\Delta T_{sat}(Z)}\right]_{OSNVG} = 2.0$$

or $$\left[\frac{\Delta T_{sub}(Z)}{\Delta T_{sat}(Z)}\right]_{OSNVG} = 6.3 \times 10^4 \, B_o^{1.25}$$, whichever is less.

This correlation is valid for water and other organic fluids over the range of pressures 1 to 138 bar, and tube diameters 2.1 to 27.1 mm. Shah states that this is a general correlation fit to experimental data with an uncertainty of ±30% and that a more accurate correlation would have to take into account detailed surface geometry, concentration of dissolved gases, and the previous flow history.

Shah also gave a correlation for the inner wall temperature superheat in the transition region from the PDB to the FDB flow regimes. They are included here since Shah introduced them with his OSNVG correlation.

FDB regime: $$\Delta T_{sat}(Z) = \frac{q''}{Y_o \, h_{fo}}$$

PDB regime: $$\Delta T_{sat}(Z) = \frac{q''}{Y_o \, h_{fo}} - \frac{\Delta T_{sub}(Z)}{Y_o}$$

where $Y_o = 230 \, B_o^{0.5}$ for $B_o \geq 0.3 \times 10^{-4}$

$Y_o = 1 + 46 \, B_o^{0.5}$ for $B_o < 0.3 \times 10^{-4}$

$B_o = q''/ G \, i_{fg}$

$\Delta T_{sat}(Z)$ is the wall superheat in °K

and all other parameters are in SI units.

The G.E. Heat Transfer Data Book[29] recommends that for a designer's use, the Shah and Saha/Zuber correlations are comparable. However, we found that better agreement with the experimental data was obtained using the modified Saha/Zuber correlation.

While in the PDB calculation mode, the subcooling at every numerical integration step(i.e. $\Delta T_{sub}(Z) = T_{sat} - T_{bulk}$) is checked against the calculated OSNVG subcooling. When the local subcooling equals or is less than the Saha/Zuber prediction, the code switches to the FDB pressure calculation procedure.

3.6 Equations for the Fully-Developed Boiling Regime

In the FDB regime, two-phase flow exists in the tube but is of a non-equilibrium nature. Variations in flow topology influence the pressure drop along the tube and in turn, the pressure drop influences the rate of vapor formation and flow topology. Pressure drop calculations are very complex, but are very important. As indicated in figures 3.6 and 3.7, the pressure drop in the FDB regime is quite significant compared to that in the SPL and PDB regimes.

The pressure drop calculation is accomplished by use of the well-known separated flow model for two-phase flow. It is assumed that the equilibrium void, α, and flow quality, x, models that one would normally use in the saturated boiling regime, can be replaced by their non-equilibrium counterparts, α' and x'. The pressure gradient terms derived from the model

of vapor and liquid flowing in a round tube at different velocities are(see Collier[24] p. 27)

$$\left[\frac{dP}{dZ}\right]_{fric} = \left[\frac{2\ f_{fo}\ G^2\ v_f}{D}\right]\ [\phi_{fo}^2]$$

$$\left[\frac{dP}{dZ}\right]_{accel} = G^2\ \frac{d}{dZ}\left[\frac{x'^2 v_g}{\alpha'} + \frac{(1 - x')^2 v_f}{(1 - \alpha')}\right]$$

$$\left[\frac{dP}{dZ}\right]_{grav} = g\ \sin\theta\left[\frac{\alpha'}{v_g} + \frac{(1 - \alpha')}{v_f}\right]$$

where f_{fo} is the Fanning SPL heated friction factor from before, θ is in degrees, α', x', and $[\phi_{fo}^2]$ are non-dimensional, and all parameters are in SI units.

These terms are numerically integrated in the computer code taking into account fluid property variations at each step along the tube length under the following assumptions:

a. The liquid and vapor phases of the flow are steady and can be treated as one-dimensional.

b. Local attainment of thermodynamic equilibrium between the phases, although this is not completely accurate.

c. Negligible liquid and vapor compressibility.

d. The physical flow properties remain constant over the differential element length.

e. The use of empirical correlations to relate the two-phase friction multiplier, ϕ_{fo}^2, non-equilibrium flow quality, x', and non-equilibrium void fraction, α', to the independent variables of the flow is accurate in describing the actual phenomenon.

The derivation of the separated flow equations is given in Kline[3] and Collier[24]. The models for the non-equilibrium void fraction, α', the non-equilibrium flow quality, x', and the two-phase friction factor multiplier, ϕ^2_{fo}, for separated flow are described next.

The non-equilibrium void equation is given by Zuber et. al.[9], later rewritten by Kroeger and Zuber[8] as

$$\alpha'(Z) = \frac{x'(Z)}{\left\{\frac{C_o(\rho_f - \rho_g)}{\rho_f}\right\}x'(Z) + \left[C_o + \frac{\bar{u}_{gj}}{u_{f\ inlet}}\right]\frac{\rho_g}{\rho_f}}$$

where C_o is the distribution parameter, $\bar{u}_{gj}$ is the drift flux velocity, $u_{f\ inlet}$ is the inlet fluid velocity, x'(Z) is the non-equilibrium flow quality and all parameters are in SI units.

As indicated, $\alpha'(Z)$ is a complex function of the non-equilibrium flow quality, liquid and vapor densities, liquid and vapor velocities and distribution profiles of the two phases. Kline found generally good pressure drop predictions using this equation so it will be continued to be used in this investigation, except with modification of the distribution parameter C_o and drift flux velocity $\bar{u}_{gj}$.

The distribution parameter used in the correlation, to account for non-uniform radial void and velocity, is determined by characteristics of the flow. Many authors assume this value to be a constant in the range of 1.13 to 1.3 for simplicity. Kline chose to use the value of 1.13

recommended by Kroeger and Zuber[8]. Hancox and Nicoll[11] introduced a model for C_o which varies with the void fraction. The expression is

$$C_o = \left[\frac{1- \exp(- C_{01}\, \alpha')}{1- \exp(-C_{01})}\right](1 + C_{02}) - C_{02}\, \alpha'$$

where $C_{01} = 19$

$$C_{02} = 1.164 - 1.6534 \times 10^{-7}\, P + 7.5098 \times 10^{-15}\, P^2$$

and all parameters are in SI units.

This relationship was derived from experimental radial void data and hypothetical radial velocity profiles. Hancox and Nicoll state that, from its basic definition, C_o must have a value near zero at the start of the significant void region(i.e. OSNVG), since the void previous to that point is concentrated in the low-velocity, near-wall region. At the other extreme, Hancox and Nicoll state that C_o should approach unity as the averaged void fraction approaches unity. C_o actually exceeds unity at intermediate values of void fraction. Kroeger and Zuber[8] concur with this theory but recommend that in absence of experimental data on flow profiles in the SCB regime, a constant C_o should be taken for the entire tube section. Both the constant and variable approaches will be addressed in this investigation. It will be shown that reasonably good pressure drop agreement is achieved using a constant value of $C_o = 1.25$. This value is used in the final code version.

The drift flux velocity(or weighted mean drift velocity) needed in the $\alpha'(Z)$ equation is given by Kroeger and Zuber[8] as

$$\bar{u}_{gj} = 1.41 \left[\frac{g\ \sigma\ (\rho_f - \rho_g)}{\rho_f^{\ 2}} \right]^{0.25}$$

where all parameters are in SI units.

The drift flux velocity describes the relative velocity between the liquid and vapor phases of SCB flow. It is a relatively minor parameter in the void fraction equation which contributes a small term for vertical flows. An almost identical equation was proposed by Dix[17]. It is given as

$$\bar{u}_{gj} = 2.9 \left[\frac{g\ \sigma\ (\rho_f - \rho_g)}{\rho_f^{\ 2}} \right]^{0.25}$$

where all the parameters are in SI units.

This expression differs from the Kroeger/Zuber equation in that the leading constant is 2.9 instead of 1.41. A comparison of the two leading constants will be made in this investigation. A leading constant of 1.41 is used in the final code version.

The non-equilibrium flow quality expression needed in both the acceleration and gravity SCB pressure drop gradient equations can be based on either the Kroeger and Zuber[8] or Levy[20] equations.

Kroeger/Zuber:

$$x'(Z) = \left[\frac{c_{pf}\ \Delta T_{sub_{(OSNVG)}}\ (Z^+ - T^*)}{i_{fg} - c_{pf}\ \Delta T_{sub_{(OSNVG)}}\ (1 - T^*)} \right]$$

where $\Delta T_{sub(OSNVG)} = (T_{sat} - T_{bulk})_{OSNVG}$, Z^+ and T^* are given below, and all parameters are in SI units.

Levy:

$$x'(Z) = x(Z) - x_{OSNVG} \exp\left[\frac{x(Z)}{x_{OSNVG}} - 1\right]$$

$$\text{where } x_{OSNVG} = \frac{i_{OSNVG} - i_{f,sat}}{i_{fg}} = - \frac{c_{pf} \left[\Delta T_{sub(Z)}\right]_{OSNVG}}{i_{fg}}$$

$$x(Z) = \text{the equilibrium flow quality} = \frac{i(Z) - i_{f,sat}}{i_{fg}}$$

and all parameters are in SI units.

Both equations were evaluated by Kline. He found that only the Kroeger/Zuber expression yielded acceptable pressure drop results. Refer to Kline[3] for further discussion of the two correlations. Because the relationship between the calculated SCB flow properties is so complex, both equations will be reinvestigated in combination with some of the other parameter correlations not reviewed by Kline. The Kroeger/Zuber non-equilibrium flow quality equation was chosen for use in the final code version.

The non-dimensional temperature profile, T^*, used in the Kroeger and Zuber[8] non-equilibrium flow quality equation above is given as

$$T^* = 1 - \exp[-Z^+]$$

or $T^* = \tanh[Z^+]$

$$\text{where } Z^+ = \frac{Z - Z_{OSNVG}}{Z_{OBB} - Z_{OSNVG}} .$$

The authors state that either form is applicable, although their plots indicate slightly higher flow quality values are predicted with the exponential form. In his investigation, Kline chose to use the hyperbolic expression. We will examine the exponential form, as well as the hyperbolic form for completeness. The hyperbolic form was chosen for use in the final code version.

The two-phase friction factor multiplier is needed to complete the description of the the frictional SCB pressure gradient term in the FDB regime. This quantity was described by Martinelli and Nelson[18] in a graphical correlation which is approximately given in equation form by Chisholm[19] as(using n=0.2)

$$[\phi_{fo}^2]_{MN} = 1 + (\gamma^2 - 1)\left[B\, x'(Z)^{0.9}(1 - x'(Z))^{0.9} + x'(Z)^{1.8}\right]$$

$$\text{where } \gamma^2 = \frac{\left[\frac{dP}{dZ}\right]_{go}}{\left[\frac{dP}{dZ}\right]_{fo}}$$

$$= \left(\frac{u_f}{u_g}\right)^{-0.2}\left(\frac{v_g}{v_f}\right)$$

and B is given for smooth pipes by

$$\gamma < 8.9 \qquad B = 2.364$$

$$\gamma \geq 8.9 \qquad B = \frac{21}{\gamma}$$

where all parameters are in SI units.

The two-phase friction factor multiplier relates the SCB frictional pressure gradient to the SPL gradient. The Martinelli/Nelson multiplier assumes that both liquid and

vapor phases are in the turbulent flow regime. The Martinelli/Nelson multiplier and the homogeneous multiplier(used by Kline) can differ by as much as a factor of two at very low pressures and flow qualities. At higher pressures, the Martinelli/Nelson and homogeneous multipliers give comparable values. The Martinelli/Nelson multiplier will replace the homogeneous multiplier in the final code version.

In the FDB region, the inner wall temperature remains at an approximately constant value as shown in figure 3.2. The temperature can be calculated from the Jens and Lottes FDB wall superheat equation, $\Delta T_{sat(OFDB)}$, using

$$T_{wall} = T_{sat} + \Delta T_{sat(OFDB)}$$

where $\Delta T_{sat(OFDB)} = 25 \left[\frac{q''}{10^6}\right]^{0.25} e^{-\left(\frac{p}{62 \times 10^5}\right)}$. As in the PDB regime, the heat transfer coefficient is calculated after-the-fact using the film drop equation.

The end of the FDB flow regime is reached when the bulk temperature, calculated from the steady state energy balance equation,

$$T_{bulk} = T_{b(inlet)} + \frac{4\ q''_{avg}\ D_o}{G\ c_{pf}\ D_i^2}\ \Delta Z\ ,$$

is equal to the local saturation temperature which is calculated at every integration step. This marks the onset of bulk boiling; no calculations are made in the saturated boiling regime.

3.7 Determination of the Flow Regime at the Tube Inlet

The flow regime at the beginning of the tube section is determined by evaluating the ONB and OSNVG correlations at the

inlet. The local saturation temperature and inlet subcooling are calculated from the inlet flow properties. The inner wall temperature is calculated using the liquid film drop equation with the heat transfer coefficient calculated from the SPL heat transfer coefficient equation. If the inner wall temperature calculated from the film drop equation equals or exceeds that value calculated from the ONB correlation, the code starts to calculate the pressure drop using the PDB procedure at the tube inlet. The attached wall void is assumed to increase linearly from zero at the inlet to the value at OSNVG. Similarly, if the calculated inlet subcooling is less than or equal to the value calculated from the OSNVG correlation, the code starts to use the FDB calculation procedure at the tube inlet, ignoring the PDB calculation routine. The attached wall void is assumed to be at the OSNVG value at the tube inlet and linearly decreases to zero at $Z = 0.25\ Z_{sat}$. It is assumed that flow and thermal boundary layers are fully developed and the the flow is fully turbulent. No tube development effects are considered in this model.

3.8 Code Output

After the code calculation has reached the end of the tube or the OBB point, whichever comes first, the calculated pressure drop, fluid and wall temperatures and flow properties along the tube are written to an output file. The basic output format of Kline's code was retained, but modified for easier reading and included output of more calculated flow quantities. During the code validation phase, additional

output files were added to store pressure and pressure drop values for comparison to the experimental data. By saving the pressure drop vs. heat flux and pressure drop vs. length output in ASCII files, plotting of the experimental results and code predictions on the same graph was easily accomplished.

The procedure for code validation and the results will be presented in the next chapter.

4. Results and Discussion

The results and discussion of major computer code modifications to Kline's model are presented in this chapter. Some of the new correlations and solution approaches identified in the literature search were implemented in revised code versions. The resulting pressure drop calculations were then compared with the selected experimental data to see if there was a general improvement in the pressure drop predictions. The following discussion of the modifications to Kline's SR-2F code is done in the logical sequence of flow regimes, taking advantage of the benefit of hindsight. However, the actual modification procedure, shown in the log of code versions assembled(appendix I), occurred in a somewhat different order. First, a couple of minor logic errors in Kline's SR-2F code were corrected. Next, the FDB regime was modified. The PDB regime was then modified, with the changes to the SPL regime worked in somewhere between the two. As a result, there may be a few occasions where more than one modification is illustrated in the figures. After the formulation of 53 code versions, we actually adopted only 12 major modifications to Kline's SR-2F code. These 12 major modifications are described in the following sections.

4.1 Procedure for Evaluating a Particular Code Version

Two types of special plots were used to evaluate the results of a particular code version. The first is a plot of the calculated pressure vs. the tube length. In order to make

this plot, the pressure at each Z location was stored in a data file during the numerical integration process in the code. The second type is an total(overall) pressure drop vs. inner wall heat flux plot. In this situation, the total pressure drop after each run was stored together with the applied heat flux level in a data file. A series of about 20 runs were made at increasing heat flux levels for each overall pressure drop vs. heat flux curve of the selected Dormer and Bergles data. With the calculated results from a particular run(pressure vs. length) or series of runs(total pressure drop vs. heat flux) in a data file, and with the experimental data for the same flow conditions also in a data file, the experimental and calculated files were combined to enable plotting for graphical comparison. The fractional difference between the experimental and calculated values was also included in the resulting data file. In total, over 3200 individual computer code runs were made during this study, yielding predicted pressure drop data for comparison to the experimental data. Because of the magnitude of data to evaluate, data comparison by computer was the most logical choice, although the resulting printout from each run was saved for later review. A small, but representative, portion of the results are presented in this report.

The code modification procedure consisted of running each code modification for the runs of the basic experimental data set and reviewing the pressure drop and fractional difference results. Once an evaluation was made from the computer

generated plots, we proceeded with the next change. The final code version, ASCB53, was checked against both the basic data sets and the additional data sets described in section 2.3 and Appendix D.

4.2 Flow Regimes Represented in the Total Pressure Drop vs. Heat Flux Plots

For the overall pressure drop vs. heat flux plots, the identification of flow regimes along the tube is only partly possible. Each point on the curve represents the pressure drop of one run. Consequently, more than one flow regime may be predicted to occur in the tube for that particular run. The significant regions of this type of plot are (1.) the all SPL region, (2.) the combination of SPL and PDB region, (3.) the all PDB region, (4.) the combination of PDB and FDB region, and (5.) the all FDB region. See figures 4.1 and 4.1.1 for a typical illustration. The regions were marked only on figures presenting the results of the final code version. Region 1 is bounded by q"=0 and the point W, where the ONB point is predicted to occur at the tube exit. Region 2 is bounded by point W and point X, where ONB occurs at the tube inlet. Region 3 is bounded by point X and point Y, where OSNVG occurs at the tube exit. Region 4 is bounded by point Y and point Z, where OSNVG occurs at the tube inlet. Region 5 is bounded by point Z and the heat flux which causes bulk boiling to occur at the tube exit. The last two regions on this type of plot correspond to individual runs having large

FDB regions in the tube and hence large overall pressure drops.

4.3 Single Phase Liquid

The only change made to Kline's model in the SPL regime calculation procedure was the replacement of the Petukhov[23] single-phase liquid heated friction factor equation with the widely-used viscosity ratio power law(VRPL). This equation, also used by Jia and Schrock[10], adjusts the isothermal friction factor to account for variation of fluid viscosity in the boundary layer. The two equations are given as

Petukhov: $$\frac{f}{f_{iso}} = \frac{1}{6}\left[7 - \frac{\mu_{bulk}}{\mu_{wall}}\right]$$

Viscosity Ratio Power Law (VRPL): $$\frac{f}{f_{iso}} = \left[\frac{\mu_{wall}}{\mu_{bulk}}\right]^{n} .$$

Owens and Schrock[5] recommended using a value of n=0.4 for water.

Computer runs using both equations were made using the flow conditions of the selected experimental data. A typical comparison of predicted overall pressure drop curves using the two expressions, along with the experimental data, is shown in figure 4.2. The difference in the use of the two equations appears to be small. Both yield fractional differences from the experimental data generally within ±20%, with the VRPL with n=0.3 giving slightly better results in the FDB regime(i.e. q" greater than about 1.0×10^6 Btu/hrft^2). At first, we were satisfied with Kline's choice of the Petukhov

equation, but the following discovery prompted a search for an alternative heated friction factor equation.

We found that there were some combinations of flow conditions which caused the Petukhov equation to become invalid during the pressure drop calculation procedure. For a few of the high heat flux Dormer and Bergles runs, the ratio μ_{bulk}/μ_{wall} became greater than 7.0, which caused f/f_{iso} to be negative. Because of this problem, it was decided to use the VRPL correlation as a substitute for the Petukhov equation. Both Dormer and Bergles[4] and Owens and Schrock[5] found this form of equation to give results which matched the experimental SPL pressure drop fairly well. However, the optimum value of n given by different researchers varies.

Many values of the exponent n have been suggested. The lower and upper limits seem to be given by Sieder and Tate[22] n=0.14 and Owens and Schrock[5] n=0.4, respectively. Dormer and Bergles[4] correlated their experimental data with a value of n=0.35 as shown in figure 4.3. It was deduced from that figure that for L/D > 32, a better value of the exponent would be 0.3. The selected experimental data listed in section 2.3 all have L/D's $\geq$ 49. Figure 4.2 compares the predicted pressure drop results using n=0.3, 0.4 and the Petukhov equation; all give comparable results. It was found that $f/f_{iso} = (\mu_{wall}/\mu_{bulk})^{0.3}$ is an acceptable choice resulting in slightly better overall pressure drop predictions than the Petukhov equation for most of the selected experimental data

and which avoids giving negative values of the friction factor.

4.4 Onset of Nucleate Boiling

The beginning of the partially developed boiling region is marked by the onset of nucleate boiling. In Kline's work, he assumed that the PDB regime started at point P for simplicity as indicated on figure 3.2. This assumption is not entirely correct because the ONB point is defined by Bergles and Rohsenow[12], Davis and Anderson[13] and others to occur at a superheat $\Delta T_{sat(ONB)}$ different than that of the approximately constant value $\Delta T_{sat(OFDB)}$ occurring in the fully-developed boiling region. The superheat is usually lower although there are conditions where it is larger. Two expressions evaluated for ONB were

Bergles and Rohsenow:

$$\Delta T_{sat(ONB)} = 0.556\left[\frac{q''}{1082\ p^{1.156}}\right]^{0.463}\ p^{0.234}$$

Davis and Anderson:

$$\Delta T_{sat(ONB)} = \frac{B}{r_{max\text{-}active}} + \frac{q''\ r_{max\text{-}active}}{k_f}$$

as previously reviewed.

The pressure drop predictions using the Bergles/Rohsenow equation are plotted together with the pressure drop results of Kline's code in figure 4.4. The calculated pressure drops are only very slightly different. Kline's code using point P effectively delays the start of the PDB regime, in relation to the starting point calculated by the Bergles/Rohsenow

equation, and hence delays the increase in the pressure drop slightly at $q" = 0.7 \times 10^6$ Btu/hrft^2.

Runs using the Davis and Anderson ONB equation were also made for the flow conditions of the basic experimental data set. The first set of runs used the maximum-active cavity radius equal to the critical radius. This assumption should yield approximately the same $\Delta T_{sat(ONB)}$ for water as the empirical Bergles/Rohsenow equation. As shown in figure 4.5, the pressure drop predictions are virtually identical for the O&S vertical tube run. The location of the ONB point along the tube calculated from the Davis/Anderson equation using r_{crit} is within 10% (calculated from $\frac{Z_{ONB(D\&A)} - Z_{ONB(B\&R)}}{Z_{ONB(B\&R)}}$) of the value predicted by the Bergles/Rohsenow equation. This slight difference appears to have little or no effect on the overall pressure drop prediction.

The only apparent difference in the two correlations occurred for the flow conditions of D&B Fig. 28. The overall pressure drop predictions using the two equations are shown in figure 4.6. For the individual code runs with q" between 1.8×10^6 and 2.7×10^6 Btu/hrft^2, a jump in the predicted overall pressure drop curve occurred. This jump, caused by a numerical error problem in the ONB computational scheme for only the smallest tube diameter(1.57 mm) runs, is less pronounced using the Davis/Anderson equation. A possible solution to this peculiarity is suggested in chapter 5. It was surmised that the Davis/Anderson equation resulted in less

of a jump because it is less sensitive to the changing pressure distribution along the tube than the Bergles/Rohsenow equation. $\Delta T_{sat(ONB)}$ calculated from Davis/Anderson is only indirectly a function of the local pressure through the local properties; the Bergles/Rohsenow equation is a direct and strong function of pressure. Thus, the Davis/Anderson equation appears to be an acceptable alternative to the Bergles/Rohsenow equation.

If it is known that the maximum-active cavity radius for the specific tube surface, $r_{max-active}$, is less than the calculated critical radius, r_{crit}, then $r_{max-active}$ should be used in the Davis/Anderson ONB equation. When it is known that $r_{max-active}$ is greater than r_{crit}, then r_{crit} should be used in the ONB equation. The critical cavity radius should be used when no information on the maximum active cavity radius is known.

Based on this study, the Davis/Anderson equation was selected for the prediction of the onset of nucleate boiling. It is also noted that since the correlation was derived using the analytical model of Hsu[14] for bubble nucleation, it is applicable to fluids other than water.

4.5 Partially-Developed Boiling Regime

In the PDB regime, a number of changes to Kline's model were examined. As before, all modifications were checked against runs of the basic experimental data set.

First, a new inner wall temperature profile was defined for the PDB regime. From figure 3.2, the actual (most probable)

inner wall temperature distribution in the PDB regime can be either approximated by (1.)the idealized but rather crude profile extending the SPL profile to point P, becoming the constant FDB value after point P, as used by Kline[3] or (2.)the linear profile from ONB to OSNVG used by Jia and Schrock[10]. The temperature profile only affects the calculation of the pressure drop through μ_{wall}, so that investigation of more refined temperature profiles did not seem necessary. A sensitivity study was conducted to measure the impact of the two profiles; only the frictional pressure drop term was examined because, as shown in figures 3.6 and 3.7, it is the largest pressure drop term in the PDB regime. The predicted frictional pressure drop results using the two temperature profiles are shown in tables 4.1 and 4.2 instead of through computer generated plots because it was difficult to distinguish and properly evaluate differences in the two profiles from pressure drop distribution plots. For the horizontal run D&B Fig. 11c(table 4.1), the maximum difference in pressure drop is only about 2.5% between the two profiles. For the vertical O&S Run 253(table 4.2), the maximum difference is approximately 3%. The difference in predicted pressure drop is small because the change in μ_{wall} between the two profiles is minor despite differences in the two temperature profiles of up to 12 °C.

Although it appears that either profile can be used in the final code version, the linear profile was selected because it results in a slightly higher, more conservative pressure drop

prediction and is closer to the actual temperature profile. It should be noted that the choice of inner wall temperature profile in the PDB regime only strongly affects the calculation of the heat transfer coefficient, which is an after-the-fact calculation in this model anyway, and hence is not critical in accurately predicting the pressure drop. It has only a small effect on the CHF prediction using the Gambill correlation.

The second modification to Kline's PDB model was based on results of a sensitivity study of the attached wall void profile in PDB. Kline assumed a linear attached wall void distribution from point P to OSNVG. The wall void fraction started at zero at point P and linearly increased to the value given by the Rouhani correlation at OSNVG as

$$\alpha_{w(OSNVG)} = \frac{4}{D_i}[1.59 \times 10^{-4}\ p^{-0.237}] \ .$$

A linear profile(shown in Fig. 3.4) is also assumed in this investigation except that the "true" ONB point is used and the Rouhani equation is multiplied by a reduction factor for very small tubes. The modified Rouhani equation is

$$\alpha_{w(OSNVG)} = \frac{4\ K_{red}}{D_i}[1.59 \times 10^{-4}\ p^{-0.237}] \ .$$

The predicted pressure drop results using selected K_{red} of 0.5 and 0.75 are shown in figure 4.7 for a run with the smallest tube diameter. This was the worst case of pressure drop agreement in the PDB regime for our experimental database because of the numerical problem encountered in the SPL-PDB

transition regime, but it illustrates the improvement possible using K_{red}.

In reducing the value of the attached wall void at OSNVG, the attached bubble layer(flow blockage) is also reduced. A reduction of 0.75 appears to yield pressure drop values which are somewhat closer to the experimental data in the all PDB region of the plot($q'' = 1.8 \times 10^6$ to 2.6×10^6 Btu/hrft^2), and more importantly, which match the experimental pressure drop values better than without a reduction factor in the steep portion of the experimental curve($q'' = 2.75 \times 10^6$ to 3×10^6 Btu/hrft^2). This is important because this steep region corresponds to individual runs with large FDB regions and pressure drops which are the most difficult to accurately calculate.

When larger tube diameter runs of the basic experimental data set were examined(using the Rouhani equation with $K_{red} = 0.75$), the predicted pressure drop results tended to be slightly less than the experimental data in the all PDB and steep regions of the overall pressure drop vs. heat flux curves. A variable reduction factor for different tube diameters was formulated as a first attempt to improve the Rouhani equation. It is presented in figure 4.8.

The reduction factor was formulated by estimating the percentage of reduction of the Rouhani equation and hence flow blockage needed to better match the experimental pressure drop data for a particular diameter tube. Figure 4.9, for a tube diameter of 2.39 mm, shows that the non-adjusted pressure drop

curve only needs a slight reduction factor to improve the agreement in the all PDB regime. The pressure drop results using the finalized variable reduction factor are also shown in figure 4.11; K_{red} equals 0.863 for this tube diameter. This reduction factor only slightly reduces the overprediction in the all PDB regime while still maintaining good agreement in the steep FDB region. For the largest D&B test section, tube diameter of 4.58 mm, no reduction of the bubble layer seemed necessary.

This scheme only showed a significant difference for the smallest diameter tube of Fig. 4.7. Use of this variable reduction factor kept the difference between the predicted and experimental pressure drop in the PDB regime to within about ±20% and greatly improved the agreement in the FDB flow regime. Further refinement of this reduction factor is recommended but left for future researchers.

Since the pressure drop calculation is sensitive to the PDB blockage model, the alternate Levy equation for the attached wall void fraction at OSNVG,

$$\alpha_{wall} = \frac{\pi\, Y_{OSNVG}}{6\, D}$$

$$\text{where } Y_{OSNVG} = 0.015\left[\frac{\sigma\, D}{\tau_{wall}}\right]^{0.5}$$

was also examined.

Jia and Schrock[10] claimed good agreement with the experimental data using the Levy equation in combination with

the Hirata et. al.[25] enhanced friction factor in the PDB regime to account for the wall bubble layer.

The Levy equation for the PDB attached wall void was first tried without any friction enhancement, and the pressure drop results were compared to the Rouhani equation(with K_{red}=1.0) as shown in figures 4.10 and 4.11. Overall pressure drop results are shown in figure 4.7. In those three figures, the Levy equation without friction enhancement predicts a smaller wall void than the Rouhani equation, resulting in lesser predicted pressure drops. For example, the attached wall void fraction at OSNVG for figure 4.10 was 53.1 times less than the Rouhani wall void fraction at OSNVG. Even with this large difference, the relatively small effect on the pressure drop predictions in Figs. 4.10 and 4.11 makes it difficult to choose between the two models. However, Hino and Ueda[26] state that the Levy equation underpredicted the actual wall void fractions they measured in their photographic studies. Because of their findings, we elected to use the Rouhani equation for the wall void fraction in the PDB regime.

The final investigation in the PDB regime dealt with the Hirata et. al.[25] isothermal enhanced friction factor used by Jia and Schrock[10] in their research. The equation is(using the Fanning friction factor definition)

$$f_{iso} = 0.0275 \left[\frac{68}{Re} + \frac{e}{D}\right]^{0.25} .$$

These authors suggested that the friction factor in the PDB regime should account for the friction caused by the non-

equilibrium growth of the attached wall bubble layer. On a local level, the growth and collapse of individual bubbles causes an effective roughness greater than that of the wall surface roughness. Kline adjusted the flow for the blockage effect in his model but assumed the bubble layer to produce the same friction as a smooth wall surface. When Hirata's enhanced friction factor was incorporated into the code, along with the Rouhani attached wall void fraction model, the predicted PDB pressure drop was slightly greater than the experimental values for all the runs of the basic experimental data set. Typical results are shown in figures 4.12 and 4.13. Both figures indicate that the friction enhancement proposed by Hirata et. al. should not be used in conjunction with the Rouhani attached wall void equation because it results in poorer agreement with the experimental data.

Since Jia and Schrock report good results with the Levy void fraction profile in combination with the Hirata et. al. bubble layer friction factor, it was decided to try that combination of equations. As shown in figure 4.14, the pressure drop distribution along the tube nearly matches the distribution from the code version using the Rouhani expression with just the smooth wall friction factor assumed. The enhanced Levy pressure drop distribution is within less than 1% of the Rouhani pressure drop distribution in the PDB regime. This result was typical for all the runs of the basic data set. This, however, did not change our decision to continue using the Rouhani model in the PDB regime, because

Hino and Ueda[26] report that the Levy equation predicted values of wall α' much less than the actual observed wall void in their photographic studies.

It is also worth noting that the the Rouhani model, as implemented in our code, does have some enhanced friction compensation in the PDB regime due to the blockage effect of the attached bubble layer. When the mass flux increases due to the blockage effect, the frictional pressure gradient is increased approximately as the square of the mass flux.

4.6 Onset of Significant Net Vapor Generation

The onset of significant net vapor generation is a very convenient and important definition in current SCB models, but it is clearly not a very precisely defined location which experimentalists can easily measure because the interpretation of "significant" has not been quantitatively defined. Nonetheless, accurately predicting the location of the OSNVG point along the tube is paramount in being able to accurately predict the pressure drop in the FDB regime. The initiation of steep pressure drop increases on the overall pressure drop vs. heat flux curves approximately corresponds to the appearance of the OSNVG point at the tube exit. Kline found that if the prediction of the OSNVG point could be made to coincide with this change in slope of the overall pressure drop vs. heat flux curve, the calculated pressure drop agreed satisfactorily with the experimental pressure drop data of Dormer and Bergles. Considerable effort was placed on the method of calculating the OSNVG point.

The two most promising general correlations found in the open literature come from Saha and Zuber[15] and Shah[16].

Saha/Zuber: $\Delta T_{sat(OSNVG)} = 0.0022\left[\frac{q'' D}{k_f}\right]$ for Pe < 70,000

$\Delta T_{sat(OSNVG)} = 153.8\left[\frac{q''}{G\, c_{pf}}\right]$ for Pe > 70,000

Shah: The lesser of:

$$\left[\frac{\Delta T_{sub(Z)}}{\Delta T_{sat(Z)}}\right]_{OSNVG} = 2.0$$

$$\left[\frac{\Delta T_{sub}(Z)}{\Delta T_{sat}(Z)}\right]_{OSNVG} = 6.3 \times 10^4 \, B_o^{1.25}$$

Because Kline showed only partial success in matching the experimental pressure data in the FDB regime with the Saha/Zuber correlation, the Shah correlation was examined as an alternative. Pressure drop distributions along the tube using both correlations are presented in figures 4.15 and 4.16, along with the experimental pressure drop data. The predicted OSNVG locations in the tube for the two code versions are

Run:	Shah	Saha/Zuber
D&B Fig. 11b	0.11529 m	0.094246 m
O&S Run 210	0.32065 m	0.24912 m

As can be seen, the OSNVG point predicted by the Shah correlation is much further downstream of the Saha/Zuber prediction. For figures 4.15 and 4.16, this effectively delayed the start of the FDB regime and caused extreme underprediction of the pressure drop in the FDB regime.

The overall pressure drop vs. heat flux results for the largest tube diameter are shown in figure 4.17. For this case, the Shah correlation gives results which are about as good as the results using the Saha/Zuber correlation. However, the predicted pressure drop results for the rest of the basic experimental data set runs(i.e. smaller tube diameters) indicated the same tendency of the Shah correlation to toward underpredict the experimental pressure drop in the FDB regime as indicated in figures 4.15 and 4.16.

Before abandoning the Shah correlation in favor of the Saha/Zuber correlation, it was decided to incorporate the heat transfer correlations given by Shah for the PDB and FDB regimes, hoping that it would improve the afore mentioned results. The results shown in figures 4.18 and 4.19 are essentially the same as in figures 4.15 and 4.16. The heat transfer correlation only affects the wall temperature profile, which has a very minor effect on the predicted pressure drop, as mentioned in section 4.5.

At that time, it was decided to continue using the Saha/Zuber correlation for OSNVG, but investigate the possibility of modifying the correlation for greater accuracy over the range of flow conditions of the selected experimental data set. Figure 4.20 is one of the worst of a few poor cases in Kline's M.S. Thesis[3] which show large differences between the predicted and experimental pressure drops. Our attempt to modify the Saha/Zuber correlation focused on inclusion of some type of diameter or heat flux effect.

Jia and Schrock and others speculated that the Saha/Zuber OSNVG correlation could be improved if an adjustment for small diameter tubes were included. As shown in figure 4.21, it appears that for tube diameters 9 mm and below, the Saha/Zuber correlation would be better represented if the high Peclet number part of the correlation(i.e. Pe > 70,000), represented by the solid horizontal line, were reduced from a subcool Stanton number, $\widetilde{St}$, of 0.0065 to 0.0057. This represents a reduction in the horizontal part of the correlation by 12.3%.

In a similar analysis, Kline estimated the OSNVG points for a number of Dormer and Bergles experimental runs and plotted them along with the Saha/Zuber correlation as shown in figure 4.22. Kline assumed that the point where the slope of the total pressure drop vs. heat flux curves started to increase rapidly approximately coincided with the appearance of the OSNVG point in the tube(at the exit). Kline estimated this point from the overall pressure drop vs. heat flux curves and plotted the corresponding OSNVG conditions against the Saha/Zuber[15] correlation. A few of these estimates are shown on Fig. 4.22. It appeared from Kline's work that some type of reduction(for small diameter tubes) of the subcool Stanton number, which defines the high Peclet number part of the correlation(Pe > 70,000), could improve the Saha/Zuber correlation.

Initially, a sensitivity study for the amount of reduction of the subcool Stanton number was undertaken. The constant $\widetilde{St}$ value at the OSNVG condition for Pe > 70,000 was reduced by 10% and 20% for all tube diameters(i.e. St = 0.0059, 0.0052, respectively). These two conditions were tested for all the runs of the basic experimental data set. Typical results are shown in figure 4.23. After reviewing all of the predicted pressure drop results, it was estimated that reduction of $\widetilde{St}$ for Pe > 70,000 of somewhere in the neighborhood of 5% to 10% would be the best overall compromise choice for all the tube diameters, heat fluxes and flow conditions of the comparison experimental data.

However, rather than settling on a single reduction factor, we looked for a modification which would better match each curve of the selected experimental data set. The parameters heat flux, tube diameter, temperature and fluid velocity were each studied for the Dormer and Bergles data points plotted in figure 4.22. It appeared that with only a few exceptions, the data points with approximately the same heat flux fell on straight lines as indicated for one heat flux(approximately 9.0×10^6 MW/m^2) in figure 4.22. The modification equation shown on figure 4.24 yielded the best improvements, of anything we examined, in the pressure drop prediction in the FDB regime. If the subcool Stanton number calculated by the modified equation in the high Pe region dropped below the -40% limit, $\tilde{St}$ would take on the value at that limit(i.e. 0.0039).

A typical comparison of the modified and unmodified Saha/Zuber correlations is shown in figure 4.20. The results were encouraging enough that this modification was incorporated into the code. Other predicted pressure drop results calculated using this modification are shown in figures 4.25 thru 4.30(for final code version ASCB53). It can be seen that the pressure drop results in the FDB regime appear to match the experimental data quite well. Figures 4.25 and 4.26 show a slight improvement in the prediction using the modified correlation over that of the unmodified Saha/Zuber correlation(used by Kline's best code version SR-2F).

Although not every run of the experimental data set showed outstanding agreement with the experimental pressure drop data, the modified Saha/Zuber correlation provided either a more accurate or somewhat more conservative(i.e. higher total pressure drop) estimate of the OSNVG point than the unmodified correlation for all runs except that in figure 4.27. It was decided that this modification to the Saha/Zuber correlation would be used as an interim adjustment until more research can be done.

4.7 Fully-Developed Boiling Regime

Accurate prediction of the pressure drop in the FDB regime is made difficult by non-equilibrium phenomena affecting the flow quality, void fraction, and phase velocities. A combination of changes were made to Kline's FDB model in order to formulate a code version which predicted pressure drop profiles that better matched the steep experimental profiles in the FDB regime.

Kline assumed a constant attached wall bubble layer(vapor void) thickness at the OSNVG value in the entire FDB regime. (However, due to a coding error, it actually grew slowly.) He did not investigate the effect of using any other types of profiles. Since vapor bubbles leave the wall surface in the FDB regime, it would be reasonable to conclude that no attached wall vapor void should exist after some transition region. The vapor void that was previously confined to the wall in the PDB regime becomes incorporated into the flow void fraction described by the α' equation. The use of a function

to represent the transition between the PDB wall void and the FDB flow void was investigated to see if better agreement with the experimental data could be achieved.

A sensitivity study of various attached wall void profiles in the FDB regime was performed. Candidate profiles are shown in figure 3.4. In summary, a constant profile, three linearly decreasing profiles and the no void profile were evaluated with runs from the basic experimental data set. The termination points for the constant void profile #1 and linearly decreasing void profiles #2, #3, #4 , and no void profile #5 can be simply described by the equation

$$Z_{termination} = Z_{OSNVG} + \frac{1}{N}(Z_{OBB} - Z_{OSNVG})$$

where N equals 0, 1 , 2 , 4, or ∞ respectively.

Typical pressure drop distribution results along the tube using the different profiles are given in figures 4.31 and 4.32 for horizontal and vertical flows conditions. The pressure drop distribution results of the linearly decreasing profile corresponding to N=2(profile #3) and the no void profile(#5) were not plotted on figure 4.32(O&S Run 253) for clarity. These figures show that the less the amount of wall void in the FDB regime, the greater the FDB pressure drop.

It was difficult to choose only one particular profile because, in some cases, the best profile would be different for each run depending on the tube diameter and flow conditions. However, the constant profile(#1) caused an underprediction of the total pressure drop of almost 35% from

the experimental data for the smallest diameter tube(i.e. D&B Fig. 28), so it was eliminated from consideration. The N=4 profile(#4) provided a FDB pressure drop distribution which almost matched the experimental data in figure 4.32 and resulted in a conservative overprediction in figure 4.31. The predicted pressure drop results from runs using the conditions of the rest of the basic experimental data set indicated that the N=4(#4) profile was a reasonable first approximation.

Because the N=4(#4) blockage profile gave adequate pressure drop results and because it is a reasonable transition model from PDB to FDB, it was selected for use in the final code version. However, this profile is not optimized so further study is needed. No other justification for its use can be given because, so far, we have found no information in the literature on how to model this attached wall void transition.

As recognized by Kline, and as seen in figures 3.6 and 3.7, the acceleration pressure drop term is the dominant term in the FDB regime. Thus, this term needs to be accurately predicted in the code in order to match the steep pressure drops of the experimental data in the FDB regime. It was discovered that the separated flow acceleration pressure gradient term, $\left[\frac{dP}{dZ}\right]_{accel}$, was extremely sensitive to the void fraction in FDB, more so than the flow quality. Sudden increases in the non-equilibrium void fraction near the tube exit for some of the calculated runs triggered large acceleration pressure gradients which resulted in large

overpredictions of the overall pressure drop as shown in figure 4.33. The void fraction and flow quality calculated at the tube exit for the run of $q" = 2.68 \times 10^6$ Btu/hrft^2 using $C_o = 1.13$ were 0.88 and 0.0091, respectively. We speculated that the void fraction value calculated may be out of the range of the Zuber et. al.[9] equation. However, since Kline found reasonable success with the Zuber et. al. equation for describing the non-equilibrium void fraction, it was decided to continue using that expression in the final code version, but modify the critical parameters in that equation in order to obtain better pressure drop predictions.

Probably the most crucial parameter in the non-equilibrium void fraction equation is the distribution parameter C_o. This value varies depending upon the two-phase flow pattern occurring in the tube. Kline assumed this value to be equal to 1.13. It is assumed that Kline chose this value because Kroeger and Zuber[8] recommend, that in the absence of experimental data on void fraction profiles, a value of $C_o = 1.13$, corresponding to bubbly flow, should be utilized. (The photographic studies of Hino and Ueda[26] confirm bubbly flow to exist in the FDB regime.) However, Collier[24] recommends, that for tube diameters less than 5 cm, and reduced pressures $P_{red} < 0.5$, C_o equal 1.2 for bubbly-turbulent flow. In addition, the original authors, Zuber et. al.[9], advise the use of $C_o = 1.25$ for circular ducts if no experimental data exists. Because such speculation exists, different values of C_o were compared in the code.

First, a sensitivity study was performed on the distribution parameter. Values of C_o equal to 1.13 and 1.3 were utilized in the computer code with typical results shown in figures 4.33 and 4.34. The void fractions calculated at the tube exit for the run with q" = 2.68 x 10^6 Btu/hrft^2 of figure 4.33 were

C_o	α'
1.13	0.88
1.3	0.36

This very large difference shows the sensitivity of the code to C_o and to the void fraction at high heat fluxes.

These figures show that the slope of the steep portion of the overall pressure drop vs. heat flux curves can be controlled by the choice of C_o. Note that the results shown in figures 4.33 and 4.34 do not use the modified OSNVG correlation as discussed previously. However, if the OSNVG points were properly predicted, then adjustment of C_o is all that would be needed to alter the slope of the overall pressure drop vs. heat flux curve to better match the curve of the experimental pressure drop data. It was difficult, as expected, to select a single value of C_o which resulted in the predicted pressure drop matching the experimental data well for all the runs of the experimental data set. Figure 4.34 shows that good agreement would be obtained for that run with $1.13 < C_o < 1.3$. The choice of C_o seemed to be particularly sensitive to the tube diameter. Figure 4.33(D = 2.39 mm) shows a greater difference from the experimental data than

does figure 4.34(D = 4.58 mm). This suggests that C_o may have a functional dependence with tube diameter. This possibility is left for investigation by future researchers.

Another possible way to estimate the distribution parameter was suggested by Jia and Schrock[10]. They used the Hancox and Nicoll[11] equation to calculate C_o. Hancox and Nicoll proposed an equation for C_o that is a function of the void fraction:

$$C_o = \left[\frac{1-\exp(-C_{01}\ \alpha)}{1-\exp(-C_{01})}\right](1+C_{02}) - C_{02}\ \alpha\ .$$

Hancox and Nicoll reasoned that C_o should vary from zero at zero void fraction to unity at a void fraction of 100%, with values greater than 1.0 in between. This seems to be what other authors have proposed as well. However, when included in code version ASCB48, the correlation produced somewhat poorer pressure drop predictions as shown in figures 4.35 and 4.36. Pressure drop predictions using C_o = 1.25 are also shown in these figures. The calculated pressure drop distribution along the tube using the Hancox/Nicoll equation for C_o is less than the experimental values. Pressure drop results using the conditions of the rest of the basic experimental data set were similar; all underpredicted the experimental data, in some cases by as much as 20%. This underprediction was a result of the Hancox/Nicoll equation predicting high values of C_o. For figure 4.33(at q" of 8.45 MW/m^2 and exit pressure of 2.07 x 10^6 Pa), C_o peaked around 1.8 at Z = 0.112 m and decreased to about 1.7 at the tube exit(Z = 0.125 m). These values of C_o were

typical for the relatively low pressures of our selected experimental data set It appeared that these values were much too high, because Zuber and Findlay[27] state that C_o should range from 1.0 to 1.5 for fully established flow profiles. (It was discovered that for higher pressures(over 28.0 x 10^5 Pa), the Hancox/Nicoll equation seemed to give more reasonable values of C_o.)

Since figures 4.35 and 4.36 show reasonable success at matching the code predicted and experimental pressure drop profiles along the tube with C_o = 1.25, and because the Hancox/Nicoll equation showed little promise for improving the pressure drop predictions in the FDB regime at pressures lower than 27.6 x 10^5 Pa, the constant value of C_o equal to 1.25 was used in the final code version as the best compromise over the range of conditions of the basic experimental data set.

Other parameters which affect the Zuber et. al. void fraction equation are the non-equilibrium flow quality, non-dimensional temperature profile(thru the Kroeger/Zuber flow quality expression), and the drift flux velocity. Expressions other than those investigated by Kline were evaluated to see if the prediction of the void fraction α', and hence the FDB pressure drop, could be improved.

An expression for the non-equilibrium flow quality is given by Levy as

$$x'(Z) = x(Z) - x_{OSNVG} \exp\left[\frac{x(Z)}{x_{OSNVG}} - 1\right] .$$

Kline evaluated the use of this equation in the computer code but neglected to combine it with the Zuber et. al. void fraction equation and some of his other code improvements. Because the equations for these parameters are so complex, the result of combining the various expressions is very difficult to predict beforehand. Changes to the computer code were made to include the Levy equation; the results are shown in figure 4.37. When it was discovered that the Levy equation dramatically overpredicted the pressure drop in the FDB regime, no further comparisons to the experimental data were attempted. It was decided to continue using the Kroeger/Zuber flow quality expression since the Levy equation gave disappointing results.

In presenting their correlation for the non-equilibrium flow quality, Kroeger and Zuber[8] suggest using either

$T^* = 1 - \exp[-Z^+]$ or

$T^* = \tanh[Z^+]$

to describe the non-dimensional temperature parameter T*. Kline elected to use the equation of the hyperbolic tangent form but never addressed using the other equation. The exponential form was substituted into the computer code yielding the results shown in figure 4.38. The exponential form of T* overpredicts the FDB pressure drop. No other runs were made after the discovery of such poor results. The results indicate that only the hyperbolic tangent form of T* should be used in the final code version of this investigation to insure agreement with the experimental data.

The last parameter investigated in the Zuber et. al. void fraction equation was the drift flux velocity $\bar{u}_{gj}$. Kline used the expression given by Kroeger and Zuber[8]

$$\bar{u}_{gj} = 1.41 \left[\frac{g\ \sigma\ (\rho_f - \rho_g)}{\rho_f^2}\right]^{0.25} \quad \text{for vertical tube flows.}$$

This term in the α' equation was inadvertently left in Kline's model for horizontal flows even though it should have been set to zero; however, the term made a negligibly small contribution in all cases he examined. (Unal[28] and Jia and Schrock[10] state that for horizontal bubbly flows, $\bar{u}_{gj}$ should be equal to zero.) To check the significance of a zero $\bar{u}_{gj}$ term for horizontal flows, it was set to zero for the horizontal tube run D&B Fig. 11a. The pressure drop distribution along the tube was almost identical to the case where the term was non-zero. This was due to the fact that $\frac{\bar{u}_{gj}}{u_{f,inlet}}$ was much less than C_o in the right-hand side term in the denominator of the α' equation. To be physically correct, the code was changed to set $\bar{u}_{gj}$ to zero for all horizontal tube runs.

Although little or no effect on the pressure drop predictions was expected, the effect of changing the leading coefficient on the $\bar{u}_{gj}$ equation was also studied. The original authors of the void fraction equation, Zuber et. al.[9], suggest the use of

$$\bar{u}_{gj} = 1.18 \left[\frac{g\ \sigma\ (\rho_f - \rho_g)}{\rho_f^2}\right]^{0.25}.$$

It was not until a later paper in which Kroeger and Zuber[8] suggest using the same equation except with a leading constant of 1.41. Dix also suggested the use of the same equation for vertically oriented tubes, but with a leading coefficient of 2.9. It was decided to check the sensitivity of the $\overline{u}_{gj}$ term in the void fraction equation by comparing the Kroeger/Zuber and Dix coefficients. Runs using each equation were made using the conditions of the vertical experimental data runs of the basic data set. Typical predicted pressure drop distributions are shown in figure 4.39; they appear to be insensitive to the choice of the coefficient. It was decided to continue using the Kroeger/Zuber equation since it was suggested by one of the same authors who formulated the void fraction equation being used in the final code version.

The final change to Kline's FDB model was to substitute the Martinelli and Nelson[18] two-phase friction factor multiplier for the homogeneous multiplier used by Kline. Although the use of the homogeneous multiplier was not entirely correct, it was a convenient and simple equation available from the literature. The Martinelli/Nelson equation is a more consistent choice for use in the frictional pressure gradient of the separated flow model. The calculated Martinelli/Nelson multiplier at the tube exit for the run shown in figure 4.40 differs only by -6% from the homogeneous multiplier, leading to a difference in the total frictional pressure drop of about the same amount. The resulting change in the total pressure drop using the two multipliers, shown in figure 4.40, is small

because the acceleration pressure drop was found to be the dominant term in the FDB regime. The very slight difference in pressure drop distributions between the two multipliers is best seen on the fractional difference plot of figure 4.40. It appears that either expression for the multiplier is satisfactory. However, the Martinelli/Nelson multiplier was chosen for use in the final code because it is the more correct separated flow two-phase friction factor multiplier.

4.8 Limitations of the Final Code Version(ASCB53)

The final code version is a selection of the best equations, correlations and changes examined in this investigation. For the most part, it satisfies our goals set at the beginning of this investigation to formulate a code to calculate pressure drops which agree with the selected experimental data sets to ±20%. However, the current calculation procedure exhibited a problem when changes in the non-equilibrium void fraction and flow quality were extremely large with each integration step (even though a minimum of 1000 steps were used in these runs). These large increases caused corresponding overprediction of the total pressure drop as seen in figures 4.26 and 4.41 at very high heat fluxes.

Although the problem was partly solved by modifying the distribution parameter in the Zuber et. al. void fraction equation, the maximum error due to this anomaly still exceeded +20% for a few runs. Figures 4.41 exhibits this peculiar behavior even though the predicted OSNVG point seems to correspond to the start of the steep slope of the experimental

data curve. Figure 4.42 shows the same trends for specific heat fluxes in the pressure drop vs. tube length format. In this case, the calculated OSNVG point seems to match the point where the experimental data curve starts to turn downward. It was initially thought that a limit on the exit subcooling could eliminate the cases where this was a problem, because the large increases in void fraction and flow quality seemed to occur for runs where the flow was calculated to be near the OBB point. However, this was not successful because there was no definite trend relating exit subcooling and the amount of pressure drop overprediction.

Closer investigation revealed that all the runs with large overprediction of the pressure drop had quite large acceleration pressure gradient terms(due to large calculated void fractions). For figures 4.26 and 4.41(the worst overprediction cases), the calculated acceleration gradients at the tube exit were

Fig. No.	Run Conditions	q" (Btu/hrft^2)	$(dP/dZ)_{accel}$
4.26	D&B Fig. 24	3.93×10^6	-6.5813×10^8 Pa/m
4.41	D&B Fig. 17	2.68×10^6	-1.2757×10^7 Pa/m

It appeared that for all the runs with fractional differences between the predicted and experimental pressure drops of within +20%, the absolute value of the pressure gradients never exceeded 3.0×10^6 Pa/m. This limit was selected so that the code would have a maximum upper deviation in the pressure drop prediction of +20%. If the calculated acceleration pressure gradient exceeds 3.0×10^6 Pa/m, the code will print a

warning to the user that the calculated pressure drop may overpredict the actual pressure drop beyond that Z location. The code still continues its calculations to the tube exit(or to the OBB point).

The only other limitation of the code occurred for some vertical tube runs with flow mass velocities less than about 2500 kg/m^2s(512 lb/ft^2s). In these cases, the pressure drops in the SPL and PDB regimes were overpredicted despite the overall pressure drop being very close to the experimental value as seen in figures 4.43 and 4.44(the only exception being figure 4.45). It was discovered that if the gravity term was deliberately set to zero in these runs, the predicted pressure drop in the SPL and PDB regimes matched the experimental data to within 1% error, but the overall pressure drop would be extremely underpredicted. This was especially puzzling because Jia and Schrock showed good agreement for the conditions of the runs shown of figures 4.43 and 4.44 using almost the same calculation procedure. Since we could not explain those discrepancies, a lower user input limit of 2500 kg/m^2s was set in order to obtain pressure drop predictions with uncertainties of no more than about $\pm$20%. The cause and solution of this problem is left for future researchers.

Some additional features were added to make the computer code more useful for designers. This work included adding approximations for one-sided heating, and adding a CHF(critical heat flux) correlation following review of several subcooled boiling CHF correlations in the literature.

4.9 One-Sided Heating Approximations

The model and correlations used in this code have assumed uniform axial and circumferential applied heat flux. However, many applications exist in the physical realm for one-sided heating. Two of the most common one-sided heat flux profiles used in modeling the actual situation are the circumferentially uniform heat flux on one half side and the cosine distribution on one half side. Under the effects of one-sided heating, the locations of average ONB, OSNVG, and OBB points along the tube are significantly changed from that of the circumferentially uniform heating case, and affect the pressure drop differently. The present correlations were modified by multiplying them by constant adjustment factors based on physical reasoning. These adjustments are presented in appendix E. The adjustment factors are only a "best guess" and must be verified against one-sided heating experimental pressure drop data, when such data becomes readily available.

4.10 Prediction of Critical Heat Fluxes

In the design of SCB cooling systems, the calculation of the critical heat flux(CHF) is as important as accurate prediction of the pressure drop. The process of comparing various CHF correlations to the experimental data was performed by Professor M.A. Hoffman. Hoffman compared many subcooled boiling CHF correlations in the literature to the CHF correlation of Gambill[30], which is based on a very extensive experimental database. He finally concluded that the Gambill CHF correlation was the best general correlation

to use because it had the broadest range of applicability with about the same uncertainty as many other more restrictive correlations. It was also found to vary in a similar way, with $u\Delta T_{sub}$, to the Rousar[31] correlation, which is valid for high $u\Delta T_{sub}$ approximately greater than 850 m°C/s. The Rousar correlation was based on a broad set of experimental data from the Aerojet Corporation. At higher $u\Delta T_{sub}$, the Gambill correlation constitutes a somewhat more conservative subcooled boiling CHF prediction than the Rousar correlation. For design purposes, Hoffman recommends that a minimum CHF safety factor of 2.0 should be applied to the Gambill correlation.

Refer to appendix F for further discussion of the Gambill CHF correlation.

5. Conclusions and Recommendations

Significant progress has been made to develop a reliable computer code to numerically integrate the SCB pressure drop equations for small diameter tubes under high heat flux conditions. Such a code is necessary in the design of SCB cooling systems because of the large pressure gradients and changing fluid properties occurring along the tube length. The current computer code is an extension of Kline's work performed in 1985. The calculation method uses the separated flow model developed for two-phase flow, but adapted to the non-equilibrium conditions of SCB using correlations for the two-phase non-equilibrium flow properties recommended by many authors. Kline's best code version was improved and computed results were checked against a wide range of experimental data. The important findings and recommendations for future research are now presented.

The computer code results indicated that the frictional pressure drop term dominated in the SPL and PDB flow regimes for both horizontal and vertical tube orientations. The acceleration pressure drop term dominated in the FDB regime for both orientations. The gravity pressure drop term was only significant in the SPL and PDB regimes, but still was less than one fourth of the frictional pressure drop. Kline's conclusion that the gravity pressure drop term is dominant in the SPL and PDB regimes is only applicable at low mass velocities(i.e. less than approximately 1500 kg/m^2s).

The heated SPL friction factor is important in the calculation of the pressure drop because it is also needed in the PDB and FDB pressure drop equations. The Petukhov correlation used by Kline was replaced with that of the viscosity-ratio power law equation, with an exponent of 0.3, because of the limitations incurred with the use of the Petukhov equation. This small change resulted in slightly better pressure drop predictions in the SPL and PDB flow regimes without degrading the agreement in the FDB regime.

The onset of nucleate boiling, as well as the onset of significant net vapor generation, need to be accurately predicted if the calculated pressure drop is to match the experimental data well. It was found that the Bergles/Rohsenow ONB correlation, and the Davis/Anderson ONB correlation using the critical radius value, gave almost the same pressure drop results. The Davis/Anderson correlation was selected because it was less sensitive to changes in the local pressure and may be used for coolants other than water with some modification. The Saha/Zuber OSNVG correlation was selected and modified slightly for heat flux dependance at high Peclet numbers to yield better overall agreement between the predicted and experimental pressure drop data.

Modeling of the attached wall bubble layer in the PDB and FDB regimes was also found to be very important. The type of profile chosen was most sensitive for the smallest diameter tubes. A linear wall void profile in PDB increasing from zero at ONB to the value given by the Rouhani equation at

OSNVG(modified for small tubes), seemed to yield good results overall. A linear decreasing profile from OSNVG to a point Z = $Z_{OSNVG} + \frac{1}{N}(Z_{OBB} - Z_{OSNVG})$, where N=4, seemed to work well. However, no justification can be given for the choice of N=4, since no information has been found in the literature to indicate how to model the bubble layer in the PDB-FDB transition region.

In the PDB regime, the attached bubble layer may cause the effective friction factor to be greater than the smooth wall friction factor. However, it was found that no enhancement of the PDB friction pressure gradient due to the PDB bubble layer roughness should be employed when the Rouhani bubble layer profile is used. In the final code version, the only enhancement to the PDB friction pressure gradient is that of the blockage effect on the mass flux.

The non-equilibrium void fraction is very important in the prediction of the pressure drop in the FDB regime. Sharp increases in the void fraction at high heat fluxes for a few runs caused large overprediction of the pressure drop. This problem was partly solved by selection of a better distribution parameter C_o. The constant value of 1.25 chosen for bubbly-turbulent flow resulted in the best agreement to the runs of our selected experimental data set.

Two limits were applied to the final code version(ASCB53) in order to keep the uncertainty range of the calculated the pressure drop along the tube to about ±20%. The first

requires that the mass flux input by the user be greater than 2500 kg/m^{2}s. For G < 2500 kg/m^{2}s, the SPL and PDB pressure drops may be greatly overpredicted. The second is a limit on the size of the acceleration pressure gradient calculated at any Z location along the tube. It was found that in order to keep the uncertainty of the pressure drop predictions to about ±20%, the acceleration pressure gradient must be less than or equal to about 3.0 x 10^6 Pa/m. A large increase in the non-equilibrium void fraction at low subcoolings is the major cause of the large acceleration gradients. When the code calculates acceleration pressure gradients above 3.0 x 10^6 Pa/m, a warning is printed on the hardcopy output that the calculated pressure drop may overpredict the actual pressure drop beyond that Z location.

It is estimated that Kline's uncertainty in his pressure drop predictions was about -30% to +45%, with deviations of pathological cases to as much as +90%.

Our final code version has been validated to give agreement with the selected experimental database for water in smooth tubes to about ±20% over the ranges

G	2500 - 10,000 kg/m^{2}s
P_{in}	2 x 10^5 - 28 x 10^5 Pa (29 - 406 psia)
q''_{inner}	0 - 12.2 MW/m^2 (0 - 3.87 x 10^6 Btu/hrft^2)
ΔT_{sub-in}	10 - 200 °C (18 - 360 °F)
L/D	49 - 127
D_i	1.5 - 4.6 mm (0.0591 - 0.1811 in)**

$$\left[\frac{dP}{dZ}\right]_{accel} \leq 3.0 \times 10^6 \text{ Pa/m (132.62 psia/ft)}$$

for vertical and horizontal tube orientations.

**We also ran the code using the conditions of two Reynolds[6] experimental data runs(inner tube diameter equal to 9.5 mm). The agreement was only fair as shown in appendix H. Kline showed good agreement using SR-2F, but he misplotted the experimental data points on for those figures. He had mistakenly plotted the experimental pressure at locations along the tube length that were all 1/2 foot off. When corrected, the plotted results of his best code SR-2F also showed only fair agreement with the experimental data. As a result, we cannot recommend using the code for inner diameters above 4.6 mm until it is verified against more large tube experimental data.

Much has been accomplished in this study to produce a well validated computer code. However, there were areas which could not be addressed thoroughly because of the time constraints of this research program. They are left for future researchers.

Because the prediction of the onset of significant net vapor generation is so crucial to accurate prediction of the FDB pressure drop, a more extensive modification to the Saha/Zuber correlation for small diameter tubes is needed to further improve the code. It is suggested that the slope of the modified correlation for Pe > 70,000 be made a function of both heat flux and diameter.

An extensive literature search for attached wall void(bubble layer) models for the PDB regime and the PDB-FDB transition regime should be undertaken. In the PDB regime, a parabolic bubble layer growth profile may help to reduce the jump in the predicted overall pressure drop curve caused by a peculiarity in the numerical integration scheme occurring only for the smallest tube diameter runs. In the FDB regime, a linearly transition profile decreasing to zero at 1/4 the distance between the OSNVG and OBB points may not be optimal. The termination point may possibly be a function of tube diameter.

The distribution parameter C_o in the Zuber et. al. void fraction equation needs to be optimized to better match the steep slope portion of the overall pressure drop vs. heat flux curves for all of the selected Dormer and Bergles data. The functional dependance of C_o on void fraction should be explored in more depth.

Investigation into the cause and solution for why the predicted pressure drop in the SPL and PDB regimes is larger than the experimental data for mass velocities less than 2500 kg/m^2s is also needed.

In order to make the code more useful in design, the non-equilibrium void fraction expression needs to be modified to allow calculation at tube orientations other than just horizontal or vertical. The modification will only effect the drift flux velocity term, which is a small term in the

comparison to other terms in the void fraction equation in all cases examined.

Other work which would extend the usefulness of such a code would include

(1.) validating the code for pressures greater than 2.8 MPa(400 psia) and heat fluxes greater than 12.2 MW/m^2(3.87 x 10^6 $Btu/hrft^2$).

(2.) properly verifying the presented one-sided heating approximations against experimental data.

(3.) extending the correlations to working fluids other than water.

(4.) extending the code model to rectangular coolant passages.

Tables and Figures

Effect of Wall temperature profiles						
Comparison in PDB regime only						
	f/f iso	f/f iso		P fric	P fric	
Z	using Twi1	using Twi2	% change	using Twi1	using Twi2	% change
0.00000	0.5503	0.5503	0.00	0.00	0.00	0.00
0.00747	0.6495	0.6340	-2.39	974.64	950.38	-2.49
0.01494	0.6618	0.6473	-2.19	1986.10	1938.70	-2.39
0.02241	0.6738	0.6603	-1.99	3036.20	2966.90	-2.28
0.02988	0.6855	0.6731	-1.80	4126.90	4036.80	-2.18
0.03735	0.6969	0.6856	-1.61	5260.30	5150.90	-2.08
0.04482	0.7080	0.6979	-1.42	6438.80	6311.40	-1.98
0.05229	0.7189	0.7099	-1.24	7664.90	7521.10	-1.88
0.05976	0.7295	0.7218	-1.06	8941.60	8782.80	-1.78
0.06723	0.7400	0.7334	-0.89	10272.00	10100.00	-1.67
0.07470	0.7502	0.7448	-0.71	11659.00	11476.00	-1.57
0.08217	0.7602	0.7560	-0.54	13108.00	12915.00	-1.47
0.08964	0.7700	0.7671	-0.38	14621.00	14421.00	-1.37
0.09711	0.7797	0.7780	-0.22	16205.00	16000.00	-1.27
0.10458	0.7892	0.7886	-0.07	17865.00	17656.00	-1.17
0.10707	0.7923	0.7922	-0.02	18435.00	18226.00	-1.13

Twi1: Linear Temperature Profile from ONB to OSNVG(ASCB47)
Twi2: Idealized Temperature Profile Used By Kline(ASCB51)

Table 4.1 Data from D&B Fig. 11c Comparing Effect of Inner Wall Temperature Profiles in PDB on Pressure Drop Predictions

Effect of Wall temperature profiles						
Comparison in SPL & PDB regime only						
	f/f iso	f/f iso		P fric(P_1)	P fric(P_2)	
Z	using Twi1	using Twi2	% change	using Twi1	using Twi2	% change
0.00000	0.7471	0.7471	0.00	0.00	0.00	0.00
0.02286	0.7640	0.7640	0.00	886.51	886.51	0.00
0.04572	0.7794	0.7794	0.00	1781.70	1781.70	0.00
0.06858	0.7933	0.7933	0.00	2684.80	2684.80	0.00
0.09144	0.8060	0.8060	0.00	3595.30	3595.30	0.00
0.09060	0.8099	0.8099	0.00	3900.40	3900.40	0.00
0.10668	0.8164	0.8137	-0.33	4206.90	4206.20	-0.02
0.12954	0.8312	0.8242	-0.85	5143.10	5128.00	-0.29
0.15240	0.8453	0.8335	-1.39	6105.40	6055.90	-0.81
0.17526	0.8585	0.8418	-1.95	7094.60	6989.50	-1.48
0.19812	0.8710	0.8574	-1.57	8111.20	7941.10	-2.10
0.22098	0.8829	0.8704	-1.41	9156.10	8925.20	-2.52
0.24384	0.8940	0.8829	-1.25	10230.00	9942.80	-2.81
0.26670	0.8980	0.8947	-0.37	11392.00	11062.00	-2.90
0.28956	0.9069	0.9059	-0.11	12614.00	12262.00	-2.79
0.30480	0.9126	0.9131	0.06	13454.00	13101.00	-2.62

Twi1: Linear Temperature Profile from ONB to OSNVG(ASCB47)
Twi2: Idealized Temperature Profile Used By Kline(ASCB51)

Table 4.2 Data from O&S Run 253 Comparing Effect of Inner Wall Temperature Profiles in PDB on Pressure Drop Predictions

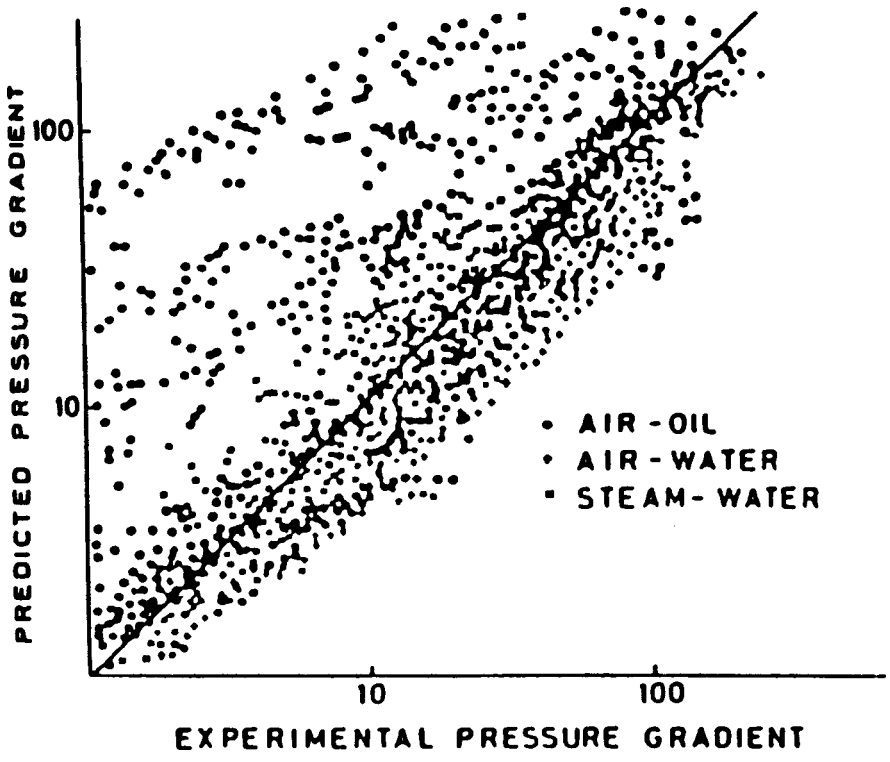

No Units Stated in Author's Paper

Figure 1.1 Hewitt Comparison of One Empirical SCB Pressure Drop Correlation with Experimental Data [Ref. 1]

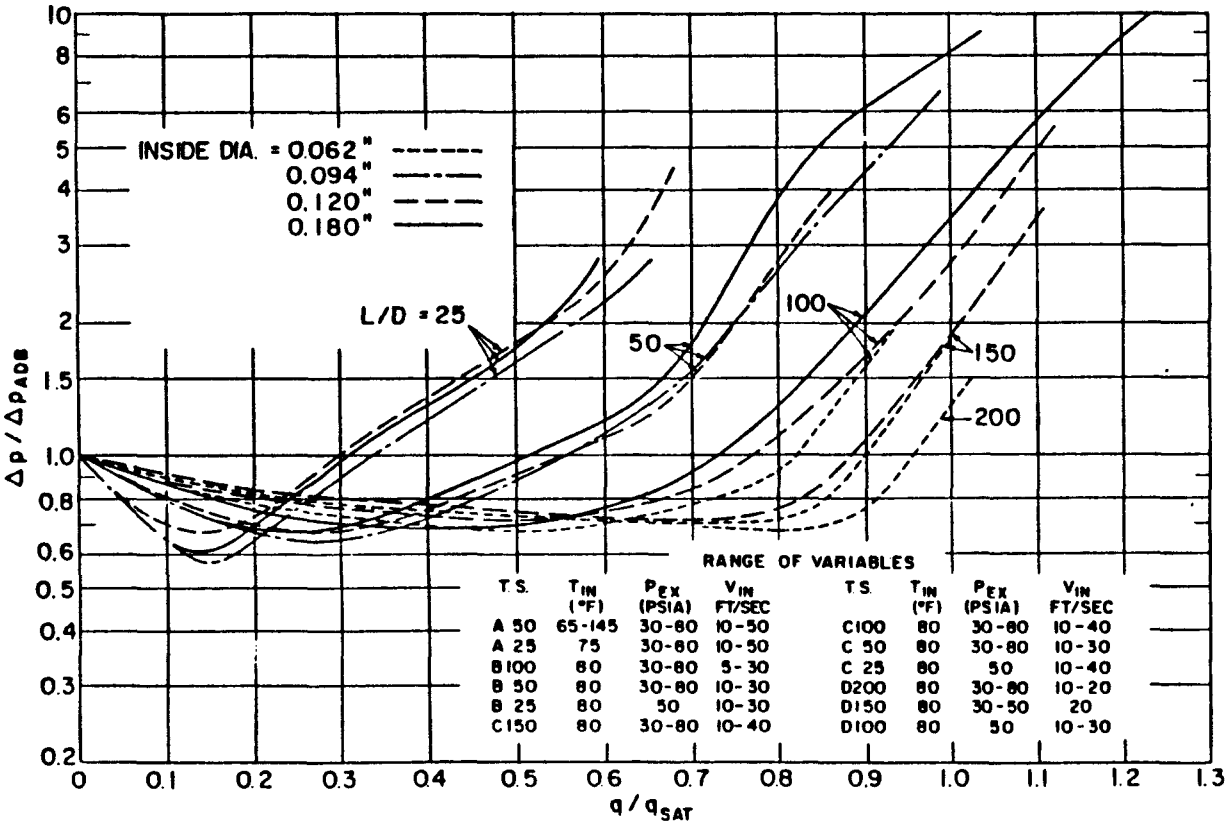

Figure 2.1 Graphical Presentation of SCB Pressure Drop Correlation of Dormer and Bergles [Ref. 4]

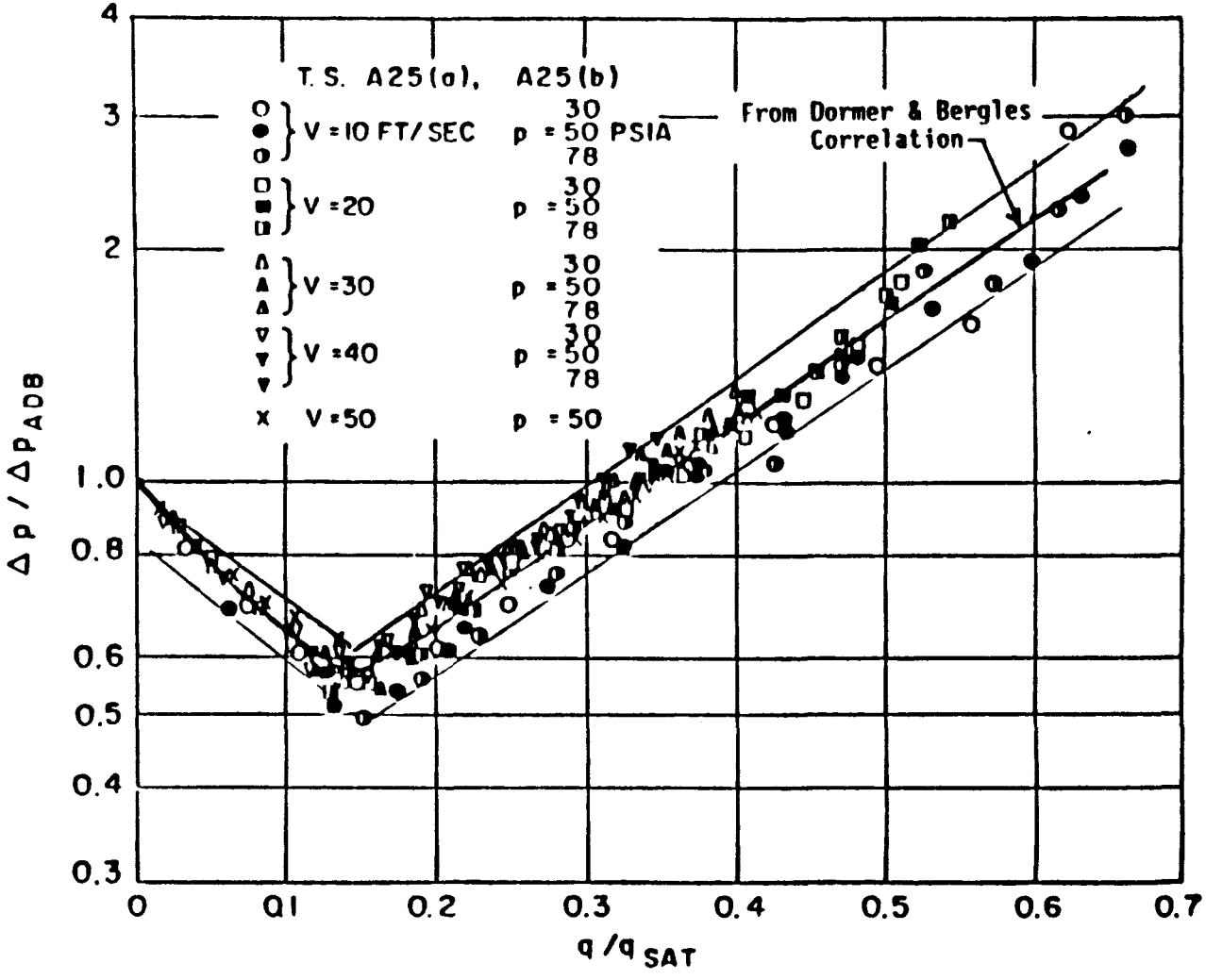

Figure 2.2 Correlation Pressure Drop Data of Dormer and Bergles for a Single Test Section [Ref. 4]

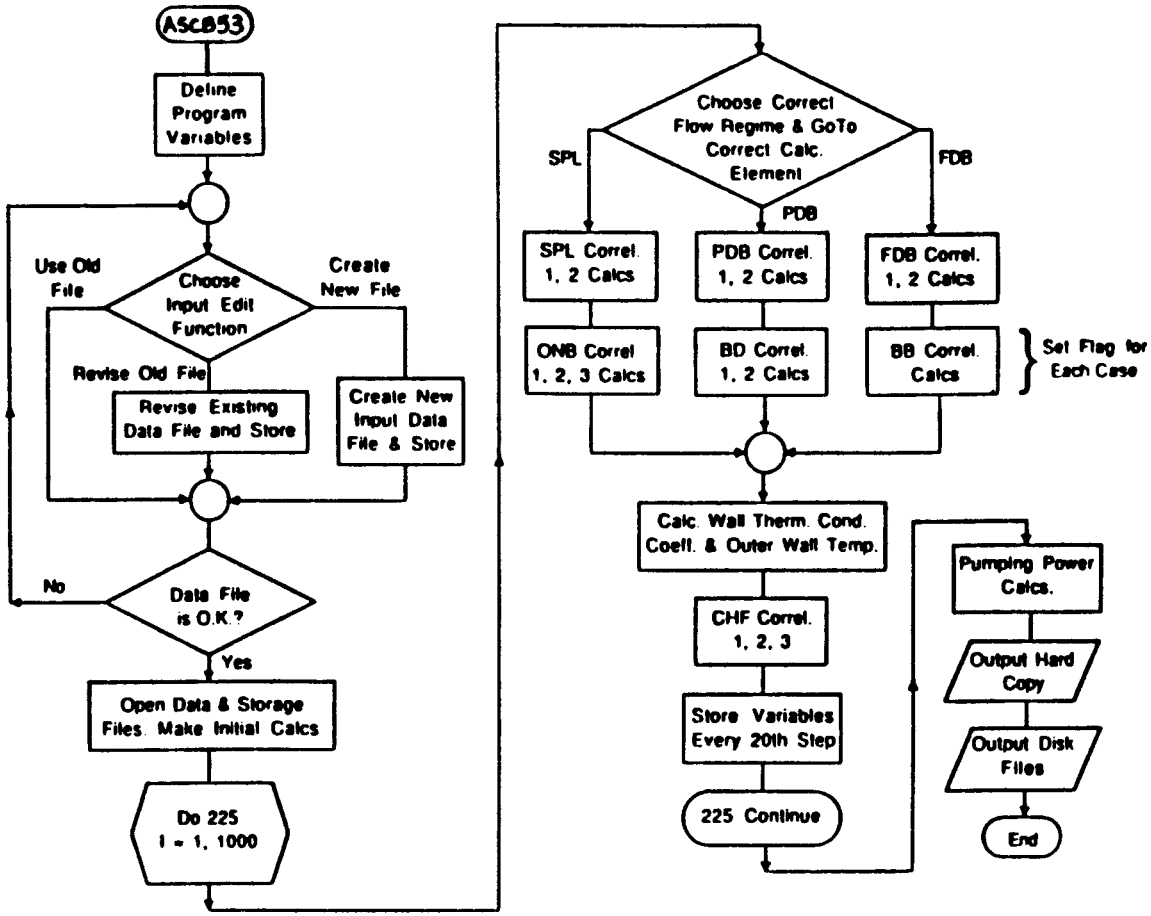

Figure 3.1 Computer Code Logic Diagram

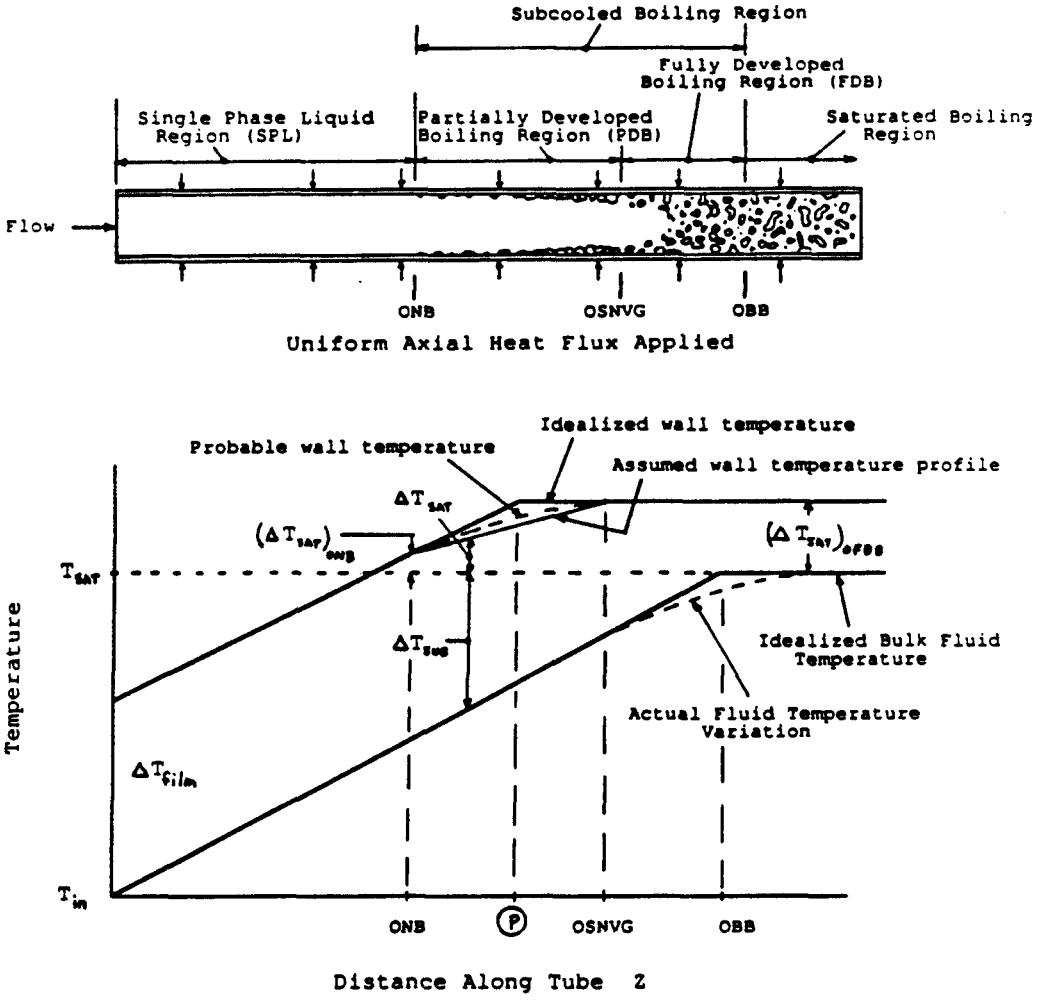

Figure 3.2 Typical Temperature Profiles Along a Heated Tube

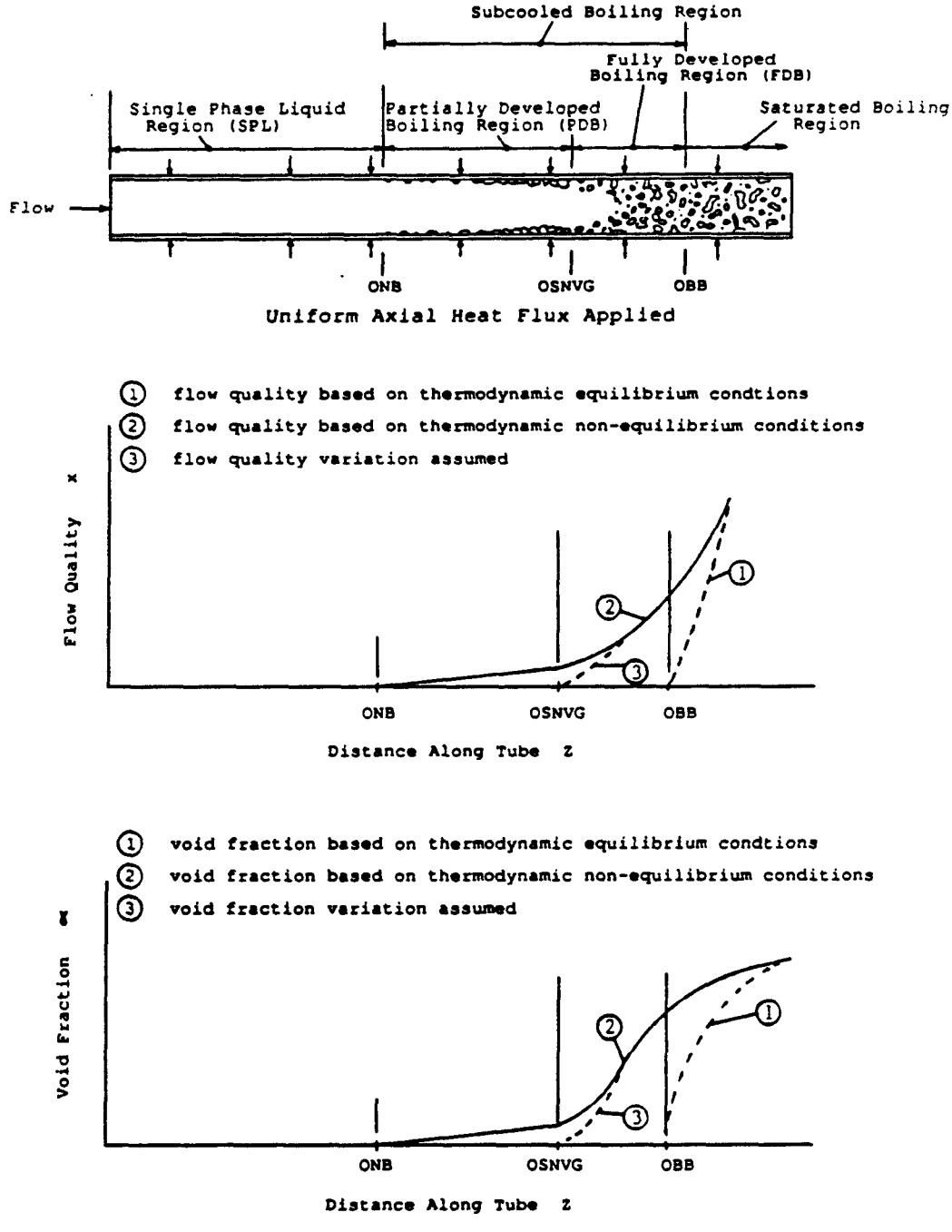

Figure 3.3 Typical Quality and Void Fraction Distributions Along Tube

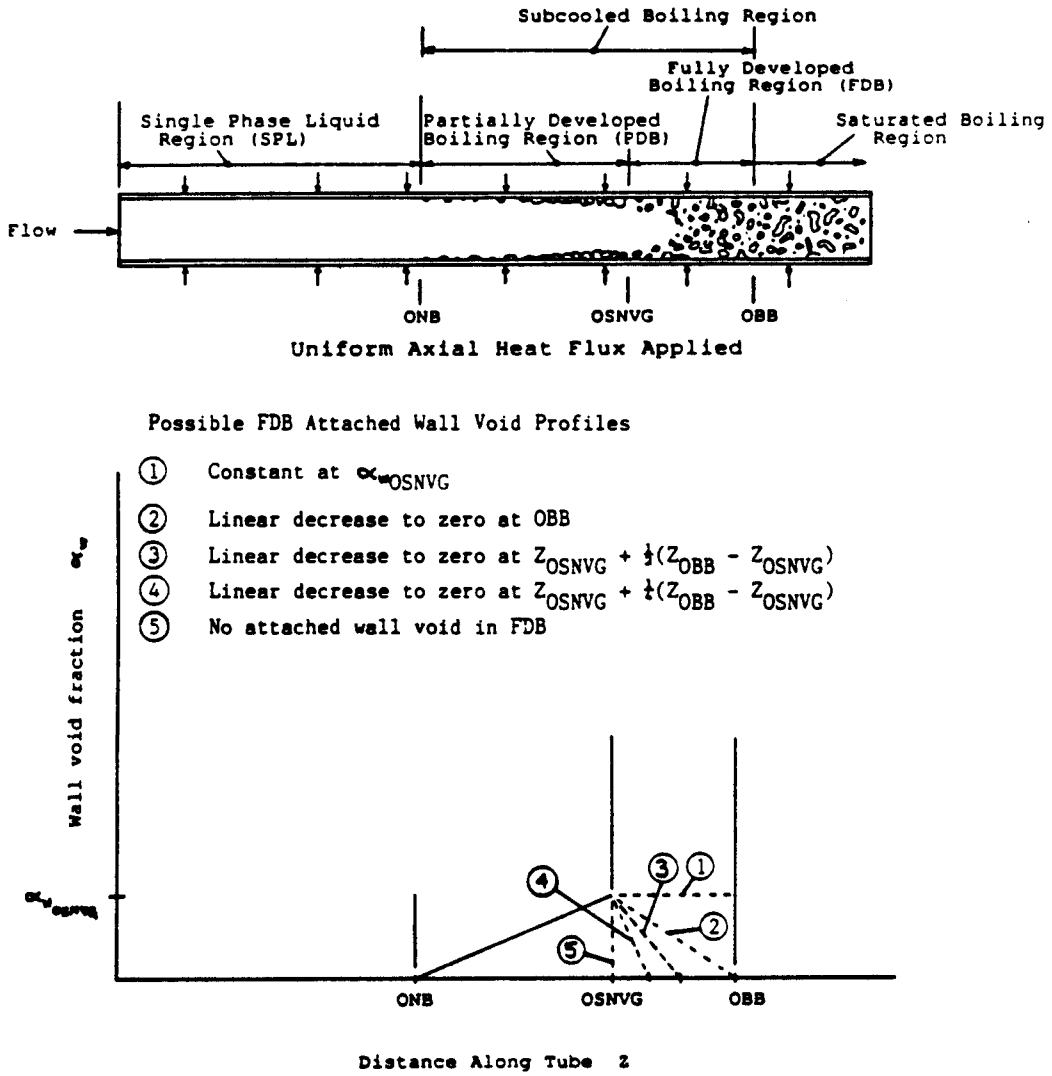

Figure 3.4 Attached Wall Void Profiles Along Tube

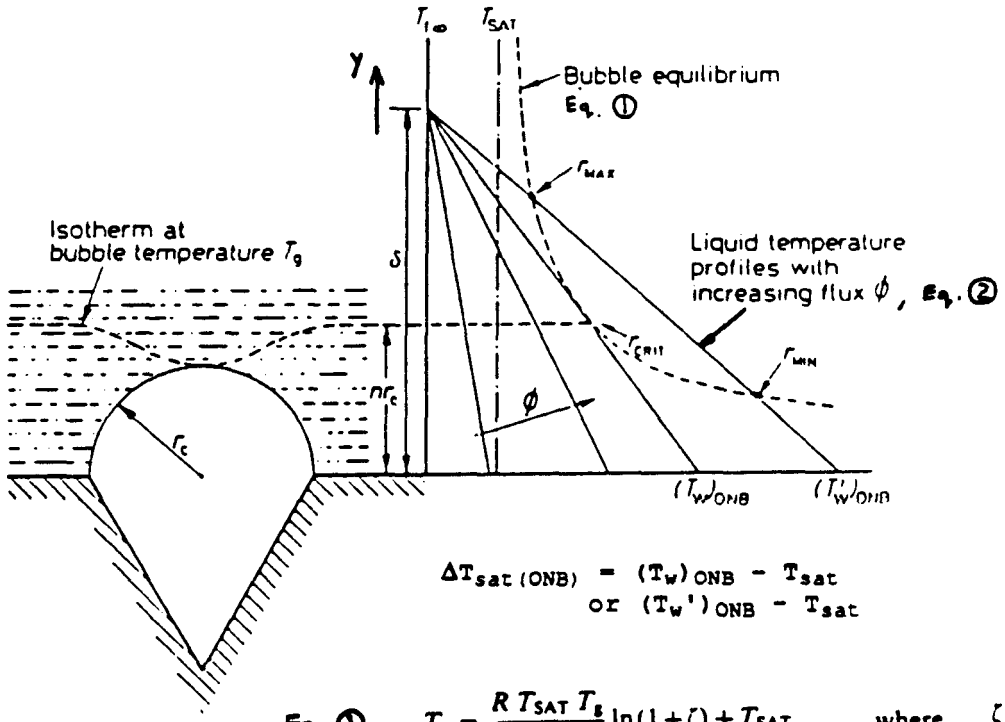

Eq. ① $$T_g = \frac{R\,T_{SAT}\,T_g}{J\,i_{fg}\,M}\ln(1+\zeta) + T_{SAT} \qquad \text{where} \quad \zeta = \left(\frac{2\sigma}{p_f\,r_c}\right)$$

Eq. ② $$T_f(y) = T_w - \left(\frac{\phi\,y}{k_f}\right)$$

Figure 3.5 Hsu Model of the Onset of Nucleate Boiling [Ref. 24]

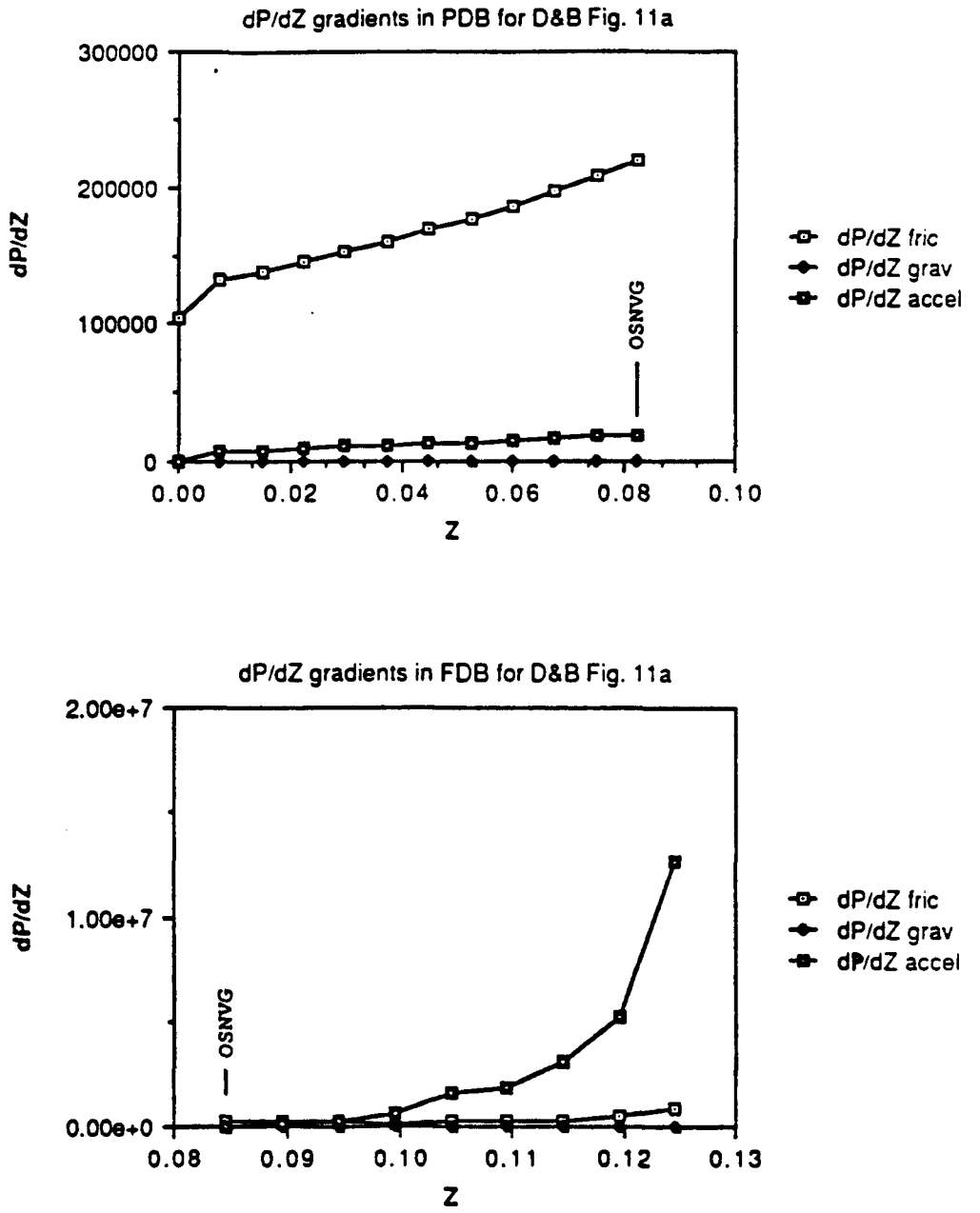

Figure 3.6 Typical dP/dZ Gradients for Horizontal Tube Flows Using Final Code Version ASCB53

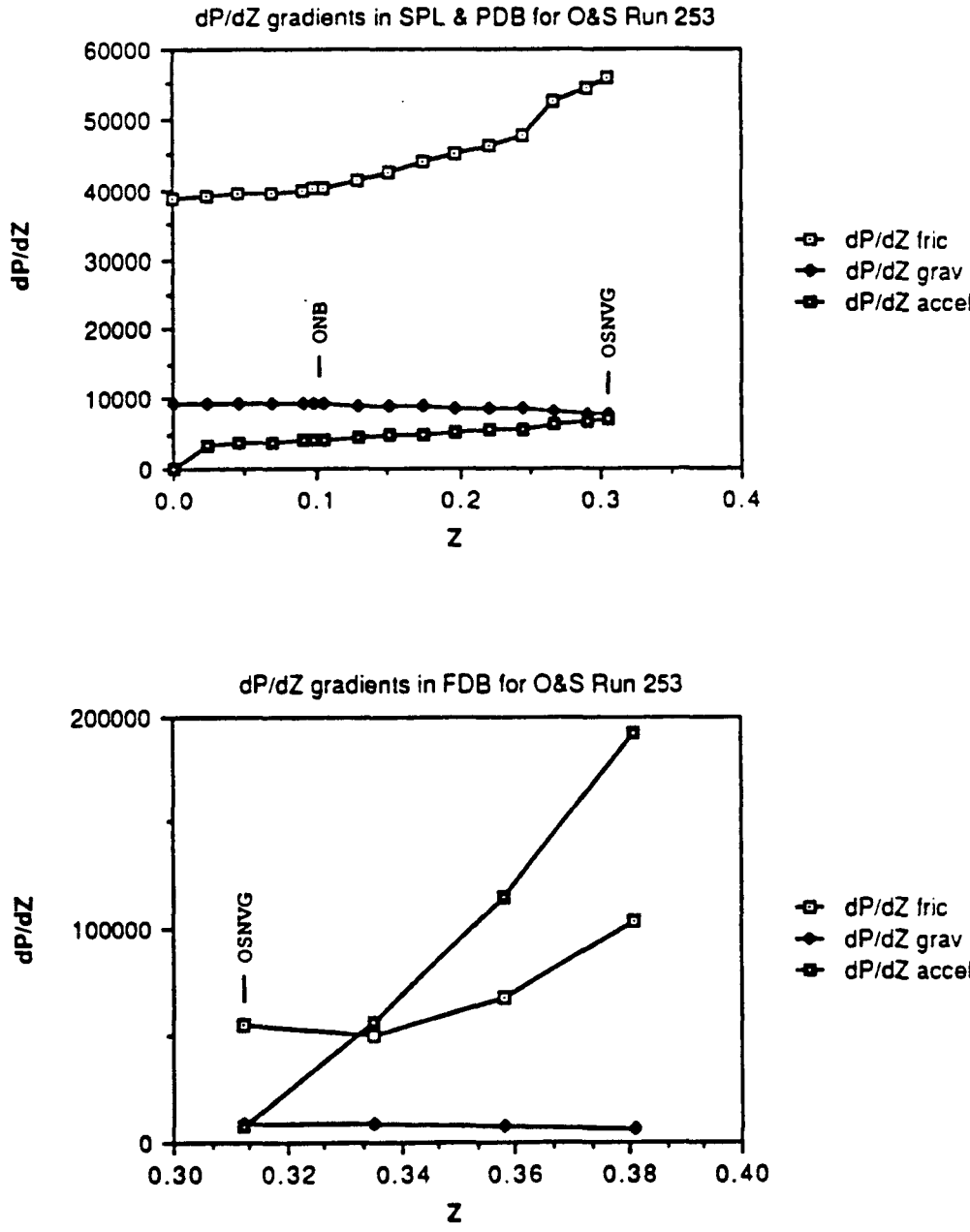

Figure 3.7 Typical dP/dZ Gradients for Vertical Tube Flows Using Final Code Version ASCB53

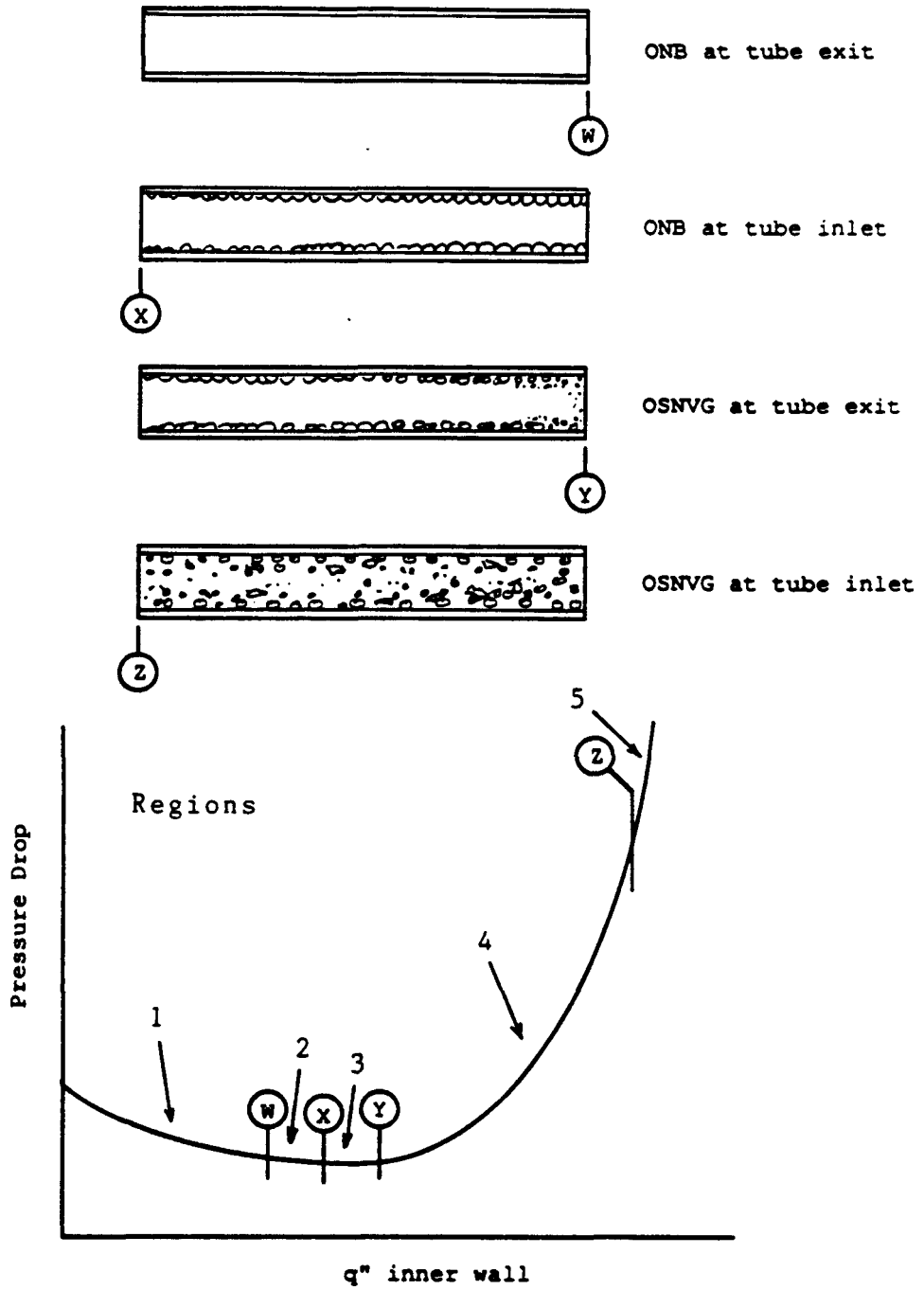

Figure 4.1 Identification of Flow Regimes for Dormer and Bergles ΔP vs. q" Curves

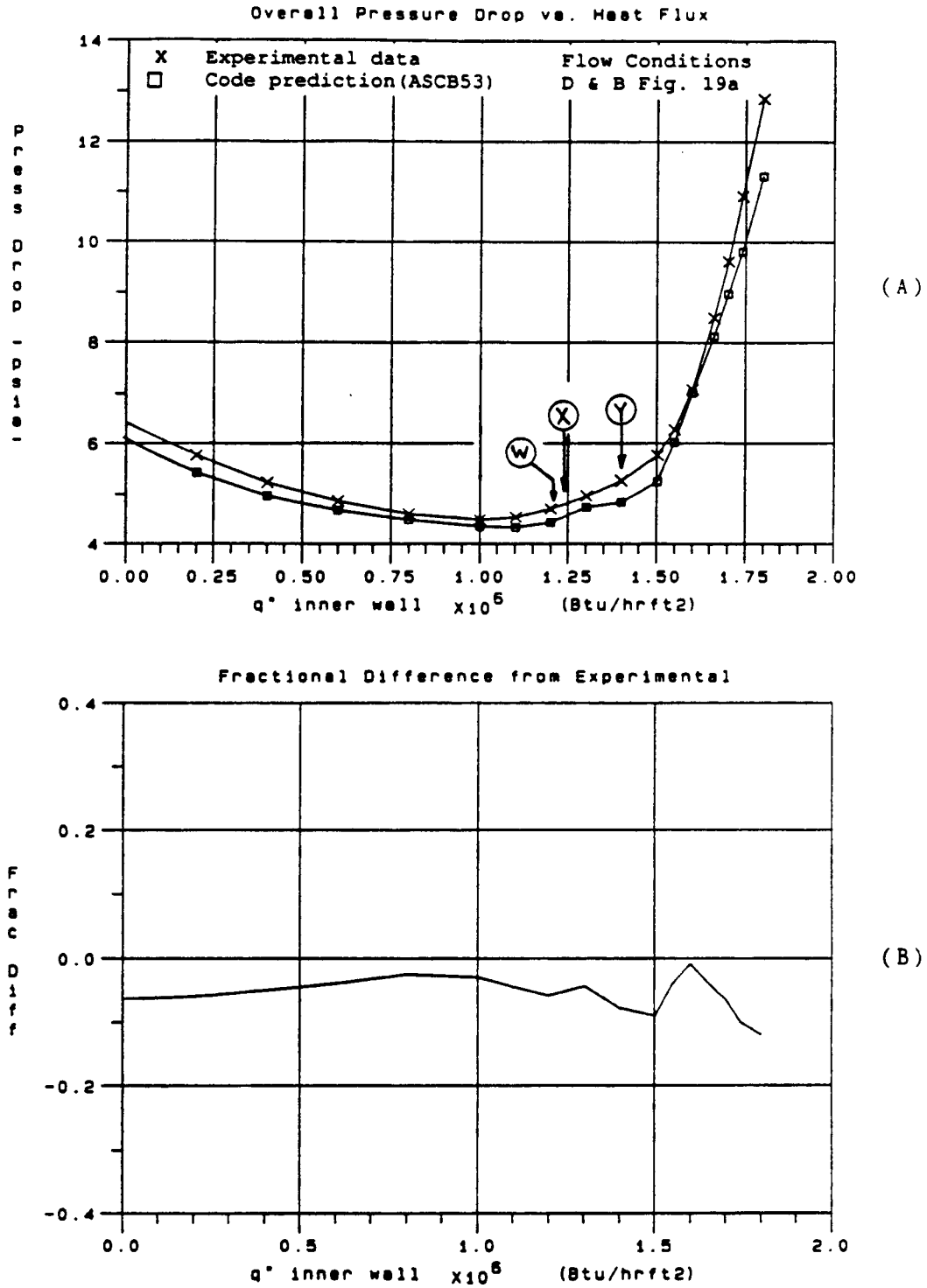

Figure 4.1.1 Comparison of Experimental and Code Predicted Overall Pressure Drop Using Final Code Version ASCB53

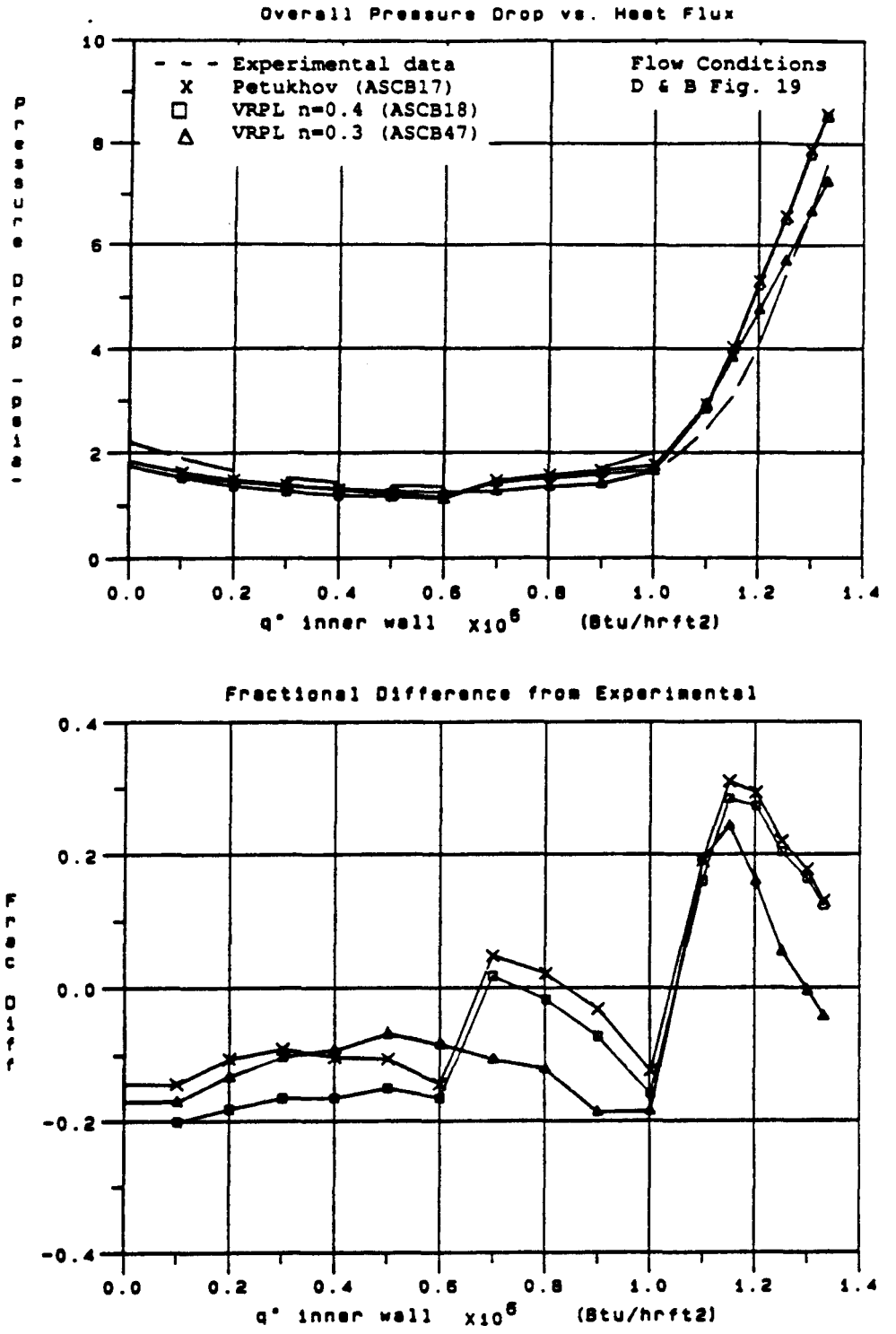

Figure 4.2 Comparison of Pressure Drop Predictions Using Petukhov and Viscosity Ratio Power Law Friction Factor Equations

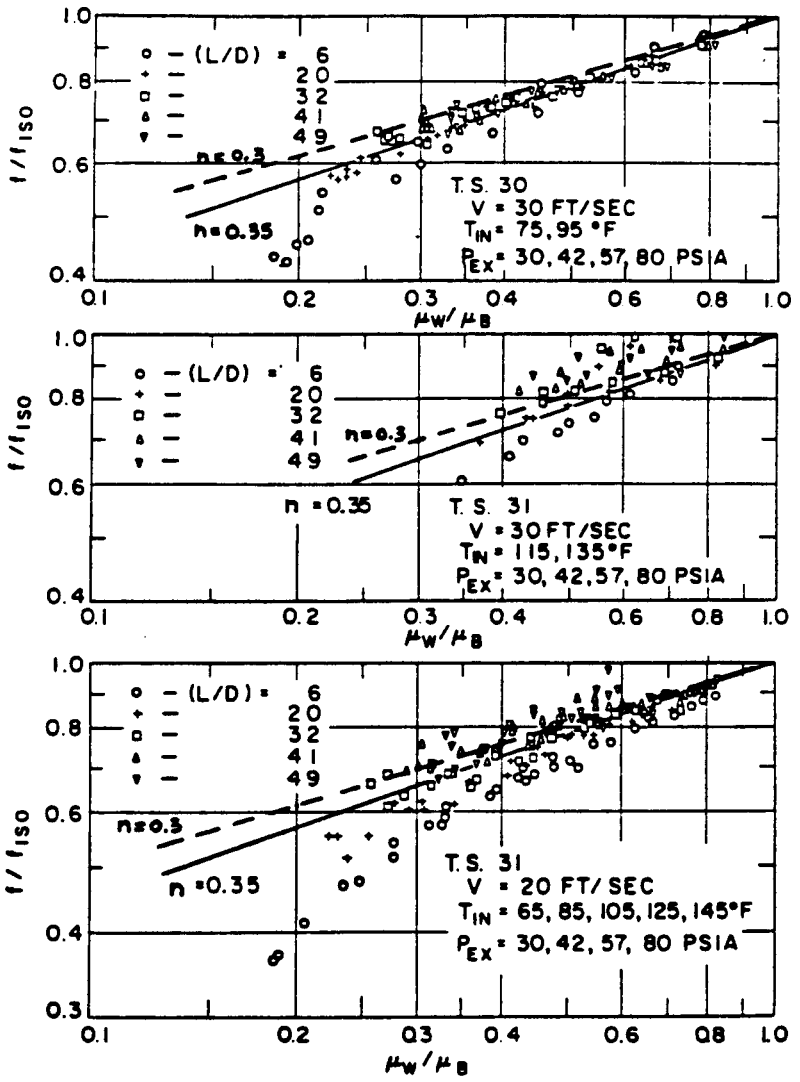

Figure 4.3 Correlation of Non-Boiling Friction Factor with Viscosity Ratio [Ref. 4]

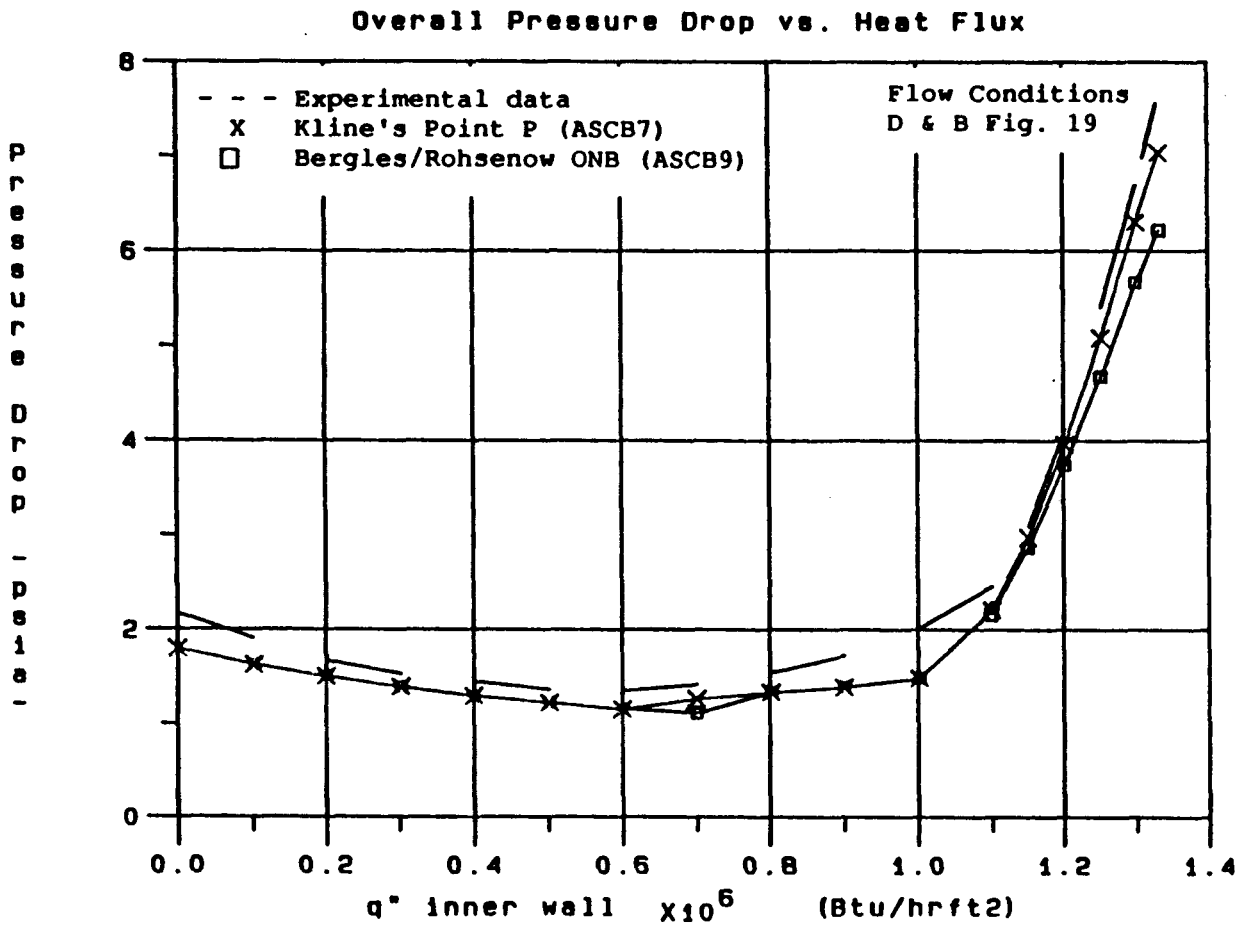

Figure 4.4 Comparison of Pressure Drop Predictions Using Bergles/ Rohsenow ONB and Kline's Point P Models for the Onset of Nucleate Boiling

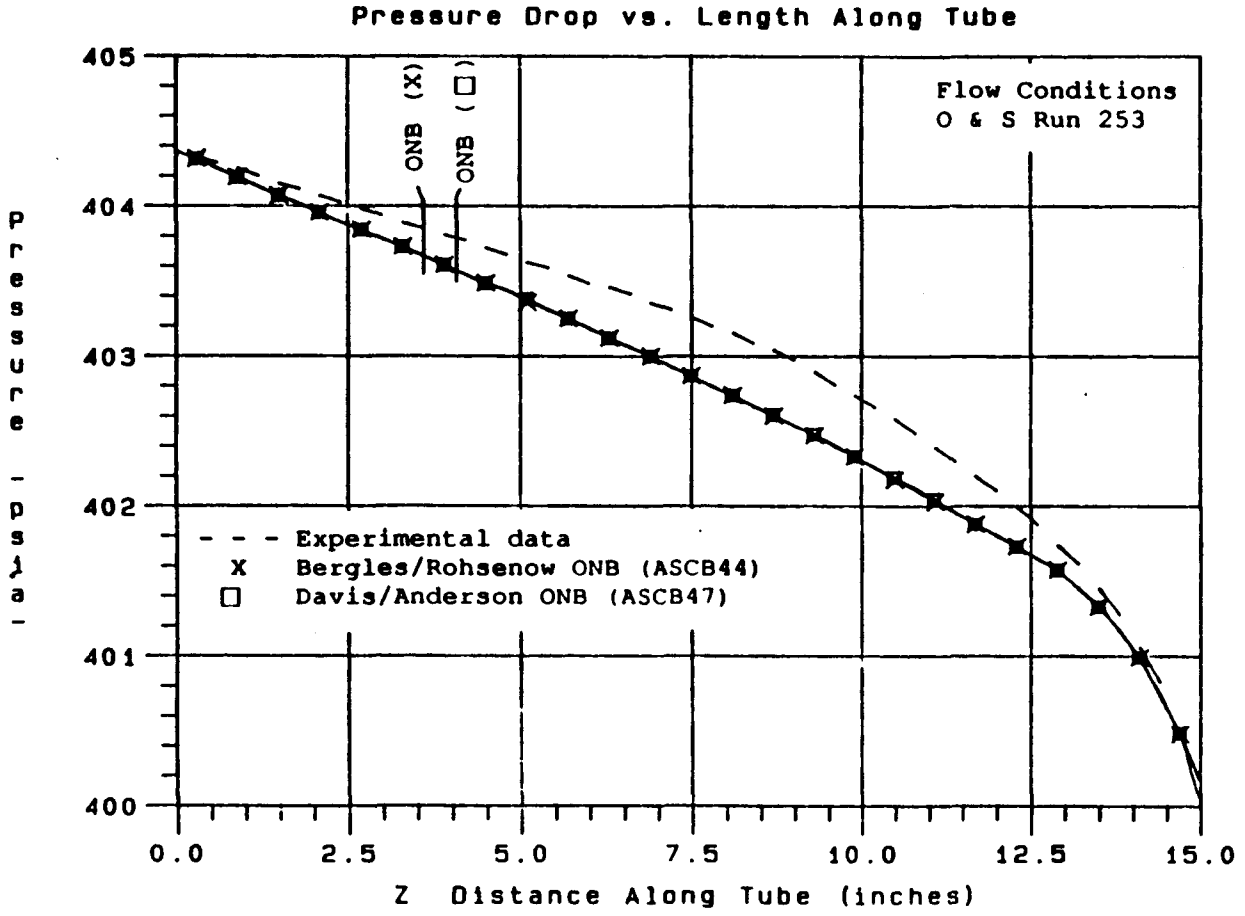

Figure 4.5 Comparison of Pressure Drop Predictions Using Bergles/ Rohsenow and Davis/Anderson ONB Correlations

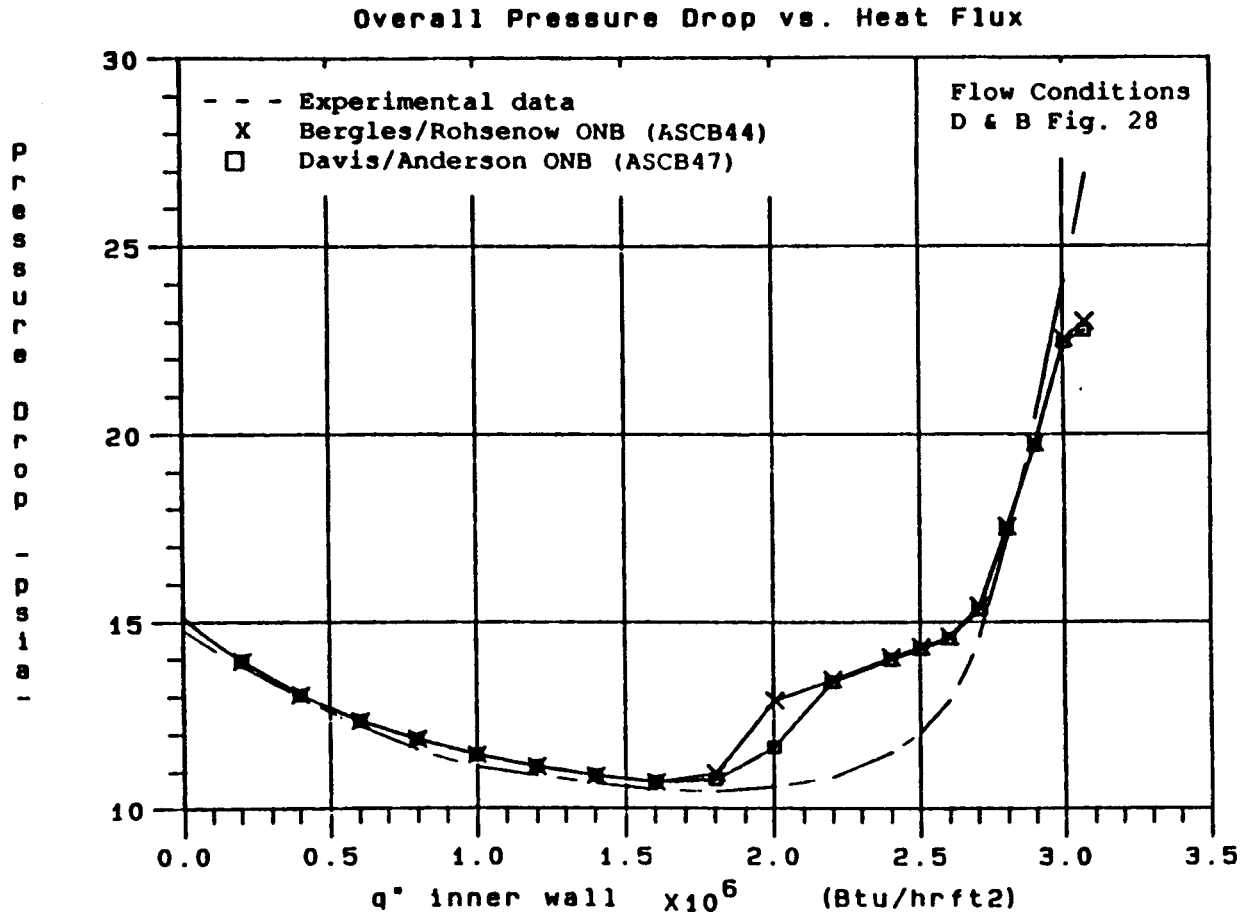

Figure 4.6 Comparison of Pressure Drop Predictions Using Bergles/ Rohsenow and Davis/Anderson ONB Correlations

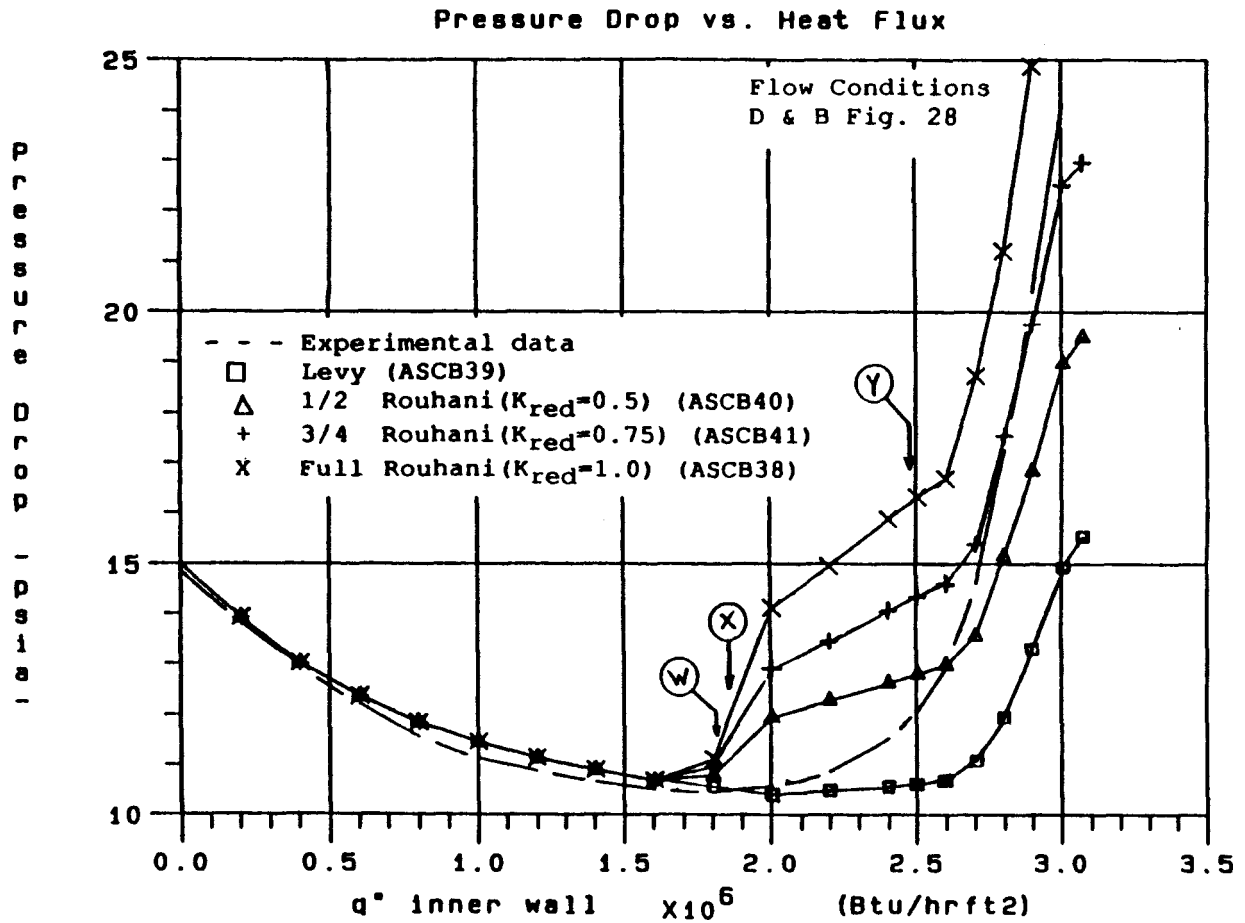

Figure 4.7 Comparison of Pressure Drop Predictions Using Various Attached Wall Void Profiles in PDB

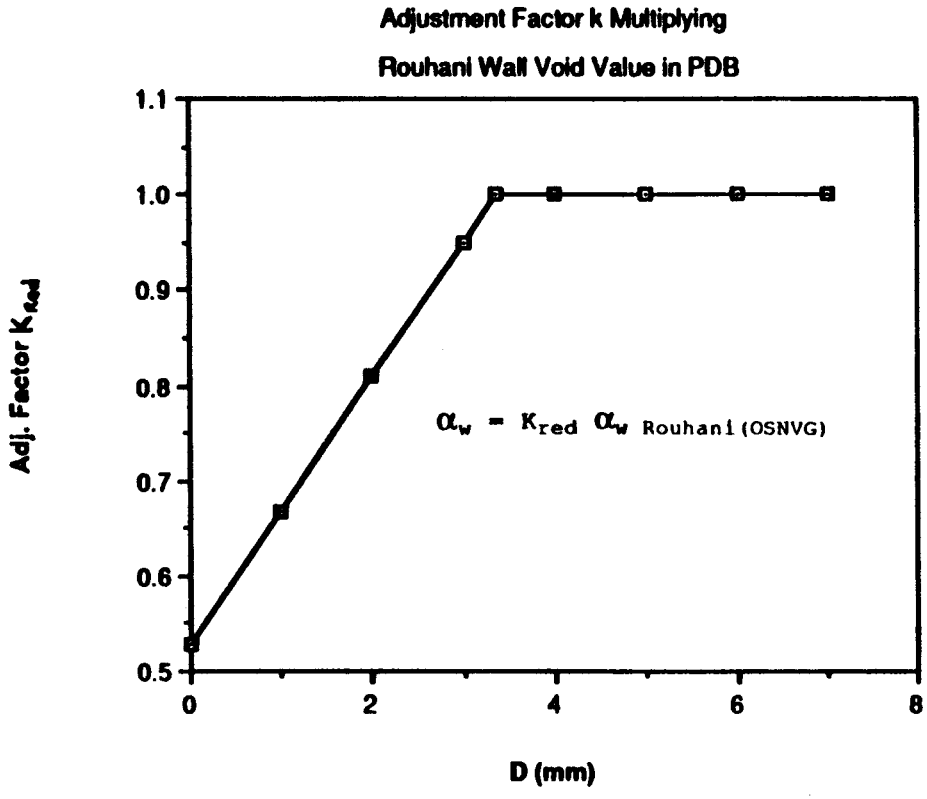

Figure 4.8 Adjustment to Rouhani Attached Wall Void for Small Tubes

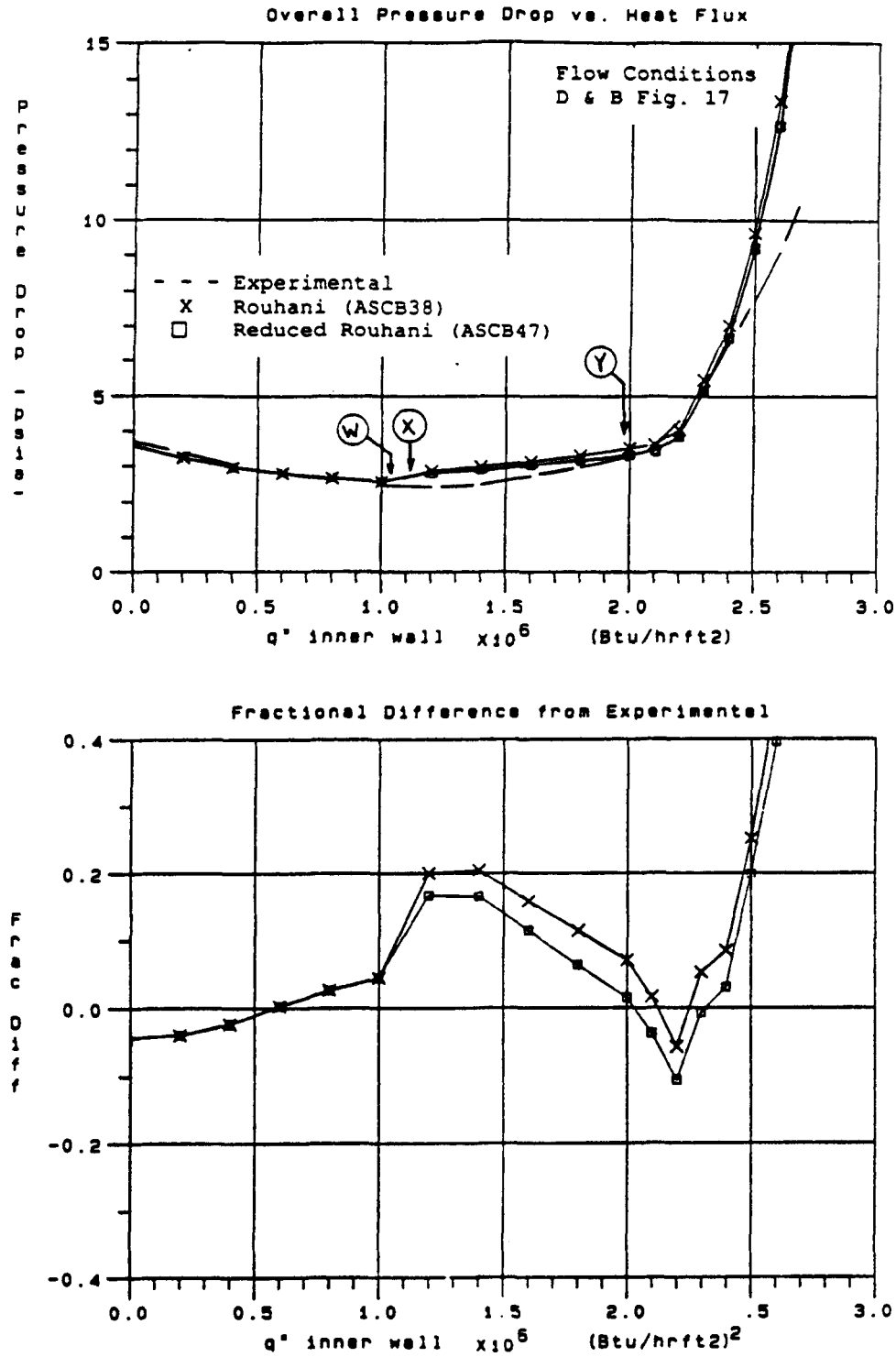

Figure 4.9 Comparison of Pressure Drop Predictions Using Rouhani and Reduced Rouhani Attached Wall Void Profiles

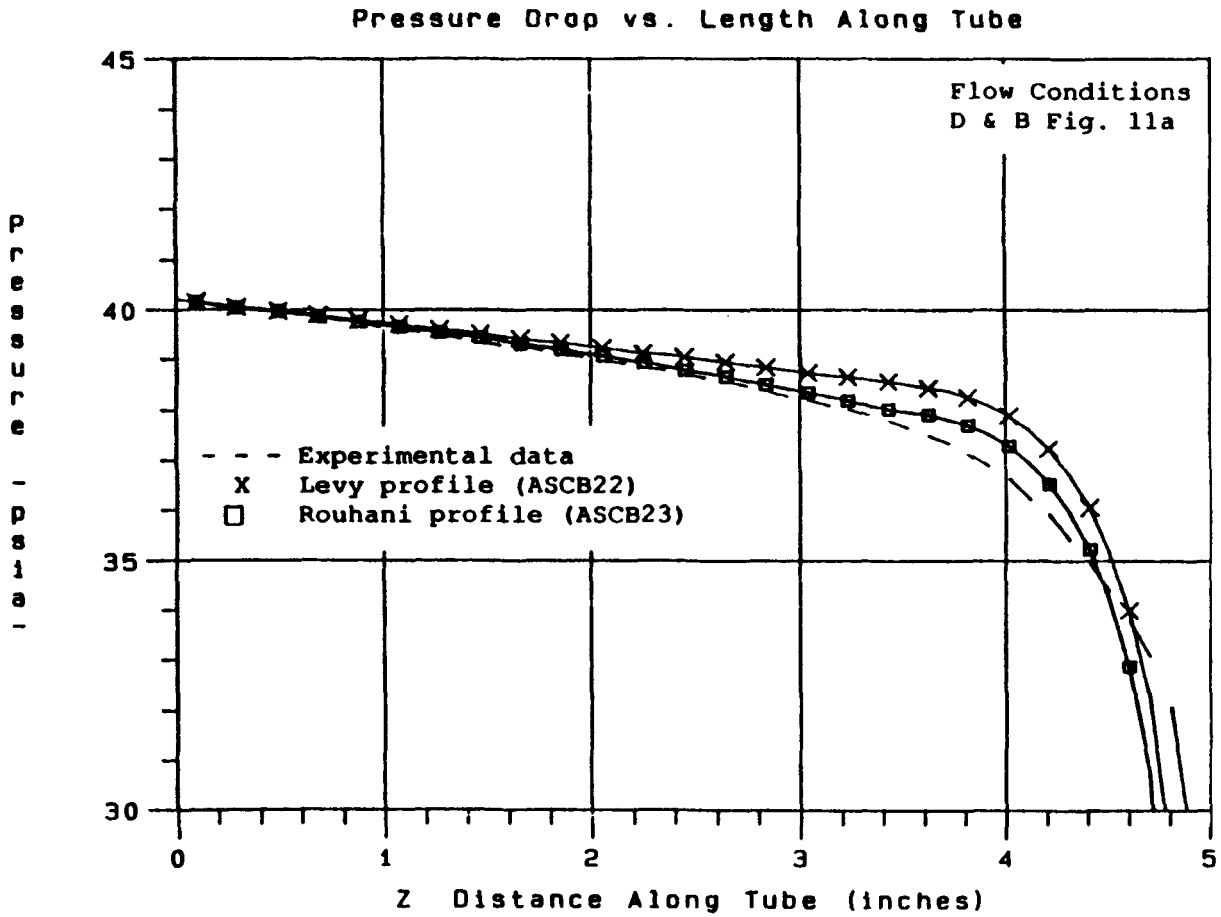

Figure 4.10 Comparison of Pressure Drop Predictions Using Levy and Rouhani Attached Wall Void Profiles in PDB

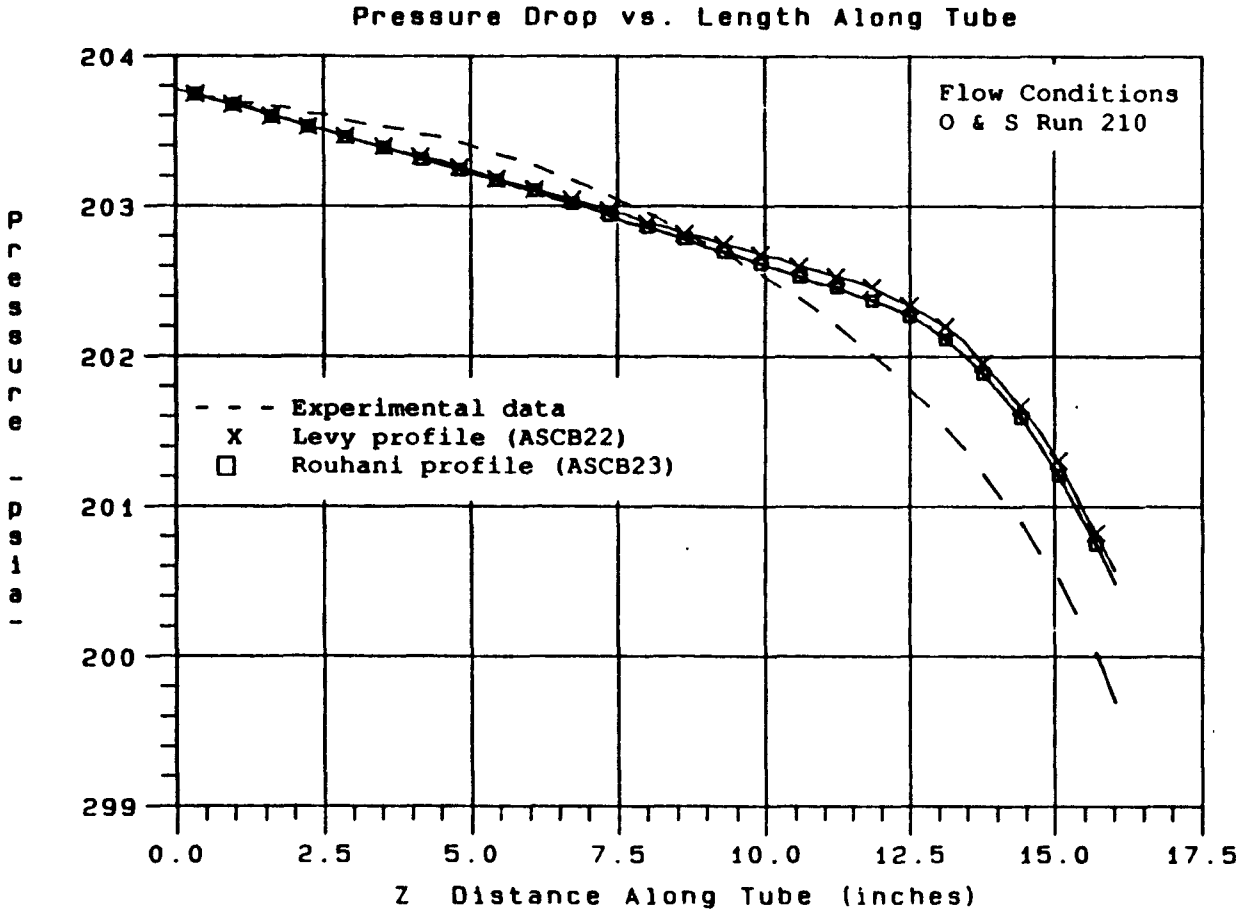

Figure 4.11 Comparison of Pressure Drop Predictions Using Levy and Rouhani Attached Wall Void Profiles in PDB

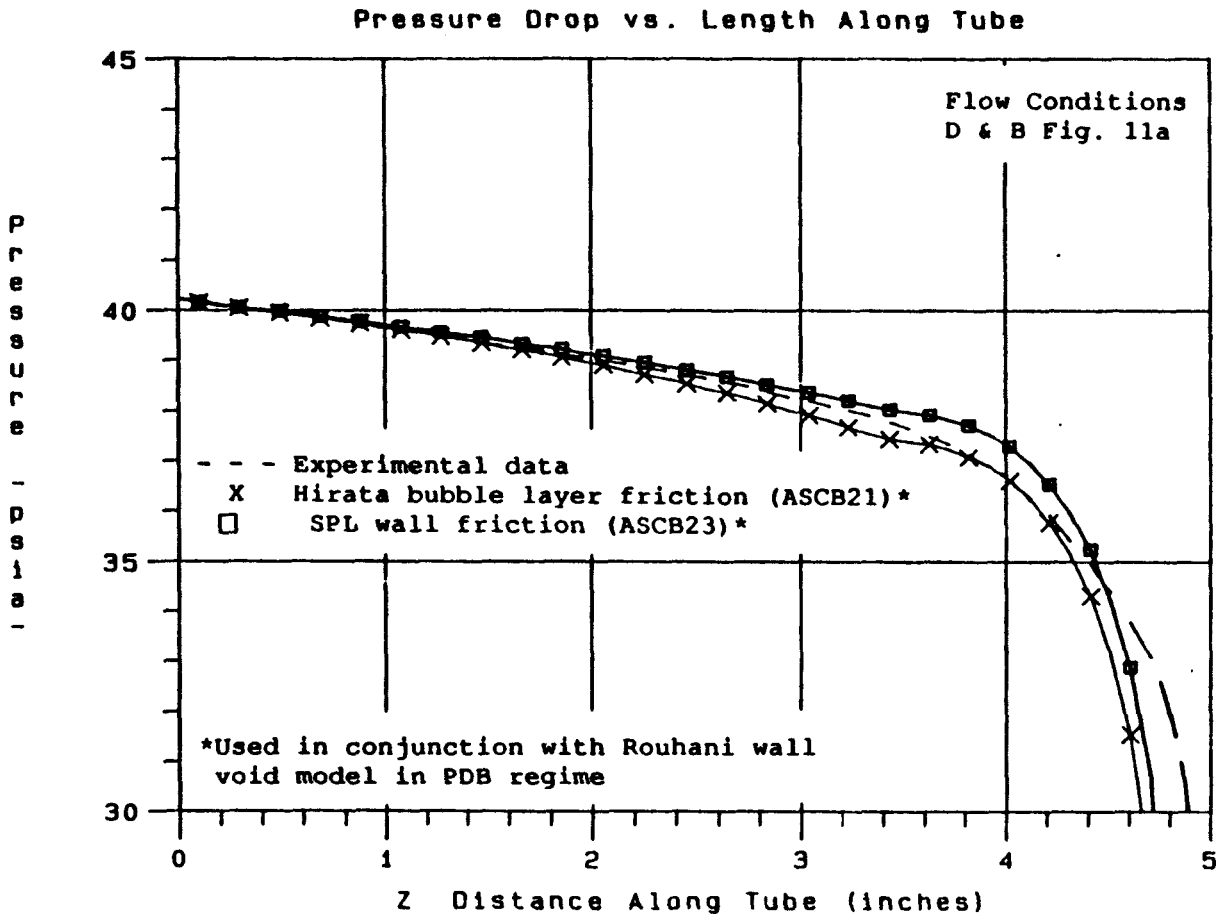

Figure 4.12 Comparison of Pressure Drop Predictions Using Hirata Bubble Layer Friction and SPL Wall Friction Factors in PDB (Both Using the Rouhani Attached Wall Void Model in PDB)

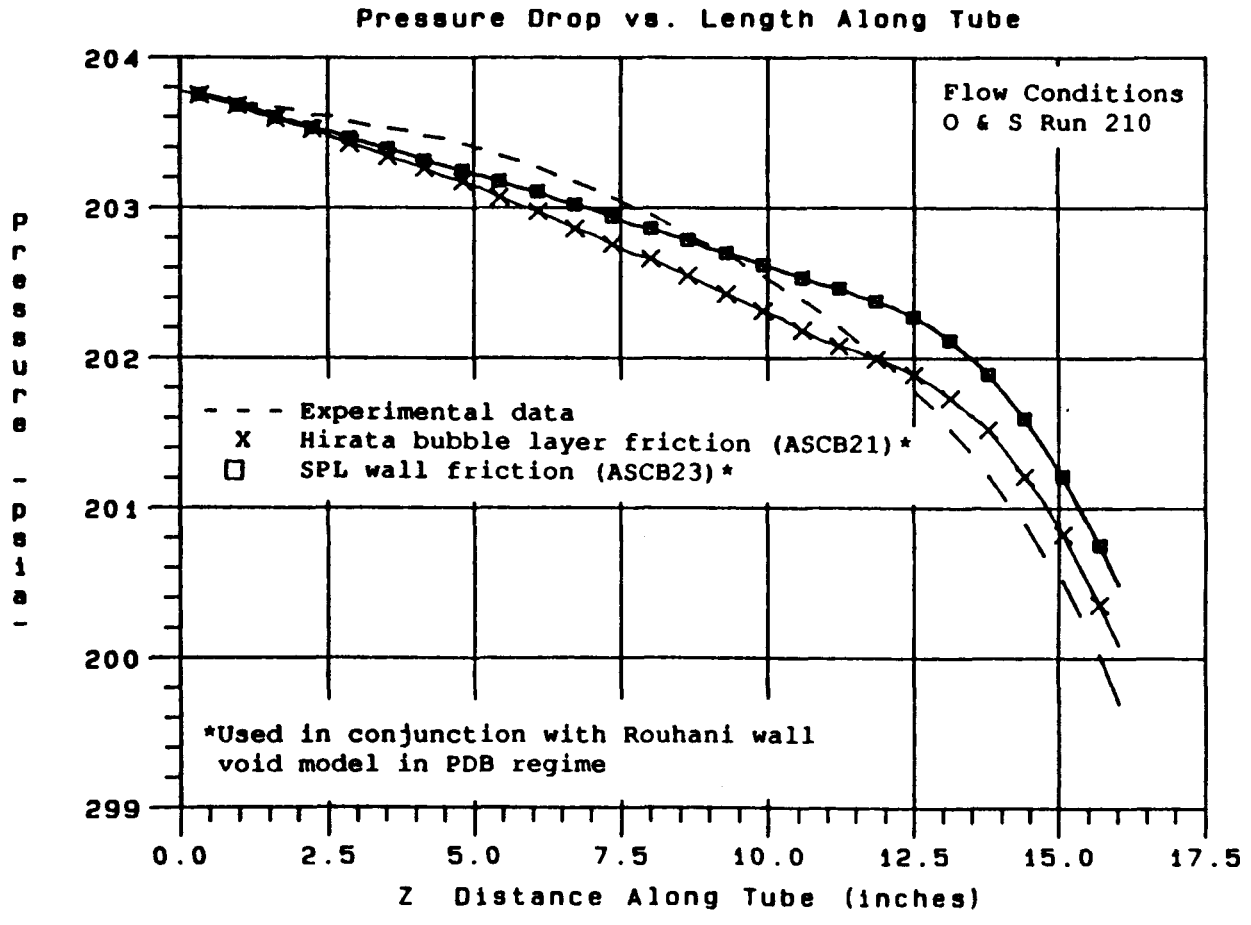

Figure 4.13 Comparison of Pressure Drop Predictions Using Hirata Bubble Layer Friction and SPL Wall Friction Factors in PDB (Both Using the Rouhani Attached Wall Void Model in PDB)

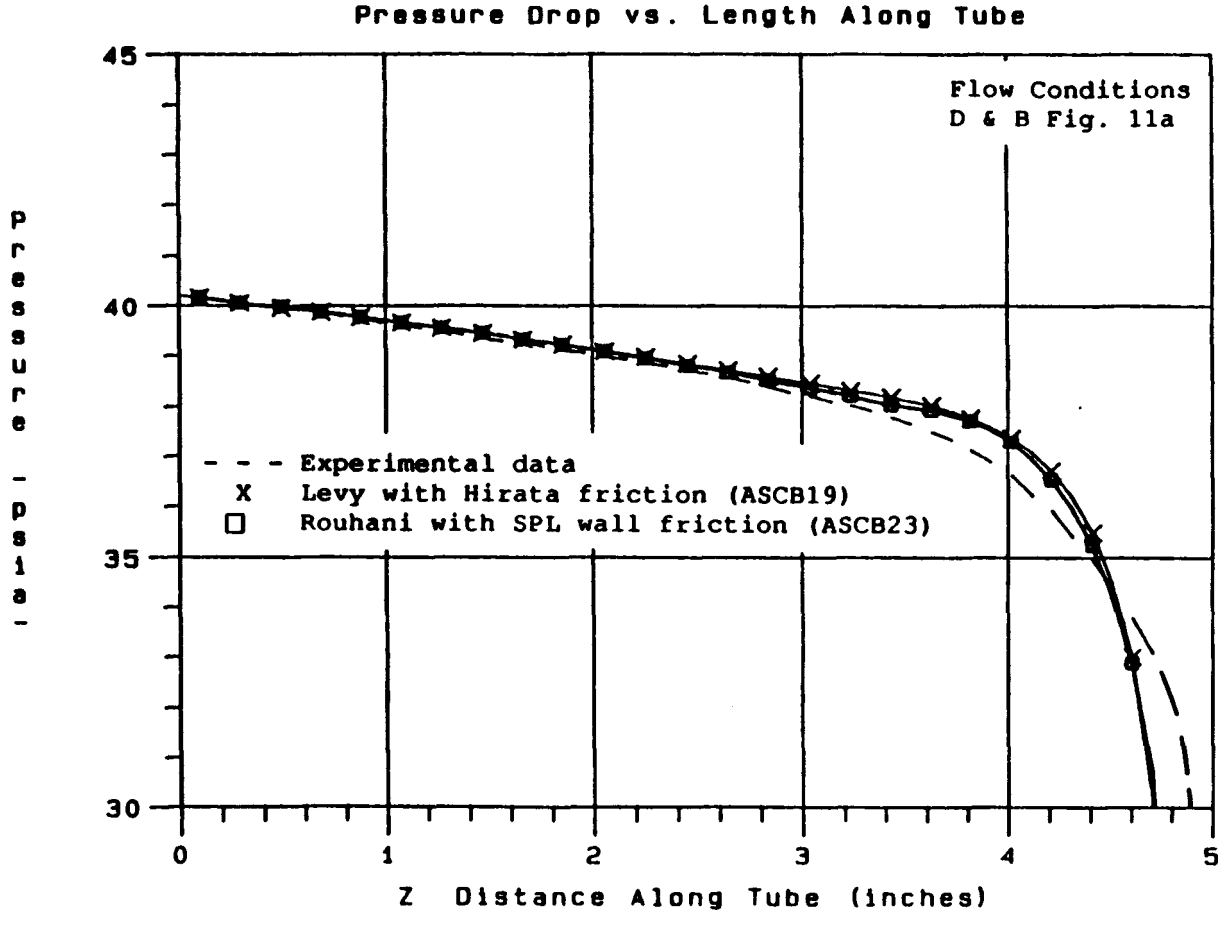

Figure 4.14 Comparison of Pressure Drop Predictions Using Two Different Combinations of Surface Friction and Attached Wall Void Models in PDB

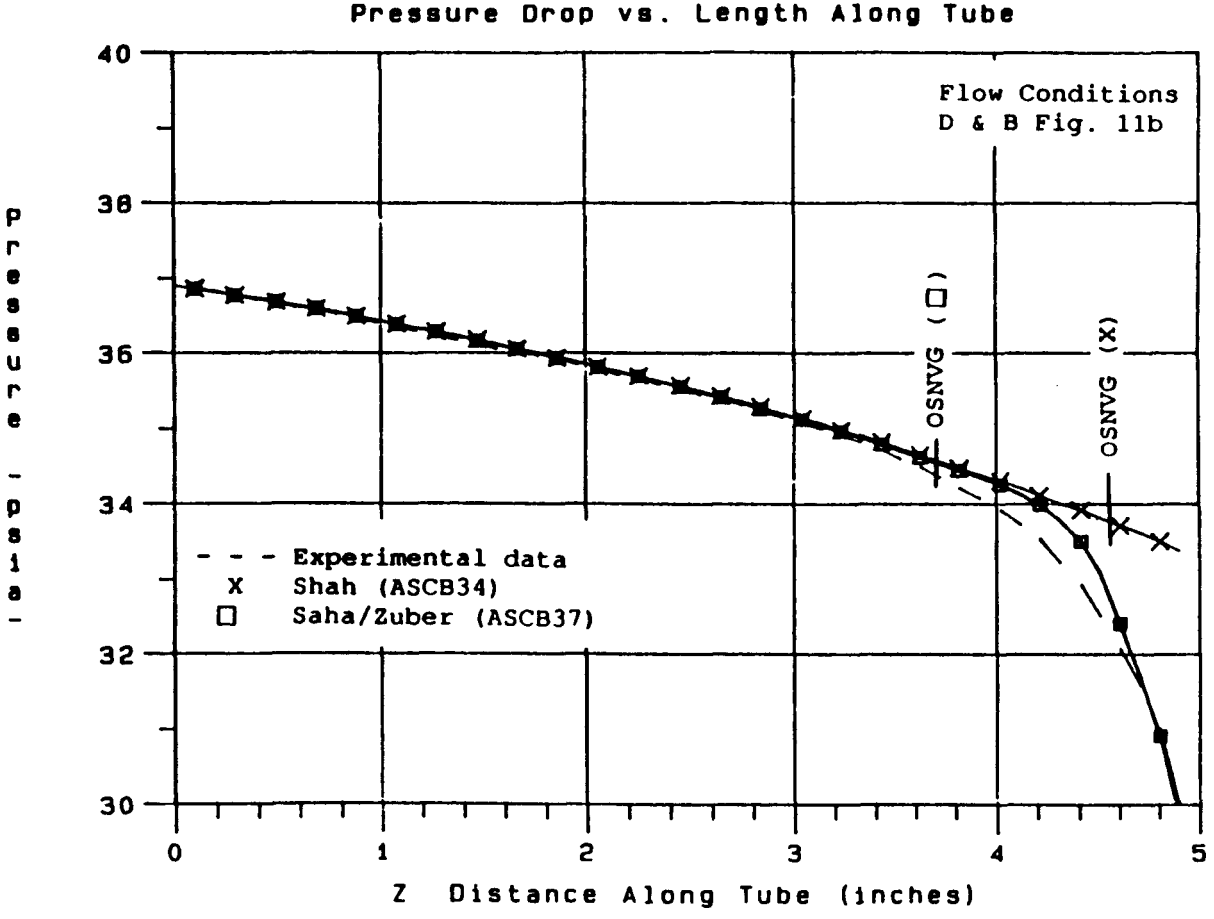

Figure 4.15 Comparison of Pressure Drop Predictions Using Saha/Zuber and Shah OSNVG Correlations

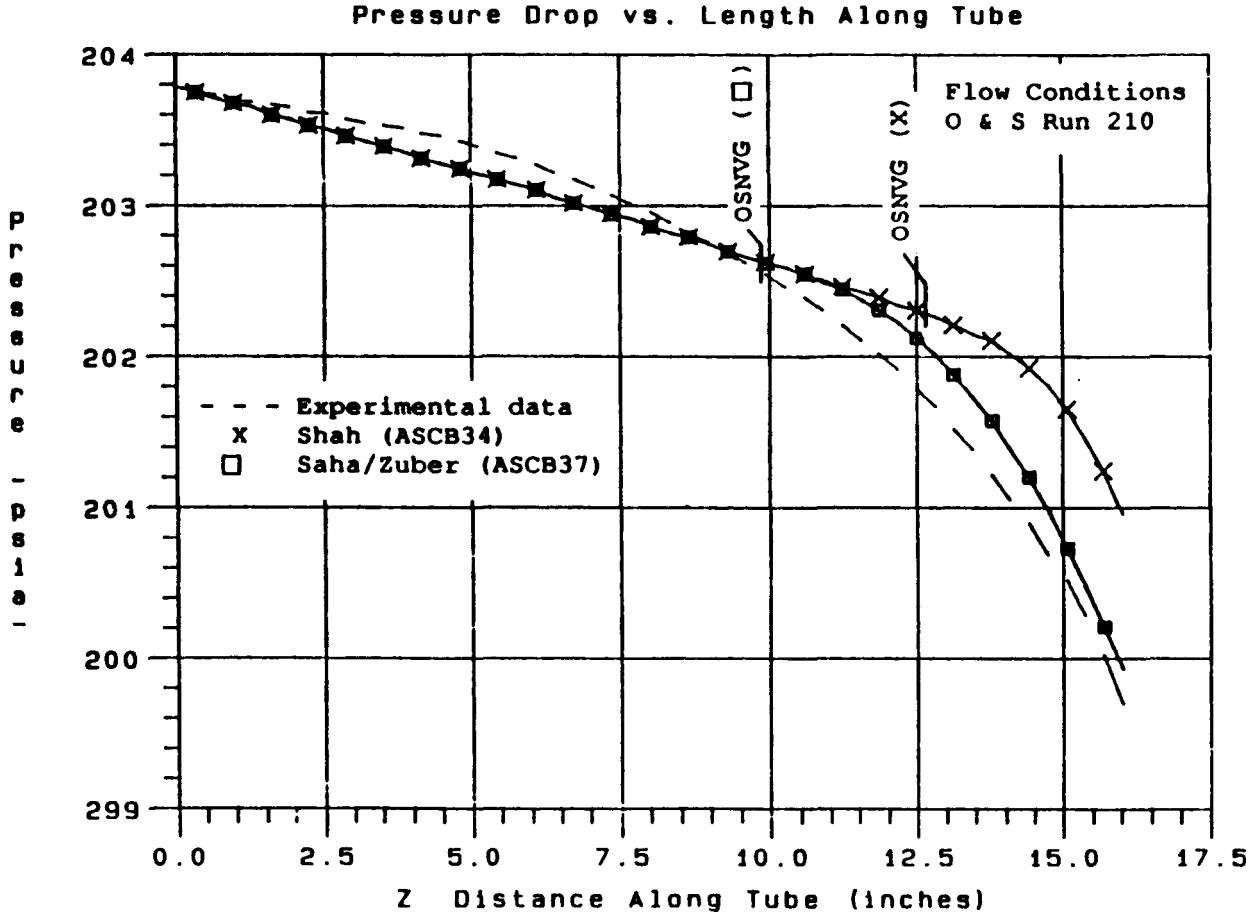

Figure 4.16 Comparison of Pressure Drop Predictions Using Saha/Zuber and Shah OSNVG Correlations

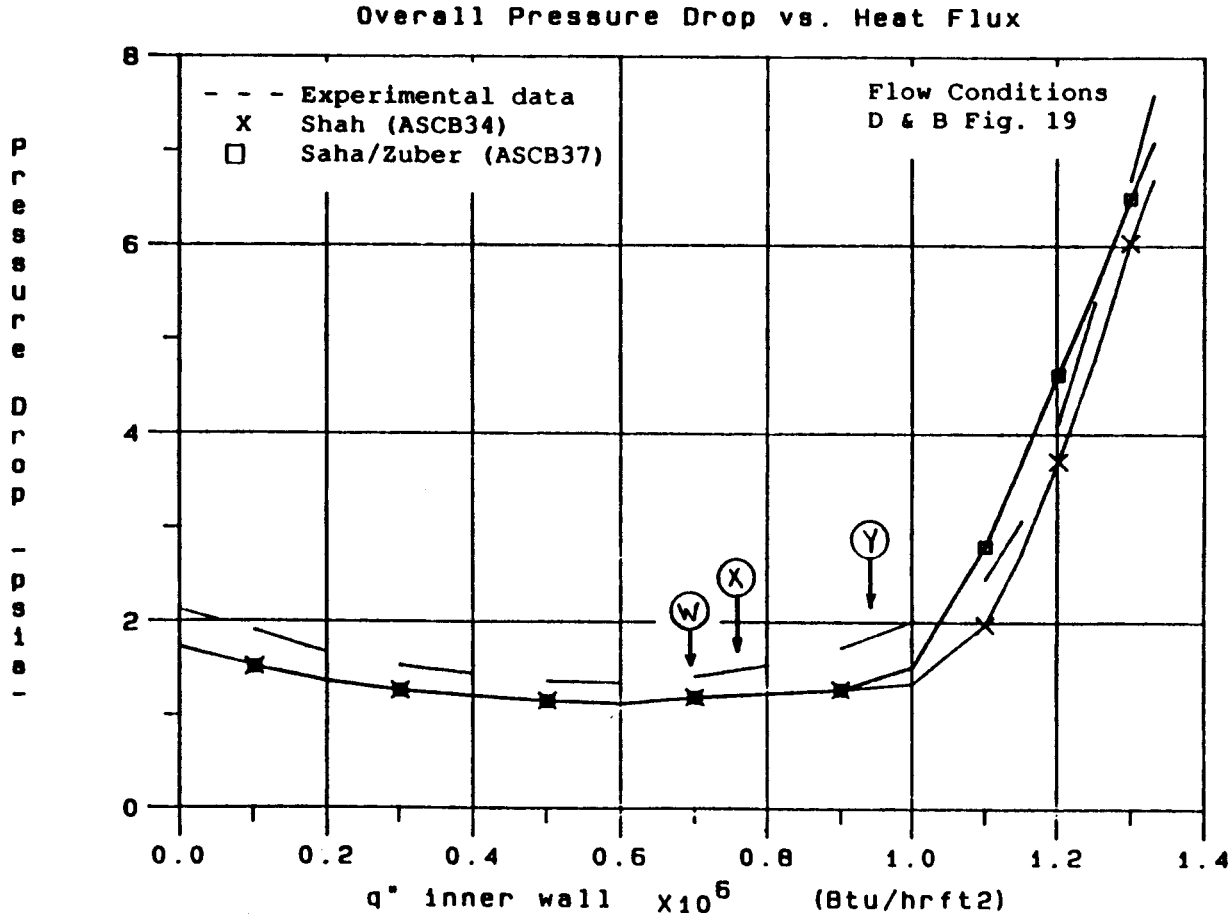

Figure 4.17 Comparison of Pressure Drop Predictions Using Saha/Zuber and Shah OSNVG Correlations

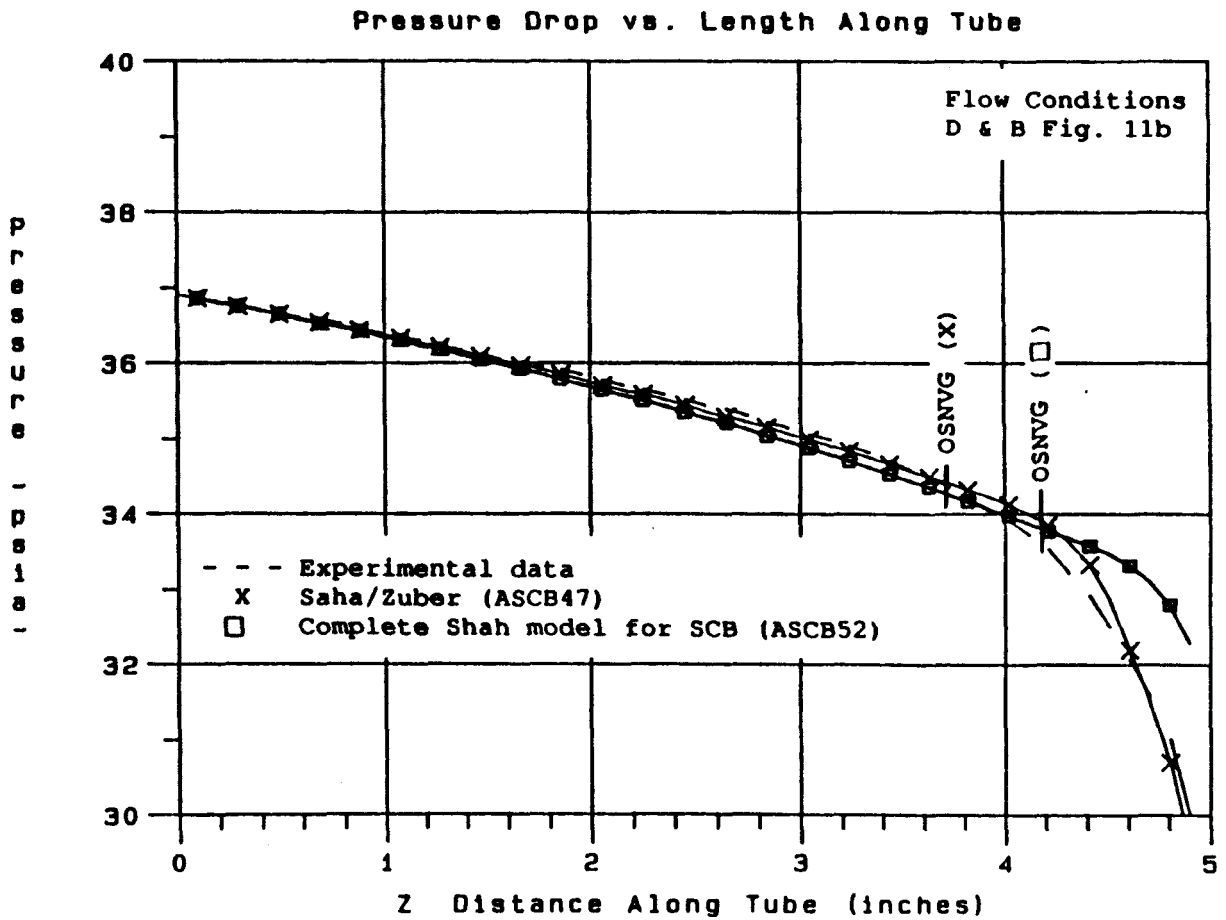

Figure 4.18 Comparison of Pressure Drop Predictions Using Saha/Zuber and Complete Shah Model for SCB

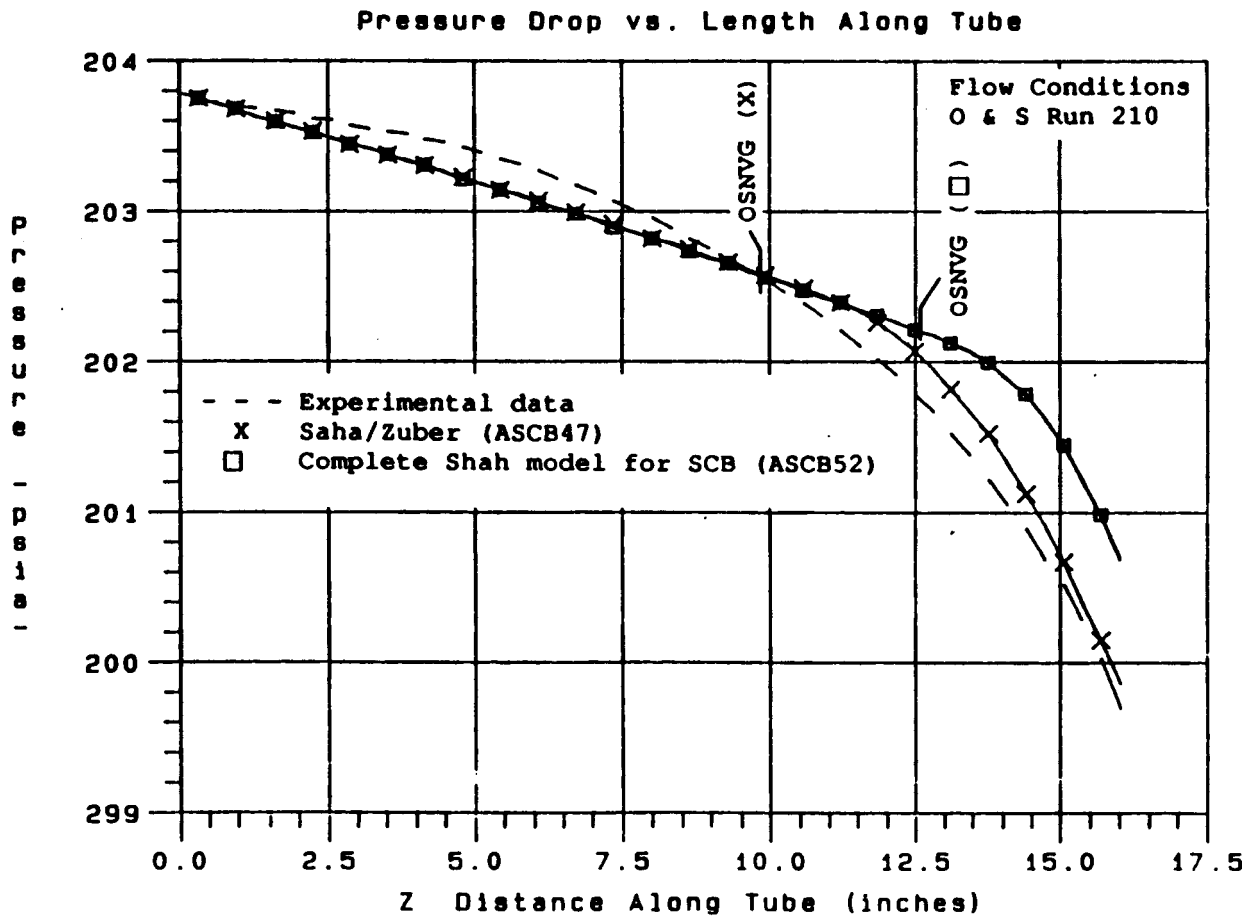

Figure 4.19 Comparison of Pressure Drop Predictions Using Saha/Zuber and Complete Shah Model for SCB

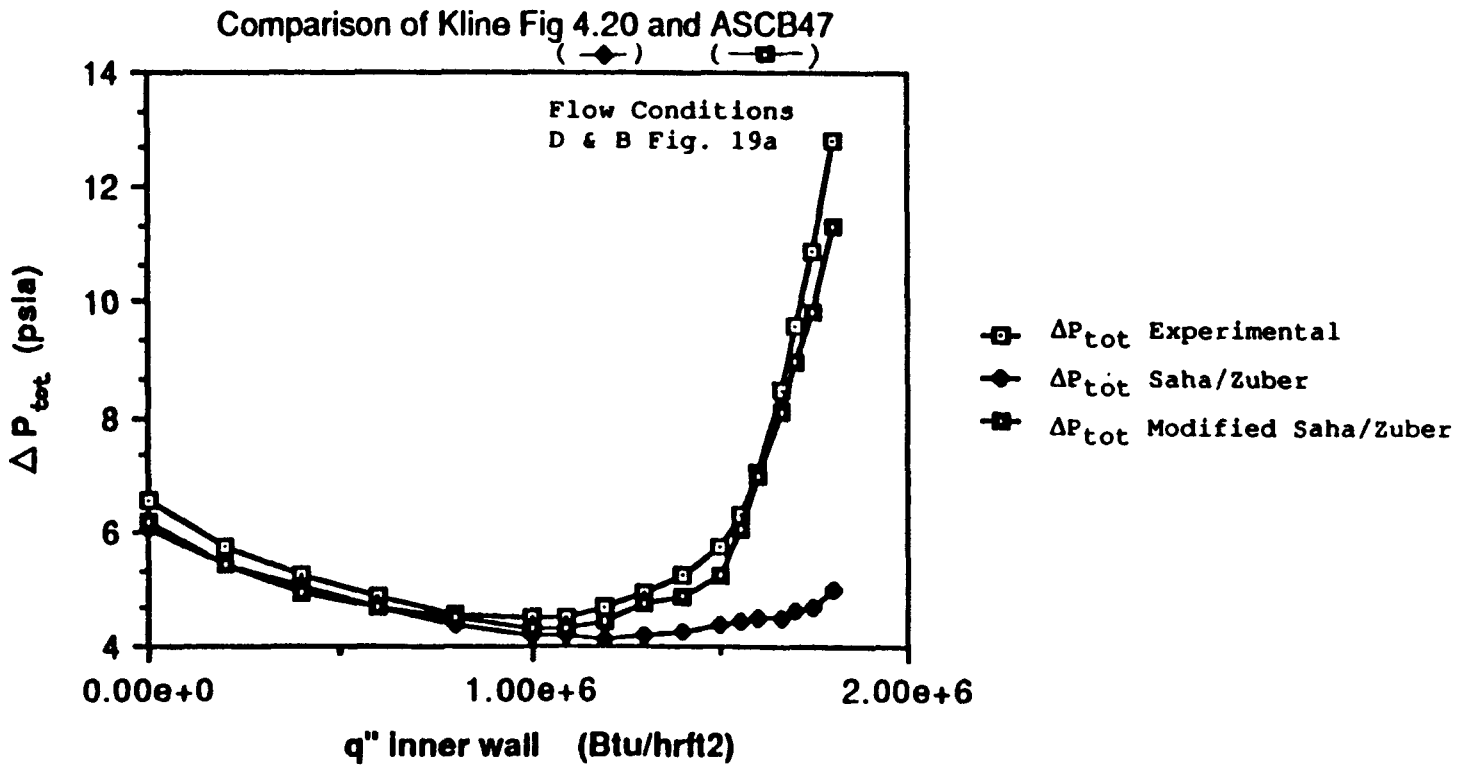

Figure 4.20 Comparison of Pressure Drop Predictions Using Saha/Zuber Correlation in Kline's SR-2F and New Modified Correlation

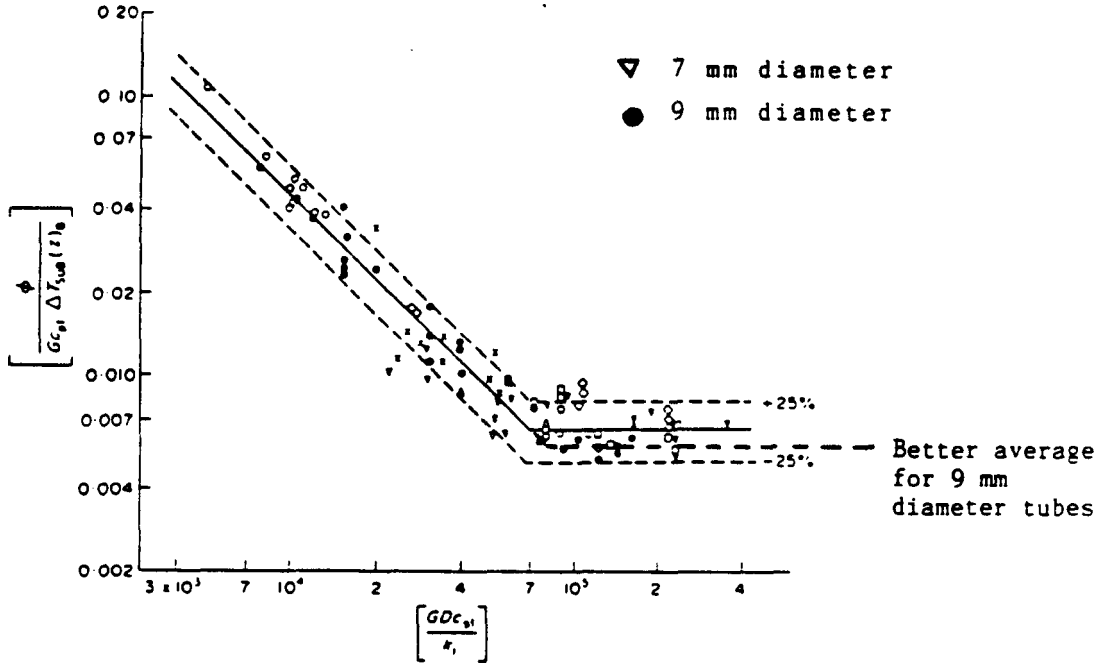

Figure 4.21 Conditions for Saha/Zuber OSNVG Point [Ref. 24]

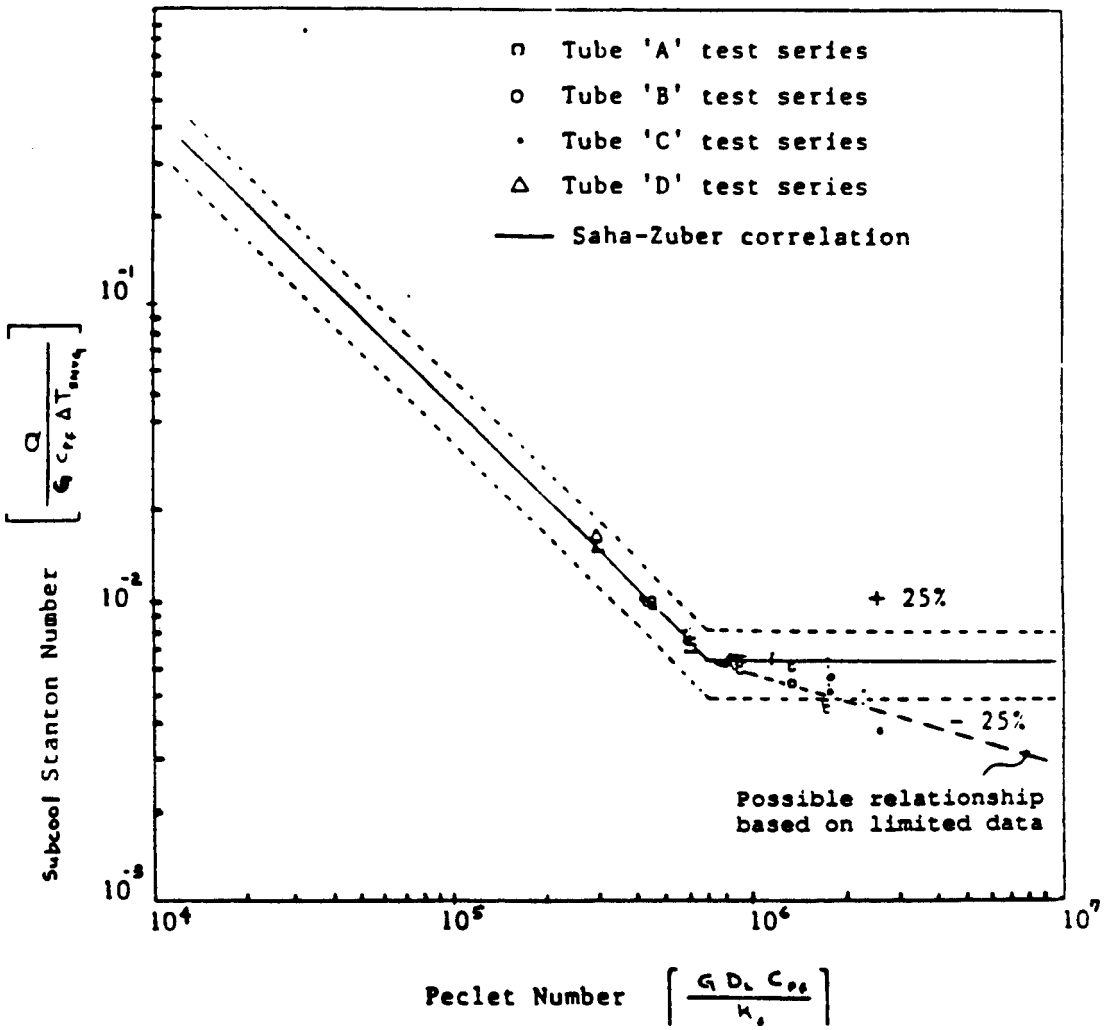

Figure 4.22 Comparison of Estimated OSNVG Points from Dormer/Bergles Experimental Data with Saha/Zuber Correlation [Ref. 3]

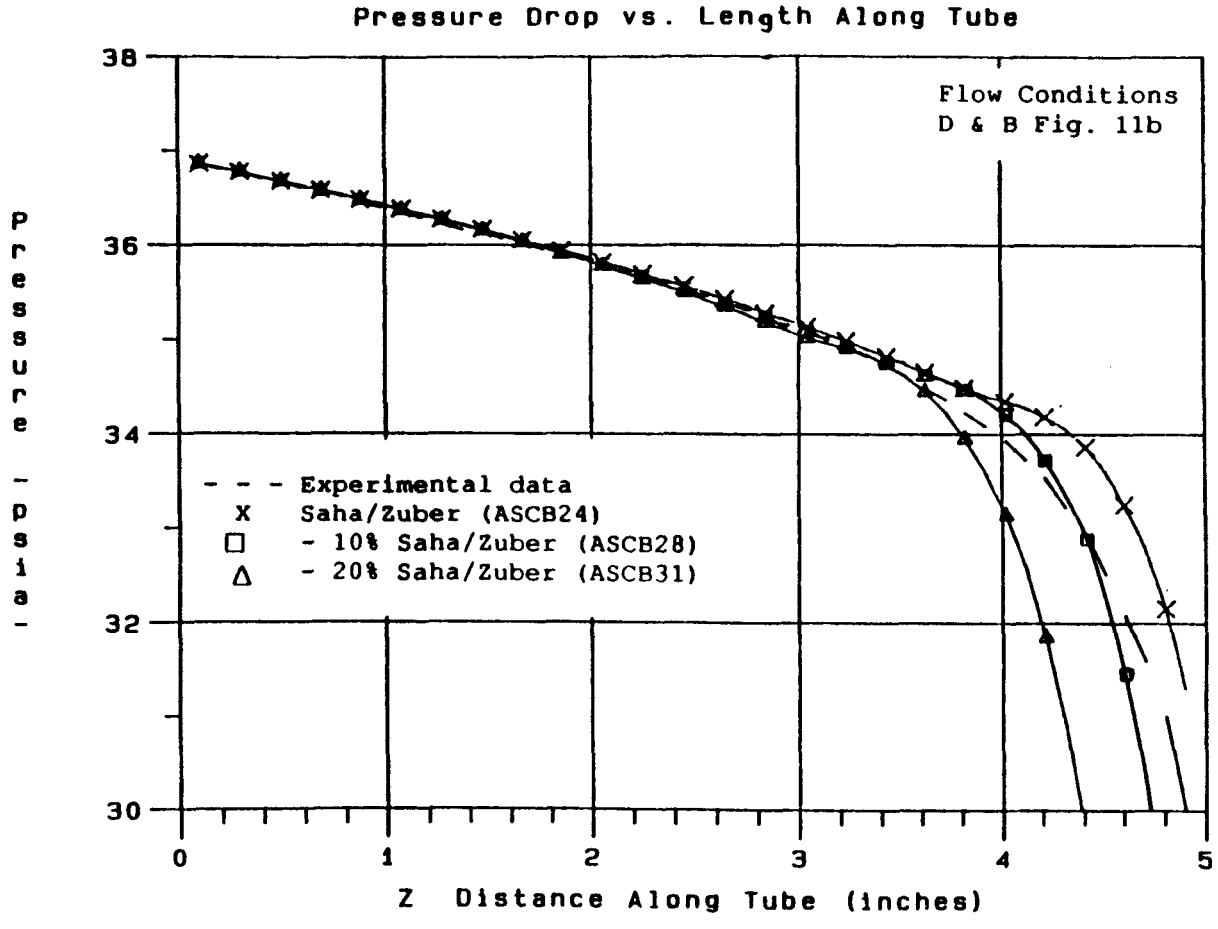

Figure 4.23 Effect of Reducing $\widetilde{St}$ in High Pe Region of Saha/Zuber Correlation

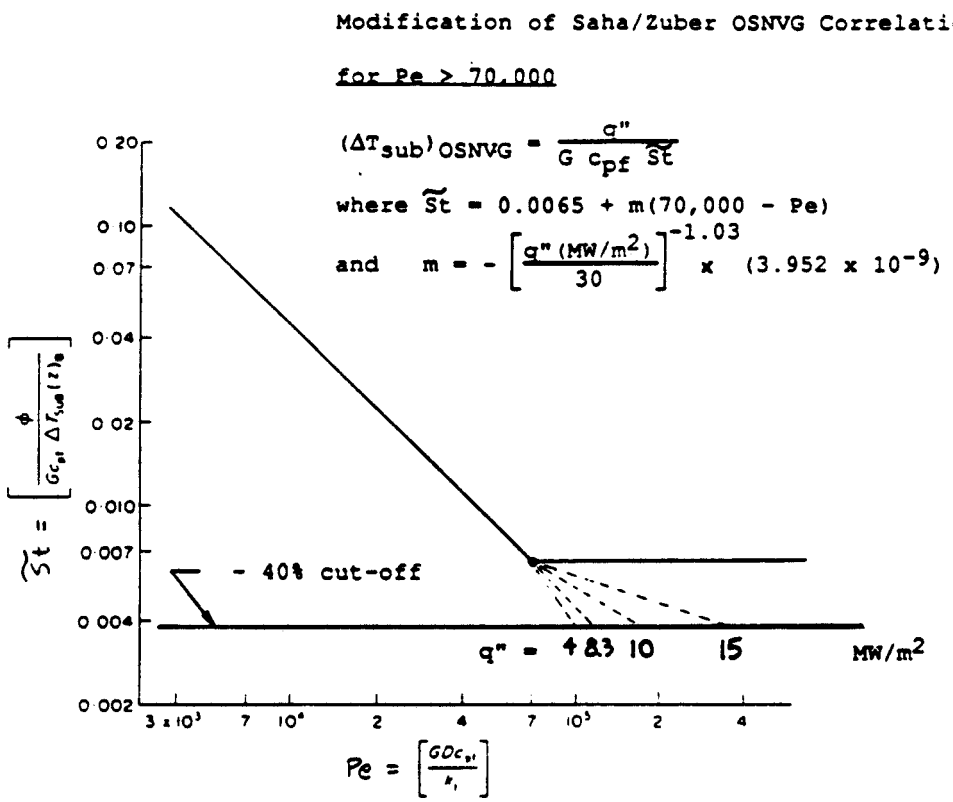

Figure 4.24 Correlation for OSNVG for the Modified Saha/Zuber Correlation

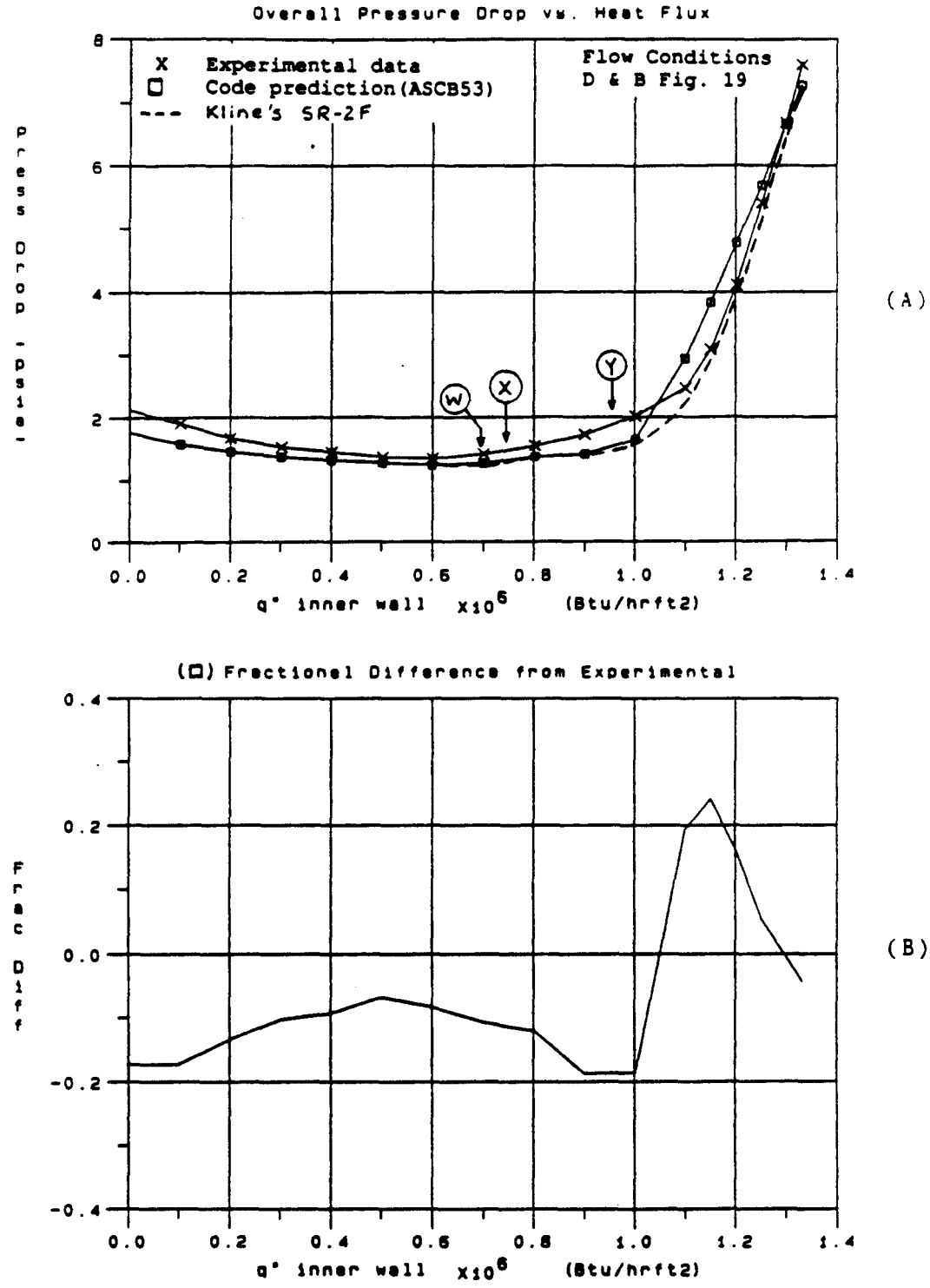

Figure 4.25 Comparison of Experimental and Code Predicted Overall Pressure Drop Results for Final Code Version ASCB53

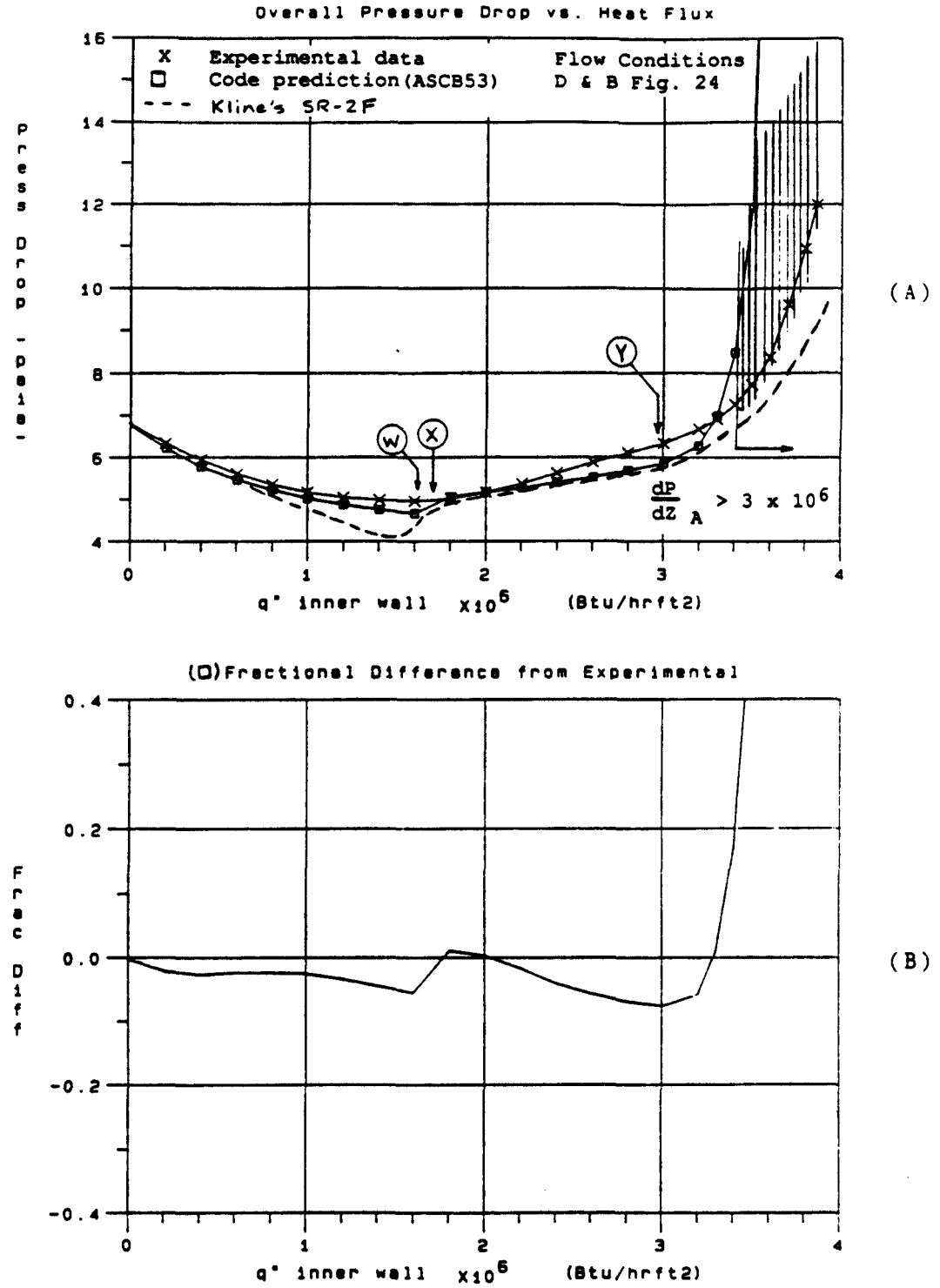

Figure 4.26 Comparison of Experimental and Code Predicted Overall Pressure Drop Results for Final Code Version ASCB53

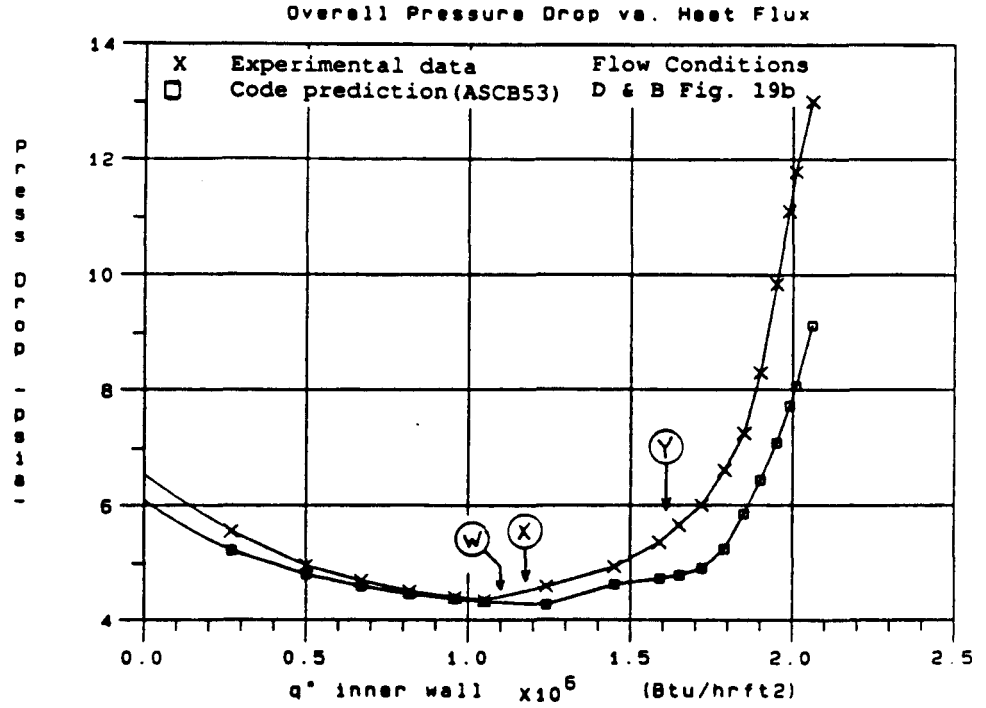

(A)

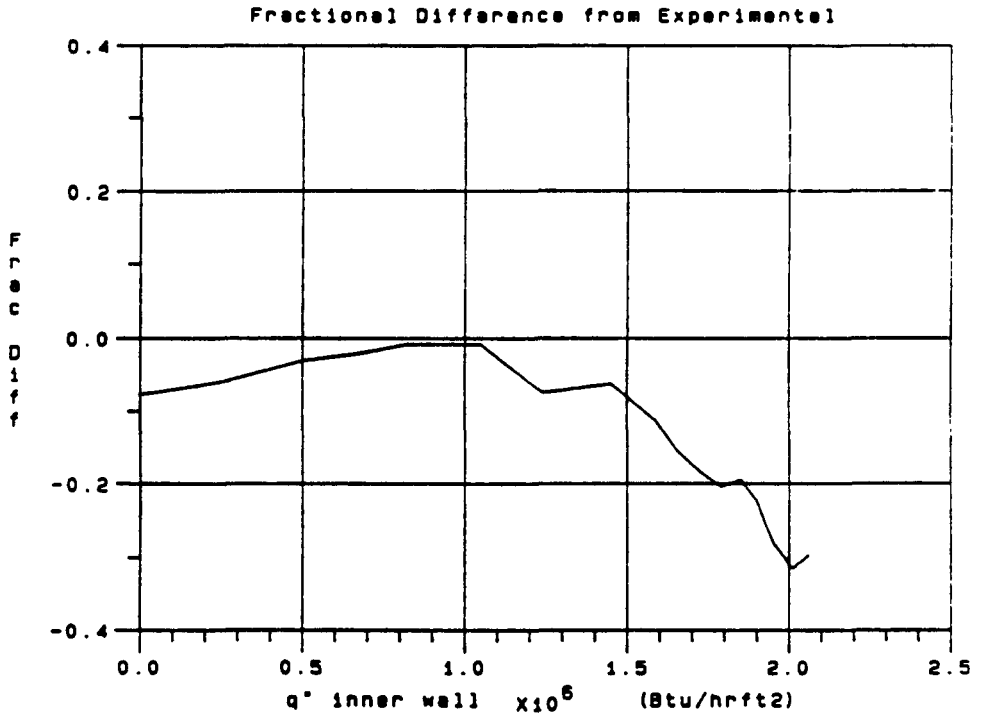

(B)

Figure 4.27 Comparison of Experimental and Code Predicted Overall Pressure Drop Results for Final Code Version ASCB53

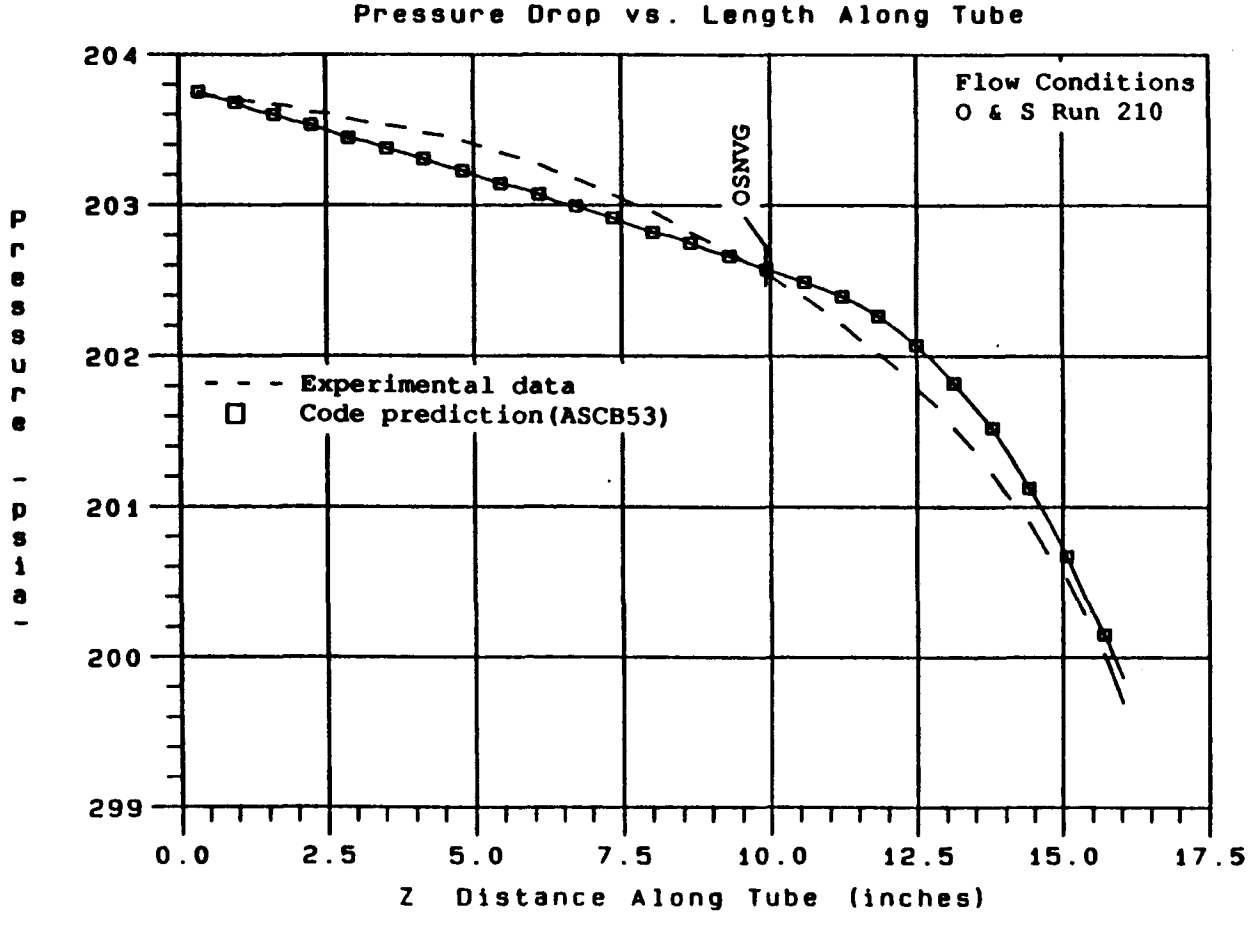

Figure 4.28 Comparison of Experimental and Code Predicted Pressure Drop Along Tube for Final Code Version ASCB53

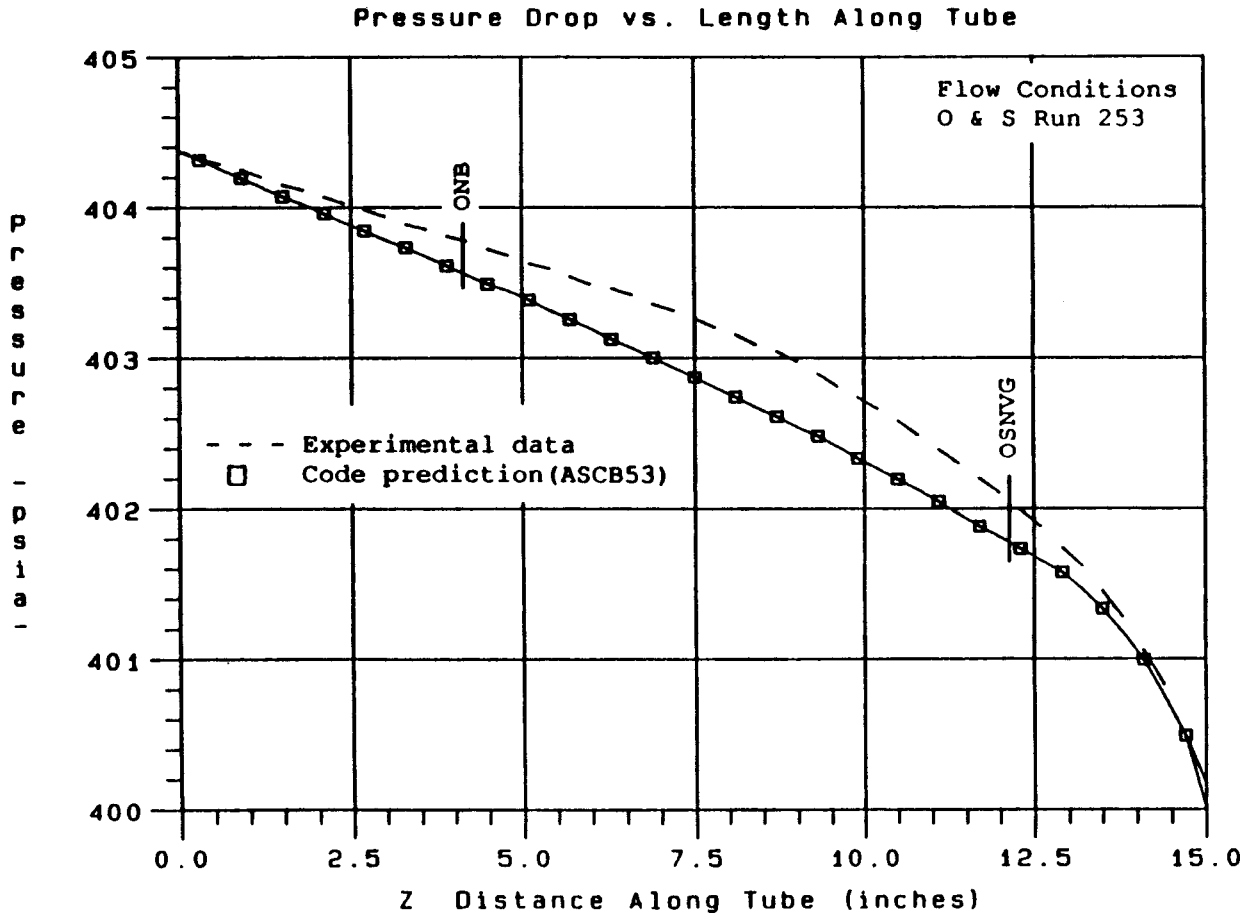

Figure 4.29 Comparison of Experimental and Code Predicted Pressure Drop Along Tube for Final Code Version ASCB53

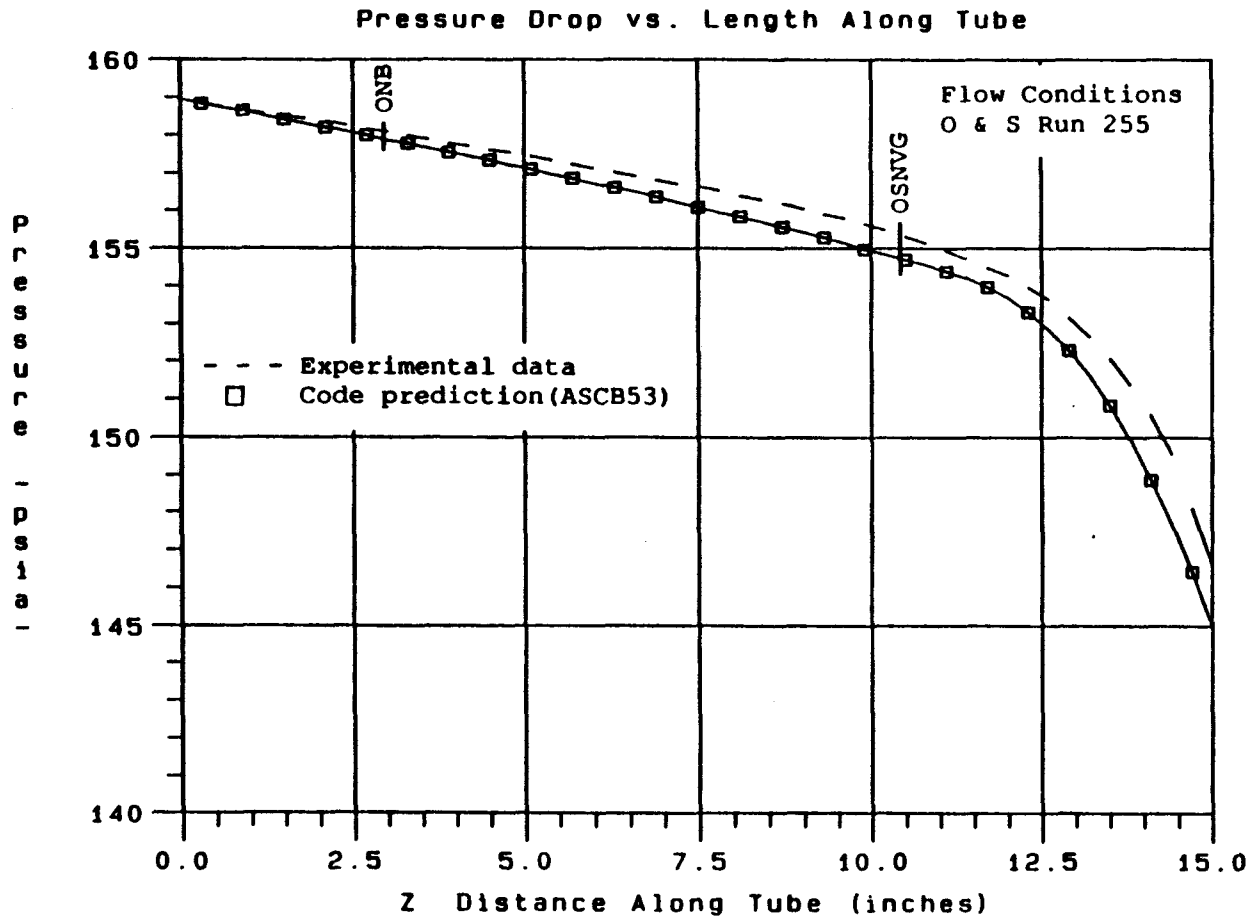

Figure 4.30 Comparison of Experimental and Code Predicted Pressure Drop Along Tube for Final Code Version ASCB53

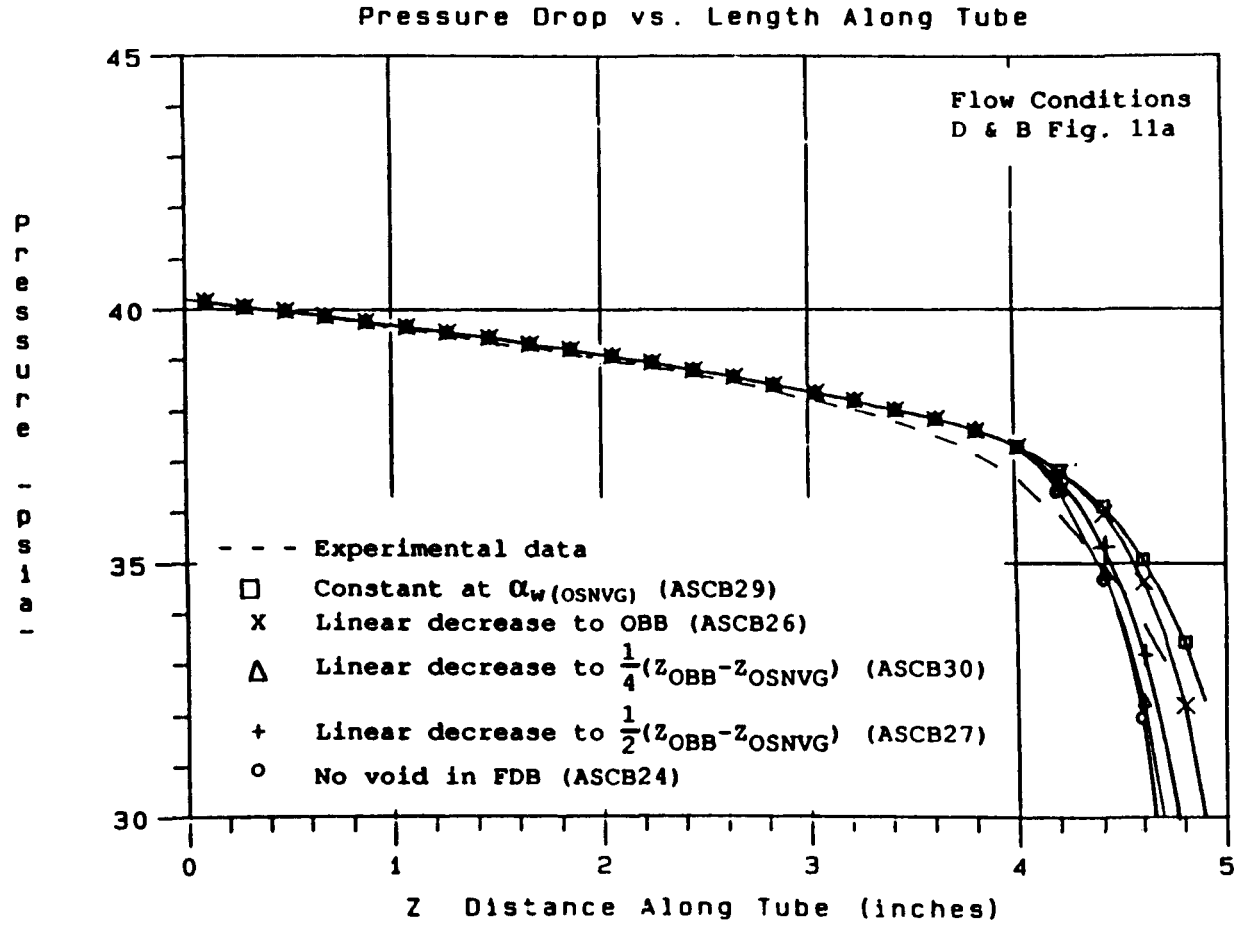

Figure 4.31 Effect of Various FDB Attached Wall Void Profiles on the Pressure Drop Predictions

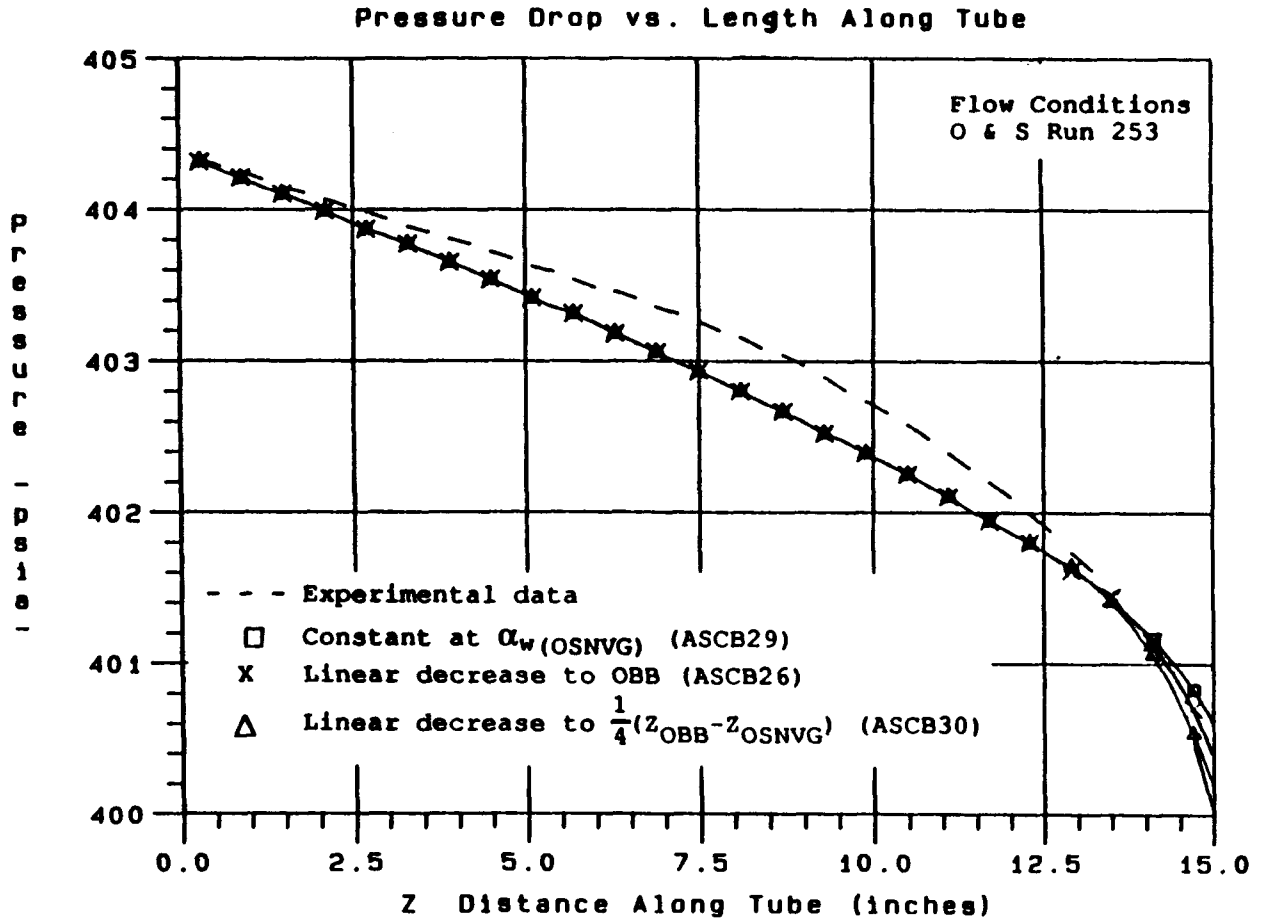

Figure 4.32 Effect of Various FDB Attached Wall Void Profiles on the Pressure Drop Predictions

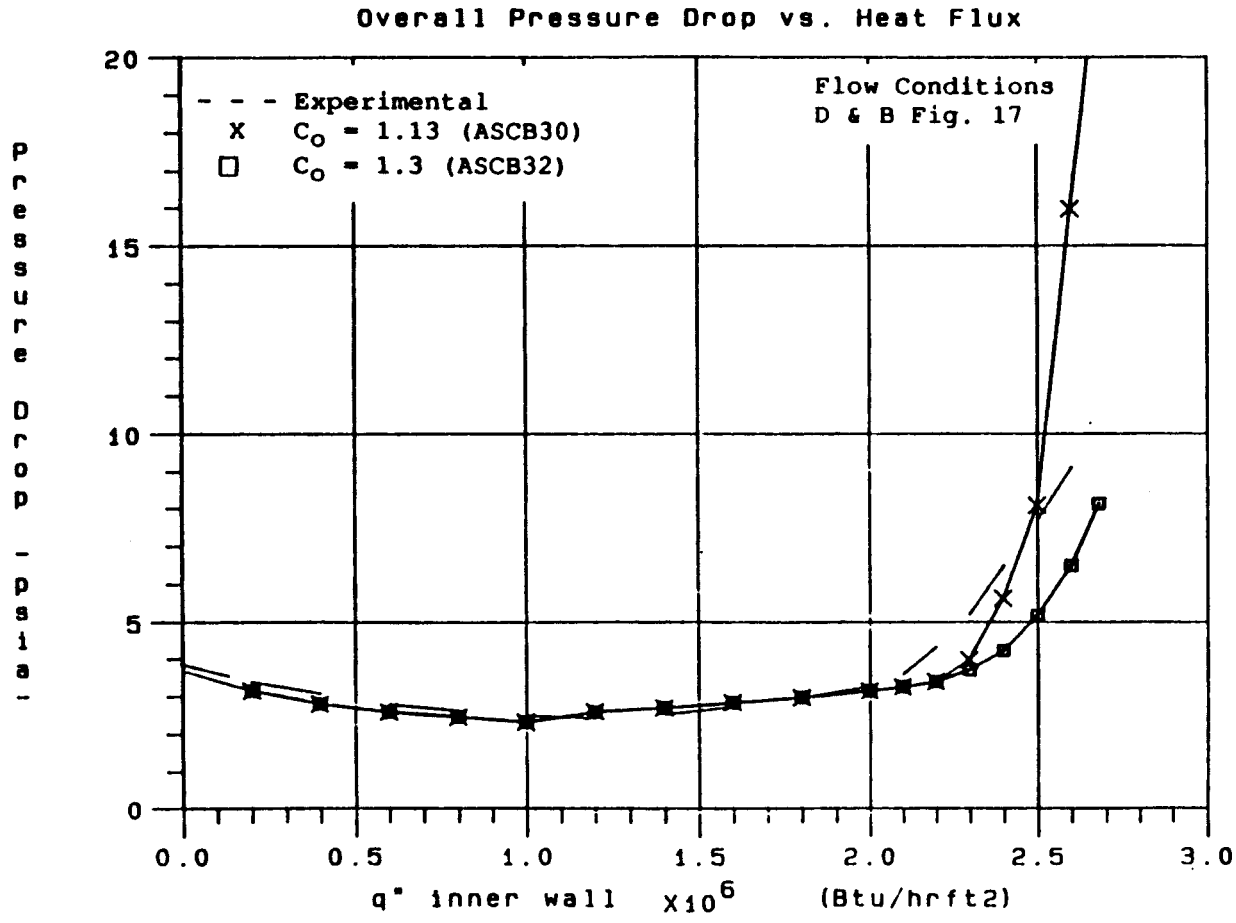

Figure 4.33 Sensitivity of Overall Pressure Drop to Changes in Flow Distribution Parameter

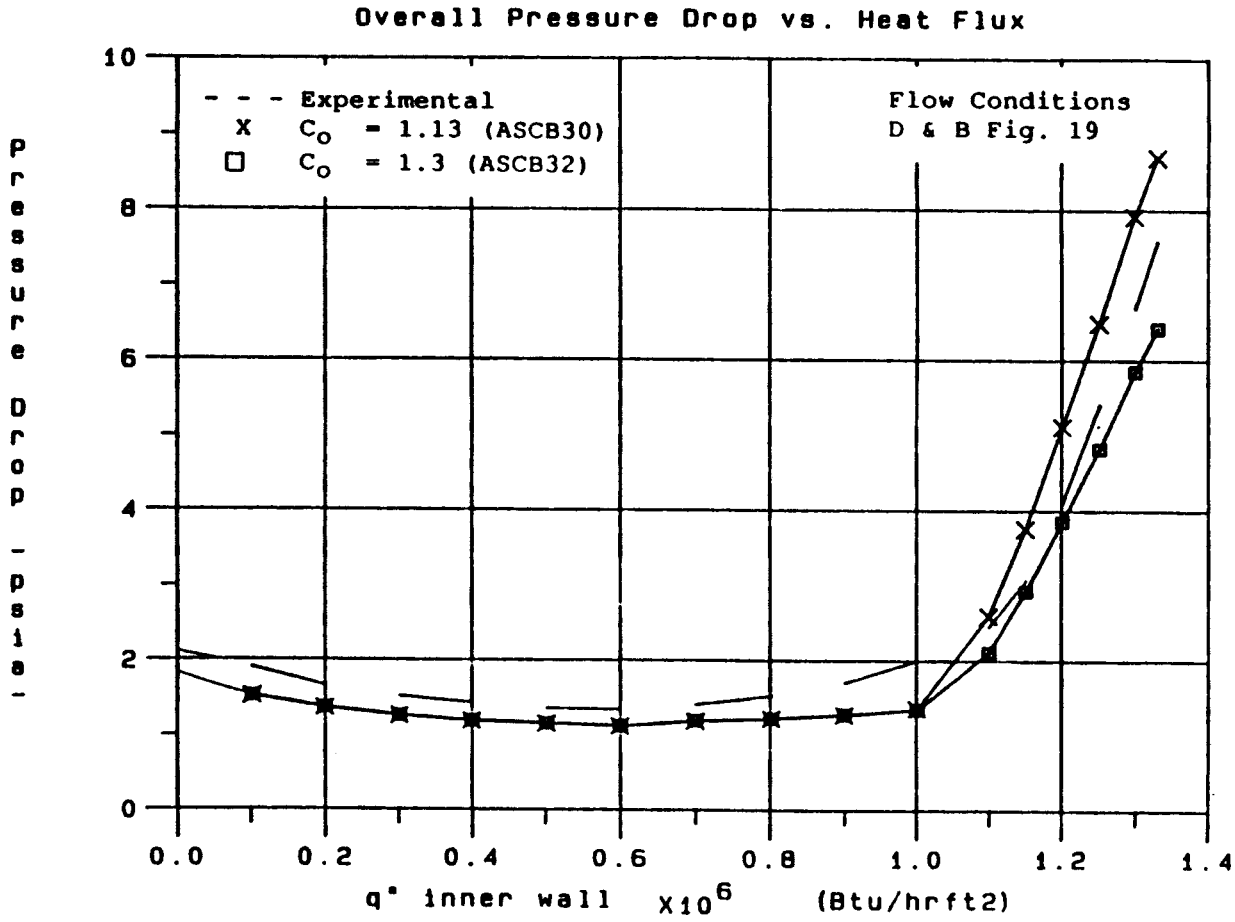

Figure 4.34 Sensitivity of Overall Pressure Drop to Changes in Flow Distribution Parameter

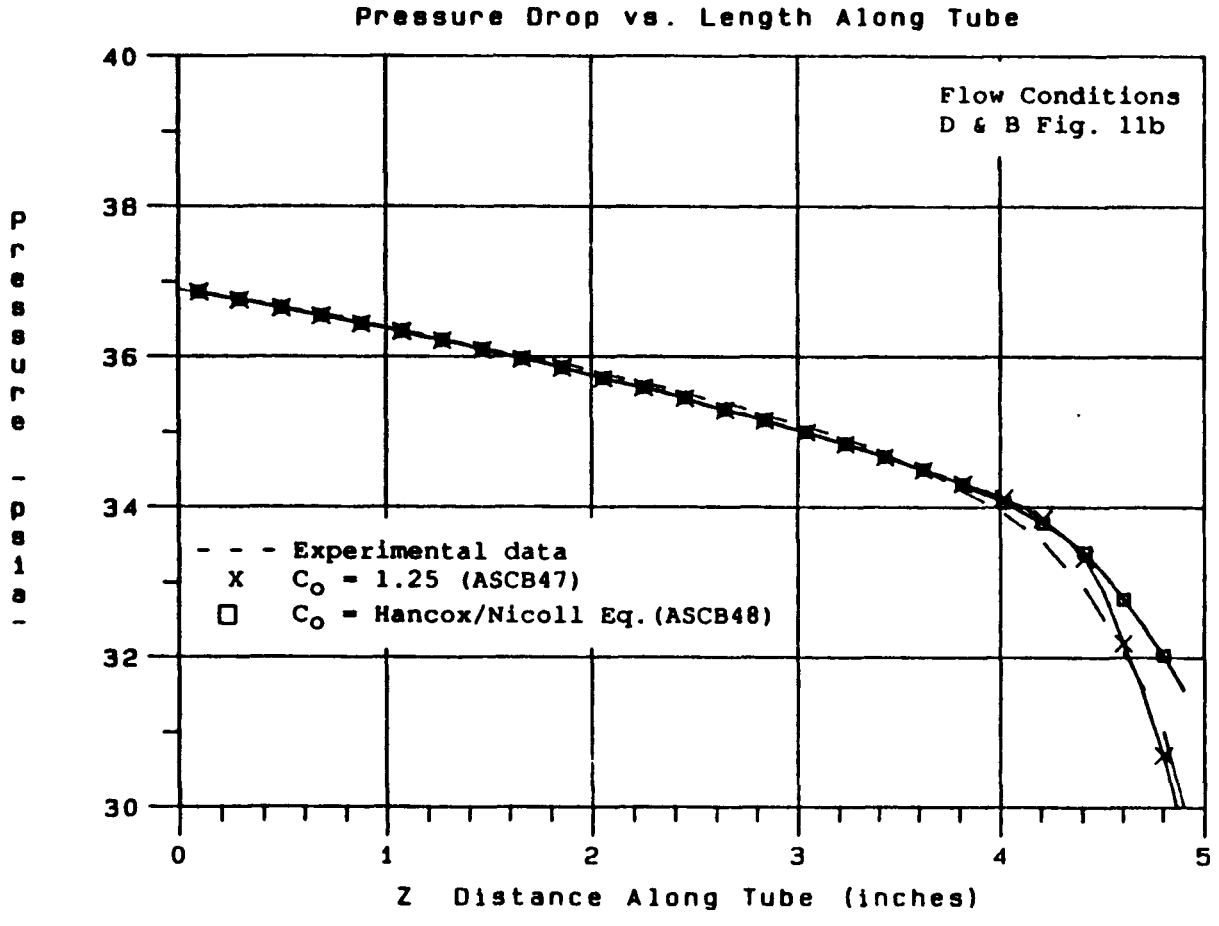

Figure 4.35 Comparison of Pressure Drop Predictions Using Constant Value and Hancox/Nicoll Distribution Parameters

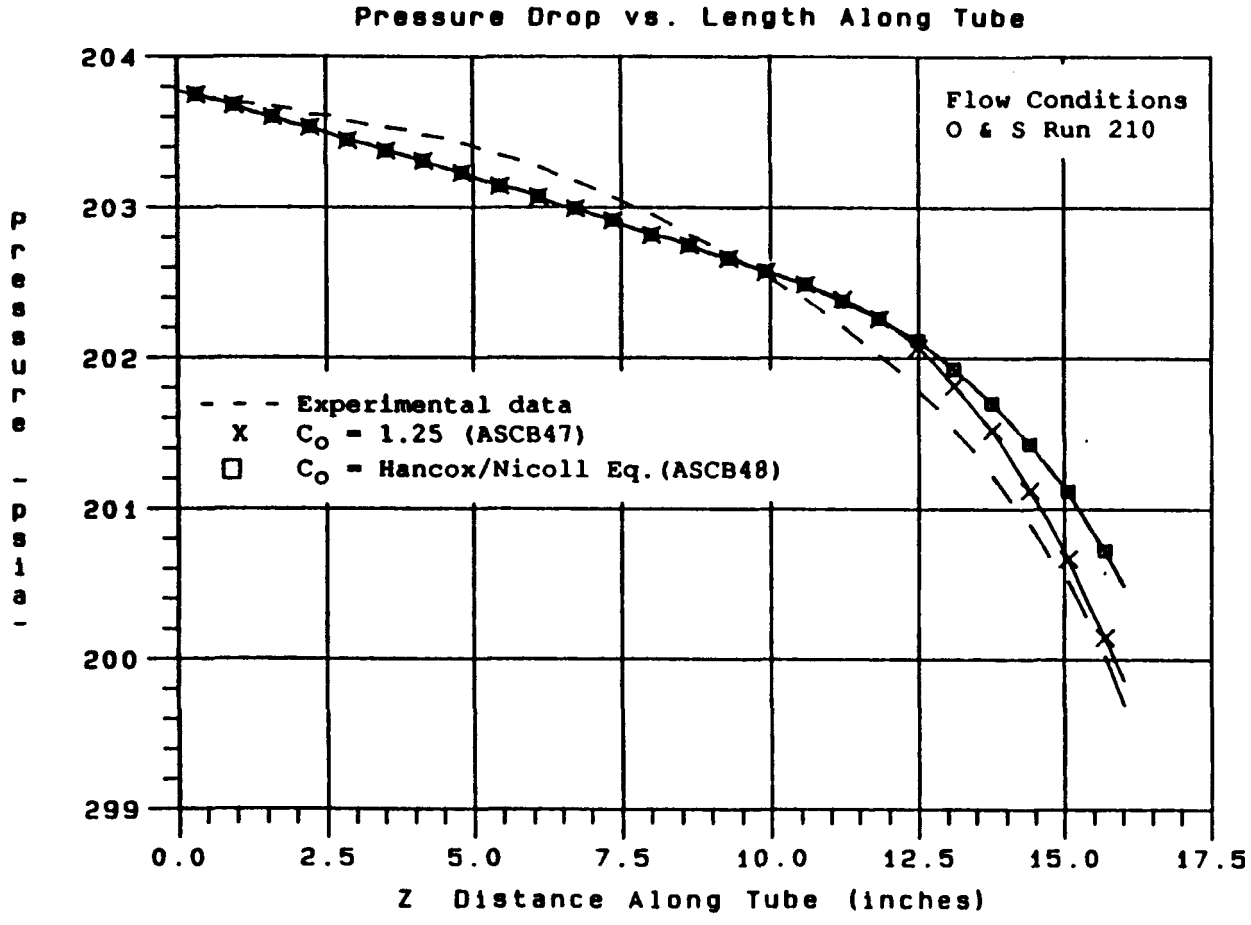

Figure 4.36 Comparison of Pressure Drop Predictions Using Constant Value and Hancox/Nicoll Distribution Parameters

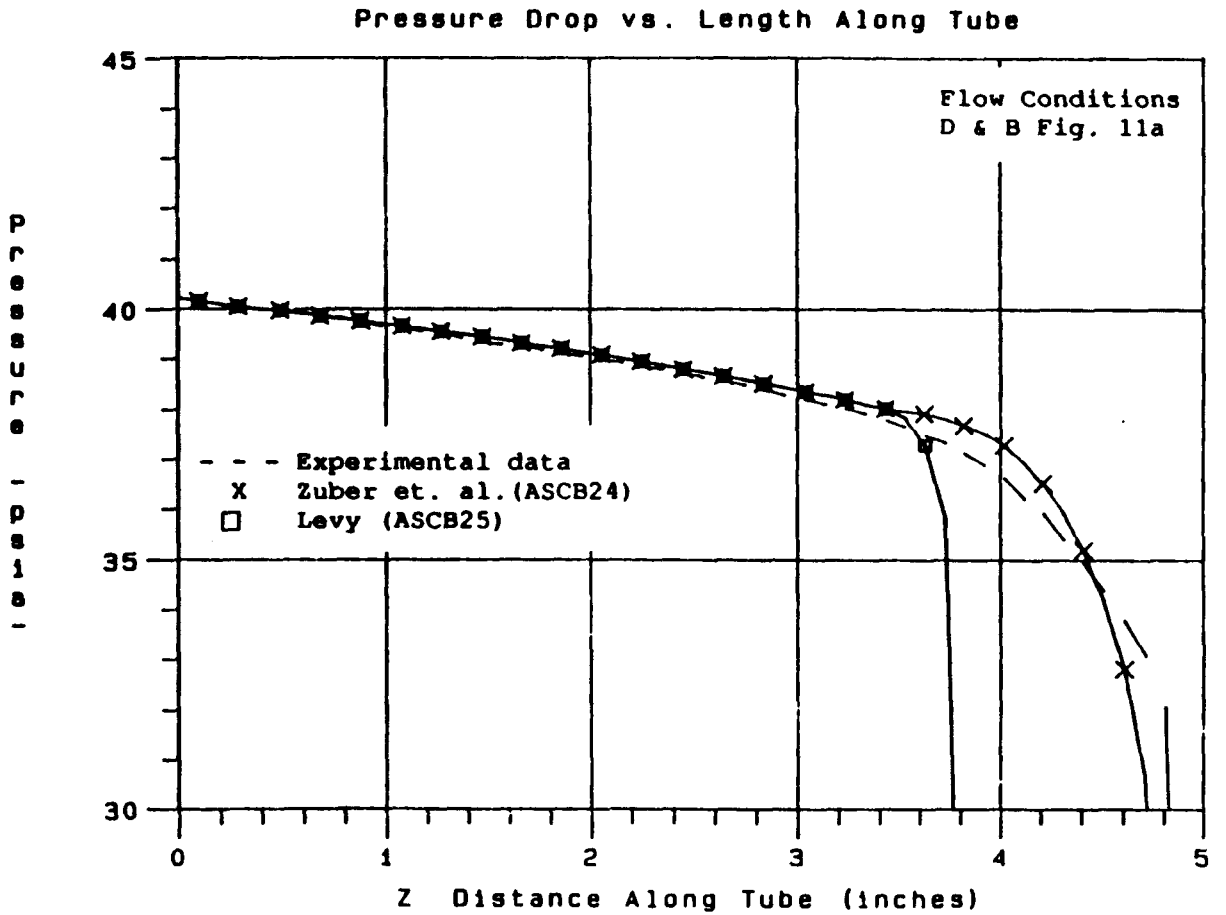

Figure 4.37 Comparison of Pressure Drop Predictions Using Levy and Zuber et. al. Flow Quality Correlations

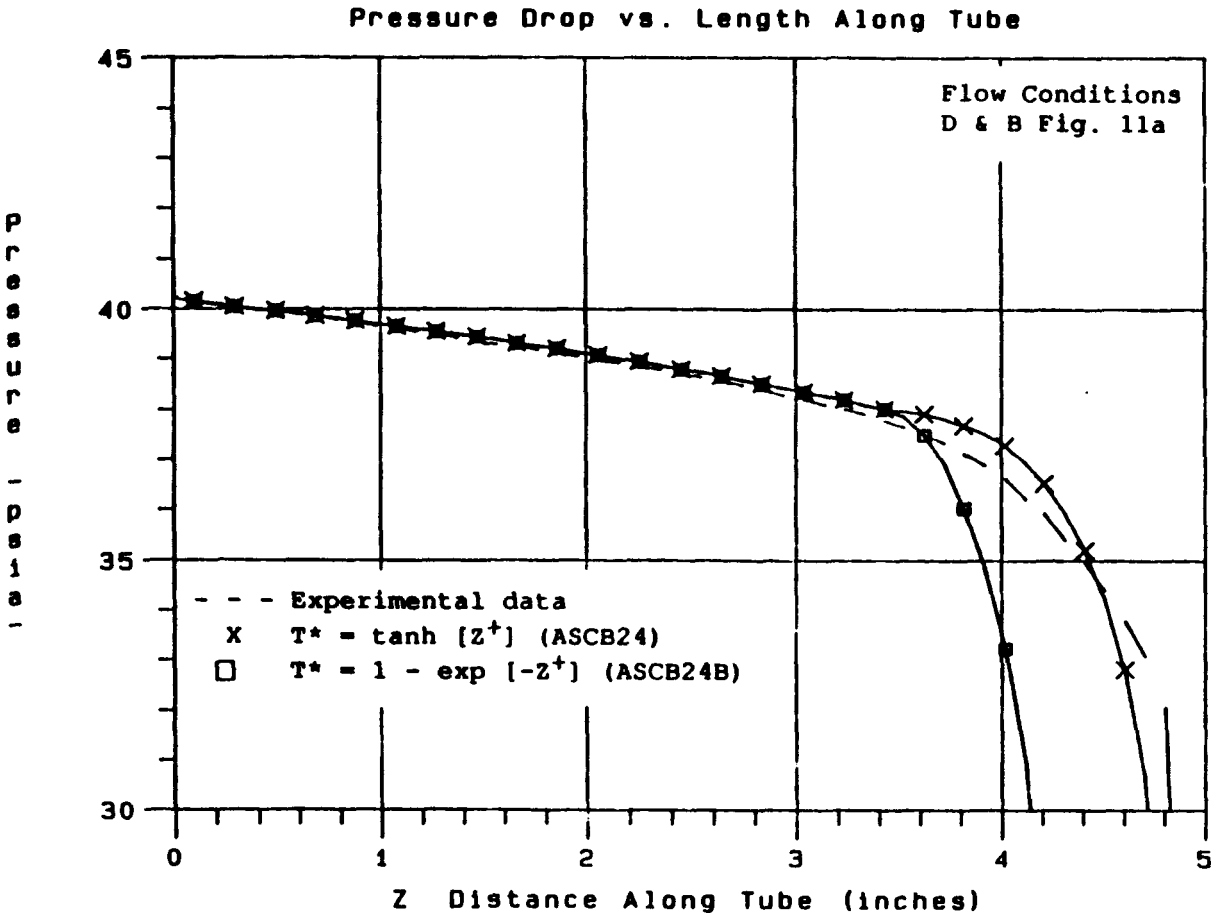

Figure 4.38 Comparison of Pressure Drop Along Tube Using Different Non-Dimensional Temperature Profiles

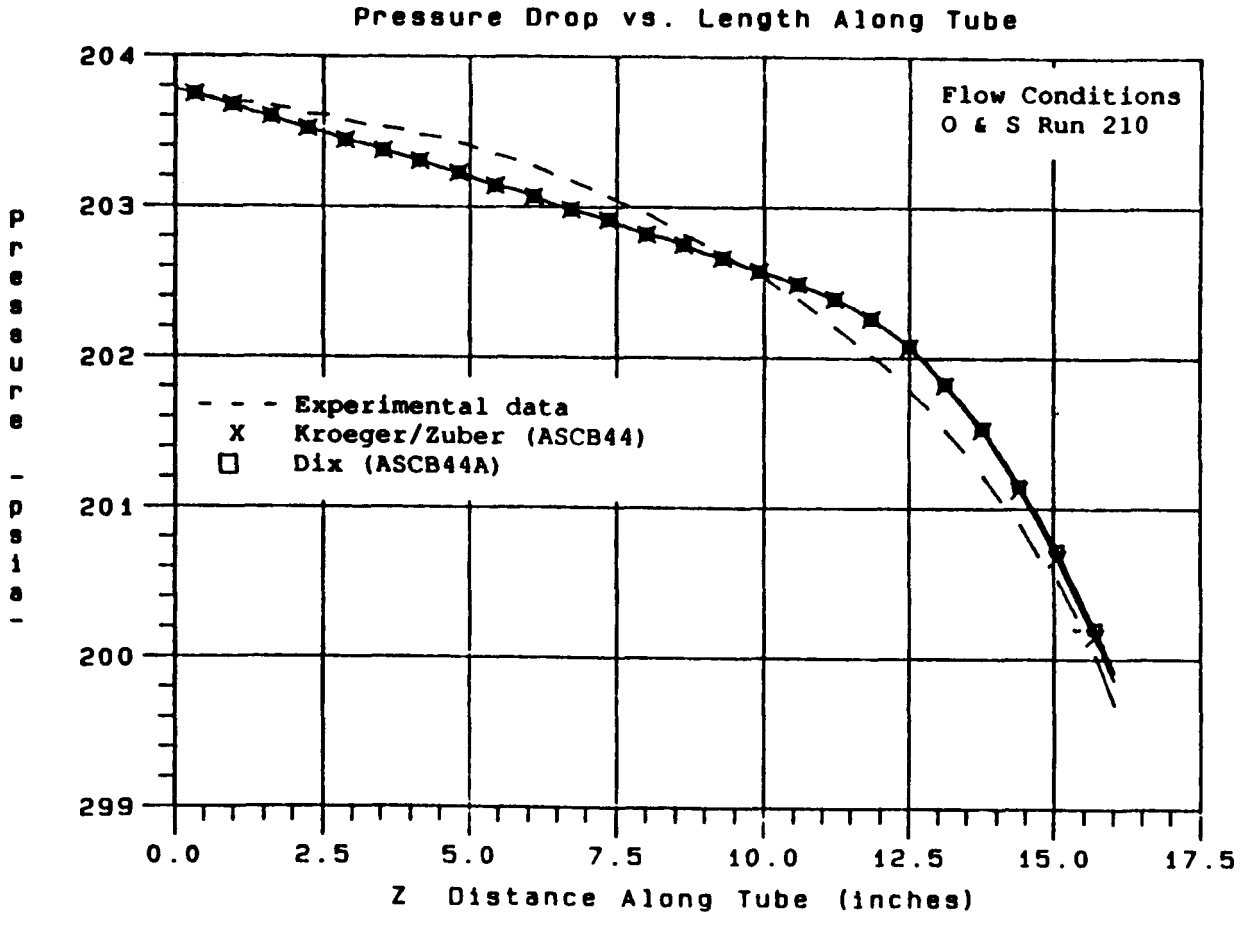

Figure 4.39 Comparison of Pressure Drop Predictions Using Kroeger/ Zuber and Dix Drift Flux Velocity Equations

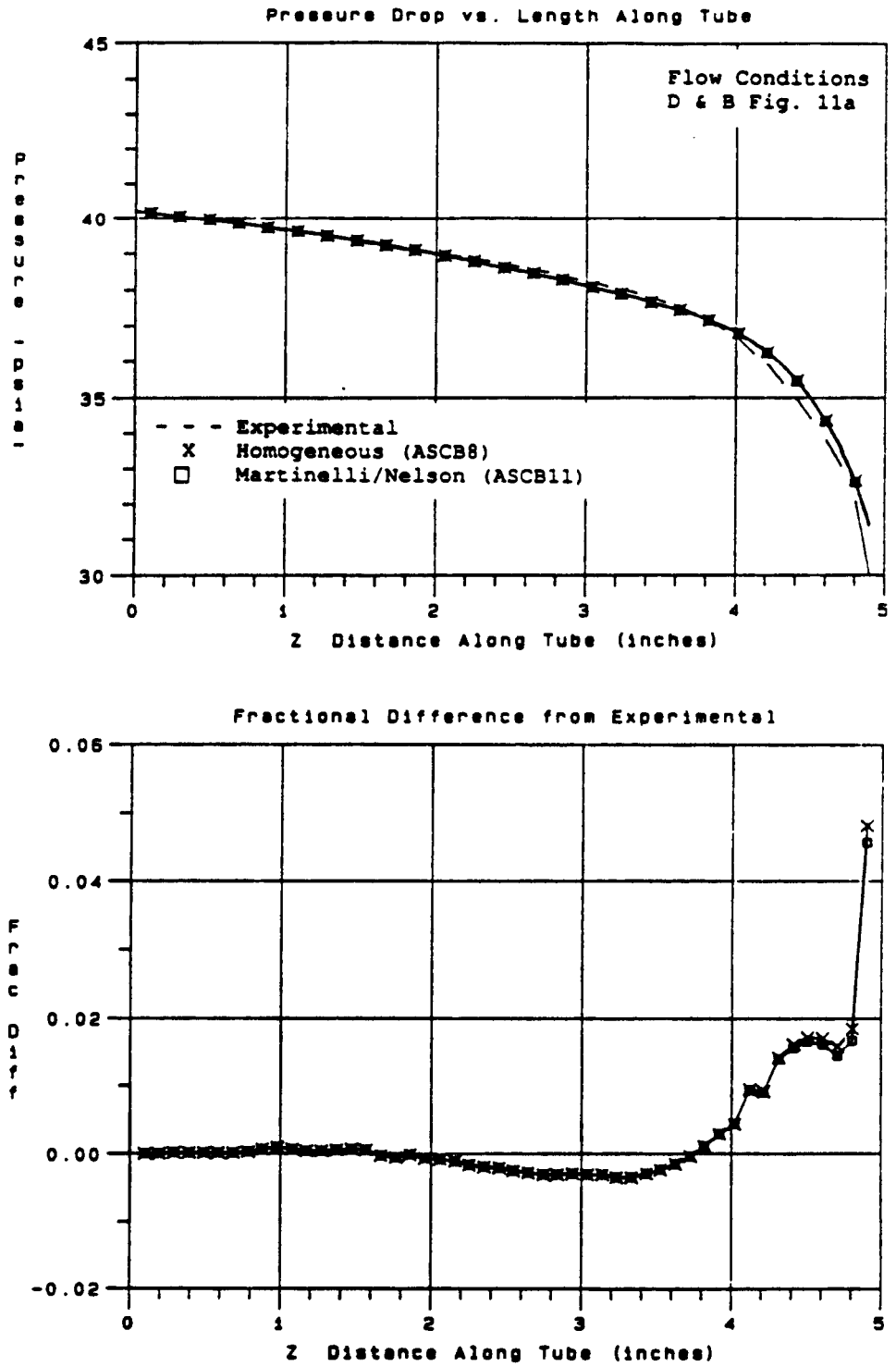

Figure 4.40 Comparison of Pressure Drop Predictions Using Homogeneous and Martinelli/Nelson Friction Factor Multipliers

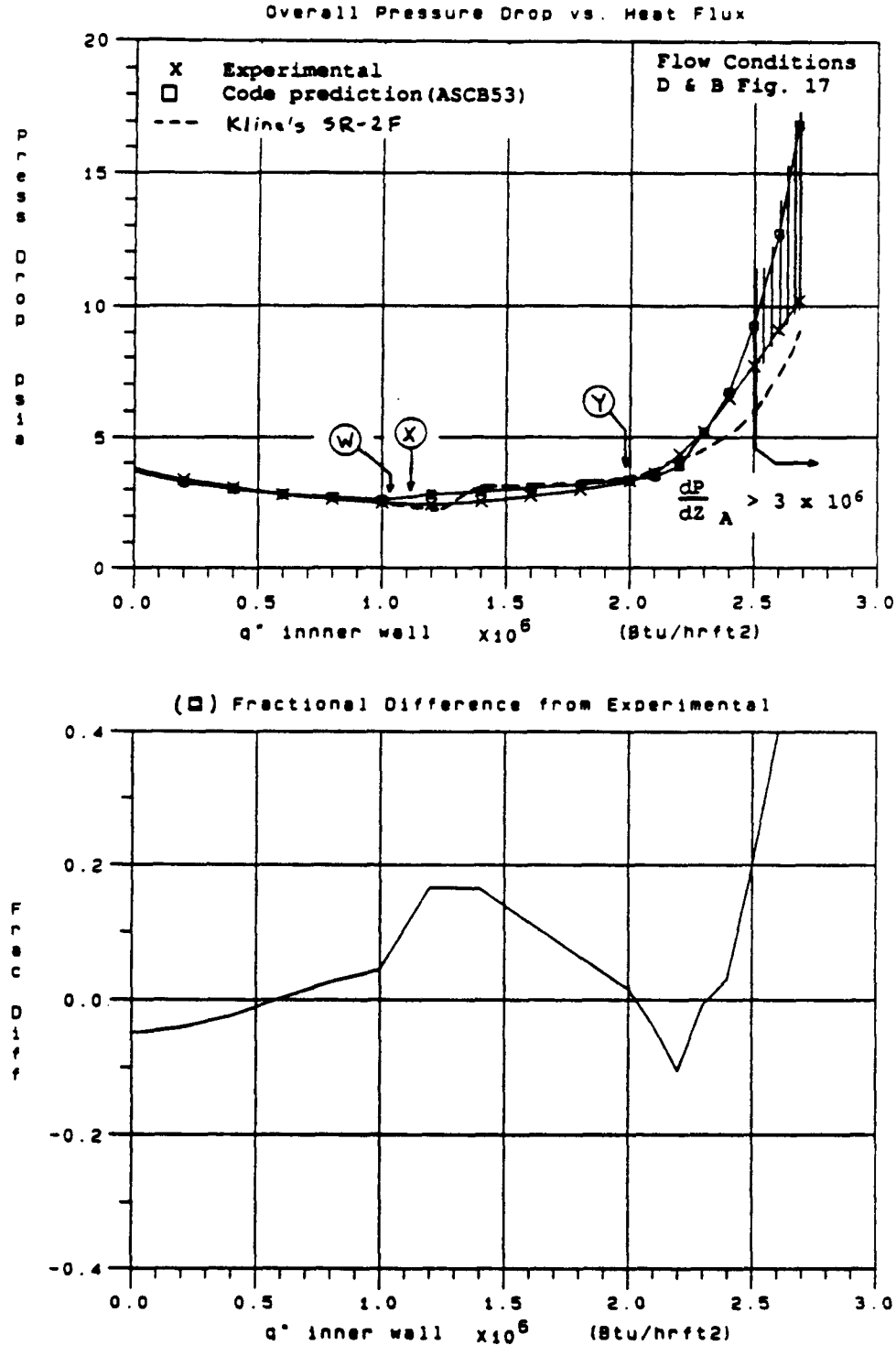

Figure 4.41 Comparison of Experimental and Code Predicted Overall Pressure Drop Results for Final Code Version ASCB53

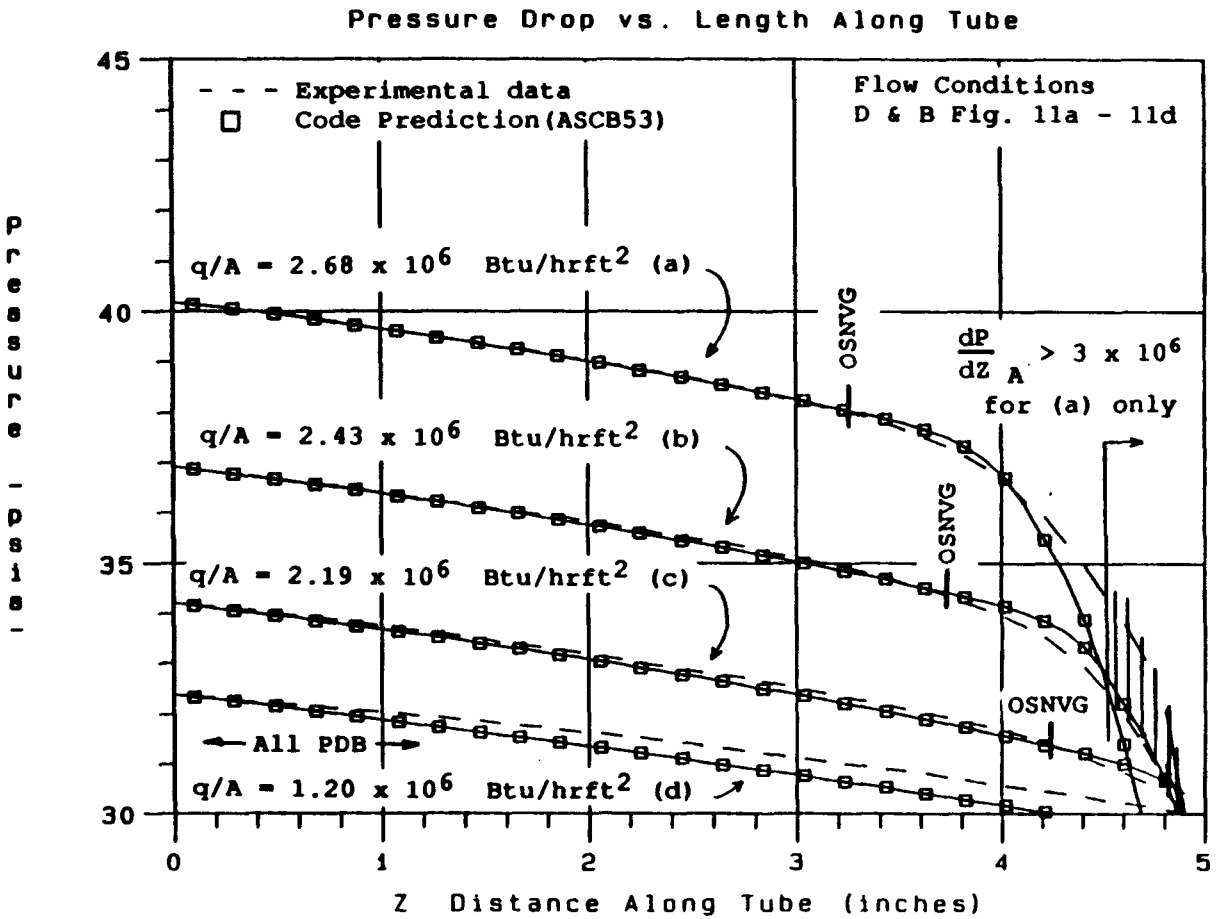

Figure 4.42 Comparison of Experimental and Code Predicted Pressure Drop Along Tube for Final Code Version ASCB53 (4 Runs Shown)

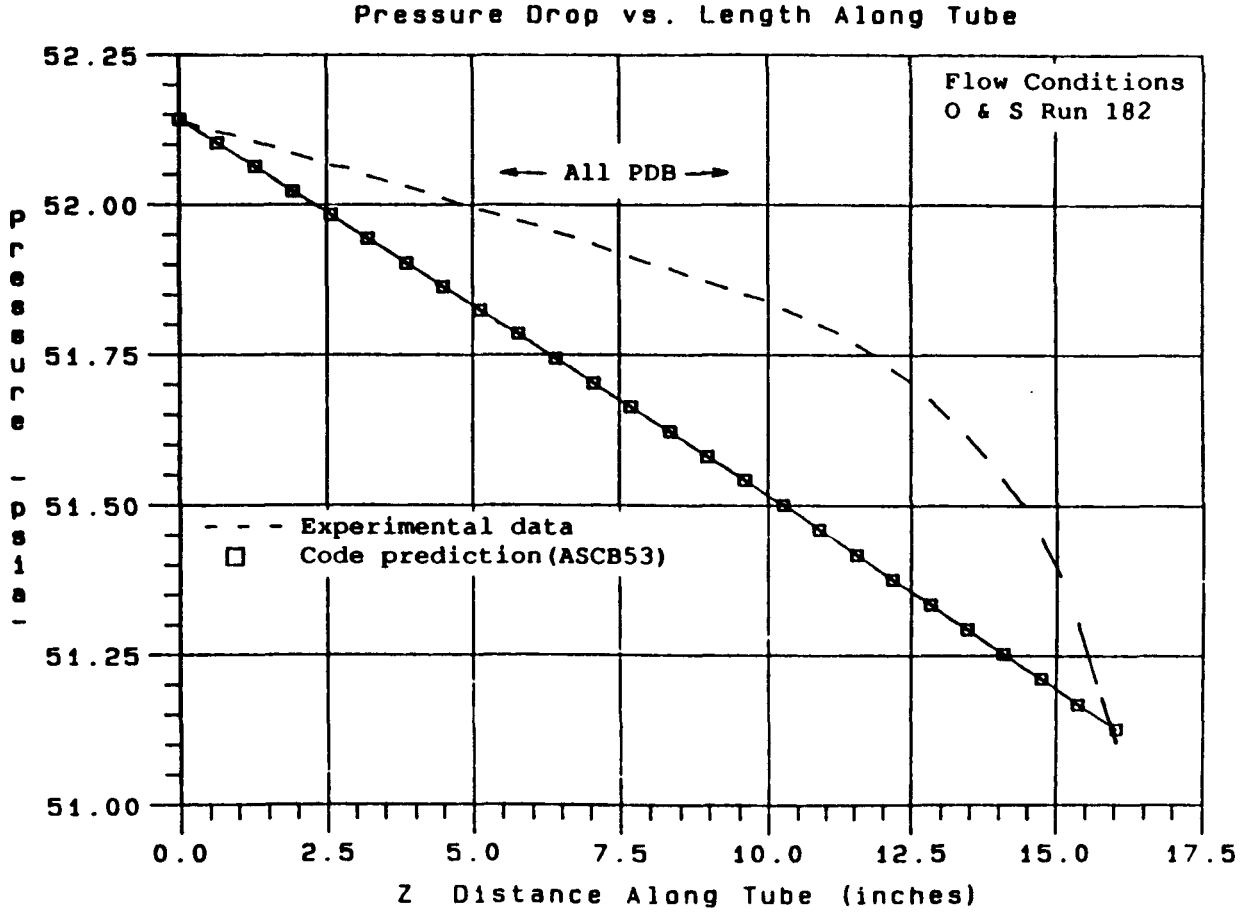

Figure 4.43 Comparison of Experimental and Code Predicted Pressure Drop Along Tube for Final Code Version ASCB53

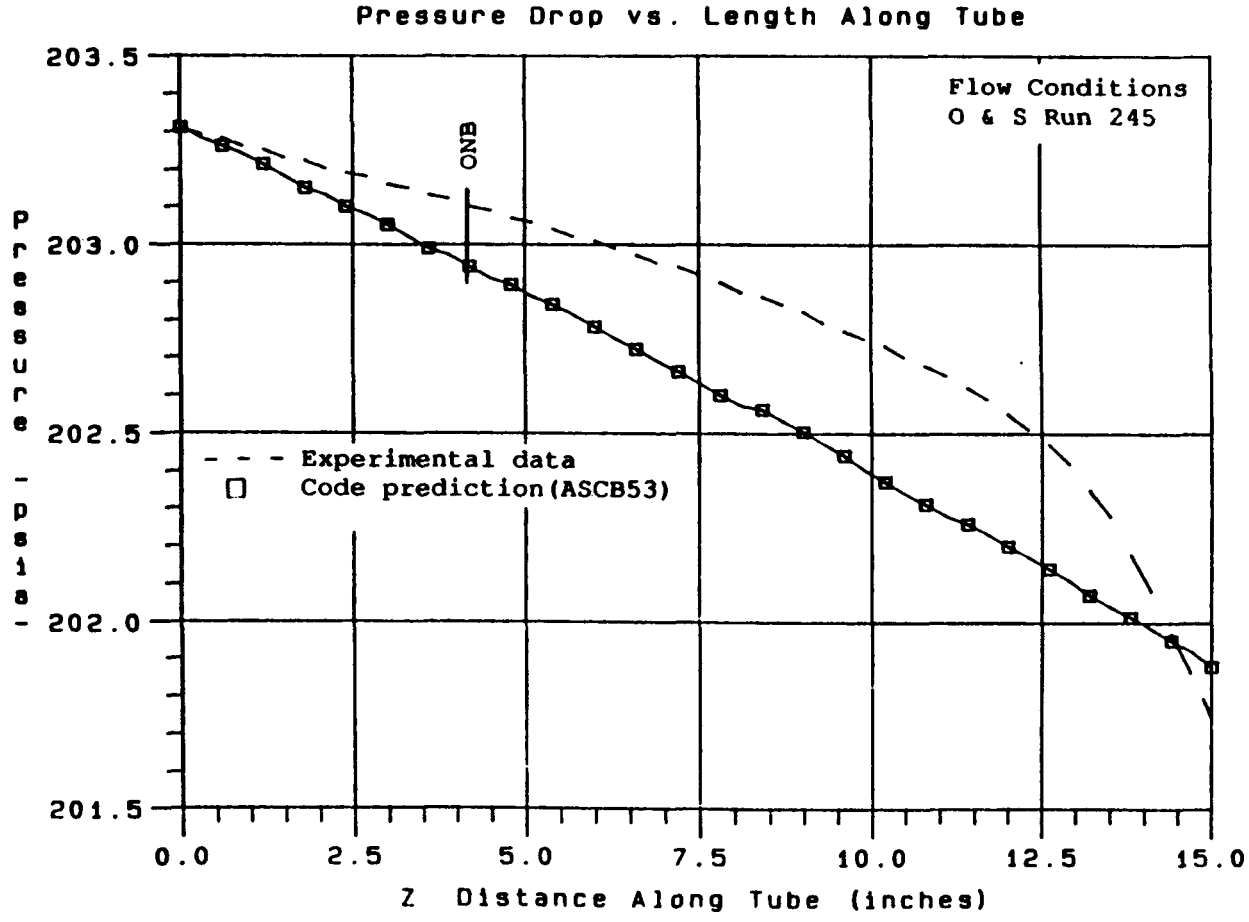

Figure 4.44 Comparison of Experimental and Code Predicted Pressure Drop Along Tube for Final Code Version ASCB53

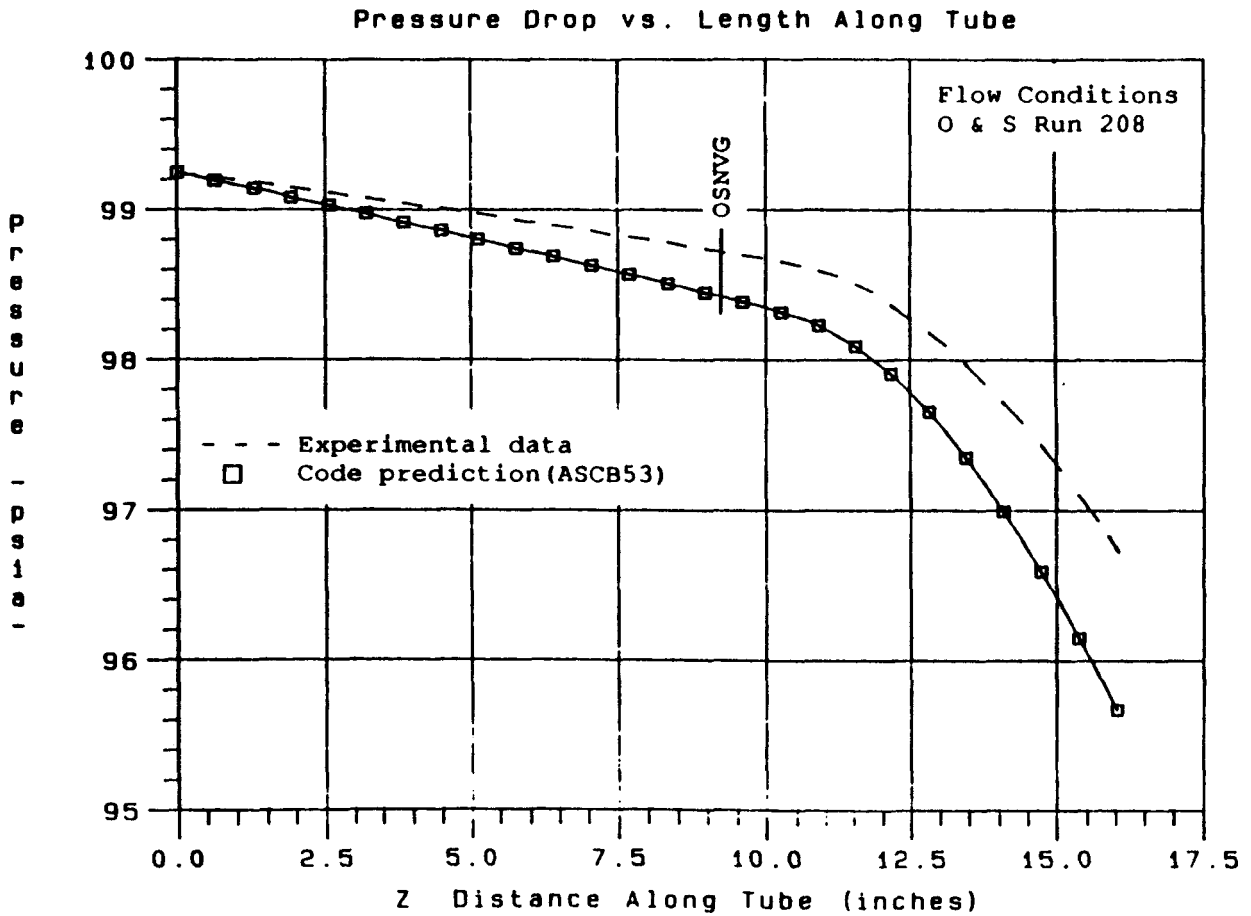

Figure 4.45 Comparison of Experimental and Code Predicted Pressure Drop Along Tube for Final Code Version ASCB53

References

1. Hewitt, G.F., "Two-Phase Flow and Its Application: Past, Present, and Future," **Heat Transfer Engineering**, Vol. 4, No. 1, pp. 67-79, Jan.-Mar. 1983.

2. Hoffman, M.A., Werner, R.W., Roose, T.R., and Carlson, G.A., "Fusion Reactor First-Wall Cooling for Very High Energy Fluxes," **Nuclear Engineering and Design**, Vol. 36, pp. 37-46, 1976.

3. Kline, C.T., "Pressure Drop Estimation Techniques for Convective Flows with Subcooled Nucleate Boiling," M.S. Thesis, Dept. of Mechanical Engineering, University of California, Davis, 1985.
   Also,
   Hoffman, M.A. and Kline, C.T., "Evaluation of Several Empirical Models for Predicting Subcooled Flow-Boiling Pressure Drops," **Multiphase Flow and Heat Transfer**, Vol. 47, pp.151-160, 1985.

4. Dormer, T. Jr., and Bergles, A.E., "Pressure Drop With Surface Boiling in Small Diameter Tubes," Technical Report No. 8767-31, Contract AF 19(604)-7344, Massachusetts Institute of Technology, Mechanical Engineering Department, September 1984.

5. Owens, W.L. and Schrock, V.E., "Local Pressure Gradients for Subcooled Boiling of Water in Vertical Tubes," ASME Paper No. 60-WA-249, 1960.

6. Reynolds, J.B., "Local Boiling Pressure Drops," Argonne National Laboratory, ANL-5178, March 1954.

7. Mendler, O.J., Rathbun, A.S., Van Huff, N.E., and Weiss, A.,"Natural Circulation Tests with Water at 800 to 2000 psia Under Nonboiling, Local Boiling, and Bulk Boiling Conditions," **ASME Journal of Heat Transfer**, August 1961.

8. Kroeger, P., and Zuber, N., "An Analysis of the Effects of Various Parameters on the Average Void Fractions in Subcooled Boiling," **International Journal of Heat and Mass Transfer**, Vol. 11, pp. 211-223, 1968.

9. Zuber, N., Staub, F., and Bijwaard, G., "Vapor Void Fraction in Subcooled Boiling and in Saturated Boiling Systems," **Proc. Third International Heat Transfer Conference**, Vol. 5, pp. 24-38, Aug. 1966, Chicago, Ill., prepared by AIChE.

10. Jia, D., and Schrock, V.E., "A Generalized Procedure for Predicting the Pressure Drop in a Subcooling Boiling Channel," **Proc. Fourth International Symposium on Multi-Phase Transport and Particulate Phenomena**, 1986, Miami, FL.

11. Hancox, W.T., and Nicoll, W.B., "A General Technique for the Prediction of Void Distribution in Non-Steady Two-Phase Forced Convection," **International Journal of Heat and Mass Transfer**, Vol. 14, pp. 1377-1394, 1971.

12. Bergles, A.E. and Rohsenow, W.M., "The Determination of Forced Convection Surface Boiling Heat Transfer," Paper 63-HT-22 presented at 6th National Heat Transfer Conference of the ASME-AIChE, Boston, August 11-14, 1963.

13. Davis, E.J. and Anderson, G.H. "The Incipience of Nucleate Boiling in Forced Convection Heat Transfer," **AIChE Journal**, Vol. 12, No. 4, pp. 774-780, July 1966.

14. Hsu, Y.Y., "On the Size of Range of Active Nucleation Cavities on a Heating Surface," **Transactions ASME Journal of Heat Transfer**, Vol. 84, p. 207, 1962.

15. Saha, P. and Zuber, N., "Point of Net Vapor Generation and Vapor Void Fraction in Subcooled Boiling," **Proc. Fifth International Heat Transfer Conference**, Vol. 4, Section B4.7, pp. 175-179, Toyko, Japan, Sept. 1974.

16. Shah, M., "A General Correlation for Heat Transfer During Subcooled Boiling in Pipes and Annuli", **ASHRAE Trans.**, Vol. 83, Pt. 1, 1977.

17. Dix, G.E., "Vapor Void Fractions for Forced Convection with Subcooled Boiling at Low Flow Rates," Paper NEDO-10491, General Electric Co., 1971.

18. Martinelli, R.C. and Nelson, D.B., "Prediction of Pressure Drop During Forced-Circulation Boiling of Water," Transactions ASME, Vol. 70, pp. 695-702, 1948.

19. Chisholm, D.,"Two-Phase Flow in Pipelines and Heat Exchangers," George Godwin Publishers, London and New York, 1983.

20. Levy, S., "Forced Convection Subcooled Boiling Prediction of Vapor Volumetric Fraction," **International Journal of Heat and Mass Transfer**, Vol. 10, pp. 951-965, 1967.

21. Rouhani, S., "Calculation of Steam Volume Fraction in Subcooled Boiling," **Journal of Heat Transfer**, pp. 158-164, February 1968.

22. Sieder, E.N. and Tate, G.E., "Heat Transfer and Pressure Drop of Liquid in Tubes," **Industrial Engineering Chemistry**, Vol. 28, pp.1429-1436, 1936.

23. Petukhov, B., "Heat Transfer and Friction in Turbulent Pipe Flow," Chapter, IV in book "Advances in Heat Transfer," Vol. 6, edited by J. Hartnett and T. Irvine, p. 503, Academic Press, 1970.

24. Collier, J., "Convective Boiling and Condensation," Second Edition, McGraw Hill Book Company, New York, NY, 1981.

25. Hirata, M. and Nishiwaki, N., "Skin Friction and Heat Transfer for Liquid Flow Over a Porous Wall with Gas Injection," **International Journal of Heat and Mass Transfer**, Vol. 6, pp. 941-949, 1963.

26. Hino, R. and Ueda, T., "Study on Heat Transfer and Flow Characteristics in Subcooled Flow Boiling-Part 1. Boiling Characteristics," **Int. J. Multiphase Flow**, Vol. 11, No. 3, pp. 269-281, 1985.

27. Zuber, N. and Findley, J., "Average Volumetric Concentration in Two-Phase Flow Systems," **Journal of Heat Transfer**, pp. 453-468, Nov. 1965.

28. Unal, H.C., "Void Fraction and Incipient Point of Boiling During the Subcooled Nucleate Flow Boiling of Water," **International Journal or Heat and Mass Transfer**, Vol. 20, pp. 409-419, Pergamon Press, 1977.

29. "Heat Transfer and Fluid Flow Data Book," Vol. 1-Heat Transfer, Corporate Research and Development, General Electric Co., Schnectady, NY, 1977.

30. Gambill, W.R., "Generalized Prediction of Burnout Heat Flux for Flowing, Subcooled, Wetting Liquids," **Chemical Engineering Symposium Series**, No. 41, Vol. 59, p. 71, 1963.

31. Rousar, D.C., "Correlation of Burnout Heat Flux for Fluids at High Velocity and High Subcooling Conditions," M.S. Thesis, Dept. of Mechanical Engineering, University of California, Davis, June 1966.

32. Kutateladze, S.S.,"Izv. Akad. Nauk, SSSR," **Otd. Tekh. Nauk**, No. 4, pp. 529-536, 1951.

33. Bonilla, C.F., "Nuclear Engineering," pp. 399-431, McGraw-Hill Book Company, New York, NY, 1957.

Appendix A

A Listing of the Final Computer Code

Version ASCB53

The following computer listing includes the main program and all the supporting subroutines

```
      PROGRAM ASCB530
C ********************COMPUTER CODE SERIES ASCB****************************
C     DATE LAST EDITED  11/5/88
C     REVISION BY: C. WONG & M.A.HOFFMAN
C     CHANGES TO MAKE ASCB53 MORE USER FRIENDLY AND COMMENTED OUT
C     FORMULAS FOR NONESSENTIAL CALCULATIONS  -- THIS IS THE FINAL CODE
C     VERSION GOING TO LIVERMORE
C ************************************************************************
C
C     THIS PROGRAM CALCULATES PRESSURE DROP, PUMPING POWER REQUIRED AND
C     THE CHF(CRITICAL HEAT FLUX) FOR WATER FLOW IN ROUND TUBES WITH
C     UNIFORM AXIAL HEAT FLUX.   IT CAN PROVIDE RESULTS FOR THE SINGLE-
C     PHASE LIQUID FLOW REGIME AND/OR THE SUBCOOLED BOILING FLOW REGIME.
C
C ************************************************************************
C     THIS CODE WAS DEVELOPED FOR THE LAWRENCE LIVERMORE NATIONAL
C     LABORATORY BY:
C       PRINCIPAL INVESTIGATOR: PROFESSOR MYRON A. HOFFMAN
C       GRADUATE STUDENTS: CHARLES KLINE(1985), CHRISTOPHER WONG(1988)
C       DEPARTMENT OF MECHANICAL ENGINEERING
C       UNIVERSITY OF CALIFORNIA, DAVIS, CA 95616
C       OCTOBER 1988
C ************************************************************************
C ****DIMENSION ALL STEPWISE STORAGE REGISTERS
C
      DIMENSION WDPDXA(51),WDPDXF(51),WDPDXG(51)
      DIMENSION WTP(51),WZP(51),WCO(51)
      DIMENSION AP123(51),GP123(51),FP123(51)
      DIMENSION WXNEZ(51),WXEZ(51),VOIDS(51),WVOIDS(51)
      DIMENSION CPS(51),DTSUBS(51),FS(51),GS(51)
      DIMENSION HS(51),KS(51),KWS(51),MUBS(51),PHILOS(51)
      DIMENSION PRBS(51),PRESS(51),GGAMBS(51)
      DIMENSION RESS(51),RHOS(51),RHOVS(51),MUWS(51)
      DIMENSION TBS(51),TPFFS(51),TSATS(51),PES(51),STANS(51)
      DIMENSION TWIS(51),TWOS(51),UDTSBS(51)
      DIMENSION XUDXS(51),VFS(51),VGS(51)
      DIMENSION TONSS(51),ZAXFS(51)
      DIMENSION GUNIF(30),DPRES(30)
      DIMENSION RCRITS(51),SFS(51)
C
C ****DIMENSION ALL STEAM PROPERTY VARIABLES
C
      DIMENSION RTSAT(182),RPRES(182),RHF(182),RHG(182),RRHOV(182),
     &  RHFG(182)
      DIMENSION RTEM(41),RCPF(41)
C
C     DIMENSION INPUT EDITOR VARIABLES
C
      DIMENSION A(14),BF(10),BD(10)
C
C ****SET REAL VARIABLE DECLARATIONS
C
      REAL L,MUB,MUW,INTPP,K,KS,KW,KWB,KW2,KW3,MUBS,MUWS,KLOSS,LU
C
C ****SET LOGICAL VARIABLE DECLARATIONS
C
C      LOGICAL LNEX,LNOP
C
C ****DECLARE CHARACTER VARIABLES
C
```

```
      CHARACTER ANSWER, DATAFL*15, DATFL2*15, DATFL3*15, TSTR*3
C
C ****EXTERNAL DECLARATION FOR FUNCTION PP FOR SUBROUTINE ZOINTI6
C
      EXTERNAL ZAXFLX
C
C ****BEGINNING MESSAGE SENT TO SCREEN
C
      WRITE(5,1)
    1 FORMAT(1H1)
      PRINT *,'                                        SCB-1A'
      PRINT *,' '
      PRINT *,' '
      PRINT *,' '
      PRINT *,' '
      PRINT *,' '
      PRINT *,'                              A Subcooled Flow Boiling'
      PRINT *,'                                    Design Code'
      PRINT *,' '
      PRINT *,' '
      PRINT *,' '
      PRINT *,' '
      PRINT *,' '
      PRINT *,' '
      PRINT *,' '
      PRINT *,' '
      PRINT *,'                    (C) University of California, Davis, 1988'
      PRINT *,' '
      WRITE(5,75)
      READ(5,82) ANSWER
      IF(ANSWER.EQ.'S')GOTO 412
      WRITE(5,1)
      PRINT *,' '
      PRINT *,' '
      PRINT *,' '
      PRINT *,' '
      PRINT *,'*************************************************************
     &************************'
      PRINT *,' THIS CODE WAS DEVELOPED FOR THE LAWRENCE LIVERMORE NATIO
     &NAL LABORATORY BY: '
      PRINT *,'      PRINCIPAL INVESTIGATOR:  Professor Myron A. Hoffman'
      PRINT *,'      GRADUATE STUDENTS:  Charles Kline(1985), Christopher
     & Wong(1988)'
      PRINT *,'      Department of Mechanical Engineering'
      PRINT *,'      University of California, Davis, CA  95616'
      PRINT *,'*************************************************************
     &************************'
      PRINT *,' '
      PRINT *,' '
      PRINT *,' '
      PRINT *,' '
      PRINT *,' '
      PRINT *,' '
      PRINT *,' '
      PRINT *,' '
      WRITE(5,75)
      READ(5,82) ANSWER
      PRINT *,' '
      PRINT *,' '
      PRINT *,' '
```

```
      PRINT *,' '
      WRITE(9,2)
    2 FORMAT(T5,'WELCOME TO THE SUBCOOLED FLOW BOILING DESIGN CODE SCB-1
     &A'/
     &,T5,'(VERSION 1A - November, 1988)'/,T9,'for the IBM PC/AT (or com
     &patibles) and the VAX 11/780'/)
      WRITE(9,*)
      PRINT *,'      This program calculates pressure drop, pumping power
     & required and the '
      PRINT *,'      CHF(Critical Heat Flux) for water flow in round tube
     &s with uniform axial'
      PRINT *,'      heat flux.  It can provide results for the single-ph
     &ase liquid flow'
      PRINT *,'      regime and/or the subcooled boiling flow regime. '
      WRITE(9,*)
      WRITE(9,*)
      WRITE(9,*)
      PRINT *,' You should be able to run SCB-1A by responding to the pr
     &ompts.  Try it!'
      PRINT *,' '
      PRINT *,' For more information, refer to the SCB-1A Code Manual.
     &It contains an example.'
      PRINT *,' '
      PRINT *,' '
      PRINT *,' '
      PRINT *,' '
      WRITE(9,75)
      READ(9,82) ANSWER
C
C ****START INPUT FILE EDITOR
C
C
C ****SELECT INPUT FILE OPERATION
C
  412 WRITE(9,1)
      PRINT *,' '
      PRINT *,' '
      WRITE(9,3)
    3 FORMAT(75HO ********************************************************
     &**********)
      WRITE(9,4)
    4 FORMAT(25HO PLEASE SELECT OPERATION)
      WRITE(9,5)
    5 FORMAT(25HO 1) USE AN OLD DATA FILE)
      WRITE(9,6)
    6 FORMAT(26HO 2) REVISE AN OLD DATA FILE)
      WRITE(9,7)
    7 FORMAT(27HO 3) CREATE A NEW DATA FILE)
      WRITE(9,8)
    8 FORMAT(43HO ENTER 0 OF YOUR CHOICE - TO EXIT, ENTER 0)
      PRINT *,'   Option (1) or (2) is recommended'
      WRITE(9,3)
      READ(9,*) NCHOICE
      IF(NCHOICE.EQ.0) THEN
        PRINT *,'*****PROGRAM EXECUTION INTERRUPTED*****'
        GOTO 999
      ENDIF
   82 FORMAT(A1)
C
C ****ENTER DATA FILE NAMES
```

```
C
      WRITE(5,12)
   12 FORMAT(1X,'PLEASE ENTER INPUT FILE NAME IN THE FORM:  INPnnn.DAT -
     & USE CAPITAL LETTERS'/,5X,'(nnn MAY BE ANY COMBINATION OF FROM 1 T
     &O 9 NUMBERS OR LETTERS)')
      READ(5,83,ERR=900) DATAFL
   83 FORMAT(A15)
      WRITE(5,*)
      WRITE(5,30)
   30 FORMAT(1X,'ENTER THE NEW OUTPUT FILE NAME IN THE FORM: OUTmmm.DAT
     &- USE CAPITAL LETTERS')
      PRINT *,' (mmm MAY BE ANY COMBINATION OF FROM 1 TO 9 NUMBERS OR LE
     &TTERS)'
      WRITE(5,11)
      READ(5,31,ERR=900) DATFL3
   31 FORMAT(A15)
      WRITE(5,13) DATAFL
   13 FORMAT(18HD WORKING ON FILE ,A15)
C     TIMEOUT LOOP
      DO 201 I=1,100
  201 CONTINUE
C
C ****TRANSFER OF EDIT CONTROL
C
      GOTO(400,401,402),NCHOICE
      PRINT *,'  IMPROPER OPERATION SELECTION'
      GOTO 999
C
C ****OPTION #1:USE AN OLD DATA FILE
C
  400 WRITE(5,14)
   14 FORMAT(25H1 ACCESSING OLD DATA FILE)
      DO 214 I=1,100
  214 CONTINUE
      GOTO 411
C
C ****OPTION #2:EDIT AN OLD FILE
C
  401 WRITE(5,15)
   15 FORMAT(39H1 RECOVERING OLD DATA FILE FOR UPDATING)
      WRITE(5,*)
      PRINT *,' *** CAUTION:  CODE RESULTS ONLY VALID IF INPUT PARAMETERS
     & ARE WITHIN VERIFIED'
      PRINT*,'                LIMITS - SEE INSTRUCTION MANUAL FOR THESE LI
     &MITS***'
      WRITE(5,*)
      OPEN(2,FILE=DATAFL,ERR=903,STATUS='OLD')
      READ(2,*) (A(I),I=1,13)
  403 WRITE(5,21) A(1)
   21 FORMAT(1X,'1) HEAT FLUX AT 0 DEGS BASED ON OUTER DIAM.  (W/M2)',
     &  T65,1PE11.4)
      WRITE(5,22) A(2)
   22 FORMAT(1X,'2) TYPE CIRCM HEAT FLUX PRFL(0-UNIF,1-HALF UNIF,2-HALF
     &COS)',T65,1PE11.4)
      WRITE(5,23) A(3)
   23 FORMAT(1X,'3) TUBE INLET MASS FLUX (KG/M2-S)',T65,1PE11.4)
      WRITE(5,24) A(4)
   24 FORMAT(1X,'4) TUBE INLET STATIC PRESSURE (PA)',T65,1PE11.4)
      WRITE(5,25) A(5)
   25 FORMAT(1X,'5) TUBE INLET BULK FLUID TEMPERATURE (DEG K)',T65,
```

```
     &  1PE11.4)
      WRITE(5,26) A(6)
   26 FORMAT(1X,'6) HEATED TUBE LENGTH (M)',T65,1PE11.4)
      WRITE(5,28) A(7)
   28 FORMAT(1X,'7) OUTSIDE TUBE DIAMETER (M)',T65,1PE11.4)
      WRITE(5,29) A(8)
   29 FORMAT(1X,'8) INSIDE TUBE DIAMETER (M)',T65,1PE11.4)
      WRITE(5,32) A(9)
   32 FORMAT(1X,'9) INLET PRESSURE LOSS COEFFICIENT KLOSS',T65,1PE11.4)
      WRITE(5,33) A(10)
   33 FORMAT(1X,'10) TUBE ANGLE FROM HORIZONTAL(EITHER 0 OR 90 DEG)',
     &  T65,1PE11.4)
      WRITE(5,35) A(11)
   35 FORMAT(1X,'11) RADIUS OF ONE MAX ACTIVE CAVITY (M) (0=RCRIT USED)'
     &  ,T65,1PE11.4)
      WRITE(5,36) A(12)
   36 FORMAT(1X,'12) NUMBER OF CALCULATION STEPS ?(1-1000, 2-2000)',
     &  T65,1PE11.4)
      WRITE(5,37) A(13)
   37 FORMAT(1X,'13) PRINT FULL WATER/STEAM PROPERTY DATA?(1-NO, 2-YES)'
     &  ,T65,1PE11.4)
      WRITE(5,86) DATFL3
   86 FORMAT(1X,'14) OUTPUT STORAGE DATA FILE NAME CHOSEN AS',
     &  T64,A15)
      WRITE(5,38)
   38 FORMAT(19HO ENTER 0 TO CHANGE)
      WRITE(5,9)
    9 FORMAT(22HO      TO EXIT, ENTER 0)
      READ(5,*) J
      IF(J.GT.14) GOTO 999
      IF(J.EQ.0)THEN
        GOTO 404
      ELSEIF(J.LE.13)THEN
        WRITE(5,39)
   39   FORMAT(24HO ENTER NEW VALUE NOW...)
        READ(5,*) A(J)
        WRITE(5,1)
        GOTO 403
      ELSEIF(J.EQ.14)THEN
        WRITE(5,30)
        READ(5,31) DATFL3
        WRITE(5,1)
        GOTO 403
      ENDIF
  404 READ(2,*) A(14)
      DO 230 I=1,A(14)
      READ(2,*) BF(I),BD(I)
  230 CONTINUE
      WRITE(5,170)
  170 FORMAT(40HO DO YOU WISH TO CHANGE ANY TUBE MATERIAL DATA PAIRS? Y
     &OR N)
      READ(5,82) ANSWER
      IF((ANSWER.EQ.'N').OR.(ANSWER.EQ.'n'))GOTO 413
      WRITE(5,40)
   40 FORMAT(43H1 NOW UPDATING TUBE MATERIAL DATA PAIRS...)
      WRITE(5,87)
   87 FORMAT(1X,'WALL THERMAL CONDUCTIVITY K NEEDS TO BE INPUT AS A FUNC
     &TION'/,1X,'OF TEMPERATURE. OBTAIN A THERMAL CONDUCTIVITY VS  TEMPE
     &RATURE'/,1X,'CURVE FOR TUBE MATERIAL USED AND PICK UP TO 10 DATA P
     &OINTS FROM'/,1X,'CURVE FOR ENTRY.'/)
```

```
405 WRITE(5,41)
 41 FORMAT(1X,'PAIR#',7X,'TEMP',7X,'THERMAL CONDUCTIVITY')
    DO 202 I=1,A(14)
    WRITE(5,42) I,BF(I),BD(I)
 42 FORMAT(1H0,2X,I3,T9,1PE9.2,1X,'DEG K',T29,E9.2,1X,'W/M-K')
202 CONTINUE
    WRITE(5,68)
 68 FORMAT(30H0 ANY CHANGES TO MAKE ? Y OR N)
    READ(5,82)ANSWER
    IF((ANSWER.EQ.'N').OR.(ANSWER.EQ.'n'))GOTO 413
    WRITE(5,78)
 78 FORMAT(59H0 DO YOU WISH TO ADD ANY DATA PAIRS(TOT MAX IO PRS)? Y O
   &R N)
    READ(5,82) ANSWER
    IF((ANSWER.EQ.'Y').OR.(ANSWER.EQ.'y'))THEN
      WRITE(5,79)
 79   FORMAT(28H0 HOW MANY ADDITIONAL PAIRS?)
      READ(5,*) NEWPAIR
      NEWNUMB=A(14)+NEWPAIR
      DO 204 J=A(14)+1,NEWNUMB
      WRITE(5,88)
 88   FORMAT(1X,'INPUT TEMPERATURE(DEG K) AND CORRESPONDING THERMAL'/,
     & 1X,'CONDUCTIVITY(W/M-K) ON SAME INPUT LINE SEPARATED BY A COMMA'/
     &,1X,'(E.G. 305.8,14.7) THEN HIT RETURN KEY --DO NOT INSERT ANY',
     & 1X,'SPACES'/)
      WRITE(5,69) J
 69   FORMAT(2X,'ENTER NEW PAIR # ',I2,'--NOW!!!')
      READ(5,*) BF(J),BD(J)
204   CONTINUE
      A(14)=NEWNUMB
      GOTO 405
    ENDIF
    WRITE(5,80)
 80 FORMAT(52H0 DO YOU WISH TO CHANGE ANY DATA PAIR VALUES? Y OR N)
    READ(5,82) ANSWER
    IF((ANSWER.EQ.'N').OR.(ANSWER.EQ.'n'))GOTO 410
    WRITE(5,43)
 43 FORMAT(29H0 ENTER PAIR NUMBER TO CHANGE)
    WRITE(5,9)
    READ(5,*) J
    IF((J.EQ.0).OR.(J.GT.A(14)))THEN
      WRITE(5,*) '  *** NO PAIRS CHANGED - CONTINUING ***'
      GOTO 410
    ELSE
      WRITE(5,88)
      READ(5,*) BF(J),BD(J)
      GOTO 405
    ENDIF
410 WRITE(5,47)
 47 FORMAT(40H0 DO YOU WISH TO DELETE ANY DATA PAIRS ?)
    READ(5,82) ANSWER
    IF((ANSWER.EQ.'Y').OR.(ANSWER.EQ.'y'))THEN
      WRITE(5,48)
 48   FORMAT(24H0 ENTER PAIR # TO DELETE)
      READ(5,*) NDELETE
      DO 205 J=NDELETE,A(14)
      BF(J)=BF(J-1)
      BD(J)=BD(J-1)
      A(14)=A(14)-1
205   CONTINUE
```

```
      GOTO 405
      ENDIF
  413 CLOSE(UNIT=2)
      WRITE(5,171)
  171 FORMAT(97HO ENTER NEW INPUT FILE NAME FOR STORING THE MODIFIED FIL
     &E)
      WRITE(5,11)
   11 FORMAT(40HO NOTE:  THIS FILE MUST NOT ALREADY EXIST)
      WRITE(5,12)
      READ(5,83,ERR=902) DATFL2
      OPEN(2,FILE=DATFL2,ERR=902,STATUS='NEW')
      WRITE(2,*) (A(J),J=1,13)
      WRITE(2,*) A(14)
      DO 235 J=1,A(14)
      WRITE(2,*) BF(J),BD(J)
  235 CONTINUE
      CLOSE(UNIT=2)
      GOTO 411
C
C ****OPTION 03:CREATE A NEW FILE FROM SCRATCH
C
  402 OPEN(2,FILE=DATAFL,ERR=901,STATUS='NEW')
      WRITE(5,49)
   49 FORMAT(26H1 CREATING A NEW DATA FILE)
      WRITE(5,50)
   50 FORMAT(32HO ENTER VALUE AFTER TEXT APPEARS)
      WRITE(5,*)
      PRINT *,' *** CAUTION:  CODE RESULTS ONLY VALID IF INPUT PARAMETERS
     & ARE WITHIN VERIFIED'
      PRINT*,'                LIMITS - SEE INSTRUCTION MANUAL FOR THESE LI
     &MITS***'
      WRITE(5,*)
      WRITE(5,91)
   91 FORMAT(1X,'1) HEAT FLUX AT O DEGS BASED ON OUTER DIAM.  (W/M2)')
      READ(5,*) A(1)
      WRITE(5,92)
   92 FORMAT(1X,'2) TYPE CIRCH HEAT FLUX PROFILE(O-UNIFORM,1-HALF UNIFOR
     &M,2-HALF COSINE')
      READ(5,*) A(2)
      WRITE(5,93)
   93 FORMAT(1X,'3) TUBE INLET MASS FLUX (KG/M2-S)')
      READ(5,*) A(3)
      WRITE(5,94)
   94 FORMAT(1X,'4) TUBE INLET STATIC PRESSUE (PA)')
      READ(5,*) A(4)
      WRITE(5,95)
   95 FORMAT(1X,'5) TUBE INLET BULK FLUID TEMPERATURE (DEG K)')
      READ(5,*) A(5)
      WRITE(5,96)
   96 FORMAT(1X,'6) HEATED TUBE LENGTH (M)')
      READ(5,*) A(6)
      WRITE(5,98)
   98 FORMAT(1X,'7) OUTSIDE TUBE DIAMETER (M)')
      READ(5,*) A(7)
      WRITE(5,99)
   99 FORMAT(1X,'8) INSIDE TUBE DIAMETER(M)')
      READ(5,*) A(8)
      WRITE(5,62)
   62 FORMAT(1X,'9) INLET PRESSURE LOSS COEFFICIENT KLOSS')
      READ(5,*) A(9)
```

```
      WRITE(5,63)
   63 FORMAT(1X,'10) TUBE ANGLE FROM HORIZONTAL(0 OR 90 DEG)')
      READ(5,*) A(10)
      WRITE(5,65)
   65 FORMAT(1X,'11) RADIUS OF ONB MAX ACTIVE CAVITY (M) (0=RCRIT USED)'
     &)
      READ(5,*) A(11)
      WRITE(5,85)
   85 FORMAT(1X,'12) NUMBER OF CALCULATION STEPS?(1-1000, 2-2000)')
      READ(5,*) A(12)
      WRITE(5,66)
   66 FORMAT(1X,'13) PRINT FULL WATER/STEAM PROPERTY DATA?(1-NO 2-YES)')
      READ(5,*) A(13)
      WRITE(5,87)
      WRITE(5,67)
   67 FORMAT(1X,'14) TOTAL NUMBER OF DATA POINTS TO BE INPUT')
      READ(5,*) A(14)
      DO 203 I=1,A(14)
      WRITE(5,88)
      WRITE(5,69) I
      READ(5,*) BF(I),BD(I)
  203 CONTINUE
      WRITE(5,73)
   73 FORMAT(16HO END DATA INPUT)
      WRITE(2,*) (A(J),J=1,13)
      WRITE(2,*) A(14)
      DO 240 J=1,A(14)
      WRITE(2,*) BF(J),BD(J)
  240 CONTINUE
      CLOSE(UNIT=2)
C     TIMEOUT LOOP
      DO 207 I=1,100
  207 CONTINUE
C
C ****ECHO BACK DATA
C

  411 WRITE(5,74)
   74 FORMAT(51HO DO YOU WISH TO VERIFY THE INPUT DATA FILE? Y OR N)
      READ(5,82) ANSWER
      IF((ANSWER.EQ.'N').OR.(ANSWER.EQ.'n')) GOTO 450
      WRITE(5,81)
   81 FORMAT(34H1 RECOVERING FILE FOR VERIFICATION)
      WRITE(5,*)
      IF(NCHOICE.EQ.2)THEN
        OPEN(2,FILE=DATFL2,ERR=903,STATUS='OLD')
      ELSE
        OPEN(2,FILE=DATAFL,ERR=903,STATUS='OLD')
      ENDIF
      READ(2,*) (A(I),I=1,13)
      WRITE(5,21) A(1)
      WRITE(5,22) A(2)
      WRITE(5,23) A(3)
      WRITE(5,24) A(4)
      WRITE(5,25) A(5)
      WRITE(5,26) A(6)
      WRITE(5,28) A(7)
      WRITE(5,29) A(8)
      WRITE(5,32) A(9)
      WRITE(5,33) A(10)
```

```
      WRITE(5,39) A(11)
      WRITE(5,36) A(12)
      WRITE(5,37) A(13)
      WRITE(5,86) DATFL3
      WRITE(5,75)
   75 FORMAT(28HO HIT RETURN KEY TO CONTINUE)
      READ(5,82) ANSWER
      READ(2,*) A(14)
      DO 245 I=1,A(14)
      READ(2,*) BF(I),BD(I)
  245 CONTINUE
      WRITE(5,87)
      WRITE(5,41)
      DO 208 I=1,A(14)
      WRITE(5,42) I,BF(I),BD(I)
  208 CONTINUE
      WRITE(5,76)
   76 FORMAT(32HO IS THIS WHAT YOU WANT?? Y OR N)
      READ(5,82) ANSWER
      IF((ANSWER.EQ.'N').OR.(ANSWER.EQ.'n'))THEN
        WRITE(5,77)
   77   FORMAT(46HO CURRENT INPUT FILE SAVED-STARTING OVER AGAIN)
        CLOSE(UNIT=2)
C       TIMEOUT LOOP
        DO 213 I=1,100
  213   CONTINUE
C
        GOTO 412
      ENDIF
      CLOSE(UNIT=2)
C
C ****END INPUT FILE EDITOR
C
C
C ****MAIN PROGRAM
C
  450 WRITE(5,100)
  100 FORMAT(38HI INPUT COMPLETE. STARTING CALCULATIONS)
      OPEN(1,FILE='STMET.DAT',ERR=903,STATUS='OLD')
      IF(NCHOICE.EQ.2)THEN
        OPEN(2,FILE=DATFL2,ERR=903,STATUS='OLD')
      ELSE
        OPEN(2,FILE=DATAFL,ERR=903,STATUS='OLD')
      ENDIF
      READ(2,*) (A(I),I=1,13)
      OPEN(3,FILE=DATFL3,ERR=901,STATUS='NEW')
C      OPEN(4,FILE='WOUTGPH.DAT',ERR=901,STATUS='NEW')
C      INQUIRE(FILE='WFLX.DAT',EXIST=LNEX,OPENED=LNOP)
C      IF(.NOT.LNEX)THEN
C        OPEN(7,FILE='WFLX.DAT',ERR=901,STATUS='NEW')
C      ELSEIF((LNEX).AND.(.NOT.LNOP))THEN
C        OPEN(7,FILE='WFLX.DAT',ERR=904,STATUS='OLD')
C      ENDIF
C      OPEN(8,FILE='WDRP.DAT',ERR=901,STATUS='NEW')
      QMAX=A(1)
      NPRFL=A(2)
      Q=A(3)
      PIN=A(4)
      TBIN=A(5)
      L=A(6)
```

```
      DOUT=A(7)
      DI=A(8)
      KLOSS=A(9)
      THETA=A(10)
      RCAV=A(11)
      ISTEPS=A(12)
      IXY=A(13)
      READ(2,*) A(14)
      NKW=A(14)
      NUNIT=2
      CALL ZLSTSB(NKW,AA1,AA2,AA3,AA4,AA5,NUNIT,BF,BD)
      DO 220 I=1,182
      READ(1,*) RTSAT(I),RPRES(I),RRHOV(I),RHF(I),RHG(I)
C  109 FORMAT(F10.4,F15.4,F15.8,F15.5,F12.2)
      RHFG(I)=RHG(I)-RHF(I)
  220 CONTINUE
      DO 221 I=1,41
      READ(1,*) RTEM(I),RCPF(I)
C  111 FORMAT(2F12.4)
  221 CONTINUE
      WRITE(3,1)
      WRITE(3,113)
  113 FORMAT(1X,30(2H-*),'     INPUTS    ',22(2H-*)//)
      WRITE(3,114) QMAX,NPRFL,G,PIN,TBIN
  114 FORMAT(5X,'APPLIED HEAT FLUX AT O DEGS BASED ON OUTER DIAM. ',
     &  10(1H-),1H=,1PE11.4,2X,'W/M2'/
     &  5X,'TYPE OF CIRCUMFERENTIAL HEAT FLUX PROFILE(0.1,OR 2)',7(1H-),
     &  1H=,I2/
     &  5X,'TUBE INLET MASS FLUX, G (BASED ON INNER DIAM.)',12(1H-),1H=,
     &  1PE11.4,2X,'KG/M2-S'
     &  /5X,'TUBE INLET STATIC PRESSURE',32(1H-),1H=,E11.4,2X,'PA'/
     &  5X,'INLET BULK FLUID TEMPERATURE',30(1H-),1H=,E11.4,2X,
     &  'KELVIN'/)
      WRITE(3,115) L,DOUT,DI,(DOUT-DI)/2.
  115 FORMAT(5X,'HEATED TUBE LENGTH',40(1H-),1H=,1PE11.4,2X,'METERS'/
     &  5X,'OUTSIDE TUBE DIAMETER, DOUT',31(1H-),1H=,E11.4,2X,
     &  'METERS'/
     &  5X,'INSIDE TUBE DIAMETER, DI',34(1H-),1H=,E11.4,2X,'METERS'/
     &  5X,'TUBE WALL THICKNESS',39(1H-),1H=,E11.4,2X,'METERS'/)
      WRITE(3,118) KLOSS,THETA,RCAV
  118 FORMAT(5X,'INLET PRESSURE LOSS COEFFICIENT, KLOSS',20(1H-),1H=,
     &  F11.5/
     &  5X,'TUBE ANGLE FROM HORIZONTAL PLANE',26(1H-),1H=,F11.5,2X,
     &  'DEGREES'/
     &  5X,'RADIUS OF ONE MAX ACTIVE CAVITY FROM USER (0=RCRIT USED)',
     &  2(1H-),1H=,1PE11.4,2X,'METERS'/)
      WRITE(3,116) ISTEPS,IXY
  116 FORMAT(5X,'NUMBER OF CALCULATION STEPS?(1-NO, 2-YES)',
     &  17(1H-),1H=,I2/
     &  5X,'PRINT FULL WATER/STEAM PROPERTY DATA?(1-1000, 2-2000)'9(1H-),
     &  1H=,I2)
      WRITE(3,117) DATFL3
  117 FORMAT(5X,'OUTPUT STORAGE DATA FILE CHOSEN AS',24(1H-),1H=,
     &  1X,A15/)
      WRITE(3,198)
  198 FORMAT(10X,'THERMAL CONDUCTIVITY AS A FUNCTION OF TEMPERATURE'//
     &  11X,'PAIR #',2X,'TEMP(DEG K)',3X,'THERMAL CONDUCTIVITY(W/M-K)
     &'/)
      DO 257 I=1,A(14)
      WRITE(3,199) I,BF(I),BD(I)
```

```
  199 FORMAT(1HO, 10X, I3, 5X, 1PE9.2, 10X, E9.2)
  257 CONTINUE
      CALL ZTSAT(PIN, RPRES, RTSAT, TSAT, IHI, ILOW, NEXIT)
      WRITE(3, 44)
   44 FORMAT(/10X, 'LIMITS OF VALIDITY: '/12X, 'PARMETER', 14X, 'UNITS', 11X,
     &   'MAIN CODE', 14X, 'GAMBILL CHF CORRELATION', 10X, 'VALUES FROM THIS
     &RUN'/)
      WRITE(3, 45) L/DI, DI, 0, PIN, GMAX
   45 FORMAT(10X, 'L/DI', 35X, '49.0 TO 127.0', 22X, '>=25.0', T113, F9.2/
     &   10X, 'INNER DIAM. DI', 9X, '(METERS)', 6X, '0.0015 TO 0.0046', 16X,
     &   '0.002 TO 0.008', T113, F6.4/
     &   10X, 'MASS FLUX, G', 11X, '(KG/M2-S)', 7X, '2500 TO 10000', 21X,
     &   '3 TO 10875', T113, F8.2/
     &   10X, 'INLET PRESSURE', 9X, '(PA)', 9X, '2.0E+05 TO 20.0E+05', 12X,
     &   '2.9E+04 TO 2.07E+07', T110, 1PE11.4/
     &   10X, 'UNIFORM HEAT FLUX', 6X, '(MW/M2)', 12X, '0 TO 12.2E+06', 12X,
     &   '3.2E+05 TO 1.18E+08', T110, E11.4)
      WRITE(3, 233) TSAT-TBIN
  233 FORMAT(10X, 'INLET DELTA-T SUBCOOL', 2X, '(DEG K)', 11X, '10 TO 200',
     &   23X, '0 TO 263', T113, F6.2)
      WRITE(3, 234) TBIN
  234 FORMAT(10X, 'INLET BULK TEMPERATURE', 1X, '(DEG K)', 6X, 'GREATER THAN
     &273.0', 20X, 'SAME', 24X, F6.2/, 46X, 'LESS THAN 644.0'/, 46X, 'LESS THAN
     &TSAT CORRESPONDING'/, 46X, 'TO INLET PRESSURE'/)
      DO 226 JLINE=1, 9
      WRITE(3, 227)
  227 FORMAT(1X, ' ')
  226 CONTINUE
C       WRITE(3, 64)
C    64 FORMAT(//1X, 99(2H-*))
C
C ****INITIAL CALCULATIONS
C
      RH=1.0
      RF=1.0
      IF(ISTEPS EQ. 1)THEN
        STEPS=1000.0
      ELSE
        STEPS=2000.0
      ENDIF
      NSTEPS=STEPS
      DIHY=DI
      BW=(DOUT-DI)/2.
      XMDA=3.14159*G*DI*DI*0.25
      DEFF=DI**2./DOUT
      DX=L/STEPS
C       CHDV=CHD(X)
C       GAX=GMAX*ZGINT1&(0., L, ZAXFLX, 10)/L
      CALL ZRHO(TBIN, PIN, RHO)
      VIN=G/RHO
      QOR=0
      THETA=THETA*(3.14159/180.0)
C
C ***SET FLAGS/COUNTERS
C
      NNN=0
      JUMP=0
      NC=0
      NEXIT=0
      N=(NSTEPS/50-1)
```

```
      MONOBEF=0
      MBOBEF=0
      MOBB=0
      IORAD=0
      ISF=0
C
C ****SET ONE-SIDED HEATING FACTORS
C
      IF(NPRFL.EQ.0)THEN
        WF1=1.0
        WF2=1.0
        WF3=1.0
        WF4=1.0
        WF5=1.0
      ELSEIF(NPRFL.EQ.1)THEN
        WF1=0.5
        WF2=1.0
        WF3=1.0
        WF4=0.5
        WF5=0.5
      ELSEIF(NPRFL.EQ.2)THEN
        WF1=0.3183
        WF2=0.866
        WF3=0.866
        WF4=0.2737
        WF5=0.2737
      ENDIF
C
C ****SET INITIAL VALUE OF TEMPERATURES AND PRESSURES
C
      TWO=TBIN
      TWI=TBIN
      TWI2=TBIN
      TWO2=TBIN
      TB=TBIN
C
C ****ZERO ALL STORAGE REGISTER VARIABLES
C
      DO 222 I=1,51
      WXNEZ(I)=0.
      WXEZ(I)=0.
      VOIDB(I)=0.
      WDPDXA(I)=0.
      WDPDXF(I)=0.
      WDPDXG(I)=0.
      WTP(I)=0.
      WZP(I)=0.
  222 CONTINUE
C
C ****SET OFDB COEFFICIENTS
C
C       JENS-LOTTES CORRELATION
        C100=0.791
        C200=0.25
        C300=-1.609E-07
C       THOM CORRELATION
C        C100=0.02252
C        C200=0.9
C        C300=-1.1509E-07
C
```

```
C ****TWO PHASE FRIC MULTIPL SET TO ONE - SEE SUBROUTINE ZUBSF2
C
      TPFF=1.0
C
C ****SET NON-EQUILIBRIUM QUALITY TO ZERO BEFORE BUBBLE DEPARTURE
C
      XNEQX=0.0
      VOID=0.0
      ITP=0.0
      IP=0.0
C
C ****CALCULATE PRESSURE DROP IN UNHEATED SECTION
C
      PRESS=PIN-XLOSS*G**2./(2.*RHO)
C      CALL ZVISC(TB,RHO,MUB)
C      CALL ZTLCW(TB,RHO,K)
C      CALL ZCPF(TB,RTEM,RCPF,CP,NEXIT)
C      IF(NEXIT.EQ.1) GOTO 800
C      CALL ZHORDOFF(0.0OR,DI,DIHY,MUB,CP,K,REB,REBF,PRB,F)
C      DPFRICUN=(G**2 /(2.*RHO))*(4.*F*LU/DI)
C      DPGRAVUN=RHO*9.807*LU*SIN(THETA)
C      DPUNHT=DPFRICUN+DPGRAVUN
C      PRESS=PRESS-DPUNHT
C
C ****START MAIN LOOP
C
      DO 225 NN=1,NSTEPS+1
C
C ****INITIALIZE CONVERGENCE COUNTERS
C
      N6=0
      N300=0
      N5=0
      N7=0
      N9=0
      LEAV=0
      ITER=0
C
C ****CALCULATE INITIAL ELEMENT VALUES
C
      NU=NN-1
      XNU=NU
      XUDX=XNU*DX
      QMAXPP=QMAX*ZAXFLX(XUDX)
      INTPP=ZQINTI&(0.,XUDX,ZAXFLX,10)
      CALL ZCPF(TB,RTEM,RCPF,CP,NEXIT)
      IF(NEXIT.EQ.1) GOTO 800
      CALL ZRHO(TB,PRESS,RHOUP)
      TB=TBIN+((QMAX*WF1*3.14159*DOUT*INTPP)/(CP*XMDA))
      CALL ZRHO(TB,PRESS,RHO)
      VF=1.0/RHO
      CALL ZVISC(TB,RHO,MUB)
      CALL ZTLCW(TB,RHO,K)
C
C ****REGIME DETERMINATION
C
      IF(NN.GT.1) GOTO 457
      CALL ZRHO(TWI,PRESS,RHOW)
      CALL ZVISC(TWI,RHOW,MUW)
      CALL ZTSAT(PRESS,RPRES,RTSAT,TSAT,IHI,ILOW,NEXIT)
```

```
      IF(NEXIT.EQ.1) GOTO 800
      IF(NM.EQ.1)THEN
        TSATIN=TSAT
      ENDIF
      XHFG=RHFG(ILOW)+(((RHFG(IHI)-RHFG(ILOW))*(PRESS-RPRES(ILOW)))/
     &  (RPRES(IHI)-RPRES(ILOW)))
      RHOV=RRHOV(ILOW)+(((RRHOV(IHI)-RRHOV(ILOW))*(PRESS-RPRES(ILOW)))/
     &  (RPRES(IHI)-RPRES(ILOW)))
      VG=1.0/RHOV
      XEQZ=-CP*(TSAT-TB)/XHFG
      CALL ZHOMOOFF(G,GOR,DI,DIHY,MUB,CP,K,REB,REBF,PRB,FDWB)
      CALL ZHTCOEFF(XUDX,REB,REBF,PRB,FDWB,CP,G,MUB,MUW,RH,TB,GMAXPP,
     &  DOUT,DI,PRESS,H,TWI,TWO,RHOW,NS,LEAV)
      IF(LEAV.EQ.1)GOTO 850
      CALL ZONB(GMAXPP,DOUT,DI,PRESS,C100,C200,C300,TSAT,TB,XHFG,K,
     &  RHOV,RCAV,WF3,SURF,RCRIT,DTJL,DTAD,DTBR,TWIONB)
      IF(TWI.GE.TWIONB)THEN
        JUMP=1
        XONB=XUDX
        TWIIN=TWI
        TWIONBIN=TWIONB
        HIN=H
        TBONB=TB
        MONBDEF=1
C ****SET UP FOR SHAH PDB ROUTINE****
C         TFLU=TB
C         H3=H
C ************************************
      ENDIF
C ****SHAH OBNVG
C       BO=GMAXPP*WF2/(GOR*XHFG)
C       IF(BO.GE.0.3E-04)THEN
C         SIO=230.0*BO**0.5
C       ELSE
C         SIO=1.0+46.0*BO**0.5
C       ENDIF
C       DTSATBD=GMAXPP*WF2/(H*SIO)
C       SHBD1=6.3E+04*BO**1.25
C       SHBD2=2.0
C       IF(SHBD1.LT.SHBD2)THEN
C         DTSBSHBD=DTSATBD*SHBD1
C       ELSE
C         DTSBSHBD=DTSATBD*SHBD2
C       ENDIF
C ****SAHA/ZUBER OBNVG
      PE=REB*PRB
C       IF(PE.LT.70000.0)THEN
C         DTSBSZ=(DI*GMAX*WF2*DOUT)/(DI*K*455.0)
C       ELSE
C         DTSBSZ=(GMAX*WF2*DOUT)/(DI*GOR*CP*0.0065)
C       ENDIF
      CALL ZMODFBD(GMAX,WF2,DOUT,DI,GOR,K,CP,PE,PESTR,DTSBSZ)
      DTSUB=TSAT-TB
      STAN=(GMAX*WF2*DOUT)/(DI*GOR*CP*DTSUB)
      IF(DTSUB.LE.DTSBSZ)THEN
C       IF(DTSUB.LE.DTSBSHBD)THEN
        NC=1
        ZBD=XUDX
        DTSUBIN=DTSUB
        TSATIN=TSAT
```

```
        CPIBD=CP
        DTSBSZIN=DTSBSZ
C        DTSHBDIN=DTSBSHBD
        TBBD=TB
        MBDBEF=1
      ENDIF
C
C ****REGIME CONTROL
C
  457 IF(NC.EQ.1)THEN
        GOTO 452
      ELSEIF(JUMP.EQ.1)THEN
        GOTO 451
      ELSE
        CALL ZRHO(TWI,PRESS,RHOW)
        CALL ZVISC(TWI,RHOW,MUW)
      ENDIF
C
C ****SINGLE PHASE LIQUID REGIME
C
      CALL ZHOMOOFF(0.0DR,DI,DIHY,MUB,CP,K,REB,REBF,PRB,FDWB)
      F=(FDWB*(MUW/MUB)**0.3)
C       F=(FDWB*(MUW/MUB)**0.3)*RF*CFF(XUDX)
      CALL ZHTCOEFF(XUDX,REB,REBF,PRB,FDWB,CP,0,MUB,MUW,RH,TB,QMAXPP,
     &  DOUT,DI,PRESS,H,TWI,TWO,RHOW,NS,LEAV)
      IF(LEAV.EQ.1)GOTO 850
      DPDXF=-(2.0*F*G*Q)/(RHO*DIHY)
      DPDXA=-((G*Q)/DX)*((1.0/RHO)-(1.0/RHOUP))
      DPDXG=-9.807*SIN(THETA)*((RHO+RHOUP)/2.0)
      IF((ABS(DPDXA).GE.3.0E+06).AND.(IGRAD.EQ.0))THEN
        IGRAD=XUDX
      ENDIF
      IF(ABS(DPDXA).GE.3.0E+06)THEN
        IGRAD=1
      ENDIF
      DPX=(DPDXF*DX)+(DPDXA*DX)+(DPDXG*DX)
      IF(NM.GT.1)THEN
        PRESS=PRESS+DPX
        FP456=FP456+(DX*DPDXF)
        AP456=AP456+(DX*DPDXA)
        GP456=GP456+(DX*DPDXG)
      ENDIF
      CALL ZTSAT(PRESS,RPRES,RTSAT,TSAT,IHI,ILOW,NEXIT)
      IF(NEXIT.EQ.1) GOTO 800
      XHFG=RHFG(ILOW)+(((RHFG(IHI)-RHFG(ILOW))*(PRESS-RPRES(ILOW)))/
     &  (RPRES(IHI)-RPRES(ILOW)))
      RHOV=RRHOV(ILOW)+(((RRHOV(IHI)-RRHOV(ILOW))*(PRESS-RPRES(ILOW)))/
     &  (RPRES(IHI)-RPRES(ILOW)))
      VG=1.0/RHOV
      XEQI=-CP*(TSAT-TB)/XHFG
      DTSUB=TSAT-TB
      CALL ZONB(QMAXPP,DOUT,DI,PRESS,C100,C200,C300,TSAT,TB,XHFG,K,
     &  RHOV,RCAV,WF3,SURF,RCRIT,DTJL,DTAD,DTBR,TWIONB)
      IF(TWI.LT.TWIONB)THEN
        GOTO 780
      ELSE
C         WRITE(3,127) XUDX,TB,TWI,TSAT
C  127    FORMAT(10X,'NUCLEATE BOILING ONB OCCURS AT',1PE11.4,
C     &     ' METERS'/10X,'BULK TEMP=',0PF10.4,' K'/10X,
C     &     'INNERWALL TEMP=',F10.4,' K'/10X,'SAT TEMP=',F10.4,' K'/)
```

```
          XONB=XUDX
          JUMP=1
          H=(GMAXPP*(DOUT/DI))/(TWIONB-TB)
C          H=(CABY(REB,PRB)*GMAXPP*(DOUT/DI))/(TWIONB-TB)
          TWI=TWIONB
          DTSUBONB=TSAT-TB
          TBONB=TB
C ****SET UP FOR SHAH PDB****
C           TFLU=TB
C           H3=H
C ****************************
          GOTO 780
        ENDIF
C
C ****PARTIALLLY DEVELOPED BOILING  REGIME
C
C ****SAHA/ZUBER MODEL FOR PDB ELEMENT 1****
  451 CALL ZRHO(TWI,PRESS,RHOW)
        CALL ZVISC(TWI,RHOW,MUW)
        PE=REB*PRB
C        IF(PE.LT.70000.0) DTSBSZ=(DI*GMAX*WF2*DOUT)/(DI*K*455.0)
C        IF(PE.GE.70000.0) DTSBSZ=(GMAX*WF2*DOUT)/(DI*GOR*CP*0.0065)
        CALL ZMODFBD(GMAX,WF2,DOUT,DI,GOR,K,CP,PE,PESTR,DTSBSZ)
C ****************************************
C ****SHAH MODEL FOR PDB REGIME ELEMENT 1****
C  451 CALL ZRHO(TSAT,PRESS,RHOW)
C        CALL ZVISC(TSAT,RHOW,MUW)
C        PE=REB*PRB
C        IF(PE.LT.70000.0) DTSBSZ=(DI*GMAX*WF2*DOUT)/(DI*K*455.0)
C        IF(PE.GE.70000.0) DTSBSZ=(GMAX*WF2*DOUT)/(DI*GOR*CP*0.0065)
C        N9=N9+1
C        IF(N9.GT.90)THEN
C          H=H3
C          WRITE(3,134) XUDX
C          WRITE(3,126) TB,TWI,TWO,GMAXPP
C          GOTO 850
C        ENDIF
C ****************************************
C        CALL ZLEVY(TB,DI,GOR,RHO,MUB,YBNV9,ZBDVO)
C        ZBDVO=0.0
        IF(DI.LT.3.3464E-03)THEN
          RHFC=0.1398*(DI/1.0E-03)+0.5291
        ELSE
          RHFC=1.0
        ENDIF
        ZBDVO=RHFC*(0.002439*3.14159*DI)/(3.14159*DI*DI*0.25*PRESS**0.237)
        TFLU=TSAT-DTSBSZ
        CALL ZCPF(TFLU,RTEM,RCPF,CP1,NEXIT)
        IF(NEXIT.EQ.1) GOTO 800
        CALL ZCPF(TBIN,RTEM,RCPF,CP2,NEXIT)
        IF(NEXIT.EQ.1) GOTO 800
        ZBD=XMDA*(CP1+CP2)*0.5*(TFLU-TBIN)/(3.14159*DOUT*GMAX*WF1)
C        ZBDOF=(GOR*CP*DI)/4.*((TSATIN-TBIN)/(GMAXPP*WF1)-1./(5.*H))
        WVOID=ZBDVO*((XUDX-XONB)/(ZBD-XONB))**WF5
        AEFF=(3.14159*DI*DI*0.25)*(1.0-WVOID)
        G=XMDA/AEFF
        DIHY=((AEFF*4.0)/3.14159)**0.50
        CALL ZHOMOGFF(G,GOR,DI,DIHY,MUB,CP,K,REB,REBF,PRB,FDWB)
C        CALL ZLEVY2(XUDX,XONB,ZBD,YBNV9,DI,REB,FLDWB)
C ****SHAH PDB MODEL ELEMENT 2****
```

```
C       CALL SHAHPDB(REB,REBF,PRB,FDWB,CP,0.0OR,MUB,MUW,RH,TSAT,TSATIN,
C      &   TBIN,QMAXPP,XHFG,XUDX,DI,DOUT,H3,H,TWI,RHOW,ITER,HFO,BIO)
C       IF(ITER.EQ.1)GOTO 451
C ***********************************
       F=(FDWB*(MUW/MUB)**0.3)
C       F=(FDWB*(MUW/MUB)**0.3)*RF*CFF(XUDX)
       DPDXF=-(2.0*F*Q*Q)/(RHO*DIHY)*TPFF
       DPDXA=-((Q*Q)/DX)*((1.0/RHO)-(1.0/RHOUP))
       DPDXG=-9.807*SIN(THETA)*((RHO+RHOUP)/2.0)*(1.0-VOID)
       IF((ABS(DPDXA).GE.3.0E+06).AND.(IGRAD.EQ.0))THEN
         ZGRAD=XUDX
       ENDIF
       IF(ABS(DPDXA).GE.3.0E+06)THEN
         IGRAD=1
       ENDIF
       DPX=(DPDXF*DX)+(DPDXA*DX)+(DPDXG*DX)
       IF(NM.GT.1)THEN
       PRESS=PRESS+DPX
       FP456=FP456+(DX*DPDXF)
       AP456=AP456+(DX*DPDXA)
       GP456=GP456+(DX*DPDXG)
       ENDIF
       CALL ZTSAT(PRESS,RPRES,RTSAT,TSAT,IHI,ILOW,NEXIT)
       IF(NEXIT.EQ.1) GOTO 800
       XHFG=RHFG(ILOW)+(((RHFG(IHI)-RHFG(ILOW))*(PRESS-RPRES(ILOW)))/
      &   (RPRES(IHI)-RPRES(ILOW)))
       RHOV=RRHOV(ILOW)+(((RRHOV(IHI)-RRHOV(ILOW))*(PRESS-RPRES(ILOW)))/
      &   (RPRES(IHI)-RPRES(ILOW)))
       VG=1.0/RHOV
       XEQZ=-CP*(TSAT-TB)/XHFG
C ****SAHA/ZUBER MODEL ELEMENT 2****
       DTJL=C100*((QMAXPP*(DOUT/DI))**C200)*EXP(C300*PRESS)
C       TWI=TSAT+DTJL
       TWIBD=TSAT+DTJL
       XMX=(TWIBD-TWIONB)/(ZBD-XONB)
       TWI=XMX*(XUDX-XONB)+TWIONB
       H=(QMAXPP*(DOUT/DI))/(TWI-TB)
C       H=(CASY(REB,PRB)*QMAXPP*(DOUT/DI))/(TWI-TB)
C ***********************************
C ****SAHA/ZUBER FORMULA FOR SUBCOOLING AT OSNVG****
       PE=REB*PRB
C       IF(PE.LT.70000.0) DTSBSZ=(DI*QMAX*WF2*DOUT)/(DI*H*459.0)
C       IF(PE.GE.70000.0) DTSBSZ=(QMAX*WF2*DOUT)/(DI*GOR*CP*0.0069)
       CALL ZMODFBD(QMAX,WF2,DOUT,DI,GOR,K,CP,PE,PESTR,DTSBSZ)
       DTSUB=TSAT-TB
       STAN=(QMAX*WF2*DOUT)/(DI*GOR*CP*DTSUB)
       IF(DTSUB.LE.DTSBSZ)THEN
         TSZ=TSAT-DTSBSZ
         NC=1
C          PRINT *,'--YIPEE'
C          WRITE(3,129) XUDX
C  129     FORMAT(10X,'BUBBLE DETACHMENT VIA SAHA-ZUBER AT',1PE11.4,
C      &      ' METERS')
C          WRITE(3,130) TB,TSAT,DTSUB
C  130     FORMAT(10X,'BULK TEMP=',F10.4,' K'/10X,'SAT TEMP=',F10.4,' K'
C      &      /10X,'DTSUB=',F10.4,' K')
C ***********************************************
C ****SHAH FORMULA FOR SUBCOOLING AT BD****
C       DTSATBD=QMAXPP*WF2/(HFO*BIO)
C       SHBD1=6.3E+04*B0**1.25
```

```
C       SHBD2=2.0
C       IF(SHBD1.LT.SHBD2)THEN
C         DTSBSHBD=DTSATBD*SHBD1
C       ELSE
C         DTSBSHBD=DTSATBD*SHBD2
C       ENDIF
C       DTSUB=TSAT-TB
C       IF(DTBUB.LE.DTSBSHBD)THEN
C         TSH=TSAT-DTSBSHBD
C         NC=1
C         WRITE(3,169) XUDX
C  169    FORMAT(10X,'BUBBLE DETACHMENT VIA SHAH SCB AT',1PE11.4,
C     &      ' METERS')
C         WRITE(3,130) TB,TSAT,DTSUB
C  130    FORMAT(10X,'BULK TEMP=',F10.4,' K'/10X,'SAT TEMP=',F10.4,' K'
C     &      /10X,'DTSUB=',F10.4,' K')
C ****************************************
C ****SAHA/ZUBER MODEL ELEMENT 3****
        CALL ZCPAVER(AVCP,TSAT,TBZ,RTEM,RCPF,NEXIT)
        IF(NEXIT.EQ.1) GOTO 800
        XEQZ=-(AVCP*DTSBSZ)/XHFG
C ***********************************
C ****SHAH PDB MODEL ELEMENT 3****
C         CALL ZCPAVER(AVCP,TSAT,TSH,RTEM,RCPF,NEXIT)
C         IF(NEXIT.EQ.1) GOTO 800
C         XEQZ=-(AVCP*DTSBSHBD)/XHFG
C ***********************************
        XNEQZ=0.0
        CPZBD=AVCP
        ZBD=XUDX
        TBBD=TB
        DTSUBBD=TSAT-TB
        VOID=1.0E-15
        DPUPF=DPDXF
        AUP1O=1.0/RHO
        DPUPG=-9.807*SIN(THETA)*RHO*(1.0-VOID)
        ZSAT=(G*AVCP*(TSAT-TBIN)*DI)/(4.0*QMAX*WF1*(DOUT/DI))
      ENDIF
      GOTO 780
C
C ****FULLY DEVELOPED BOILING REGIME
C
  452 CALL ZRHO(TW1,PRESS,RHOW)
      CALL ZVISC(TW1,RHOW,MUW)
C       ZBDVO=0.0
C       ZBDVO=(0.002435*3.14159*DI)/(3.14159*DI*DI*0.25*
C     &   PRESS**0.237)
C       IF(DI.LT.2.0E-03)THEN
        WXX1=(ZSAT-ZBD)/4.0+ZBD
        WVOID=ZBDVO*((WXX1-XUDX)/(WXX1-ZBD))*WF5
C       ELSE
C         WVOID=ZBDVO*((ZSAT-XUDX)/(ZSAT-ZBD))
C       ENDIF
      IF(WVOID.LE.0.0)THEN
        WVOID=0.0
      ENDIF
      AEFF=(3.14159*DI*DI*0.25)*(1.0-WVOID)
      G=XMDA/AEFF
      DIHY=((AEFF*4.0)/3.14159)**0.5
      CALL ZHOMOGFF(G,GOR,DI,DIHY,MUB,CP,K,REB,REBF,PRB,FDWB)
```

```
      F=(FDWB*(MUW/MUB)**0.3)
C       F=(FDWB*(MUW/MUB)**0.3)*RF*CFF(XUDX)
      CALL ZCPAVER(AVCPI,TSAT,TBIN,RTEM,RCPF,NEXIT)
      IF(NEXIT.EQ.1) GOTO 800
      ISAT=(G*AVCPI*(TSAT-TBIN)*DI)/(4.0*QMAX*WF1*(DOUT/DI))
      ZP=(XUDX-ZBD)/(ISAT-ZBD)
      CALL ZUBSF3(TSAT,TB,AVCP,XHFG,RHO,G,DI,DIHY,DX,RHOV,ZP,CPZBD,
     &  DTSBSZ,THETA,F,TPFF,AUP1O,DPUPF,DPUPG,VIN,DPDXG,DPDXA,DPDXF,
     &  DPX1,VOID,ZA1O,ZDPF,ZDPG,XNEQZ,XEQZ,ZTP,CO,WF4)
      PRES1=PRESS+DPX1
      CALL ZTSAT(PRES1,RPRES,RTSAT,TSAT1,IHI,ILOW,NEXIT)
      IF(NEXIT.EQ.1) GOTO 800
      XHFG=RHFG(ILOW)+(((RHFG(IHI)-RHFG(ILOW))*(PRES1-RPRES(ILOW)))/
     &  (RPRES(IHI)-RPRES(ILOW)))
      RHOV=RRHOV(ILOW)+(((RRHOV(IHI)-RRHOV(ILOW))*(PRES1-RPRES(ILOW)))/
     &  (RPRES(IHI)-RPRES(ILOW)))
      VG=1.0/RHOV
      IF(TB.GE.TSAT1)THEN
C       WRITE(3,132)
C 132   FORMAT(1X,'TSAT OCCURS BEFORE TUBE EXIT')
C       WRITE(3,133) XUDX,TB,TSAT1
C 133   FORMAT(12X,'BULK BOILING POSITION=',1PE11.4,' METERS'/
C     &    12X,'BULK TEMP=',E11.4,' K'/12X,'SAT TEMP=',E12.4,' K'/)
        IF(NM.LT.NSTEPS)THEN
          ZOBB=XUDX
          NOBB=1
        ENDIF
        NEXIT=1
        TSAT=TSAT1
        GOTO 800
      ELSE
        TSAT=TSAT1
        PRESS=PRES1
        FP456=FP456+(DPDXF*DX)
        AP456=AP456+(DPDXA*DX)
        GP456=GP456+(DPDXG*DX)
        IF((ABS(DPDXA).GE.3.0E+06).AND.(IGRAD.EQ.0))THEN
          ZGRAD=XUDX
        ENDIF
        IF(ABS(DPDXA).GE.3.0E+06)THEN
          IGRAD=1
        ENDIF
        DPUPG=ZDPG
        DPUPF=ZDPF
        AUP1O=ZA1O
C ****JENS/LOTTES OR THOM MODEL FOR FDB REGIME****
        DTJL=C1OO*((QMAXPP*(DOUT/DI))**C2OO)*EXP(C3OO*PRESS)
        TWI=TSAT+DTJL
        H=(QMAXPP*(DOUT/DI))/(TWI-TB)
C         H=(CASY(REB,PRB)*QMAXPP*(DOUT/DI))/(TWI-TB)
C ************************************************
C ****SHAH MODEL FOR FDB REGIME****
C         CALL SHAHFDB(XUDX,REBF,PRB,FDWB,CP,G,GOR,DI,MUB,MUW,RH,
C     &  QMAXPP,XHFG,TSAT,TSATIN,TB,TBIN,H,TWI)
C ***********************************
        DTBUB=TSAT-TB
        PE=REB*PRB
        STAN=(QMAX*WF2*DOUT)/(DI*GOR*CP*DTBUB)
      ENDIF
C
```

```
C ****CALCULATION OF THERMAL CONDUCTIVITY COEFF
C
  780 N6=N6+1
      IF(N6 GT. 50)THEN
        KW=KW2
        WRITE(3, 134) XUDX
  134   FORMAT(1X, '50 ITERATIONS - OUTER WALL TEMP LOOP NOT CONVERGENT ',
     &     'AT POSITION =', 1PE11. 4, ' METERS')
        WRITE(3, 126) TB, TWI, TWO, QMAXPP
  126   FORMAT(1X, 'BULK TEMP=', 1PE10. 3, ' K  INNNER WALL TEMP=', E10. 3,
     &     ' K  OUTER WALL TEMP=', E10. 3, ' K  HEAT FLUX=', E10. 3,
     &     ' WATTS/M2')
        GOTO 850
      ELSE
        KW=ZFIT(TWO, AA1, AA2, AA3, AA4, AA5)
        FVT=(DI/DOUT)**2. 0
        DT=QMAXPP*DOUT*ALOG(1. 0/FVT)/(4. 0*KW)
        TWO=TWI+DT
        KW2=ZFIT(TWO, AA1, AA2, AA3, AA4, AA5)
C        PRINT *, 'N6=', N6
C        PRINT *, 'KW2=', KW2
      ENDIF
      IF(ABS(1. 0-KW/KW2). GT. 1. 0E-02) GOTO 780
C
C ****CRITICAL HEAT FLUX CORRELATION
C
      VEL=G/RHO
      UDTSUB=VEL*(TSAT-TB)
C     ROUSAR'S CORRELATION
C      QROUS=6. 34E+06+6. 31E+03*UDTSUB
C     QAMBILL'S CORRELATION
      AQ=9. 81
      SIGM=ZSURTE(TSAT)
C     BERNATH'S CORRELATION TO EVALUATE WALL TEMP AT BURNOUT CONDITIONS
      TWBO=97. 0*ALOG(PRESS/6891. 0)-54. 0*(PRESS/(PRESS+103365. 0))-VEL/
     &  1. 2192
      TWBO=TWBO+273. 15
C     VALUES OF K AND KP ARE . 14 AND . 026 RESPECTIVELY
      QCAMB=0. 14*XHFG*RHOV*(SIGM*AQ*(RHO-RHOV)/RHOV**2. 0)**0. 25*
     &  (1. 0+(RHO/RHOV)**0. 923*CP*DTSUB/(25. 0*XHFG))+0. 026*K/DI*
     &  REB**0. 8*PRB**(1. 0/3. 0)*(TWBO-TB)
      IF(DI. LT. 0. 0)THEN
        QCAMB=QCAMB*(0. 008/DI)**0. 5
      ENDIF
      IF((NPRFL. EQ. 1). OR. (NPRFL. EQ. 2))THEN
        QCAMB=QCAMB*1. 3
      ENDIF
      IF(QMAX. EQ. 0. 0)THEN
        CHFSF=0. 0
      ELSE
        CHFSF=QCAMB/QMAX
      ENDIF
      IF(ISF. LT. 1)THEN
        IF(CHFSF. LT. 2. 0)THEN
        ISF=1
        CHFZ=XUDX
        ENDIF
      ENDIF
C
C ****STORE COMPUTED VARIABLES EVERY 20TH STEP
```

```
C
  456 N=N+1
      IF(N.GE.NSTEPS/50)THEN
  800 N=0
      NNN=NNN+1
      KWS(NNN)=KW
      KS(NNN)=K
      RHOS(NNN)=RHO
      MUBS(NNN)=MUB
      MUWS(NNN)=MUW
      QS(NNN)=Q
      ZAXFS(NNN)=ZAXFLX(XUDX)
      TSATS(NNN)=TSAT
      TBS(NNN)=TB
      CPS(NNN)=CP
      VFS(NNN)=VF
      VQS(NNN)=VQ
C      CFHS(NNN)=CFH(XUDX)
C      CFFS(NNN)=CFF(XUDX)
C      CASYS(NNN)=CASY(REB,PRB)
      TWIS(NNN)=TWI
      TWOS(NNN)=TWO
C      GROUSS(NNN)=GROUS
      QQAMBS(NNN)=QQAMB
      SFS(NNN)=CHFSF
      FS(NNN)=F
      HS(NNN)=H
      PHILOS(NNN)=F/FDWS
      PES(NNN)=PE
      STANS(NNN)=STAN
      RHOVS(NNN)=RHOV
      FP123(NNN)=FP456
      AP123(NNN)=AP456
      QP123(NNN)=QP456
      DTSUBS(NNN)=DTSUB
      UDTSBS(NNN)=UDTSUB
      TONBS(NNN)=TWIONB
      XUDXS(NNN)=XUDX
      PRESSS(NNN)=PRESS
      REBS(NNN)=REBF
      PRBS(NNN)=PRB
      TPFFS(NNN)=TPFF
      RCR1TS(NNN)=RCR1T
      WDPDXA(NNN)=DPDXA
      WDPDXF(NNN)=DPDXF
      WDPDXQ(NNN)=DPDXQ
C      IF(NC.GE.1)THEN
        WXNEZ(NNN)=XNEQZ
        WXEZ(NNN)=XEQZ
        VOIDS(NNN)=VOID
        WVOIDS(NNN)=WVOID
        WTP(NNN)=ZTP
        WZP(NNN)=ZP
        WCO(NNN)=CO
C      ENDIF
      IF(NEXIT.EQ.1) GOTO 850
      ENDIF
  225 CONTINUE
C      PRINT *,'-- DP=',PIN-PRESSS(NNN)
C
```

```
C ****FRACTIONAL PRESSURE DROP AND PUMPING POWER
C
  850 PFRAC=(PIN-PRESS)/PIN
      CALL ZRHO(TB,PRESS,RHO)
      PPUMP=3.14159*(PIN-PRESS)*DI**2.0*G/(4.0*RHO)
      IF(NPRFL.EQ.0)THEN
        PTHERM=QMAX*DOUT*XUDX
C         PTHERM=QMAX*CHD(XUDX)*DOUT*XUDX
      ELSEIF(NPRFL.EQ.1)THEN
        PTHERM=QMAX*0.5*DOUT*XUDX
C         PTHERM=QMAX*0.5*CHD(XUDX)*DOUT*XUDX
      ELSEIF(NPRFL.EQ.2)THEN
        PTHERM=QMAX*0.5*DOUT*XUDX
C         PTHERM=QMAX*0.5*CHD(XUDX)*DOUT*XUDX
      ENDIF
      IF(PTHERM.LE.0.0)THEN
        PRATIO=0.0
      ELSE
        PRATIO=PPUMP/PTHERM
      ENDIF
      IF(XUDX.EQ.0)THEN
        PPUMPA=0.0
      ELSE
        PPUMPA=PPUMP/(XUDX*(DI+2.0*BW))
      ENDIF
C
C ****PREDICTION OF ONB,BD,OBB IF NOT OCCURING IN TUBE
C
      TBSLPI=(TBS(2)-TBIN)/(L/50.0)
      IF(TBSLPI.EQ.0.0)GOTO 254
      TBSLPE=(TBS(NNN)-TBS(NNN-1))/(L/50.0)
      IF(TBSLPE.EQ.0.0)GOTO 254
      IF(JUMP.LT.1)THEN
        TBONB=TWIONB-(QMAXPP*DOUT)/(H*DI)
        XONB=(TBONB-TBIN)/TBSLPE+L
        INREGM=1
C         WRITE(3,172) XONB
C  172    FORMAT(/10X,'PREDICTED ONB OCCURS AT ',1PE11.4,2X,'METERS')
C         WRITE(3,175) TBONB
C  175    FORMAT(10X,'PREDICTED BULK TEMP ',1PE11.4,2X,'DEG R')
      ENDIF
      IF(MONBDEF.EQ.1)THEN
        TBONB=TWIONBIN-(QMAXPP*DOUT)/(HIN*DI)
        XONB=(TBONB-TBIN)/TBSLPI
        INREGM=2
C         WRITE(3,172) XONB
C         WRITE(3,175) TBONB
      ENDIF
      IF(NC.LT.1)THEN
        TBBD=TSATS(NNN)-DTSBSZ
C         TBBD=TSAT-DTSBSHBD
        ZBD=(TBBD-TBIN)/TBSLPE+L
C         WRITE(3,173) ZBD
C  173    FORMAT(/10X,'PREDICTED BD PT OCCURS AT ',1PE11.4,2X,'METERS')
C         WRITE(3,175) TBBD
      ENDIF
      IF(MBDBEF.EQ.1)THEN
        TBBD=TSATIN-DTSBSZIN
C         TBBD=TSATIN-DTSBSHIN
        ZBD=(TBBD-TBIN)/TBSLPI
```

```
        INREGM=3
C         WRITE(3,173) ZBD
C         WRITE(3,175) TBBD
        ENDIF
        IF(MOBB.LT.1)THEN
          ZOBB=(TSATB(NNN)-TBB(NNN))/TBSLPE+L
C         WRITE(3,174) ZOBB
C  174    FORMAT(/10X,'PREDICTED OBB OCCURS AT ',1PE11.4,2X,'METERS')
        ENDIF
C       WRITE(3,*) ' EXIT SUBCOOLING = ',TSAT-TB
C
C ****PRINT INSTRUCTIONS
C
  234 WRITE(3,1)
      WRITE(3,137)
  137 FORMAT(/1X,20(2H-*),'  OUTPUTS  ',27(2H-*)//)
      WRITE(3,176)
  176 FORMAT(10X,'NOTE:  ZERO DEVELOPMENT LENGTHS ASSUMED AT HEATED INLET
     &'/)
      IF((MONBBEF.LT.1).AND.(MBDBEF.LT.1))THEN
        WRITE(3,177)
  177   FORMAT(10X,'HEATED INLET IS IN THE SPL REGIME (AT Z=0.0000E+00 M
     &ETERS)'/)
      ELSEIF(MONBBEF.EQ.1)THEN
        WRITE(3,192)
  192   FORMAT(10X,'HEATED INLET IS IN THE PDB REGIME (AT Z=0.0000E+00 M
     &ETERS)'/)
      ELSEIF(MBDBEF.EQ.1)THEN
        WRITE(3,193)
  193   FORMAT(10X,'HEATED INLET IS IN THE FDB REGIME (AT Z=0.0000E+00 M
     &ETERS)'/)
      ENDIF
      IF(MONBBEF.EQ.1)THEN
        WRITE(3,178) XONB,TBONB,TSATIN-TBONB
  178   FORMAT(10X,'ONB PREDICTED TO OCCUR BEFORE HEATED INLET AT Z=',
     &  1PE11.4,2X,'METERS'/15X,'PREDICTED ONB BULK TEMPERATURE=',
     &  E11.4,2X,'DEG K'/15X,'PREDICTED ONB DELTA-T SUBCOOL=',
     &  E11.4,2X,'DEG K'/)
      ENDIF
      IF(MBDBEF.EQ.1)THEN
        WRITE(3,179) ZBD,TBBD,TSATIN-TBBD
  179   FORMAT(10X,'OBNVG PREDICTED TO OCCUR BEFORE TUBE INLET AT Z=',
     &  1PE11.4,2X,'METERS'/15X,'PREDICTED OBNVG BULK TEMPERATURE=',
     &  E11.4,2X,'DEG K'/15X,'PREDICTED OBNVG DELTA-T SUBCOOL=',
     &  E11.4,2X,'DEG K'/)
      ENDIF
      IF((MONBBEF.LT.1).AND.(JUMP.EQ.1))THEN
        WRITE(3,180) XONB,TBONB,DTSUBONB
  180   FORMAT(10X,'ONB(ONSET OF NUCLEATE BOILING) OCCURS AT Z=',
     &  1PE11.4,2X,'METERS'/15X,'ONB BULK TEMPERATURE=',E11.4,2X,
     &  'DEG K'/15X,'ONB DELTA-T SUBCOOL=',E11.4,2X,'DEG K'/)
      ENDIF
      IF(JUMP.LT.1)THEN
        WRITE(3,196) XONB
  196   FORMAT(10X,'ONB(ONSET OF NUCLEATE BOILING) PREDICTED TO OCCUR AT
     & Z=',1PE11.4,2X,'METERS'/)
      ENDIF
      IF((MBDBEF.LT.1).AND.(NC.EQ.1))THEN
        WRITE(3,181) ZBD,TBBD,DTSUBBD
  181   FORMAT(10X,'OBNVG(ONSET OF SIGNIFICANT NET VAPOR GENERATION) OCC
```

```
     &URB AT',1PE11.4,2X,'METERS'/15X,'OSNVG BULK TEMPERATURE=',
     &  E11.4,2X,'DEG K'/15X,'OSNVG DELTA-T SUBCOOL=',E11.4,2X,
     &  'DEG K'/)
      ENDIF
      IF(NC.LT.1)THEN
        WRITE(3,197) ZBD
  197   FORMAT(10X,'OSNVG(ONSET OF SIGNIFICANT NET VAPOR GENERATION) PRE
     &DICTED TO OCCUR AT Z=',1PE11.4,2X,'METERS'/)
      ENDIF
      IF(MOBB.LT.1)THEN
      IF((JUMP.LT.1).AND.(NC.LT.1))THEN
        WRITE(3,182) L
  182   FORMAT(10X,'HEATED EXIT IS IN THE BPL REGIME AT Z=',1PE11.4,
     &  2X,'METERS'/)
      ELSEIF((JUMP.EQ.1).AND.(NC.LT.1))THEN
        WRITE(3,183) L
  183   FORMAT(10X,'HEATED EXIT IS IN THE FDB REGIME AT Z=',1PE11.4,
     &  2X,'METERS'/)
      ELSEIF(NC.EQ.1)THEN
        WRITE(3,184) L
  184   FORMAT(10X,'HEATED EXIT IS IN THE FDB REGIME AT Z=',1PE11.4,
     &  2X,'METERS'/)
      ENDIF
      ENDIF
      IF(MOBB.EQ.1)THEN
        WRITE(3,185) ZOBB,TBOBB
  185   FORMAT(10X,'BULK BOILING OCCURS BEFORE HEATED EXIT AT Z=',
     &    1PE11.4,2X,'METERS'/15X,'OBB BULK TEMPERATURE=',E11.4,
     &    2X,'DEG K')
      ELSEIF((MOBB.LT.1).AND.(ZOBB.GT.0.0))THEN
        WRITE(3,186) ZOBB
  186 FORMAT(10X,'OBB(ONSET OF BULK BOILING) PREDICTED TO OCCUR AT Z='
     &  ,1PE11.4,2X,'METERS'/)
      ENDIF
      WRITE(3,194) RCAV
  194 FORMAT(10X,'MAXIMUM ACTIVE SURFACE CAVITY RADIUS =',1PE11.4,2X,
     &  'METERS')
      WRITE(3,160) RCRIT
  160 FORMAT(10X,'CALCULATED CRITICAL SURFACE CAVITY RADIUS =',1PE11.4,
     &  2X,'METERS'/)
      IF(ISF.EQ.1)THEN
        WRITE(3,189) CHFZ
  189   FORMAT(10X,'****WARNING**** CHF SAFETY FACTOR LESS THAN 2.0 AT Z
     &=',1PE11.4,2X,'METERS'/)
      ENDIF
      IF(MOBB.LT.1)THEN
        WRITE(3,187) CHFSF
  187   FORMAT(10X,'EXIT CHF(CRITICAL HEAT FLUX) SAFETY FACTOR=',
     &  1PE11.4/)
      ELSEIF(MOBB.EQ.1)THEN
        WRITE(3,190) CHFSF
  190   FORMAT(10X,'CHF(CRITICAL HEAT FLUX) SAFETY FACTOR=',1PE11.4,
     &  2X,'AT OBB POINT'/)
      ENDIF
      IF(IGRAD.EQ.1)THEN
        WRITE(3,195) ZGRAD,ZGRAD
  195   FORMAT(10X,'****WARNING****  DP/DZ ACCEL > 3.0E+06 PA/M AT Z=',
     &    1PE11.4,2X,'METERS'/
     &    10X,'PRESSURE DROP MAY BE OVERPREDICTED AFTER Z=',E11.4,2X,
     &    'METERS'/)
```

```
      ENDIF
      WRITE(3,138) PIN-PRESS(NNN),PFRAC,PPUMP,PTHERM,PRATIO
  138 FORMAT(//10X,'TOTAL PRESSURE DROP IN HEATED LENGTH',22(1H-),
     &   1H=,1PE11.4,2X,'PA'/
     &   15X,'FRACTIONAL PRESSURE DROP IN HEATED LENGTH',12(1H-),
     &   1H=,E11.4/
     &   15X,'PUMPING POWER FOR HEATED LENGTH',22(1H-),1H=,E11.4,
     &   2X,'WATTS'/
     &   15X,'THERMAL POWER REMOVED',32(1H-),1H=,E11.4,2X,
     &   'WATTS'/
     &   15X,'PUMPING-TO-THERMAL POWER RATIO',23(1H-),1H=,E11.4/)
      DO 220 JLINE=1,21
      WRITE(3,227)
  227 CONTINUE
  220 CONTINUE
      WRITE(3,1)
      WRITE(3,140)
  140 FORMAT(T69,'INNER WALL',T82,'OUTER WALL',T98,'CORE',T123,'LOCAL')
      WRITE(3,141)
  141 FORMAT(T30,'SATURATION',T46,'BULK',T57,'DELTA-T',T71,'TEMP.',
     &   T84,'TEMP.',T96,'REYNOLDS',T110,'LIQUID',T120,'HEAT TRANSFER')
      WRITE(3,142)
  142 FORMAT(T5,'POSITION',T18,'PRESSURE',T33,'TEMP.',T46,'TEMP.',
     &   T57,'SUBCOOL',T69,'AT 0 DEGS',T82,'AT 0 DEGS',T97,'NUMBER',
     &   T110,'PRANDTL',T120,'COEFFICIENT')
      WRITE(3,143)
  143 FORMAT(T5,'(METERS)',T20,'(PA)',T32,'(DEG K)',T49,'(DEG K)',
     &   T57,'(DEG K)',T70,'(DEG K)',T83,'(DEG K)',T96,'RE(D-EFF)',T110,
     &   'NUMBER',T122,'(W/M2-K)'/)
      WRITE(3,144) (XUDXS(I),PRESS(I),TSATS(I),TBS(I),DTSUBS(I),
     &   TWIS(I),TWOS(I),RES(I),PRS(I),HS(I),I=1,NNN)
  144 FORMAT(10(2X,1PE11.4))
      WRITE(3,1)
      WRITE(3,145)
  145 FORMAT(T16,'LIQ. FANNING',T30,'TWO-PHASE')
      WRITE(3,146)
  146 FORMAT(T16,'FRIC. FACTOR',T33,'M-N',T49,'DP/DZ',T58,'DP/DZ',T71,
     &   'DP/DZ',T83,'DELTA-P',T96,'DELTA-P',T109,'DELTA-P',T122,
     &   'DELTA P')
      WRITE(3,147)
  147 FORMAT(T5,'POSITION',T18,'HEATING',T31,'FRICTION',T45,'FRIC.',
     &   T58,'GRAV.',T71,'ACCEL.',T84,'FRIC.',T97,'GRAV.',T110,
     &   'ACCEL.',T123,'TOTAL')
      WRITE(3,148)
  148 FORMAT(T5,'(METERS)',T18,'ADJUSTED',T30,'MULTIPLIER',T49,
     &   '(PA/M)',T58,'(PA/M)',T71,'(PA/M)',T85,'(PA)',T98,'(PA)',
     &   T111,'(PA)',T124,'(PA)'/)
      WRITE(3,149) (XUDXS(I),FS(I),TPFFS(I),WDPDXF(I),WDPDXG(I),
     &   WDPDXA(I),ABS(FP123(I)),ABS(GP123(I)),ABS(AP123(I)),ABS(
     &     FP123(I)+GP123(I)+AP123(I)),I=1,NNN)
  149 FORMAT(10(2X,1PE11.4))
      WRITE(3,1)
      WRITE(3,150)
  150 FORMAT(T31,'NON-EQUIL',T44,'ATTACHED',T59,'WALL BUBBLE',T72,
     &   'CORE')
      WRITE(3,151)
  151 FORMAT(T18,'NON-EQUIL',T33,'FLOW',T46,'WALL',T58,'LAYER',
     &   T72,'MASS',T96,'GAMBILL',T111,'CHF')
      WRITE(3,152)
  152 FORMAT(T5,'POSITION',T20,'FLOW',T33,'VOID',T46,'VOID',T57,
     &   'THICKNESS',T72,'FLUX',T97,'CHF',T110,'SAFETY')
```

```
      WRITE(3,188)
  188 FORMAT(T5,'(METERS)',T19,'QUALITY',T31,'FRACTION',T44,'FRACTION',
     &   T57,'(METERS)',T70,'(KG/M2-S)',T96,'(W/M2)',T110,'FACTOR'/)
      WRITE(3,191) (XUDXS(I),WXNEZ(I),VOIDS(I),WVOIDS(I),
     &  DI*WVOIDS(I)/4.0,QS(I),QQAMBS(I),SFS(I),I=1,NNN)
  191 FORMAT(6(2X,1PE11.4),T94,E11.4,2X,E11.4)
      WRITE(3,1)
      WRITE(3,196)
  196 FORMAT(T70,'MUW(TWI)',T110,'SUBCOOL',T124,'CO')
      WRITE(3,197)
  197 FORMAT(T5,'POSITION',T19,'CP(TS)',T32,'VF(TS)',T45,'VG(TS)',T57,
     &   'MUB(TS)',T69,'AT 0 DEGS',T85,'KS',T99,'PE',T112,'ST',T123,
     &   'DISTR')
      WRITE(3,199)
  199 FORMAT(T5,'(METERS)',T18,'(J/KG-K)',T32,'(M3/KG)',T45,'(M3/KG)',
     &   T57,'(NS/M2)',T70,'(NS/M2)',T83,'(W/M-K)',T97,'NUMBER',T110,
     &   'NUMBER',T123,'PARAM'/)
      WRITE(3,198) (XUDXS(I),CPS(I),VFS(I),VGS(I),MUBS(I),MUWS(I),
     &  KS(I),PES(I),STANS(I),WCO(I),I=1,NNN)
  198 FORMAT(10(2X,1PE11.4))
      IF(IXY EQ 2)THEN
        WRITE(3,1)
        WRITE(3,101)
  101   FORMAT(63X,'SAT',14X,'SAT')
        WRITE(3,102)
  102   FORMAT(44X,'VAPOR',12X,'LIQUID',12X,'VAPOR')
        WRITE(3,103)
  103   FORMAT(9X,'TSAT',14X,'PSAT',12X,'DENSITY',10X,'ENTHALPY',
     &  10X,'ENTHALPY')
        WRITE(3,104)
  104   FORMAT(10X,'(K)',14X,'(PA)',12X,'(KG/M3)',11X,'(J/KG)',
     &    12X,'(J/KG)'/)
        DO 255 I=1,182
        WRITE(3,106) I,RTSAT(I),RPRES(I),RRHOV(I),RHF(I),RHG(I)
  106   FORMAT(I4,F10.4,3X,F15.4,3X,F15.8,3X,F15.4,3X,F15.2)
  255   CONTINUE
        WRITE(3,1)
        WRITE(3,107)
  107   FORMAT(30X,'SAT')
        WRITE(3,108)
  108   FORMAT(29X,'LIQUID')
        WRITE(3,109)
  109   FORMAT(9X,'TSAT',19X,'SP  HEAT')
        WRITE(3,110)
  110   FORMAT(10X,'(K)',19X,'(J/KG-K)')
        DO 256 I=1,41
        WRITE(3,112) I,RTEM(I),RCPF(I)
  112   FORMAT(I4,F12.5,10X,F12.5)
  256 CONTINUE
      ENDIF
C      WRITE(3,199)
C  199 FORMAT(////5X,'**********************************************',
C     &   '**********')

C
C ****WRITE DATA TO GRAPH FILE
C
C       DO 250 I=1,NNN
C       WRITE(4,165) XUDXS(I),TBS(I),TSATS(I),TWIS(I),TWOS(I),PRESS(I)
C  165 FORMAT(1X,6(2X,1PE11.4))
```

```
C  250 CONTINUE
C       IF(.NOT.LNEX)THEN
C         WRITE(7,166) QMAX*(DOUT/DI),PRESSS(1)-PRESSS(NNN)
C  166    FORMAT(2(2X,1PE11.4))
C       ELSEIF(LNEX)THEN
C         DO 252 I=1,90
C         READ(7,166,END=458) QUNIF(I),DPRES(I)
C  252    CONTINUE
C  458    NREC=I-1
C         REWIND 7
C         QUNIF(NREC+1)=QMAX*(DOUT/DI)
C         DPRES(NREC+1)=PRESSS(1)-PRESSS(NNN)
C         DO 253 I=1,NREC+1
C         WRITE(7,166) QUNIF(I),DPRES(I)
C  253    CONTINUE
C       ENDIF
C       DO 251 I=1,NNN
C       WRITE(8,167) XUDXS(I),PRESSS(I)
C  167 FORMAT(2(2X,1PE11.4))
C  251 CONTINUE
C
C ****END ROUTINE
C
  899 CLOSE(UNIT=1)
      CLOSE(UNIT=2)
      CLOSE(UNIT=3)
C      CLOSE(UNIT=4)
C      CLOSE(UNIT=7)
C      CLOSE(UNIT=8)
      PRINT *,'    CALCULATIONS COMPLETE - END PROGRAM'
      GOTO 999
C
C ****ERROR MESSAGES
C
  900 WRITE(5,*) '  IMPROPER FILE NAME - EXITING PROGRAM'
      GOTO 999
  901 WRITE(5,*) '  ERROR OPENING FILE - EXITING PROGRAM'
      GOTO 999
  902 WRITE(5,*) '  ERROR STORING CORRECTIONS - EXITING PROGRAM'
      GOTO 999
  903 WRITE(5,*) '  ERROR OPENING DATA FILE - EXITING PROGRAM'
      GOTO 999
  904 WRITE(5,*) '  ERROR OPENING OLD FILE FOR ADDITIONS - EXITING'
C
  999 END
```

Supporting Subroutines

```
C
C *** THIS SUBROUTINE CALCULATES THE ISOTHERMAL FRICTION
C *** FACTOR(FANNING) AND RETURNS REB AND PRB
C
      SUBROUTINE ZHOMOGFF(Q,GOR,DI,DIHY,MUB,CP,K,REB,REBF,PRB,FDWB)
C
      REAL MUB,MUW,K
      REB=GOR*DI/MUB
      REBF=Q*DIHY/MUB
      PRB=MUB*CP/K
      IF(REBF.LE.1.0E+06)THEN
        FDWB=0.046/REBF**0.2
C       FDWB=.079/REBF**0.25
      ELSE
        FDWB=0.0246/REBF**0.155
      ENDIF
C
      RETURN
      END
```

```
C
C *** THIS SUBROUTINE CALCULATES FLUID ONLY HEAT TRANSFER
C *** COEFFICIENT AND RETURNS INNER WALL TEMPERATURE
C *** AND RHOW & MUW
C
      SUBROUTINE ZHTCOEFF(XUDX,REB,REBF,PRB,FDWB,CP,G,MUB,MUW,RH,TB,
     &  QMAXPP,DOUT,DI,PRESS,H,TWI,TWO,RHOW,N5,LEAV)
C
      REAL MUB,MUW
      XPM=ZXFPM(REB)
      XHB=0.445*FDWB*CP*G*((REB*0.0001)**0.0685)*(PRB**(-0.53))
  100 N5=N5+1
      IF(N5.GT.50)THEN
        H=H2
        WRITE(3,125) XUDX
        WRITE(3,126) TB,TWI,TWO,QMAXPP
  125   FORMAT(2X,'50 ITERATIONS - INNER WALL TEMP LOOP NOT
     &    CONVERGENT AT POSITION',1PE11.4,' METERS')
  126   FORMAT(1X,'BULK TEMP=',1PE10.3,' K  INNER WALL TEMP=',
     &  E10.3,' K  OUTER WALL TEMP=',E10.3,' K  HEAT FLUX=',
     &  E10.3,' WATTS/M2')
        LEAV=1
        RETURN
      ENDIF
      H=XHB*((MUB/MUW)**XPM)*RH
C      H=XHB*((MUB/MUW)**XPM)*RH*CFH(XUDX)
      TWI=TB+((QMAXPP*DOUT)/(H*DI))
C      TWI=TB+((QMAXPP*CASY(REB,PRB)*DOUT)/(H*DI))
      CALL ZRHO(TWI,PRESS,RHOW)
      CALL ZVISC(TWI,RHOW,MUW)
      H2=XHB*((MUB/MUW)**XPM)*RH
C      H2=XHB*((MUB/MUW)**XPM)*RH*CFH(XUDX)
C      PRINT *,'H2=',H2
      IF(ABS(1.-H/H2).GT.1.0E-03)THEN
      GOTO 100
      ENDIF
C
      RETURN
      END
```

```
C
C ****SUBROUTINE TO CALCULATE THE WALL SUPER HEAT AT ONB USING
C      THE DAVIS/ANDERSON, BERGLES/ROHSENOW, AND OFDB CORRELATIONS
C
      SUBROUTINE ZONB(QMAXPP,DOUT,DI,PRESS,C100,C200,C300,TSAT,
     &   TB,XHFG,K,RHOV,RCAV,WF3,SURF,RCRIT,DTJL,DTAD,DTBR,TWIONB)
C
      REAL K
C
C JENB/LOTTES OFDB USED BY KLINE
      DTJL=C100*(((QMAXPP*WF3*(DOUT/DI))**C200)*EXP(C300*PRESS)
      TWIONBJL=TSAT+DTJL
C
C DAVIS/ANDERSON ONB WITH RCAV OR RCRIT
      SURF=ZSURTE(TB)
      B=2.0*SURF*TSAT/(XHFG*RHOV)
        RCRIT=((B*K)/((QMAXPP+1.0E-03)*WF3))**0.5
      IF(RCAV.EQ.0.0)THEN
        DTAD=((8.0*SURF*QMAXPP*WF3*TSAT)/(XHFG*K*RHOV))**0.5
      ELSE
        DTAD=(B/RCAV)+(QMAXPP*WF3*RCAV/K)
      ENDIF
      TWIONBAD=TSAT+DTAD
C
C BERGLES/ROHSNOW ONB CORRELATION
      DTBR=0.556*(QMAXPP*WF3/(1082.0*(PRESS/1.05E+05)**1.156))**
     &   (0.463*(PRESS/1.0E+05)**0.0234)
      TWIONBBR=TSAT+DTBR
C
      TWIONB=TWIONBAD
C
      RETURN
      END
```

```
      SUBROUTINE ZMODFBD(QMAX,WF2,DOUT,DI,QOR,K,CP,PE,PESTR,DTSBSZ)
C
C     THIS SUBROUTINE DETERMINES THE ADJUSTED BD PREDICTION OF THE
C     SAHA-ZUBER CORRELATION BASED ON TRENDS OF KLINE FIG 4.17A
C
      IF(QMAX.EQ.0.0)GOTO 10
      PESTR=70000.0
C      PESTR=20839263.33*DI+37276.54
      IF(PE.LT.70000.0)THEN
        DTSBSZ=(DI*QMAX*DOUT)/(DI*K*455.0)
C      ELSEIF((PE.GE.70000.0).AND.(PE.LT.PESTR))THEN
C        DTSBSZ=(QMAX*DOUT)/(DI*QOR*CP*0.0065)
C      ELSEIF((PE.GE.PESTR).AND.(PE.LT.300000.0))THEN
C        BDM=9.9564E-06*DI-6.1605E-09
C        STNM=0.0065+BDM*(PESTR-PE)
C        DTSBSZ=(QMAX*DOUT)/(DI*QOR*CP*STNM)
C      ELSEIF(PE.GE.300000.0)THEN
C        BDM=9.9564E-06*DI-6.1605E-09
C        STNM=0.0065+BDM*(PESTR-300000.0)
C        DTSBSZ=(QMAX*DOUT)/(DI*QOR*CP*STNM)
C      ENDIF
      ELSEIF((PE.GE.70000.0).AND.(DI.GE.7.0E-03))THEN
        DTSBSZ=(QMAX*DOUT)/(DI*QOR*CP*0.0065)
      ELSEIF((PE.GE.70000.0).AND.(DI.LT.7.0E-03))THEN
        BDM=-(((QMAX*(DOUT/DI)/1.0E+06)/30.0)**(-1.03))*3.952E-09
        STNM=0.0065+BDM*(PE-70000.0)
        IF(STNM.LE.0.0039)THEN
          STNM=0.0039
        ENDIF
        DTSBSZ=(QMAX*DOUT)/(DI*QOR*CP*STNM)
      ENDIF
      GOTO 20
   10 DTSBSZ=0.0
   20 CONTINUE
      RETURN
      END
```

```
      SUBROUTINE ZUBSF3(TSAT,TB,AVCP,XHFG,RHO,G,DI,DIHY,DX,RHOV,
     &    ZP,CPZBD,DTSBSZ,THETA,F,TPFF,AUP1O,DPUPF,DPUPG,VIN,DPDXG,
     &    DPDXA,DPDXF,DPX,VOID,ZA1O,ZDPF,ZDPG,XNEQZ,XEQZ,TP,CO,WF4)
C
C  THIS SUBROUTINE DETERMINES THE TWO PHASE PRESSURE GRADIENT (DPDX)
C  FOR SEPARATED FLOW USING THE ZUBER FLOW QUALITY MODEL,
C  THE ZUBER VOID MODEL, AND HOMOGENEOUS TWO-PHASE FRICTION FACTOR
C
C       N1=0
        DTSUB=TSAT-TB
        XEQZ=-(AVCP*DTSUB)/(XHFG)*WF4
C               TP=1-EXP(-ZP)
                TP=TANH(ZP)
C       IF(ABS((TP-ZP)/ZP).LE.1.0E-10)THEN
C         TP=TP+1.0E-12
C       ENDIF
        XNEQZ=(DTSBSZ*(ZP-TP)*CPZBD)/(XHFG+(DTSBSZ*(1.000-TP)*
     &  CPZBD))*WF4
C       PRINT *,'ZP=',ZP
C       PRINT *,'TP=',TP
C       PRINT *,'CP=',CPZBD
C       PRINT *,'DTSUBSZ=',DTSBSZ
C       PRINT *,'WF4=',WF4
C       PRINT *,'XNEQZ=',XNEQZ
         IF(XNEQZ.EQ.0.0)THEN
          XNEQZ=XNEQZ+1.0E-15
        ENDIF
        A300=1.41
C        A300=2.9
C  100   N1=N1+1
C        IF(N1.GT.150)THEN
C          WRITE(5,*) 'WARNING - CO LOOP NOT CONVERGENT AT 150'
C        WRITE(5,*) 'VOID=',VOID
C          GOTO 200
C        ENDIF
C         CO1=19
C        CO2=0.2
C         CO2=1.164-1.6934E-07*PRESS+7.9078E-15*PRESS**2.0
C         CO=(1-EXP(-CO1*VOID))/(1-EXP(-CO1))*(1+CO2)-CO2*VOID
        CO=1.29
        XST=ZSURTE(TSAT)
        VGJ=A300*((((9.807)*(RHO-RHOV)*(XST))/(RHO*RHO))**(0.250))*
     &  (SIN(THETA))
        A100=(CO/RHO)*(RHO-RHOV)*(XNEQZ)
        A200=(RHOV/RHO)*CO
        A300=(RHOV/RHO)*(VGJ/VIN)*(SIN(THETA))
        VOID=(XNEQZ)/(A100+A200+A300)
C         WRITE(5,*) 'VOID=',VOID
C        IF(ABS(1-VOID/VOID1).GT.1.0E-02)THEN
C          VOID=VOID1
C          GOTO 100
C        ENDIF
  200   ZA1O=((XNEQZ*XNEQZ)/(VOID*RHOV))+
     &         (((1.00-XNEQZ)*(1.000-XNEQZ))/((1.000-VOID)*(RHO)))
        DPDXA=-((G*G)/(DX))*(ZA1O-AUP1O)
        ZDPG=-(9.807)*(SIN(THETA))*((VOID*RHOV)+((1.000-VOID)*RHO))
        DPDXG=0.5*(ZDPG+DPUPG)
C *****  HOMOGENEOUS TPFF
                VF=1.00/RHO
                VG=1.00/RHOV
```

```
                VFO=VO-VF
                CALL ZVISC(TB,RHO,FVIS)
                CALL ZVISC(TSAT,RHOV,GVIS)
                B10=FVIS-GVIS
                B100=XNEQZ*(VFO/VF)
                B200=XNEQZ*(B10/GVIS)
                B300=(1.00+B200)**0.25
C                TPFF=1.0
C               TPFF=(1.000+B100)/(B300)
C               WRITE(3,300) TPFF
C300            FORMAT('  TPFF = ',F20.10)
C ***** M-N TPFF ****
        REGO=G*DI/GVIS
        REFO=G*DI/FVIS
        FGO=0.046*REGO**(-0.2)
        FFO=0.046*REFO**(-0.2)
        DPDZFGO=(2.0*FGO*G*G)/(DI*RHOV)
        DPDZFFO=(2.0*FFO*G*G)/(DI*RHO)
        GMA=(DPDZFGO/DPDZFFO)**0.5
C        GMA=((FVIS/GVIS)**(-0.2)*(VG/VF))**0.5
        IF(GMA.GE.8.9)THEN
          C=21.0
C           B=21.0/GMA
        ELSE
          C=2.364*GMA-1/GMA
C           B=2.364
        ENDIF
        B=(C*GMA-2.0**1.8+2.0)/(GMA**2.0-1)
C ***** MN TPFF WITH CHISHOLM CORRECTION
C         IF(GMA.LE.9.5)THEN
C           IF(G.LE.300.0)THEN
C             B=4.8
C           ELSEIF((G.GT.300.0).AND.(G.LT.1900.0))THEN
C             B=2400.0/G
C           ELSEIF(G.GE.1900.0)THEN
C             B=55.0/G**0.5
C           ENDIF
C         ELSEIF((GMA.GT.9.5).AND.(GMA.LT.28.0))THEN
C           IF(G.LE.600.0)THEN
C             B=520.0/(GMA*G**0.5)
C           ELSEIF(G.GT.600.0)THEN
C             B=21.0/GMA
C           ENDIF
C         ELSEIF(GMA.GE.28.0)THEN
C           B=15000.0/(GMA**2.0*G**0.5)
C         ENDIF
        TPFF=1+(GMA**2.0-1)*(B*XNEQZ**0.9*(1-XNEQZ)**0.9+XNEQZ**1.8)
C         TPFF=0.7*TPFF
        ZDPF=-((2.0*F*G*G)/(DIHY*RHO))*TPFF
C       ZDPF=-((2.0*F*G*G)/(DI*RHO))*TPFF
        DPDXF=0.5*(ZDPF+DPUPF)
        DPX=(DPDXF*DX)+(DPDXA*DX)+(DPDXG*DX)
        RETURN
        END
```

```
      SUBROUTINE  ZLSTSQ(NPT,AA,BB,CC,DD,EE,NUNIT,F,D)
C
C     THIS IS A SUBROUTINE THAT DOES A LEAST SQUARES CURVE FIT
C     ON A DATA SET.   THE DATA IS READ IN THROUGH THE
C     SUBROUTINE IN PAIRS_ THE INDEPENDENT(FREE) VARIABLE AND
C     THE CORRESPONDING DEPENDENT VARIABLE.
C     IF THE INPUT CONSISTS OF ONE THROUGH FIVE VARIABLE
C     PAIRS, A CURVE FIT EQUAL IN ORDER TO ^THE NUMBER OF
C     INPUT VARIABLE PAIRS MINUS ONE^ RESULTS.
C     FOR INPUT OF MORE THAN FIVE VARIABLE PAIRS A
C     FOURTH ORDER FIT RESULTS.
C     THE MAXIMUM NUMBER OF PAIRS ALLOWED IS 100.
C     THE SUBROUTINE IS CALLED BY  ZLSTSQ(NPT,AA,BB,CC,DD,EE).
C     ^NPT^ IS THE NUMBER OF PAIRS OF POINTS THROUGH WHICH
C     THE LEAST SQUARES FIT IS DESIRED.
C     ^NPT^ MUST BE SPECIFIED IN THE PART OF THE CODE
C     CALLING  ZLSTSQ(NPT,AA,BB,CC,DD,EE).
C     AA,BB,CC,DD,EE ARE THE COEFFICIENTS OF THE
C     FIT EQUATION,  I.E.,
C     Y = AA + BB*X + CC*X**2 + DD*X**3 + EE*X**4
C     THE DATA IS READ IN THROUGH THIS SUBROUTINE IN
C     THE FOLLOWING FORMAT;
C
C       READ(2,2) FREE,DEP
C     2 FORMAT(2E15.5)
C
C     EXAMPLE
C
C       READ(2,4) NPT
C     4 FORMAT(I3)
C       CALL  ZLSTSQ(NPT,AA,BB,CC,DD,EE)
C
C     AA,BB,CC,DD,EE ARE NOW VARIABLES COMMON TO THE
C     PART OF THE CODE CALLING  ZLSTSQ AND MAY BE USED IN
C     ANY MANNER ACCORDINGLY.
C
C     IT SHOULD BE NOTED THAT THIS SUBROUTINE HAS ANOTHER
C     SUBROUTINE INTERNAL TO IT - SUBROUTINE ZGAUSSY(A,B,X,N).
C     ZGAUSSY SOLVES A SYSTEM OF LINEAR SIMULTANEOUS
C     EQUATIONS USING GAUSSIAN ELIMINATION.
C     IF THE EQUATIONS READ IN TO ZGAUSSY ARE NOT
C     LINEARLY INDEPENDENT, THE SUBROUTINE WILL PRINT OUT
C     ^EQUATIONS ARE NOT INDEPENDENT^.
C
      DIMENSION A(5,5),B(5),X(5),TP(9)
      DIMENSION D(10),F(10)
      DO 81 NI=1,5
   81 X(NI)=0.
      DO 20 N=1,NPT
      READ(NUNIT,*) FREE,DEP
C     2 FORMAT(1PE11.4,2X,1PE11.4)
      D(N)=DEP
   20 F(N)=FREE
      IF(NPT.EQ.1)GO TO 51
      IF(NPT.GT.5)GO TO 61
      NX=NPT
      NT=2*NPT-1
      GO TO 62
   61 NT=9
      NX=5
```

```
 62 TP(1)=NPT
    DO 30 K=2,NT
    TP(K)=0.
    DO 40 I=1,NPT
 40 TP(K)=TP(K)+F(I)**(K-1)
 30 CONTINUE
    B(1)=0.
    DO 50 J=1,NPT
 50 B(1)=B(1)+D(J)
    DO 60 L=2,NX
    B(L)=0.
    DO 70 M=1,NPT
 70 B(L)=B(L)+D(M)*F(M)**(L-1)
 60 CONTINUE
    DO 31 I=1,5
    DO 31 K=1,5
 31 A(I,K)=TP(I+K-1)
    CALL IGAUSSY(A,B,X,NX)
    AA=X(1)
    GO TO 89
 51 AA=D(1)
 89 BB=X(2)
    CC=X(3)
    DD=X(4)
    EE=X(5)
    RETURN
    END
```

```
      SUBROUTINE ZGAUSSY(A,B,X,N)
C     SOLUTION OF SIMULTANEOUS EQUATIONS BY GAUSS ELIMINATION
      DIMENSION A(5,5),B(5),X(5)
C     BEGINNING OF ELIMINATION PROCESS
      DO 28 K=1,N
C     MOVING LARGEST COEFFICIENT INTO DIAGONAL POSITION
      AMAX=0.
      DO 4 I=K,N
      IF(ABS(A(I,K))-ABS(AMAX))4,4,2
    2 AMAX=A(I,K)
      IMAX=I
    4 CONTINUE
C     TESTING FOR CONVERGENCE
      IF(ABS(AMAX)-0.1E-15)10,10,14
   10 WRITE(3,12)
   12 FORMAT('   EQUATIONS ARE NOT INDEPENDENT  ')
      RETURN
C     EXCHANGING ROW IMAX AND ROW K
   14 BTEMP=B(K)
      B(K)=B(IMAX)
      B(IMAX)=BTEMP
      DO 18 J=K,N
      ATEMP=A(K,J)
      A(K,J)=A(IMAX,J)
   18 A(IMAX,J)=ATEMP
C     SUBTRACTING A(I,K)/A(K,K) TIMES TERM IN THE FIRST EQN FROM OTHERS
      KPLUS=K+1
      IF(K-N)22,26,26
   22 DO 24 I=KPLUS,N
      B(I)=B(I)-B(K)*A(I,K)/A(K,K)
      ACON=A(I,K)
      DO 24 J=K,N
   24 A(I,J)=A(I,J)-A(K,J)*ACON/A(K,K)
   28 CONTINUE
C     BACK SUBSTITUTION
      L=N
   32 SUM=0.
      IF(L-N)34,38,38
   34 LPLUS=L+1
      DO 36 J=LPLUS,N
   36 SUM=SUM+A(L,J)*X(J)
   38 CONTINUE
      X(L)=(B(L)-SUM)/A(L,L)
      IF(L-1)42,42,40
   40 L=L-1
      GO TO 32
   42 RETURN
      END
```

```
      SUBROUTINE ZCPF(TEMPK,RTEM,RCPF,CP,NEXIT)
C  THIS SUBROUTINE DETERMINES THE ISOBARIC SPECIFIC HEAT OF
C  SATURATED LIQUID FOR A GIVEN TEMPERATURE
      DIMENSION RTEM(41),RCPF(41)
      DO 100 I=1,41
      IF(TEMPK.GT.RTEM(I)) GO TO 100
      IHI=I
      ILOW=I-1
      IF(ILOW.LE.0) GO TO 101
      CP=RCPF(ILOW)+(((RCPF(IHI)-RCPF(ILOW))*(TEMPK-RTEM(ILOW)))/
     &    (RTEM(IHI)-RTEM(ILOW)))
      GO TO 105
100   CONTINUE
101   WRITE(3,300) TEMPK
300   FORMAT(' ZCPF SUBROUTINE:TEMP OUT OF TABLE RANGE
     &  273.15 - 643 K   TEMP K =',F20.8)
      NEXIT=1
105   RETURN
      END
```

```
      SUBROUTINE ZCPAVER(AVCP,T2,T1,RTEM,RCPF,NEXIT)
C  THIS SUBROUTINE DETERMINES THE AVERAGE ISOBARIC SPECIFIC
C  HEAT OF WATER BETWEEN TWO TEMPERATURES
      DIMENSION RTEM(41),RCPF(41)
      DTRAN=T2-T1
      IDT=IFIX(DTRAN)
      IF(IDT.LT.1) GO TO 200
      ICOUN=1
      TRUNK=AINT(DTRAN)
      ITOP=IFIX(2.000*TRUNK)
      XDT=DTRAN/(2.000*TRUNK)
      XT=T1+(0.5*XDT)
      CALL ZCPF(XT,RTEM,RCPF,CPSUM,NEXIT)
       IF(NEXIT.EQ.1) GO TO 400
50    CONTINUE
      XT=XT+XDT
      CALL ZCPF(XT,RTEM,RCPF,CPXT,NEXIT)
       IF(NEXIT.EQ.1) GO TO 400
      CPSUM=CPSUM+CPXT
      ICOUN=ICOUN+1
      IF(ICOUN.GE.ITOP) GO TO 100
      GO TO 50
100   CONTINUE
      AVCP=(XDT*CPSUM)/(DTRAN)
      RETURN
200   CONTINUE
      XT=T1+(0.5*DTRAN)
      CALL ZCPF(XT,RTEM,RCPF,AVCP,NEXIT)
400   RETURN
      END
```

```
      SUBROUTINE ZRHO(TEMPK,PRESS,RHO)
C  THIS SUBROUTINE DETERMINES DENSITY OF EITHER (A) COMPRESSED
C  LIQUID OR (B) SATURATED LIQUID FOR GIVEN VALUES OF TEMPERATURE
C  AND PRESSURE
      TC1=647.3
      PC1=2.2120E7
      SPVC1=0.00317
      THETA=(TEMPK)/TC1
      BETA=PRESS/PC1
      A1=0.8438375405
      A2=9.362162162E-4
      A3=1.720
      A4=0.07342278489
      A5=0.04975858870
      A6=0.6537154300
      A7=1.1500000E-6
      A8=1.510800000E-5
      A9=0.1418800
      A10=7.002753165
      A11=2.995284926E-4
      A12=0.20400
      CA11=7.982692717
      CA12=-0.02616971843
      CA13=0.001522411790
      CA14=0.02284279054
      CA15=242.1647003
      CA16=1.269716088E-10
      CA17=2.074838328E-7
      CA18=2.174020350E-8
      CA19=1.105710498E-9
      CA20=12.93441934
      CA21=1.308119072E-5
      CA22=6.047626338E-14
      Y=1.0000-(A1*THETA*THETA)-(A2*((THETA)**(-6)))
      UL=(A3*Y*Y)-(2.00*A4*THETA)+(2.00*A5*BETA)
      IF(UL.LE.0.00000000) GO TO 400
      GO TO 405
400   CONTINUE
      Z=Y
      GO TO 412
405   Z=Y+((UL)**(0.500))
412   CONTINUE
         C100=0.000
      IF(Z.GT.0.000) C100=CA11*A9*((Z)**(-9.00/17.00))
      C200=CA12+(CA13*THETA)+(CA14*THETA*THETA)+
     &  (CA15*((A6-THETA)**(10)))+(CA16/(A7+((THETA)**(19))))
      C300=(CA17+(2.00*CA18*BETA)+(3.00*CA19*BETA*BETA))/
     &        (A8+((THETA)**(11)))
      C400=CA20*((THETA)**(18))*((A9)+(THETA*THETA))*
     &        (((-3.00)*((A10+BETA)**(-4)))+A11)
      C500=(3.00*CA21*(A12-BETA)*BETA*BETA)+(4.000*CA22*BETA*BETA*
     &        BETA*((THETA)**(-20)))
      RHO=1.0000000/((SPVC1)*(C100+C200-C300-C400+C500))
      RETURN
      END
```

```
      SUBROUTINE ZVISC(TEMPK,RHOD,VISC)
C  THIS SUBROUTINE DETERMINES DYNAMIC VISCOSITY OF EITHER
C  (A)COMPRESSED LIQUID, (B)SATURATED LIQUID, OR(C)SATURATED
C  VAPOR FOR GIVEN VALUES OF TEMPERATURE AND DENSITY
      DIMENSION B(6,5)
      TS=647.27
      DS=317.763
      A0=0.0181583
      A1=0.0177624
      A2=0.0105287
      A3=-0.0036744
      B(1,1)=0.501938
      B(1,2)=0.235622
      B(1,3)=-0.274637
      B(1,4)=0.145831
      B(1,5)=-0.0270448
      B(2,1)=0.162888
      B(2,2)=0.789393
      B(2,3)=-0.743539
      B(2,4)=0.263129
      B(2,5)=-0.0253093
      B(3,1)=-0.130356
      B(3,2)=0.673665
      B(3,3)=-0.959456
      B(3,4)=0.347247
      B(3,5)=-0.0267758
      B(4,1)=0.907919
      B(4,2)=1.207552
      B(4,3)=-0.687343
      B(4,4)=0.213486
      B(4,5)=-0.0822904
      B(5,1)=-0.551119
      B(5,2)=0.0670665
      B(5,3)=-0.497089
      B(5,4)=0.100754
      B(5,5)=0.0602253
      B(6,1)=0.146543
      B(6,2)=-0.0843370
      B(6,3)=0.195286
      B(6,4)=-0.032932
      B(6,5)=-0.0202595
      TK=TEMPK
      TT=TS/TK
      TT1=TK/TS
      DD=RHOD/DS
      UO=(TT1**0.500)/(A0+(A1*TT)+(A2*TT*TT)+(A3*TT*TT*TT))
      D100=DD-1.00000
      T100=TT-1.00000
      SUM=0.00000
      DO 85 I=1,6
      DO 88 J=1,5
      ITP=I-1
      IDP=J-1
      SUM=SUM+(B(I,J)*((T100)**(ITP))*((D100)**(IDP)))
88    CONTINUE
85    CONTINUE
      U100=DD*SUM
      VISC=UO*EXP(U100)*(1.0E-6)
      RETURN
      END
```

```
      SUBROUTINE ZTLCW(TEMPK,RHO,FKOND)
C  THIS SUBROUTINE DETERMINES THERMAL CONDUCTIVITY OF
C  EITHER (A)SATURATED WATER OR (B)COMPRESSED WATER FOR GIVEN
C  VALUES OF TEMPERATURE AND DENSITY
      TS=647.3
      A0=1.02811E-2
      A1=2.99621E-2
      A2=1.96146E-2
      A3=-4.22464E-3
      B0=-3.97070E-1
      B1=4.00302E-1
      B2=1.06000
      BB1=-1.71587E-1
      BB2=2.39219
      DS=317.7
      D1=7.01309E-2
      D2=1.18520E-2
      D3=1.69937E-3
      D4=-1.02000
      C1=6.42857E-1
      C2=-4.11717
      C3=-6.17937
      C4=3.08976E-3
      C5=8.22994E-2
      C6=1.00932E+1
      TK=TEMPK
      TT=TK/TS
      E10=TT-1.00000
      E12=ABS(E10)
      DTS=E12+C4
      IF(TT.LT.1.0000) GO TO 100
      S=1.0000/DTS
      GO TO 105
100   S=C6/((DTS)**(0.6))
105   CONTINUE
      Q=2.00000+(C5/((DTS)**(0.6)))
      R=Q+1.0000
      DD=RHO/DS
      DDI=DS/RHO
      E20=(C2*((TT)**(1.5)))+(C3*(DDI**5))
      E200=D4*EXP(E20)
      E19=(Q/R)*(1.0000-((DD)**(R)))
      E190=D3*S*((DD)**(Q))*EXP(E19)
      E18=C1*(1.0000-(DD**2.8))
      E180=(DD**1.8)*EXP(E18)
      E170=((D1)/(TT**10))+D2
      DLAM=(E170*E180)+E190+E200
      E21=BB1*(DD+BB2)*(DD+BB2)
      BLAM=B0+(B1*DD)+(B2*EXP(E21))
      ZLAM=(TT**0.500)*(A0+(A1*TT)+(A2*TT*TT)+(A3*TT*TT*TT))
      FKOND=ZLAM+BLAM+DLAM
      RETURN
      END
```

```
      SUBROUTINE ZTSAT(PRESS,RPRES,RTSAT,TSAT,IHI,ILOW,NEXIT)
C  THIS SUBROUTINE DETERMINES THE SATURATION TEMPERATURE FOR A
C  GIVEN PRESSURE
      DIMENSION RPRES(182),RTSAT(182)
      DO 100 I=1,182
      IF(PRESS.GT.RPRES(I)) GO TO 100
      IHI=I
      ILOW=I-1
      IF(ILOW.LE.0) GO TO 101
     TSAT=RTSAT(ILOW)+(((RTSAT(IHI)-RTSAT(ILOW))*(PRESS-RPRES(ILOW)))/
     &       (RPRES(IHI)-RPRES(ILOW)))
      GO TO 105
100   CONTINUE
101   WRITE(3,300) PRESS
300   FORMAT(' ZTSAT SUBROUTINE:PRESS OUT OF TABLE RANGE: PRESS N/M2='
     &          ,F25.10)
      NEXIT=1
105   RETURN
      END
```

```
      FUNCTION ZSURTE(TEMPK)
C  THIS FUNCTION DETERMINES THE SURFACE TENSION AT THE
C  LIQUID-VAPOR INTERFACE FOR A GIVEN TEMPERATURE
      TC=647.15
      TK=TEMPK
      C10=(TC-TK)/TC
      B=0.2358
      BB=-0.625
      U=1.256
      C100=C10**U
      C200=1.0000+(BB*C10)
      ZSURTE=B*C100*C200
      RETURN
      END
```

```
      FUNCTION  ZGINT16(XMIN,XMAX,F,NINT)
C   THIS IS A 16 POINT GAUSSIAN INTEGRATION ROUTINE.
      DIMENSION U(8),R(8),T(8)
      EXTERNAL F
      IF(NTEST-13579) 1,2,1
    1 NTEST=13579
      U(1)=-9.894009349E-1
      U(2)=-9.445750230E-1
      U(3)=-8.656312024E-1
      U(4)=-7.554044083E-1
      U(5)=-6.178762444E-1
      U(6)=-4.580167776E-1
      U(7)=-2.816035507E-1
      U(8)=-9.501250977E-2
      R(1)=2.715247939E-2
      R(2)=6.225392297E-2
      R(3)=9.515851168E-2
      R(4)=1.246289712E-1
      R(5)=1.495959888E-1
      R(6)=1.691565193E-1
      R(7)=1.826034151E-1
      R(8)=1.894506104E-1
    2 Q=XMIN
      XN=NINT
      DQ=(XMAX-XMIN)/XN
      DQ5=DQ*.5
      DO 3 K=1,8
    3 T(K)=DQ5*U(K)
      ZGINT16=0.
      DO 5 L=1,NINT
      PM=Q+DQ5
      DO 4 N=1,8
    4  ZGINT16= ZGINT16+(F(PM+T(N)) + F(PM-T(N)))*R(N)
    5 Q=Q+DQ
      ZGINT16=DQ5* ZGINT16
      RETURN
      END
```

```
      FUNCTION ZXFPM(RE)
C     THIS FUNCTION CALCULATES EXPONENT ON VISCOSITY RATIO
C     FOUND IN SINGLE PHASE FULLY DEVELOPED TURBULENT FORCED
C     CONVECTION (SMOOTH PIPE) HEAT TRANSFER CORRELATION VIA
C      GE R&D HEAT TRANSFER MANUAL VOL 1.  PER UCD LIBRARY
      IF(RE.LT.2100.0) ZXFPM=0.14
      IF(RE.GE.2100.0.AND.RE.LT.12500.0) ZXFPM=.02+((0.12/10400.0)*
     &       (12500.0-RE))
      IF(RE.GE.12500.0.AND.RE.LT.25000.0) ZXFPM=.05-((0.03/12500.0)*
     &       (25000.0-RE))
      IF(RE.GE.25000.0.AND.RE.LT.50000.0) ZXFPM=.08-((0.03/25000.0)*
     &       (50000.0-RE))
      IF(RE.GE.50000.0) ZXFPM=.08
      RETURN
      END
```

```
      FUNCTION ZFIT(T,A,B,C,D,E)
C  THIS FUNCTION EVALUATES THE LEAST SQUARES CURVE FIT AT A POINT,
C  FOR THE CORRESPONDING TEMPERATURE AND COEFFICIENTS.
C*****FOLLOWING FORM FOR ZFIT CHANGED TO IMPROVE OPERATION.  (LAPPA/7/78)
      ZFIT=((((E*T)+D)*T+C)*T+B)*T+A
      RETURN
      END
```

```
      FUNCTION ZAXFLX(X)
C  THIS FUNCTION GIVES THE AXIAL DISTRIBUTION OF THE HEAT FLUX,
C  NORMALIZED TO UNITY AT THE MAXIMUM HEAT FLUX.
      ZAXFLX=1.
      RETURN
      END
```

Appendix B

Sample Video Screens Showing Input
File Editing Features of Code

```
                                SCB-1A


                        A Subcooled Flow Boiling
                              Design Code



                    (C) University of California, Davis, 1988

 HIT RETURN KEY TO CONTINUE
```

```
*******************************************************************************
 THIS CODE WAS DEVELOPED FOR THE LAWRENCE LIVERMORE NATIONAL LABORATORY BY:
     PRINCIPAL INVESTIGATOR:  Professor Myron A. Hoffman
     GRADUATE STUDENTS:  Charles Kline(1985), Christopher Wong(1988)
     Department of Mechanical Engineering
     University of California, Davis, CA  95616
*******************************************************************************




  HIT RETURN KEY TO CONTINUE
```

Screens #1 and #2

```
   WELCOME TO THE SUBCOOLED FLOW BOILING DESIGN CODE SCB-1A
   (VERSION 1A - November, 1988)
       for the IBM PC/AT (or compatibles) and the VAX 11/780

     This program calculates pressure drop, pumping power required and the
     CHF(Critical Heat Flux) for water flow in round tubes with uniform axial
     heat flux.  It can provide results for the single-phase liquid flow
     regime and/or the subcooled boiling flow regime.


 You should be able to run SCB-1A by responding to the prompts.  Try it!

 For more information, refer to the SCB-1A Code Manual. It contains an example.



 HIT RETURN KEY TO CONTINUE
```

```
 ********************************************************************************

 PLEASE SELECT OPERATION

 1) USE AN OLD DATA FILE

 2) REVISE AN OLD DATA FILE

 3) CREATE A NEW DATA FILE

 ENTER # OF YOUR CHOICE - TO EXIT, ENTER 0
   Option (1) or (2) is recommended

 ********************************************************************************
2
PLEASE ENTER INPUT FILE NAME IN THE FORM:  INPnnn.DAT - USE CAPITAL LETTERS
    (nnn MAY BE ANY COMBINATION OF FROM 1 TO 5 NUMBERS OR LETTERS)
INP32.DAT

ENTER THE NEW OUTPUT FILE NAME IN THE FORM: OUTmmm.DAT - USE CAPITAL LETTERS
 (mmm MAY BE ANY COMBINATION OF FROM 1 TO 5 NUMBERS OR LETTERS)

 NOTE: THIS FILE MUST NOT ALREADY EXIST
OUT32.DAT
```

Screens #3 and #4

```
 RECOVERING OLD DATA FILE FOR UPDATING

 *** CAUTION: CODE RESULTS ONLY VALID IF INPUT PARAMETERS ARE WITHIN VERIFIED
              LIMITS - SEE INSTRUCTION MANUAL FOR THESE LIMITS***

1) HEAT FLUX AT 0 DEGS BASED ON OUTER DIAM. (W/M2)              5.4107E+06
2) TYPE CIRCM HEAT FLUX PRFL(0-UNIF,1-HALF UNIF,2-HALF COS)     0.0000E+00
3) TUBE INLET MASS FLUX (KG/M2-S)                               8.0715E+03
4) TUBE INLET STATIC PRESSURE (PA)                              2.3580E+05
5) TUBE INLET BULK FLUID TEMPERATURE (DEG K)                    3.0259E+02
6) HEATED TUBE LENGTH (M)                                       1.2450E-01
7) OUTSIDE TUBE DIAMETER (M)                                    3.0480E-03
8) INSIDE TUBE DIAMETER (M)                                     2.3876E-03
9) INLET PRESSURE LOSS COEFFICIENT KLOSS                        0.0000E+00
10) TUBE ANGLE FROM HORIZONTAL(EITHER 0 OR 90 DEG)              0.0000E+00
11) RADIUS OF ONB MAX ACTIVE CAVITY (M) (0=RCRIT USED)          0.0000E+00
12) NUMBER OF CALCULATION STEPS ?(1-1000, 2-2000)               1.0000E+00
13) PRINT FULL WATER/STEAM PROPERTY DATA?(1-NO, 2-YES)          1.0000E+00
14) OUTPUT STORAGE DATA FILE NAME CHOSEN AS                    OUT32.DAT

 ENTER # TO CHANGE

     TO EXIT, ENTER 0
0

 DO YOU WISH TO CHANGE ANY TUBE MATERIAL DATA PAIRS? Y OR N
Y
```

```
 NOW UPDATING TUBE MATERIAL DATA PAIRS...
WALL THERMAL CONDUCTIVITY K NEEDS TO BE INPUT AS A FUNCTION
OF TEMPERATURE. OBTAIN A THERMAL CONDUCTIVITY VS. TEMPERATURE
CURVE FOR TUBE MATERIAL USED AND PICK UP TO 10 DATA POINTS FROM
CURVE FOR ENTRY.

PAIR#       TEMP        THERMAL CONDUCTIVITY

    1   2.80E+02 DEG K      1.47E+01 W/M-K

    2   6.00E+02 DEG K      1.87E+01 W/M-K

    3   1.00E+03 DEG K      2.37E+01 W/M-K

 ANY CHANGES TO MAKE ? Y OR N
Y

 DO YOU WISH TO ADD ANY DATA PAIRS(TOT MAX 10 PRS)? Y OR N
N

 DO YOU WISH TO CHANGE ANY DATA PAIR VALUES? Y OR N
N

 DO YOU WISH TO DELETE ANY DATA PAIRS ?
N

 ENTER NEW INPUT FILE NAME FOR STORING THE MODIFIED FILE

 NOTE: THIS FILE MUST NOT ALREADY EXIST
PLEASE ENTER INPUT FILE NAME IN THE FORM:  INPnnn.DAT - USE CAPITAL LETTERS
    (nnn MAY BE ANY COMBINATION OF FROM 1 TO 5 NUMBERS OR LETTERS)
```

File Editing Screens

Appendix C

Sample Output File Printout from Computer Code

-* INPUTS -*

APPLIED HEAT FLUX AT 0 DEGS BASED ON OUTER DIAM.------------=	5.4107E+06	W/M2
TYPE OF CIRCUMFERENTIAL HEAT FLUX PROFILE(0,1,OR 2)--------=	0	
TUBE INLET MASS FLUX, G (BASED ON INNER DIAM.)-------------=	6.0715E+03	KG/M2-S
TUBE INLET STATIC PRESSURE--------------------------------=	2.3580E+05	PA
INLET BULK FLUID TEMPERATURE------------------------------=	3.0259E+02	KELVIN
HEATED TUBE LENGTH--=	1.2450E-01	METERS
OUTSIDE TUBE DIAMETER, DOUT-------------------------------=	3.0480E-03	METERS
INSIDE TUBE DIAMETER, DI----------------------------------=	2.3876E-03	METERS
TUBE WALL THICKNESS---------------------------------------=	3.3020E-04	METERS
INLET PRESSURE LOSS COEFFICIENT, KLOSS--------------------=	0.00000	
TUBE ANGLE FROM HORIZONTAL PLANE--------------------------=	0.00000	DEGREES
RADIUS OF ONB MAX ACTIVE CAVITY FROM USER (0=RCRIT USED)--=	0.0000E+00	METERS
NUMBER OF CALCULATION STEPS?(1-NO, 2-YES)-----------------=	1	
PRINT FULL WATER/STEAM PROPERTY DATA?(1-1000, 2-2000)-----=	1	
OUTPUT STORAGE DATA FILE CHOSEN AS------------------------=	OUT32.DAT	

THERMAL CONDUCTIVITY AS A FUNCTION OF TEMPERATURE

PAIR #	TEMP(DEG K)	THERMAL CONDUCTIVITY(W/M-K)
1	2.80E+02	1.47E+01
2	6.00E+02	1.87E+01
3	1.00E+03	2.37E+01

LIMITS OF VALIDITY:

PARMETER	UNITS	MAIN CODE	GAMBILL CHF CORRELATION	VALUES FROM THIS RUN
L/DI		49.0 TO 127.0	>=25.0	52.14
INNER DIAM, DI	(METERS)	0.0015 TO 0.0046	0.002 TO 0.008	0.0024
MASS FLUX, G	(KG/M2-S)	2500 TO 10000	3 TO 10875	6071.50
INLET PRESSURE	(PA)	2.0E+05 TO 28.0E+05	2.9E+04 TO 2.07E+07	2.3580E+05
UNIFORM HEAT FLUX	(MW/M2)	0 TO 12.2E+06	3.2E+05 TO 1.18E+08	5.4107E+06
INLET DELTA-T SUBCOOL	(DEG K)	10 TO 200	0 TO 263	96.06
INLET BULK TEMPERATURE	(DEG K)	GREATER THAN 273.0 LESS THAN 644.0 LESS THAN TSAT CORRESPONDING TO INLET PRESSURE	SAME	302.59

```
-*-*-*-*-*-*-*-*-*-*-*-*-*-*-*-*-*-*-*-*-*-*-*-*-*-*-*-*-*-* OUTPUTS -*-*-*-*-*-*-*-*-*-*-*-*-*-*-*-*-*-*-*-*-*-*-*-*-*-*-*-*-*-*

NOTE: ZERO DEVELOPMENT LENGTHS ASSUMED AT HEATED INLET

HEATED INLET IS IN THE PDB REGIME (AT Z=0.0000E+00 METERS)

ONB PREDICTED TO OCCUR BEFORE HEATED INLET AT Z=-1.9041E-01  METERS
     PREDICTED ONB BULK TEMPERATURE= 2.1575E+02  DEG K
     PREDICTED ONB DELTA-T SUBCOOL= 1.8290E+02  DEG K

OSNVG(ONSET OF SIGNIFICANT NET VAPOR GENERATION) OCCURS AT 1.0769E-01  METERS
     OSNVG BULK TEMPERATURE= 3.5152E+02  DEG K
     OSNVG DELTA-T SUBCOOL= 4.4317E+01  DEG K

HEATED EXIT IS IN THE FDB REGIME AT Z= 1.2450E-01  METERS

OSB(ONSET OF BULK BOILING) PREDICTED TO OCCUR AT Z= 2.0432E-01  METERS

MAXIMUM ACTIVE SURFACE CAVITY RADIUS = 0.0000E+00  METERS
CALCULATED CRITICAL SURFACE CAVITY RADIUS = 1.4966E-06  METERS

EXIT CHF(CRITICAL HEAT FLUX) SAFETY FACTOR= 2.3537E+00


TOTAL PRESSURE DROP IN HEATED LENGTH----------------------= 2.6089E+04  PA
     FRACTIONAL PRESSURE DROP IN HEATED LENGTH------------= 1.1064E-01
     PUMPING POWER FOR HEATED LENGTH----------------------= 7.9447E-01  WATTS
     THERMAL POWER REMOVED--------------------------------= 2.0532E+03  WATTS
     PUMPING-TO-THERMAL POWER RATIO-----------------------= 3.8694E-04
```

POSITION (METERS)	PRESSURE (PA)	SATURATION TEMP. (DEG K)	BULK TEMP. (DEG K)	DELTA-T SUBCOOL (DEG K)	INNER WALL TEMP. AT 0 DEGS (DEG K)	OUTER WALL TEMP. AT 0 DEGS (DEG K)	CORE REYNOLDS NUMBER RE(D-EFF)	LIQUID PRANDTL NUMBER	LOCAL HEAT TRANSFER COEFFICIENT (W/M2-K)
0.0000E+00	2.3580E+05	3.9863E+02	3.0259E+02	9.6033E+01	4.2501E+02	5.3752E+02	1.7957E+04	5.4911E+00	5.6424E+04
2.4900E-03	2.3547E+05	3.9860E+02	3.0373E+02	9.4873E+01	4.2529E+02	5.3765E+02	1.8436E+04	5.3453E+00	5.6820E+04
4.9800E-03	2.3513E+05	3.9856E+02	3.0487E+02	9.3691E+01	4.2558E+02	5.3792E+02	1.8921E+04	5.2057E+00	5.7222E+04
7.4700E-03	2.3479E+05	3.9851E+02	3.0600E+02	9.2508E+01	4.2586E+02	5.3817E+02	1.9412E+04	5.0718E+00	5.7631E+04
9.9600E-03	2.3444E+05	3.9846E+02	3.0714E+02	9.1324E+01	4.2613E+02	5.3843E+02	1.9909E+04	4.9432E+00	5.8047E+04
1.2450E-02	2.3409E+05	3.9841E+02	3.0827E+02	9.0140E+01	4.2641E+02	5.3869E+02	2.0412E+04	4.8198E+00	5.8469E+04
1.4940E-02	2.3373E+05	3.9836E+02	3.0941E+02	8.8955E+01	4.2668E+02	5.3894E+02	2.0921E+04	4.7011E+00	5.8899E+04
1.7430E-02	2.3337E+05	3.9831E+02	3.1054E+02	8.7770E+01	4.2695E+02	5.3919E+02	2.1437E+04	4.5870E+00	5.9336E+04
1.9920E-02	2.3300E+05	3.9826E+02	3.1168E+02	8.6583E+01	4.2722E+02	5.3944E+02	2.1959E+04	4.4773E+00	5.9781E+04
2.2410E-02	2.3263E+05	3.9821E+02	3.1282E+02	8.5397E+01	4.2749E+02	5.3969E+02	2.2487E+04	4.3717E+00	6.0233E+04
2.4900E-02	2.3225E+05	3.9816E+02	3.1395E+02	8.4209E+01	4.2776E+02	5.3994E+02	2.3021E+04	4.2702E+00	6.0694E+04
2.7390E-02	2.3187E+05	3.9811E+02	3.1509E+02	8.3022E+01	4.2802E+02	5.4018E+02	2.3561E+04	4.1725E+00	6.1162E+04
2.9880E-02	2.3148E+05	3.9805E+02	3.1622E+02	8.1834E+01	4.2828E+02	5.4042E+02	2.4107E+04	4.0784E+00	6.1639E+04
3.2370E-02	2.3109E+05	3.9800E+02	3.1735E+02	8.0645E+01	4.2854E+02	5.4066E+02	2.4660E+04	3.9877E+00	6.2124E+04
3.4860E-02	2.3069E+05	3.9794E+02	3.1849E+02	7.9456E+01	4.2880E+02	5.4090E+02	2.5219E+04	3.9001E+00	6.2618E+04
3.7350E-02	2.3029E+05	3.9789E+02	3.1962E+02	7.8266E+01	4.2905E+02	5.4114E+02	2.5784E+04	3.8157E+00	6.3122E+04
3.9840E-02	2.2988E+05	3.9783E+02	3.2076E+02	7.7075E+01	4.2930E+02	5.4137E+02	2.6356E+04	3.7342E+00	6.3634E+04
4.2330E-02	2.2946E+05	3.9778E+02	3.2189E+02	7.5884E+01	4.2955E+02	5.4160E+02	2.6933E+04	3.6555E+00	6.4157E+04
4.4820E-02	2.2904E+05	3.9772E+02	3.2303E+02	7.4692E+01	4.2980E+02	5.4183E+02	2.7518E+04	3.5794E+00	6.4689E+04
4.7310E-02	2.2862E+05	3.9766E+02	3.2416E+02	7.3500E+01	4.3005E+02	5.4206E+02	2.8108E+04	3.5061E+00	6.5232E+04
4.9800E-02	2.2819E+05	3.9760E+02	3.2529E+02	7.2308E+01	4.3029E+02	5.4229E+02	2.8705E+04	3.4352E+00	6.5785E+04
5.2290E-02	2.2775E+05	3.9753E+02	3.2642E+02	7.1112E+01	4.3053E+02	5.4251E+02	2.9308E+04	3.3666E+00	6.6349E+04
5.4780E-02	2.2730E+05	3.9747E+02	3.2756E+02	6.9914E+01	4.3076E+02	5.4273E+02	2.9918E+04	3.3002E+00	6.6925E+04
5.7270E-02	2.2685E+05	3.9740E+02	3.2869E+02	6.8716E+01	4.3100E+02	5.4294E+02	3.0534E+04	3.2360E+00	6.7513E+04
5.9760E-02	2.2639E+05	3.9734E+02	3.2982E+02	6.7518E+01	4.3123E+02	5.4316E+02	3.1157E+04	3.1739E+00	6.8113E+04
6.2250E-02	2.2593E+05	3.9727E+02	3.3095E+02	6.6318E+01	4.3146E+02	5.4337E+02	3.1787E+04	3.1136E+00	6.8725E+04
6.4740E-02	2.2546E+05	3.9720E+02	3.3208E+02	6.5118E+01	4.3168E+02	5.4358E+02	3.2423E+04	3.0553E+00	6.9351E+04
6.7230E-02	2.2498E+05	3.9713E+02	3.3321E+02	6.3917E+01	4.3190E+02	5.4379E+02	3.3066E+04	2.9988E+00	6.9990E+04
6.9720E-02	2.2449E+05	3.9706E+02	3.3434E+02	6.2717E+01	4.3212E+02	5.4399E+02	3.3715E+04	2.9441E+00	7.0642E+04
7.2210E-02	2.2400E+05	3.9699E+02	3.3547E+02	6.1515E+01	4.3234E+02	5.4419E+02	3.4372E+04	2.8911E+00	7.1308E+04
7.4700E-02	2.2350E+05	3.9692E+02	3.3660E+02	6.0313E+01	4.3255E+02	5.4439E+02	3.5035E+04	2.8397E+00	7.1989E+04
7.7190E-02	2.2300E+05	3.9684E+02	3.3773E+02	5.9111E+01	4.3276E+02	5.4458E+02	3.5705E+04	2.7898E+00	7.2686E+04
7.9680E-02	2.2248E+05	3.9677E+02	3.3886E+02	5.7907E+01	4.3297E+02	5.4477E+02	3.6382E+04	2.7414E+00	7.3398E+04
8.2170E-02	2.2196E+05	3.9669E+02	3.3999E+02	5.6703E+01	4.3317E+02	5.4496E+02	3.7066E+04	2.6944E+00	7.4128E+04
8.4660E-02	2.2143E+05	3.9661E+02	3.4112E+02	5.5497E+01	4.3337E+02	5.4514E+02	3.7758E+04	2.6488E+00	7.4874E+04
8.7150E-02	2.2089E+05	3.9653E+02	3.4224E+02	5.4291E+01	4.3356E+02	5.4532E+02	3.8456E+04	2.6044E+00	7.5638E+04
8.9640E-02	2.2034E+05	3.9645E+02	3.4337E+02	5.3084E+01	4.3375E+02	5.4550E+02	3.9163E+04	2.5613E+00	7.6421E+04
9.2130E-02	2.1979E+05	3.9637E+02	3.4449E+02	5.1878E+01	4.3394E+02	5.4568E+02	3.9879E+04	2.5196E+00	7.7222E+04
9.4620E-02	2.1922E+05	3.9629E+02	3.4562E+02	5.0671E+01	4.3413E+02	5.4585E+02	4.0596E+04	2.4790E+00	7.8043E+04
9.7110E-02	2.1865E+05	3.9621E+02	3.4674E+02	4.9463E+01	4.3431E+02	5.4601E+02	4.1323E+04	2.4396E+00	7.8885E+04
9.9600E-02	2.1807E+05	3.9612E+02	3.4787E+02	4.8254E+01	4.3448E+02	5.4618E+02	4.2059E+04	2.4012E+00	7.9749E+04
1.0209E-01	2.1747E+05	3.9604E+02	3.4899E+02	4.7044E+01	4.3465E+02	5.4634E+02	4.2803E+04	2.3639E+00	8.0635E+04
1.0458E-01	2.1687E+05	3.9595E+02	3.5011E+02	4.5832E+01	4.3482E+02	5.4649E+02	4.3554E+04	2.3275E+00	8.1545E+04
1.0707E-01	2.1626E+05	3.9586E+02	3.5124E+02	4.4620E+01	4.3498E+02	5.4664E+02	4.4314E+04	2.2921E+00	8.2480E+04
1.0956E-01	2.1565E+05	3.9577E+02	3.5236E+02	4.3408E+01	4.3494E+02	5.4660E+02	4.4693E+04	2.2577E+00	8.3447E+04
1.1205E-01	2.1503E+05	3.9568E+02	3.5348E+02	4.2197E+01	4.3485E+02	5.4652E+02	4.4940E+04	2.2242E+00	8.4889E+04
1.1454E-01	2.1436E+05	3.9558E+02	3.5460E+02	4.0981E+01	4.3476E+02	5.4643E+02	4.5162E+04	2.1917E+00	8.6172E+04
1.1703E-01	2.1360E+05	3.9547E+02	3.5572E+02	3.9751E+01	4.3465E+02	5.4633E+02	4.5354E+04	2.1600E+00	8.7509E+04
1.1952E-01	2.1266E+05	3.9533E+02	3.5684E+02	3.8493E+01	4.3452E+02	5.4621E+02	4.5514E+04	2.1292E+00	8.8919E+04
1.2201E-01	2.1142E+05	3.9514E+02	3.5795E+02	3.7187E+01	4.3434E+02	5.4604E+02	4.5632E+04	2.0991E+00	9.0431E+04
1.2450E-01	2.0971E+05	3.9488E+02	3.5907E+02	3.5810E+01	4.3409E+02	5.4581E+02	4.5696E+04	2.0698E+00	9.2078E+04

POSITION (METERS)	LIQ. FANNING FRIC. FACTOR HEATING ADJUSTED	TWO-PHASE M-N FRICTION MULTIPLIER	DP/DZ FRIC. (PA/M)	DP/DZ GRAV. (PA/M)	DP/DZ ACCEL. (PA/M)	DELTA-P FRIC. (PA)	DELTA-P GRAV. (PA)	DELTA-P ACCEL. (PA)	DELTA P TOTAL (PA)
0.0000E+00	3.5689E-03	1.0000E+00	-1.1065E+05	0.0000E+00	0.0000E+00	0.0000E+00	0.0000E+00	0.0000E+00	0.0000E+00
2.4900E-03	4.1358E-03	1.0000E+00	-1.2963E+05	0.0000E+00	-5.2837E+03	3.2089E+02	0.0000E+00	1.2906E+01	3.3380E+02
4.9800E-03	4.1414E-03	1.0000E+00	-1.3123E+05	0.0000E+00	-5.4689E+03	6.4575E+02	0.0000E+00	2.6356E+01	6.7211E+02
7.4700E-03	4.1468E-03	1.0000E+00	-1.3286E+05	0.0000E+00	-5.7278E+03	9.7464E+02	0.0000E+00	4.0368E+01	1.0150E+03
9.9600E-03	4.1522E-03	1.0000E+00	-1.3452E+05	0.0000E+00	-5.9554E+03	1.3076E+03	0.0000E+00	5.4911E+01	1.3625E+03
1.2450E-02	4.1574E-03	1.0000E+00	-1.3620E+05	0.0000E+00	-6.1868E+03	1.6448E+03	0.0000E+00	7.0013E+01	1.7148E+03
1.4940E-02	4.1625E-03	1.0000E+00	-1.3791E+05	0.0000E+00	-6.3858E+03	1.9861E+03	0.0000E+00	8.5669E+01	2.0718E+03
1.7430E-02	4.1675E-03	1.0000E+00	-1.3964E+05	0.0000E+00	-6.6247E+03	2.3318E+03	0.0000E+00	1.0188E+02	2.4337E+03
1.9920E-02	4.1724E-03	1.0000E+00	-1.4141E+05	0.0000E+00	-6.8308E+03	2.6818E+03	0.0000E+00	1.1865E+02	2.8004E+03
2.2410E-02	4.1772E-03	1.0000E+00	-1.4320E+05	0.0000E+00	-7.0776E+03	3.0362E+03	0.0000E+00	1.3598E+02	3.1722E+03
2.4900E-02	4.1819E-03	1.0000E+00	-1.4503E+05	0.0000E+00	-7.2911E+03	3.3952E+03	0.0000E+00	1.5388E+02	3.5491E+03
2.7390E-02	4.1864E-03	1.0000E+00	-1.4688E+05	0.0000E+00	-7.5082E+03	3.7587E+03	0.0000E+00	1.7232E+02	3.9310E+03
2.9880E-02	4.1909E-03	1.0000E+00	-1.4877E+05	0.0000E+00	-7.7291E+03	4.1269E+03	0.0000E+00	1.9136E+02	4.3183E+03
3.2370E-02	4.1953E-03	1.0000E+00	-1.5069E+05	0.0000E+00	-7.9929E+03	4.4999E+03	0.0000E+00	2.1097E+02	4.7108E+03
3.4860E-02	4.1995E-03	1.0000E+00	-1.5265E+05	0.0000E+00	-8.2605E+03	4.8776E+03	0.0000E+00	2.3117E+02	5.1088E+03
3.7350E-02	4.2037E-03	1.0000E+00	-1.5464E+05	0.0000E+00	-8.4940E+03	5.2603E+03	0.0000E+00	2.5196E+02	5.5123E+03
3.9840E-02	4.2078E-03	1.0000E+00	-1.5667E+05	0.0000E+00	-8.6523E+03	5.6480E+03	0.0000E+00	2.7334E+02	5.9214E+03
4.2330E-02	4.2117E-03	1.0000E+00	-1.5873E+05	0.0000E+00	-8.9734E+03	6.0408E+03	0.0000E+00	2.9534E+02	6.3362E+03
4.4820E-02	4.2156E-03	1.0000E+00	-1.6084E+05	0.0000E+00	-9.1795E+03	6.4388E+03	0.0000E+00	3.1792E+02	6.7568E+03
4.7310E-02	4.2194E-03	1.0000E+00	-1.6298E+05	0.0000E+00	-9.4299E+03	6.8421E+03	0.0000E+00	3.4113E+02	7.1832E+03
4.9800E-02	4.2232E-03	1.0000E+00	-1.6516E+05	0.0000E+00	-9.6437E+03	7.2508E+03	0.0000E+00	3.6495E+02	7.6157E+03
5.2290E-02	4.2268E-03	1.0000E+00	-1.6739E+05	0.0000E+00	-9.9864E+03	7.6649E+03	0.0000E+00	3.8941E+02	8.0543E+03
5.4780E-02	4.2304E-03	1.0000E+00	-1.6967E+05	0.0000E+00	-1.0210E+04	8.0847E+03	0.0000E+00	4.1448E+02	8.4992E+03
5.7270E-02	4.2338E-03	1.0000E+00	-1.7199E+05	0.0000E+00	-1.0437E+04	8.5102E+03	0.0000E+00	4.4021E+02	8.9504E+03
5.9760E-02	4.2372E-03	1.0000E+00	-1.7436E+05	0.0000E+00	-1.0712E+04	8.9416E+03	0.0000E+00	4.6659E+02	9.4081E+03
6.2250E-02	4.2406E-03	1.0000E+00	-1.7678E+05	0.0000E+00	-1.0992E+04	9.3789E+03	0.0000E+00	4.9363E+02	9.8725E+03
6.4740E-02	4.2438E-03	1.0000E+00	-1.7924E+05	0.0000E+00	-1.1233E+04	9.8222E+03	0.0000E+00	5.2135E+02	1.0344E+04
6.7230E-02	4.2470E-03	1.0000E+00	-1.8176E+05	0.0000E+00	-1.1524E+04	1.0272E+04	0.0000E+00	5.4976E+02	1.0822E+04
6.9720E-02	4.2501E-03	1.0000E+00	-1.8434E+05	0.0000E+00	-1.1820E+04	1.0728E+04	0.0000E+00	5.7882E+02	1.1307E+04
7.2210E-02	4.2531E-03	1.0000E+00	-1.8697E+05	0.0000E+00	-1.2168E+04	1.1190E+04	0.0000E+00	6.0860E+02	1.1799E+04
7.4700E-02	4.2561E-03	1.0000E+00	-1.8966E+05	0.0000E+00	-1.2340E+04	1.1659E+04	0.0000E+00	6.3907E+02	1.2298E+04
7.7190E-02	4.2590E-03	1.0000E+00	-1.9241E+05	0.0000E+00	-1.2694E+04	1.2135E+04	0.0000E+00	6.7024E+02	1.2805E+04
7.9680E-02	4.2618E-03	1.0000E+00	-1.9522E+05	0.0000E+00	-1.2928E+04	1.2618E+04	0.0000E+00	7.0218E+02	1.3320E+04
8.2170E-02	4.2646E-03	1.0000E+00	-1.9810E+05	0.0000E+00	-1.3349E+04	1.3108E+04	0.0000E+00	7.3488E+02	1.3843E+04
8.4660E-02	4.2673E-03	1.0000E+00	-2.0104E+05	0.0000E+00	-1.3588E+04	1.3605E+04	0.0000E+00	7.6831E+02	1.4373E+04
8.7150E-02	4.2699E-03	1.0000E+00	-2.0406E+05	0.0000E+00	-1.3881E+04	1.4109E+04	0.0000E+00	8.0253E+02	1.4912E+04
8.9640E-02	4.2725E-03	1.0000E+00	-2.0714E+05	0.0000E+00	-1.4229E+04	1.4621E+04	0.0000E+00	8.3754E+02	1.5459E+04
9.2130E-02	4.2750E-03	1.0000E+00	-2.1030E+05	0.0000E+00	-1.4486E+04	1.5141E+04	0.0000E+00	8.7329E+02	1.6015E+04
9.4620E-02	4.2775E-03	1.0000E+00	-2.1354E+05	0.0000E+00	-1.4849E+04	1.5669E+04	0.0000E+00	9.0987E+02	1.6579E+04
9.7110E-02	4.2799E-03	1.0000E+00	-2.1687E+05	0.0000E+00	-1.5169E+04	1.6205E+04	0.0000E+00	9.4728E+02	1.7153E+04
9.9600E-02	4.2822E-03	1.0000E+00	-2.2027E+05	0.0000E+00	-1.5547E+04	1.6750E+04	0.0000E+00	9.8553E+02	1.7735E+04
1.0209E-01	4.2845E-03	1.0000E+00	-2.2377E+05	0.0000E+00	-1.5883E+04	1.7303E+04	0.0000E+00	1.0247E+03	1.8327E+04
1.0458E-01	4.2867E-03	1.0000E+00	-2.2736E+05	0.0000E+00	-1.6227E+04	1.7863E+04	0.0000E+00	1.0646E+03	1.8929E+04
1.0707E-01	4.2889E-03	1.0000E+00	-2.3104E+05	0.0000E+00	-1.6579E+04	1.8435E+04	0.0000E+00	1.1056E+03	1.9541E+04
1.0956E-01	4.3001E-03	1.0001E+00	-2.2561E+05	0.0000E+00	-1.9603E+04	1.9006E+04	0.0000E+00	1.1489E+03	2.0155E+04
1.1205E-01	4.3142E-03	1.0014E+00	-2.1736E+05	0.0000E+00	-3.6158E+04	1.9357E+04	0.0000E+00	1.2161E+03	2.0773E+04
1.1454E-01	4.3287E-03	1.0052E+00	-2.0950E+05	0.0000E+00	-7.1549E+04	2.0088E+04	0.0000E+00	1.3478E+03	2.1436E+04
1.1703E-01	4.3438E-03	1.0134E+00	-2.0229E+05	0.0000E+00	-1.3257E+05	2.0600E+04	0.0000E+00	1.5995E+03	2.2200E+04
1.1952E-01	4.3596E-03	1.0284E+00	-1.9604E+05	0.0000E+00	-2.2986E+05	2.1096E+04	0.0000E+00	2.0477E+03	2.3143E+04
1.2201E-01	4.3766E-03	1.0539E+00	-1.9113E+05	0.0000E+00	-3.8104E+05	2.1577E+04	0.0000E+00	2.8040E+03	2.4381E+04
1.2450E-01	4.3950E-03	1.0957E+00	-1.8813E+05	0.0000E+00	-6.1837E+05	2.2049E+04	0.0000E+00	4.0401E+03	2.6089E+04

POSITION (METERS)	NON-EQUIL FLOW QUALITY	NON-EQUIL FLOW VOID FRACTION	ATTACHED WALL VOID FRACTION	WALL BUBBLE LAYER THICKNESS (METERS)	CORE MASS FLUX (KG/M2-S)	GAMBILL CHF (W/M2)	CHF SAFETY FACTOR
0.0000E+00	0.0000E+00	0.0000E+00	0.0000E+00	0.0000E+00	6.0715E+03	2.0417E+07	3.7735E+00
2.4900E-03	0.0000E+00	0.0000E+00	4.2055E-03	2.5103E-06	6.0971E+03	2.0316E+07	3.7548E+00
4.9800E-03	0.0000E+00	0.0000E+00	8.4159E-03	5.0234E-06	6.1230E+03	2.0213E+07	3.7357E+00
7.4700E-03	0.0000E+00	0.0000E+00	1.2631E-02	7.5397E-06	6.1492E+03	2.0108E+07	3.7163E+00
9.9600E-03	0.0000E+00	0.0000E+00	1.6852E-02	1.0059E-05	6.1756E+03	2.0000E+07	3.6964E+00
1.2450E-02	0.0000E+00	0.0000E+00	2.1080E-02	1.2582E-05	6.2022E+03	1.9890E+07	3.6761E+00
1.4940E-02	0.0000E+00	0.0000E+00	2.5313E-02	1.5109E-05	6.2292E+03	1.9778E+07	3.6554E+00
1.7430E-02	0.0000E+00	0.0000E+00	2.9553E-02	1.7640E-05	6.2564E+03	1.9664E+07	3.6343E+00
1.9920E-02	0.0000E+00	0.0000E+00	3.3801E-02	2.0176E-05	6.2839E+03	1.9548E+07	3.6128E+00
2.2410E-02	0.0000E+00	0.0000E+00	3.8056E-02	2.2716E-05	6.3117E+03	1.9429E+07	3.5909E+00
2.4900E-02	0.0000E+00	0.0000E+00	4.2319E-02	2.5260E-05	6.3398E+03	1.9309E+07	3.5686E+00
2.7390E-02	0.0000E+00	0.0000E+00	4.6589E-02	2.7809E-05	6.3682E+03	1.9186E+07	3.5460E+00
2.9880E-02	0.0000E+00	0.0000E+00	5.0868E-02	3.0363E-05	6.3969E+03	1.9062E+07	3.5230E+00
3.2370E-02	0.0000E+00	0.0000E+00	5.5156E-02	3.2923E-05	6.4259E+03	1.8935E+07	3.4995E+00
3.4860E-02	0.0000E+00	0.0000E+00	5.9453E-02	3.5488E-05	6.4553E+03	1.8806E+07	3.4757E+00
3.7350E-02	0.0000E+00	0.0000E+00	6.3761E-02	3.8059E-05	6.4850E+03	1.8675E+07	3.4514E+00
3.9840E-02	0.0000E+00	0.0000E+00	6.8079E-02	4.0636E-05	6.5150E+03	1.8541E+07	3.4267E+00
4.2330E-02	0.0000E+00	0.0000E+00	7.2408E-02	4.3220E-05	6.5454E+03	1.8405E+07	3.4017E+00
4.4820E-02	0.0000E+00	0.0000E+00	7.6748E-02	4.5811E-05	6.5762E+03	1.8268E+07	3.3762E+00
4.7310E-02	0.0000E+00	0.0000E+00	8.1099E-02	4.8408E-05	6.6073E+03	1.8128E+07	3.3504E+00
4.9800E-02	0.0000E+00	0.0000E+00	8.5461E-02	5.1012E-05	6.6389E+03	1.7986E+07	3.3241E+00
5.2290E-02	0.0000E+00	0.0000E+00	8.9842E-02	5.3626E-05	6.6708E+03	1.7842E+07	3.2975E+00
5.4780E-02	0.0000E+00	0.0000E+00	9.4237E-02	5.6250E-05	6.7032E+03	1.7695E+07	3.2704E+00
5.7270E-02	0.0000E+00	0.0000E+00	9.8647E-02	5.8882E-05	6.7360E+03	1.7546E+07	3.2429E+00
5.9760E-02	0.0000E+00	0.0000E+00	1.0307E-01	6.1523E-05	6.7692E+03	1.7395E+07	3.2150E+00
6.2250E-02	0.0000E+00	0.0000E+00	1.0751E-01	6.4174E-05	6.8029E+03	1.7242E+07	3.1867E+00
6.4740E-02	0.0000E+00	0.0000E+00	1.1197E-01	6.6834E-05	6.8370E+03	1.7087E+07	3.1579E+00
6.7230E-02	0.0000E+00	0.0000E+00	1.1644E-01	6.9503E-05	6.8716E+03	1.6929E+07	3.1288E+00
6.9720E-02	0.0000E+00	0.0000E+00	1.2093E-01	7.2182E-05	6.9067E+03	1.6770E+07	3.0994E+00
7.2210E-02	0.0000E+00	0.0000E+00	1.2543E-01	7.4871E-05	6.9423E+03	1.6608E+07	3.0695E+00
7.4700E-02	0.0000E+00	0.0000E+00	1.2996E-01	7.7571E-05	6.9784E+03	1.6444E+07	3.0392E+00
7.7190E-02	0.0000E+00	0.0000E+00	1.3450E-01	8.0282E-05	7.0150E+03	1.6278E+07	3.0086E+00
7.9680E-02	0.0000E+00	0.0000E+00	1.3906E-01	8.3005E-05	7.0522E+03	1.6110E+07	2.9775E+00
8.2170E-02	0.0000E+00	0.0000E+00	1.4364E-01	8.5740E-05	7.0899E+03	1.5940E+07	2.9460E+00
8.4660E-02	0.0000E+00	0.0000E+00	1.4825E-01	8.8488E-05	7.1282E+03	1.5767E+07	2.9141E+00
8.7150E-02	0.0000E+00	0.0000E+00	1.5287E-01	9.1249E-05	7.1671E+03	1.5592E+07	2.8818E+00
8.9640E-02	0.0000E+00	0.0000E+00	1.5752E-01	9.4023E-05	7.2067E+03	1.5415E+07	2.8490E+00
9.2130E-02	0.0000E+00	0.0000E+00	1.6219E-01	9.6808E-05	7.2468E+03	1.5236E+07	2.8160E+00
9.4620E-02	0.0000E+00	0.0000E+00	1.6688E-01	9.9609E-05	7.2876E+03	1.5055E+07	2.7825E+00
9.7110E-02	0.0000E+00	0.0000E+00	1.7159E-01	1.0242E-04	7.3291E+03	1.4872E+07	2.7486E+00
9.9600E-02	0.0000E+00	0.0000E+00	1.7633E-01	1.0525E-04	7.3713E+03	1.4687E+07	2.7143E+00
1.0209E-01	0.0000E+00	0.0000E+00	1.8110E-01	1.0810E-04	7.4142E+03	1.4499E+07	2.6796E+00
1.0458E-01	0.0000E+00	0.0000E+00	1.8590E-01	1.1096E-04	7.4579E+03	1.4308E+07	2.6445E+00
1.0707E-01	0.0000E+00	0.0000E+00	1.9072E-01	1.1384E-04	7.5024E+03	1.4116E+07	2.6089E+00
1.0956E-01	5.8118E-08	3.7292E-05	1.9155E-01	1.0837E-04	7.4183E+03	1.3931E+07	2.5747E+00
1.1205E-01	8.1270E-07	5.2218E-04	1.6750E-01	9.9981E-05	7.2931E+03	1.3747E+07	2.5406E+00
1.1454E-01	3.4933E-06	2.2445E-03	1.5248E-01	9.1013E-05	7.1638E+03	1.3560E+07	2.5062E+00
1.1703E-01	9.8889E-06	6.3375E-03	1.3630E-01	8.1359E-05	7.0297E+03	1.3369E+07	2.4709E+00
1.1952E-01	2.2663E-05	1.4424E-02	1.1874E-01	7.0874E-05	6.8895E+03	1.3171E+07	2.4343E+00
1.2201E-01	4.5960E-05	2.8849E-02	9.9403E-02	5.9335E-05	6.7417E+03	1.2962E+07	2.3956E+00
1.2450E-01	8.6619E-05	5.3024E-02	7.7739E-02	4.6402E-05	6.5833E+03	1.2735E+07	2.3537E+00

POSITION (METERS)	CP(TB) (J/KG-K)	VF(TB) (M3/KG)	VG(TB) (M3/KG)	MUB(TB) (NS/M2)	MUW(TWI) AT 0 DEGS (NS/M2)	KB (W/M-K)	PE NUMBER	SUBCOOL ST NUMBER	CO DISTR PARAM
0.0000E+00	4.1789E+03	1.0040E-03	7.9895E-01	8.0726E-04	1.1027E-04	6.1435E-01	9.8606E+04	2.8342E-03	0.0000E+00
2.4900E-03	4.1787E+03	1.0044E-03	7.5996E-01	7.8797E-04	1.7904E-04	6.1600E-01	9.8338E+04	2.8696E-03	0.0000E+00
4.9800E-03	4.1787E+03	1.0047E-03	7.6098E-01	7.6940E-04	1.7868E-04	6.1762E-01	9.8081E+04	2.9058E-03	0.0000E+00
7.4700E-03	4.1788E+03	1.0051E-03	7.6202E-01	7.5154E-04	1.7832E-04	6.1921E-01	9.7828E+04	2.9430E-03	0.0000E+00
9.9600E-03	4.1788E+03	1.0055E-03	7.6308E-01	7.3435E-04	1.7796E-04	6.2078E-01	9.7581E+04	2.9811E-03	0.0000E+00
1.2450E-02	4.1788E+03	1.0059E-03	7.6415E-01	7.1779E-04	1.7761E-04	6.2233E-01	9.7339E+04	3.0202E-03	0.0000E+00
1.4940E-02	4.1788E+03	1.0063E-03	7.6525E-01	7.0183E-04	1.7727E-04	6.2386E-01	9.7101E+04	3.0605E-03	0.0000E+00
1.7430E-02	4.1788E+03	1.0067E-03	7.6636E-01	6.8645E-04	1.7693E-04	6.2536E-01	9.6868E+04	3.1018E-03	0.0000E+00
1.9920E-02	4.1789E+03	1.0071E-03	7.6749E-01	6.7161E-04	1.7659E-04	6.2684E-01	9.6640E+04	3.1443E-03	0.0000E+00
2.2410E-02	4.1789E+03	1.0076E-03	7.6863E-01	6.5729E-04	1.7625E-04	6.2830E-01	9.6417E+04	3.1879E-03	0.0000E+00
2.4900E-02	4.1791E+03	1.0080E-03	7.6980E-01	6.4346E-04	1.7592E-04	6.2974E-01	9.6201E+04	3.2327E-03	0.0000E+00
2.7390E-02	4.1793E+03	1.0085E-03	7.7099E-01	6.3012E-04	1.7559E-04	6.3115E-01	9.5992E+04	3.2788E-03	0.0000E+00
2.9880E-02	4.1796E+03	1.0090E-03	7.7219E-01	6.1722E-04	1.7527E-04	6.3254E-01	9.5787E+04	3.3262E-03	0.0000E+00
3.2370E-02	4.1799E+03	1.0094E-03	7.7342E-01	6.0476E-04	1.7495E-04	6.3391E-01	9.5586E+04	3.3750E-03	0.0000E+00
3.4860E-02	4.1801E+03	1.0099E-03	7.7467E-01	5.9271E-04	1.7464E-04	6.3525E-01	9.5389E+04	3.4253E-03	0.0000E+00
3.7350E-02	4.1804E+03	1.0104E-03	7.7594E-01	5.8105E-04	1.7432E-04	6.3658E-01	9.5196E+04	3.4772E-03	0.0000E+00
3.9840E-02	4.1806E+03	1.0109E-03	7.7723E-01	5.6977E-04	1.7402E-04	6.3788E-01	9.5008E+04	3.5306E-03	0.0000E+00
4.2330E-02	4.1809E+03	1.0114E-03	7.7854E-01	5.5884E-04	1.7371E-04	6.3917E-01	9.4823E+04	3.5858E-03	0.0000E+00
4.4820E-02	4.1812E+03	1.0120E-03	7.7988E-01	5.4826E-04	1.7341E-04	6.4043E-01	9.4642E+04	3.6428E-03	0.0000E+00
4.7310E-02	4.1815E+03	1.0125E-03	7.8124E-01	5.3802E-04	1.7312E-04	6.4167E-01	9.4468E+04	3.7016E-03	0.0000E+00
4.9800E-02	4.1820E+03	1.0130E-03	7.8262E-01	5.2809E-04	1.7282E-04	6.4289E-01	9.4297E+04	3.7622E-03	0.0000E+00
5.2290E-02	4.1824E+03	1.0136E-03	7.8404E-01	5.1846E-04	1.7254E-04	6.4409E-01	9.4131E+04	3.8252E-03	0.0000E+00
5.4780E-02	4.1828E+03	1.0141E-03	7.8548E-01	5.0912E-04	1.7226E-04	6.4527E-01	9.3968E+04	3.8903E-03	0.0000E+00
5.7270E-02	4.1832E+03	1.0147E-03	7.8694E-01	5.0006E-04	1.7198E-04	6.4643E-01	9.3809E+04	3.9577E-03	0.0000E+00
5.9760E-02	4.1836E+03	1.0153E-03	7.8843E-01	4.9127E-04	1.7170E-04	6.4757E-01	9.3653E+04	4.0276E-03	0.0000E+00
6.2250E-02	4.1840E+03	1.0159E-03	7.8995E-01	4.8274E-04	1.7143E-04	6.4868E-01	9.3501E+04	4.1000E-03	0.0000E+00
6.4740E-02	4.1844E+03	1.0165E-03	7.9150E-01	4.7445E-04	1.7117E-04	6.4978E-01	9.3351E+04	4.1752E-03	0.0000E+00
6.7230E-02	4.1848E+03	1.0171E-03	7.9307E-01	4.6640E-04	1.7091E-04	6.5086E-01	9.3206E+04	4.2532E-03	0.0000E+00
6.9720E-02	4.1854E+03	1.0177E-03	7.9468E-01	4.5858E-04	1.7065E-04	6.5192E-01	9.3067E+04	4.3340E-03	0.0000E+00
7.2210E-02	4.1860E+03	1.0183E-03	7.9631E-01	4.5098E-04	1.7040E-04	6.5296E-01	9.2932E+04	4.4181E-03	0.0000E+00
7.4700E-02	4.1865E+03	1.0189E-03	7.9798E-01	4.4360E-04	1.7015E-04	6.5398E-01	9.2799E+04	4.5055E-03	0.0000E+00
7.7190E-02	4.1871E+03	1.0196E-03	7.9968E-01	4.3641E-04	1.6991E-04	6.5498E-01	9.2670E+04	4.5965E-03	0.0000E+00
7.9680E-02	4.1877E+03	1.0202E-03	8.0141E-01	4.2942E-04	1.6967E-04	6.5597E-01	9.2544E+04	4.6914E-03	0.0000E+00
8.2170E-02	4.1883E+03	1.0209E-03	8.0318E-01	4.2262E-04	1.6943E-04	6.5693E-01	9.2421E+04	4.7904E-03	0.0000E+00
8.4660E-02	4.1888E+03	1.0215E-03	8.0498E-01	4.1600E-04	1.6920E-04	6.5788E-01	9.2301E+04	4.8938E-03	0.0000E+00
8.7150E-02	4.1894E+03	1.0222E-03	8.0682E-01	4.0956E-04	1.6898E-04	6.5880E-01	9.2184E+04	5.0018E-03	0.0000E+00
8.9640E-02	4.1900E+03	1.0229E-03	8.0869E-01	4.0328E-04	1.6876E-04	6.5971E-01	9.2070E+04	5.1148E-03	0.0000E+00
9.2130E-02	4.1908E+03	1.0236E-03	8.1061E-01	3.9717E-04	1.6854E-04	6.6060E-01	9.1962E+04	5.2328E-03	0.0000E+00
9.4620E-02	4.1915E+03	1.0243E-03	8.1256E-01	3.9122E-04	1.6833E-04	6.6147E-01	9.1858E+04	5.3565E-03	0.0000E+00
9.7110E-02	4.1922E+03	1.0250E-03	8.1455E-01	3.8543E-04	1.6813E-04	6.6232E-01	9.1756E+04	5.4864E-03	0.0000E+00
9.9600E-02	4.1930E+03	1.0257E-03	8.1659E-01	3.7977E-04	1.6793E-04	6.6316E-01	9.1656E+04	5.6229E-03	0.0000E+00
1.0209E-01	4.1937E+03	1.0264E-03	8.1867E-01	3.7426E-04	1.6773E-04	6.6398E-01	9.1560E+04	5.7665E-03	0.0000E+00
1.0458E-01	4.1945E+03	1.0271E-03	8.2079E-01	3.6888E-04	1.6754E-04	6.6478E-01	9.1466E+04	5.9178E-03	0.0000E+00
1.0707E-01	4.1952E+03	1.0278E-03	8.2296E-01	3.6364E-04	1.6736E-04	6.6556E-01	9.1374E+04	6.0775E-03	0.0000E+00
1.0956E-01	4.1959E+03	1.0286E-03	8.2515E-01	3.5852E-04	1.6740E-04	6.6632E-01	9.1286E+04	6.2461E-03	1.2500E+00
1.1205E-01	4.1967E+03	1.0293E-03	8.2737E-01	3.5353E-04	1.6750E-04	6.6707E-01	9.1201E+04	6.4243E-03	1.2500E+00
1.1454E-01	4.1977E+03	1.0301E-03	8.2976E-01	3.4867E-04	1.6760E-04	6.6780E-01	9.1122E+04	6.6133E-03	1.2500E+00
1.1703E-01	4.1986E+03	1.0308E-03	8.3253E-01	3.4392E-04	1.6772E-04	6.6851E-01	9.1045E+04	6.8164E-03	1.2500E+00
1.1952E-01	4.1996E+03	1.0316E-03	8.3598E-01	3.3928E-04	1.6787E-04	6.6920E-01	9.0972E+04	7.0375E-03	1.2500E+00
1.2201E-01	4.2005E+03	1.0324E-03	8.4057E-01	3.3475E-04	1.6807E-04	6.6988E-01	9.0900E+04	7.2831E-03	1.2500E+00
1.2450E-01	4.2015E+03	1.0332E-03	8.4698E-01	3.3033E-04	1.6835E-04	6.7054E-01	9.0831E+04	7.5614E-03	1.2500E+00

Appendix D

Flow Conditions for Each of the Experimental Data Runs Selected and Flow Parameter Plots of the Two Major Experimental Datasets Reviewed

Experimental Data Flow Conditions

Designation	Parameter	SI Units	English Units
D&B Fig. 11a*:	q/A	8.46×10^6 W/m^2	2.68×10^6 Btu/hrft
	V	6.1 m/s	20 ft/s
	T	302.59 deg K	85 deg F
	P_{ex}	2.07×10^5 Pa	30 psia
	D_i	2.3876 mm	0.094 in
	G	6071.5 kg/m^{2}s	1243.5 lb/ft^{2}s
	L	0.1245 m	4.9 in
	L/D	52	
D&B Fig. 11b:	q/A	7.67×10^6 W/m^2	2.43×10^6 Btu/hrft^2
	V	6.1 m/s	20 ft/s
	T	302.59 deg K	85 deg F
	P_{ex}	2.07×10^5 Pa	30 psia
	D_i	2.3876 mm	0.094 in
	G	6071.5 kg/m^{2}s	1243.5 lb/ft^{2}s
	L	0.1245 m	4.9 in
	L/D	52	
D&B Fig. 11c:	q/A	6.91×10^6 W/m^2	2.19×10^6 Btu/hrft^2
	V	6.1 m/s	20 ft/s
	T	302.59 deg K	85 deg F
	P_{ex}	2.07×10^5 Pa	30 psia
	D_i	2.3876 mm	0.094 in
	G	6071.5 kg/m^{2}s	1243.5 lb/ft^{2}s
	L	0.1245 m	4.9 in
	L/D	52	
D&B Fig. 11d:	q/A	3.78×10^6 W/m^2	1.2×10^6 Btu/hrft^2
	V	6.1 m/s	20 ft/s
	T	302.59 deg K	85 deg F
	P_{ex}	2.07×10^5 Pa	30 psia
	D_i	2.3876 mm	0.094 in
	G	6071.5 kg/m^{2}s	1243.5 lb/ft^{2}s
	L	0.1245 m	4.9 in
	L/D	52	

*Note: Letter designation after number is our notation refering to one overall pressure drop vs. heat flux curve appearing on the Dormer and Bergles figure.

Designation	Parameter	SI Units	English Units
D&B Fig. 17:	T.S. 31		
	V	6.1 m/s	20 ft/s
	T	302.59 deg K	85 deg F
	P_{ex}	2.07×10^5 Pa	30 psia
	D_i	2.3876 mm	0.094 in
	G	6071.5 kg/m^{2}s	1243.5 lb/ft^{2}s
	L	0.1245 m	4.9 in
	L/D	52	
	Inner Wall Heat Flux Levels:		
	0, 0.63, 1.26, 1.89, 2.52, 3.15, 3.78, 4.42, 5.05, 5.68, 6.31, 6.62, 6.94, 7.25, 7.57, 7.89, 8.2, 8.45 MW/m^2		
	0, 0.2, 0.4, 0.6, 0.8, 1.0, 1.2, 1.4, 1.6, 1.8, 2.0, 2.1, 2.2, 2.3, 2.4, 2.5, 2.6, 2.68 $\times 10^6$ Btu/hrft^2		
D&B Fig. 19:	T.S. B100		
	V	3.05 m/s	10 ft/s
	T	299.82 deg K	80 deg F
	P_{ex}	5.38×10^5 Pa	78 psia
	D_i	4.5847 mm	0.1805 in
	G	3038.6 kg/m^{2}s	622.33 lb/ft^{2}s
	L	0.4572 m	18.0 in
	L/D	100	
	Inner Wall Heat Flux Levels:		
	0, 3.15, 6.31, 9.46, 1.26, 1.58, 1.89, 2.21, 2.52, 2.84, 3.15, 3.47, 3.63, 3.78, 3.94, 4.1, 4.19 MW/m^2		
	0, 0.1, 0.2, 0.3, 0.4, 0.5, 0.6, 0.7, 0.8, 0.9, 1.0, 1.1, 1.15, 1.2, 1.25, 1.3, 1.33 $\times 10^6$ Btu/hrft^2		

Designation	Parameter	SI Units	English Units
D&B Fig. 28:	T.S. D100		
	V	9.14 m/s	30 ft/s
	T	299.82 deg K	80 deg F
	P_{ex}	3.45 x 10^5 Pa	50 psia
	D_i	1.5748 mm	0.062 in
	G	9115.6 kg/m^2s	1866.96 lb/ft^2s
	L	0.1509 m	5.94 in
	L/D	96	
	Inner Wall Heat Flux Levels:		
	0, 0.63, 1.26, 1.89, 2.52, 3.15, 3.78, 4.42, 5.05, 5.68, 6.31, 6.94, 7.57, 7.89, 8.2, 8.52, 8.83, 9.15, 9.46, 9.68 MW/m^2		
	0, 0.2, 0.4, 0.6, 0.8, 1.0, 1.2, 1.4, 1.6, 1.8, 2.0, 2.2, 2.4, 2.5, 2.6, 2.7, 2.8, 2.9, 3.0, 3.07 x 10^6 Btu/hrft^2		
D&B Fig. 19a:	T.S. B100		
	V	6.096 m/s	20 ft/s
	T	299.82 deg K	80 deg F
	P_{ex}	3.4474 x 10^5 Pa	50 psia
	D_i	4.5847 mm	0.1805 in
	G	6076.8 kg/m^2s	1244.59 lb/ft^2s
	L	0.4572 m	18.0 in
	L/D	100	
	Inner Wall Heat Flux Levels:		
	0, 0.63, 1.26, 1.89, 2.52, 3.15, 3.47, 3.78, 4.1, 4.42, 4.73, 4.89, 5.05, 5.24, 5.36, 5.49, 5.68 MW/m^2		
	0, 0.2, 0.4, 0.6, 0.8, 1.0, 1.1, 1.2, 1.3, 1.4, 1.5, 1.55, 1.6, 1.66, 1.7, 1.74, 1.8 x 10^6 Btu/hrft^2		

Designation	Parameter	SI Units	English Units
D&B Fig. 24:	T.S. 50b		
	V	9.144 m/s	30 ft/s
	T	299.82 deg K	80 deg F
	P_{ex}	2.0684 x 10^5	30 psia
	D_i	3.0734 mm	0.121 in
	G	9114.6 kg/m^2s	1866.8 lb/ft^2s
	L	0.1499 m	5.9 in
	L/D	49	
	Inner Wall Heat Flux Levels:		
	0, 0.63, 1.26, 1.89, 2.52, 3.15, 3.78, 4.42, 5.05, 5.68, 6.31, 6.94, 7.57, 8.2, 8.83, 9.46, 10.1, 10.4, 10.7, 11.0, 11.4, 11.7, 12.0, 12.2 MW/m^2		
	0, 0.2, 0.4, 0.6, 0.8, 1.0, 1.2, 1.4, 1.6, 1.8, 2.0, 2.2, 2.4, 2.6, 2.8, 3.0, 3.2, 3.3,3.4, 3.5, 3.6, 3.7, 3.8, 3.86 x 10^6 Btu/hrft^2		
D&B Fig. 19b:	T.S. B100		
	V	6.096 m/s	20 ft/s
	T	299.82 deg K	80 deg F
	P_{ex}	5.4481 x 10^5 Pa	78 psia
	D_i	4.5847 mm	0.1805 in
	G	6077.2 kg/m^2s	1244.7 lb/m^2s
	L	0.4572 m	18.0 in
	L/D	100	
	Inner Wall Heat Flux Levels:		
	0, 0.85, 1.58, 2.11, 2.59, 3.03, 3.31, 3.91, 4.57, 5.01, 5.2, 5.42, 5.65, 5.83, 5.99, 6.15, 6.28, 6.34, 6.5 MW/m^2		
	0, 0.27, 0.5, 0.67, 0.82, 0.96, 1.05, 1.24, 1.45, 1.59, 1.65, 1.72, 1.79, 1.85, 1.9, 1.95, 1.99, 2.01, 2.06 x 10^6 Btu/hrft^2		

Designation	Parameter	SI Units	English Units
Reynolds #115:	q/A	5.48×10^5 W/m^2	1.7×10^5 Btu/hrft^2
	T	375.37 deg K	216.0 deg F
	P_{in}	3.0675×10^5 Pa	44.49 psia
	D_i	9.5250 mm	0.375 in
	G	3181.4 kg/m^{2}s	651.6 lb/ft^{2}s
	L	1.8288 m	6.0 ft
	L/D	192	
Reynolds #129:	q/A	9.59×10^5 W/m^2	3.04×10^5 Btu/hrft^2
	T	381.48 deg K	227.0 deg F
	P_{in}	6.8630×10^5 Pa	99.54 psia
	D_i	9.5250 mm	0.375 in
	G	3181.4 kg/m^{2}s	651.6 lb/ft^{2}s
	L	1.8288 m	6.0 ft
	L/D	192	
O&S Run 182:	q/A	8.96×10^5 W/m^2	2.84×10^5 Btu/hrft^2
	T	366.48 deg K	200 deg F
	P_{in}	3.5970×10^5 Pa	52.17 psia
	D_i	4.633 mm	0.1824 in
	G	1734.82 kg/m^{2}s	355 lb/ft^{2}s
	L	0.4064 m	16.0 in
	L/D	88	
O&S Run 210:	q/A	3.48×10^6 W/m^2	1.10×10^6 Btu/hrft^2
	T	368.7 deg K	204.0 deg F
	P_{in}	1.4040×10^6 Pa	203.63 psia
	D_i	4.633 mm	0.1824 in
	G	3198.05 kg/m^{2}s	355 lb/ft^{2}s
	L	0.4064 m	16.0 in
	L/D	88	
O&S Run 245:	q/A	1.79×10^6 W/m^2	5.66×10^5 Btu/hrft^2
	T	351.2 deg K	172.5 deg F
	P_{in}	1.4010×10^6 Pa	203.2 psia
	D_i	2.9990 mm	0.1181 in
	G	1987.18 kg/m^{2}s	407.0 lb/ft^{2}s
	L	0.3810 m	15 in
	L/D	127	

Designation	Parameter	SI Units	English Units
O&S Run 253:	q/A	4.01 x 10^6 W/m^2	1.27 x 10^6 Btu/hrft^6
	T	359.5 deg K	187.5 deg F
	P_{in}	2.7850 x 10^6 Pa	403.93 psia
	D_i	2.9990 mm	0.1181 in
	G	3617.94 kg/m^2s	741.0 lb/ft^2s
	L	0.3810 m	15 in
	L/D	127	
O&S Run 208:	q/A	2.07 x 10^6 W/m^2	6.57 x 10^5 Btu/hrft^2
	T	368.15 deg K	203.0 deg F
	P_{in}	6.8427 x 10^5 Pa	99.22 psia
	D_i	4.633 mm	0.1824 in
	G	2475.43 kg/m^2s	507.0 lb/ft^2s
	L	0.4064 m	16.0 in
	L/D	88	
O&S Run 215:	q/A	3.53 x 10^6 W/m^2	1.12 x 10^6 Btu/hrft^2
	T	364.26 deg K	196.0 deg F
	P_{in}	2.7746 x 10^6 Pa	402.31 psia
	D_i	4.633 mm	0.1824 in
	G	2285.01 kg/m^2s	468 lb/m^2s
	L	0.4064 m	16.0 in
	L/D	88	
O&S Run 255:	q/A	3.91 x 10^6 W/m^2	1.24 x 10^6 Btu/hrft^2
	T	364.82 deg K	197.0 deg F
	P_{in}	1.0959 x 10^6 Pa	158.99 psia
	D_i	2.9990 mm	0.1181 in
	G	5321.94 kg/m^2s	1090.0 lb/ft^2s
	L	0.3810 m	15 in
	L/D	127	

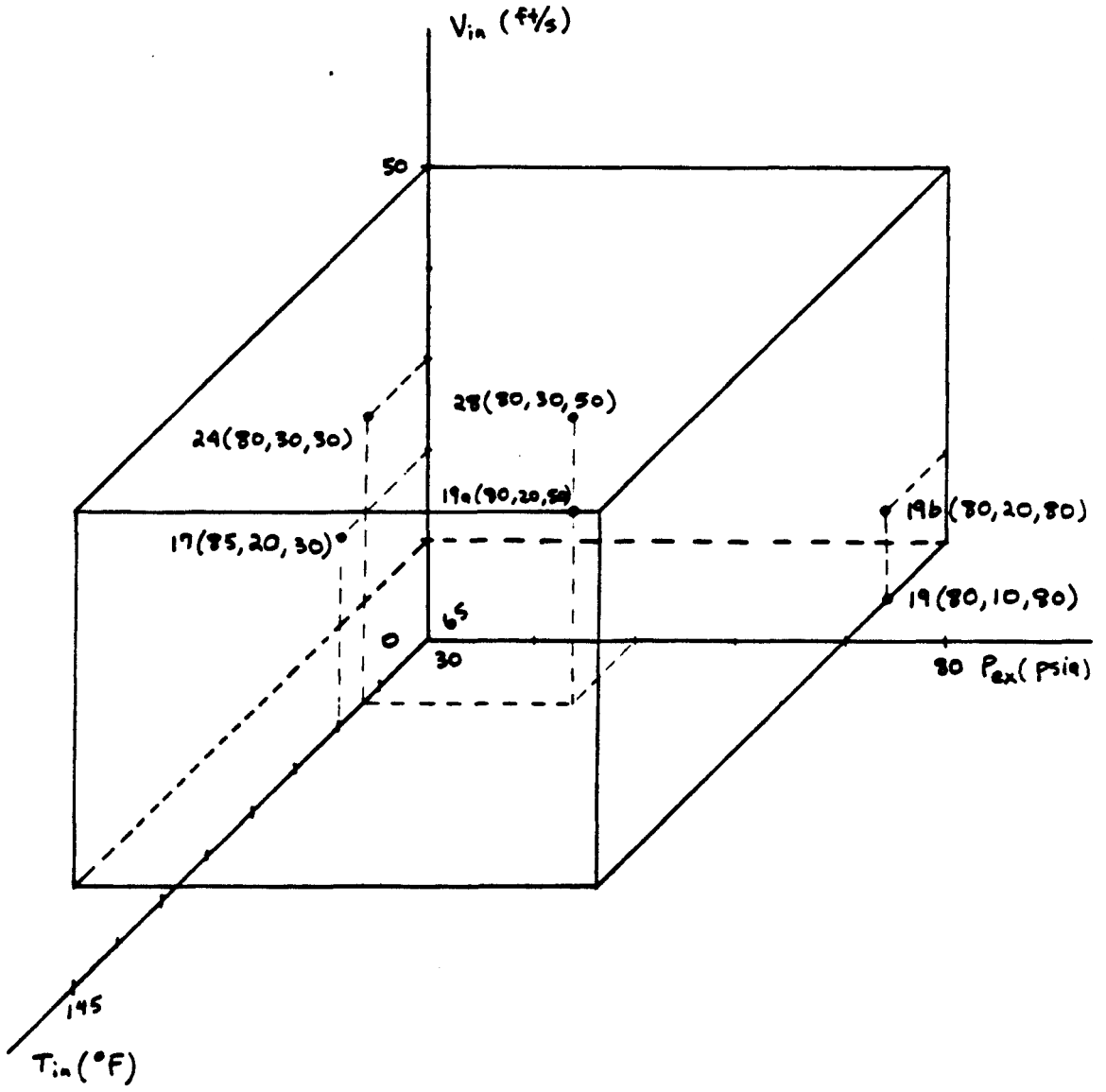

Dormer and Bergles Flow Parameter Space

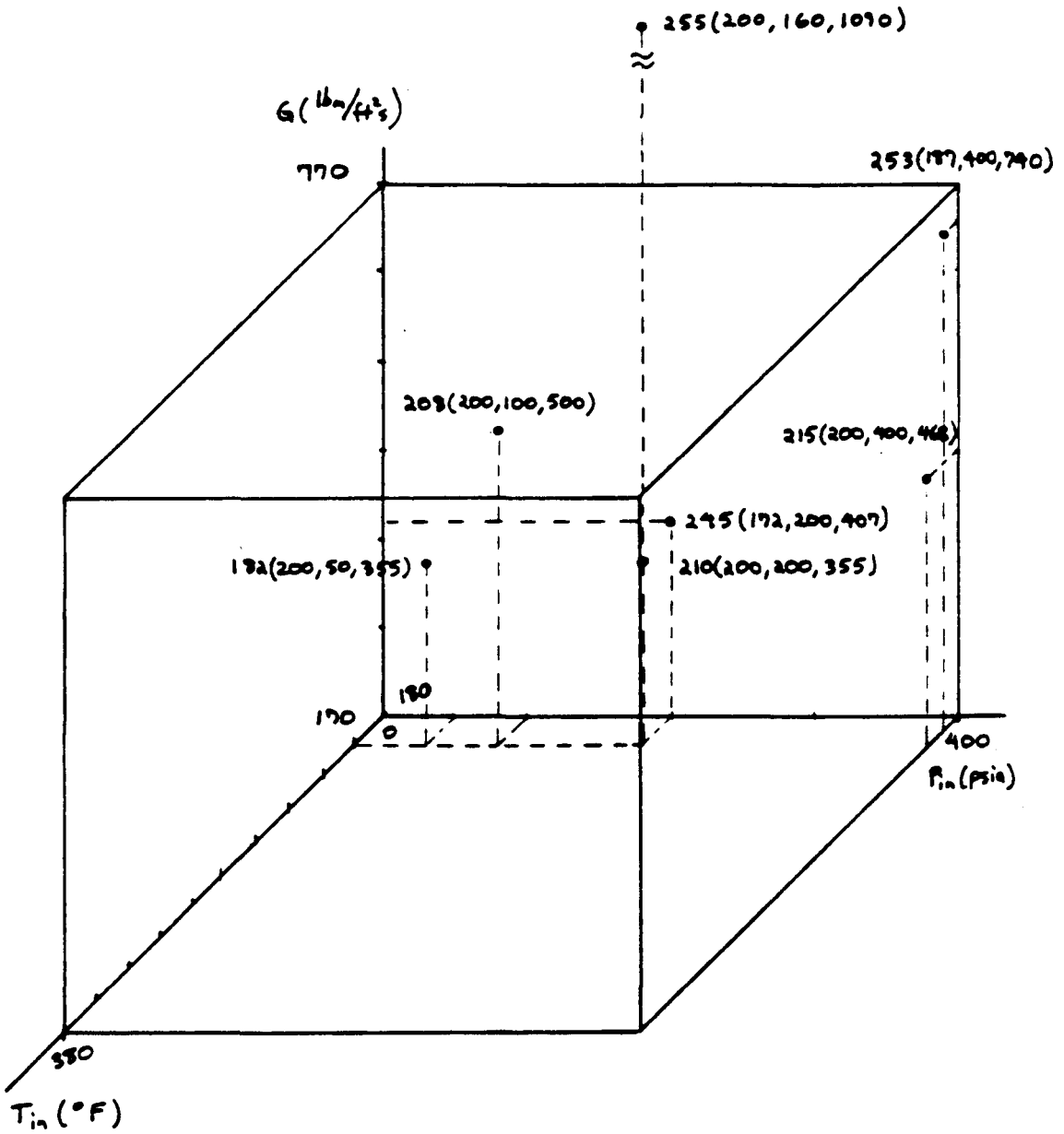

Owens and Schrock Flow Parameter Space

Dormer and Bergles Flow Parameter Space

N(T,V,P) N = D&B Figure Number

T = Inlet Temperature

P = Exit Pressure

V = Inlet Velocity

Dormer and Bergles presented most of their experimental data in overall pressure drop vs. heat flux curves for a variety of combinations of temperatures, velocities and pressures. Each point on the above figure represents a number of overall pressure drop vs. heat flux curves at different tube diameters. One factor influencing our choice of experimental data for use in the code validation procedure was the need to pick curves which covered a sufficiently wide range of flow parameters. The temperature, velocity, pressure plot shows the flow conditions of the data we selected. We also included at least one run for each of the test sections that Dormer and Bergles had examined in order to validate the code over a range of tube diamters.

Owens and Schrock Parameter Space

N(T,P,G) N = O&S Run Number

T = Inlet Temperature

G = Inlet Mass Flux

P = Inlet Pressure

A parameter space plot of the Owens and Schrock experimental data is shown similarly in the next figure. The

same reasoning was used to select experimental data for the code validation from their database.

Appendix E

Estimation of One-Sided Heating Adjustment Factors

The current set of equations used in the final code version ASCB53 to calculate the pressure drop assume that a circumferential and axial uniform heat flux is applied to the tube surface. However, there are many SCB cooling system designs which make use of heating from only one side of the tube. In order to modify the current code for these situations, two axially uniform, one-sided profiles have been considered. They are the (1.) one-sided uniform, and (2.) one-sided cosine profiles. It is assumed that the present uniform heating equations can be multiplied by reducing factors to account for approximately half the heat added to the tube. This method is meant only as a first approximation to the actual physical situation and must be verified by comparison to the experimental data under one-sided heating conditions.

The three types of heating profiles are listed below. The current equations are based on profile P0, but modified for profiles P1 and P2.

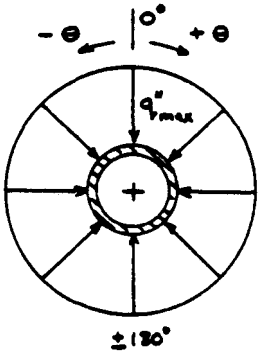

P0: $q''(\theta)$ = constant

= q_{max}

for $-180° < \theta < +180°$

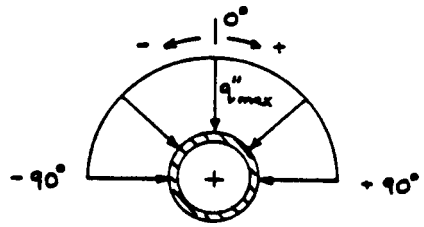

P1: $q''(q) = q''_{max}$

for $-90° < \theta < +90°$

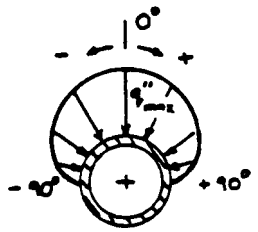

P2: $q''(\theta) = q''_{max}\cos(\theta)$

for $-90° < \theta < +90°$

The amount of heat into the tube will first affect the steady state energy balance equation. The average q" energy into the tube(from -180° to + 180°) is found for profiles P1 and P2 using the definition of an average.

$$\text{P1: } q'' = \frac{\int_{-\pi}^{-\pi/2} 0 \, d\theta + \int_{-\pi/2}^{0} q''_{max} d\theta + \int_{0}^{\pi/2} q''_{max} d\theta + \int_{\pi/2}^{\pi} 0 \, d\theta}{\pi - (-\pi)}$$

$$= \frac{q''_{max}}{2}$$

In similar fashion,

$$P2: \quad q'' = \frac{q''_{max}}{\pi}$$

These q" equations are then substituted into equations using an average q"(i.e. the energy balance equation)

$$\tilde{T}_b(z) = T_{b_{in}} + \frac{4\ n_1\ q''_{max}}{G\ D\ c_{pf}}$$

where

$$n_1 = 1.0 \text{ for P0}$$

$$= 0.5 \text{ for P1}$$

$$= \frac{1}{\pi} \quad \text{for P2} .$$

The predicted onset of significant net vapor generation and the bulk boiling points are then calculated from the same equation, however rearranged as

$$\tilde{z}_{OSNVG} = \frac{G\ c_{pf}}{\pi\ D\ n_1\ q''_{max}} (T_{b_{OSNVG}} - T_{b_{in}})$$

$$\tilde{z}_{OBB} = \frac{G\ c_{pf}}{\pi\ D\ n_1\ q''_{max}} (T_{sat} - T_{b_{in}}) .$$

The adjustment for equations utilizing local q" values(i.e. ONB and SCB equations) are made in a similar manner. The half-sided uniform heating case will be presented first, followed by the half-cosine case.

In both one-sided heating cases, it is idealized that vapor generation can take place only on the heated portion of the tube surface. For illustrative purposes, assume that the tube can be divided into two halves with heating occuring on the top half only. For the uniform one-sided heating case, vapor

generation on the top half would ideally occur at the same rate as in the full uniform heating case. Thus, the ONB and OSNVG points would be predicted at the same $\Delta T_{sat\,(ONB)}$ and $\Delta T_{sub\,(OSNVG)}$, respectively. No vapor is assumed to be generated from the bottom half and the ONB and OSNVG points are not defined for the bottom half. This means that the adjustment factors for the ONB and OSNVG ΔT's should be equal to 1.0. Keep in mind that the bulk temperature rises along the tube only half as fast as in the full uniform heating case. Intuition tells us that the distances of ONB and OSNVG from the tube inlet should be approximately twice their corresponding full uniform heating values; hence requiring adjustment factors of 1.0 on $\Delta T_{sat\,(ONB)}$ and $\Delta T_{sub\,(OSNVG)}$ because factors of less than 1.0 would cause those distances to be less than twice the full uniform heating values.

Because one-half the vapor is formed along the tube as compared to the full uniform case, the adjustment factors on the attached wall bubble layer and flow quality would correspondingly be 0.5. Because the void fraction α' is a direct function of flow quality x', an adjustment of x' will effectively adjust α'.

The adjusted equations for uniform one-half-sided heating are given as

$$\widetilde{\Delta T}_{sat\,(OSNVG)} = n_2\ 0.0022\left[\frac{q''\ D}{k_f}\right] \qquad \text{for Pe} < 70{,}000$$

$$\widetilde{\Delta T}_{sat\,(OSNVG)} = n_2\ 153.8\left[\frac{q''}{G\ c_{pf}}\right] \qquad \text{for Pe} > 70{,}000$$

$$\widetilde{\widetilde{St}} = n_2 \left[\frac{q''}{G\ c_{pf}\ \Delta T_{sub}}\right]$$

where $n_2 = 1.0$ for P0
$= 1.0$ for P1

$$\widetilde{\Delta T}_{sat(ONB)} = \frac{B}{r_{max\text{-}active}} + n_3 \frac{q''\ r_{max\text{-}active}}{k_f}$$

where $n_3 = 1.0$ for P0
$= 1.0$ for P1

$$\widetilde{x'(Z)} = n_4 \left[\frac{c_{pf}\ \Delta T_{sub(OSNVG)}\ (Z^+ - T^*)}{i_{fg} - c_{pf}\ \Delta T_{sub(OSNVG)}\ (1 - T^*)}\right]$$

$$\widetilde{\alpha'(Z)} = \frac{x'(Z)}{\left\{\frac{C_o(\rho_f - \rho_g)}{\rho_f}\right\} x'(Z) + \left[C_o + \frac{\bar{u}_{gj}}{u_{f\ inlet}}\right] \frac{\rho_g}{\rho_f}}$$

where $n_4 = 1.0$ for P0
$= 0.5$ for P1

$$\widetilde{\alpha'}_{wall} = n_5\ \alpha'_{wall}$$

where $n_5 = 1.0$ for P0
$= 0.5$ for P1

The heat transfer coefficient in the top half is given by the same equations used for the full heating case, hence no

adjustment factors are needed. For the bottom half, no heat is assumed to be transfered.

For the one-sided cosine heating profile, it is assumed that heat applied near $\theta = -90°$ and $+90°$ contributes minimally to the heating of the fluid and vapor generation because of the cooling effect of the non-heated liquid on the bottom half of the tube. Thus, the end sections of the $q''(\theta)$ curve with $q'' < 0.5\ q''_{max}$ will be ignored as a rough first approximation. This assumption is illustrated below.

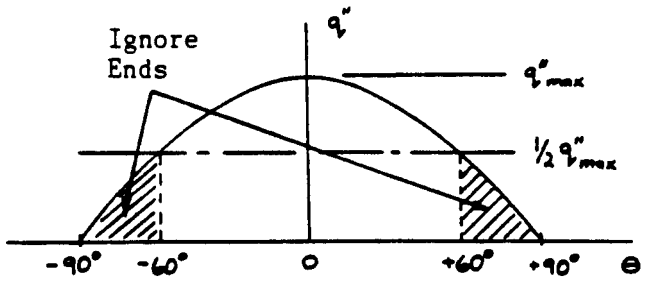

The total q" now into the tube is calculated as

$$q''_{tot'} = \int_{-\pi/2}^{+\pi/2} q''_{max} \cos(\theta)\ d\theta$$

$$= \sqrt{3}\ q''_{max}$$

as compared to

$$q''_{tot} = \int_{-\pi/2}^{+\pi/2} q''_{max} \cos(\theta)\ d\theta$$

$$= 2\ q''_{max}$$

for the full one-sided cosine q" profile. The total q" now into the tube(i.e. $q"_{tot'}$) can be thought of as being reduced by a factor of

$$\left[\frac{q"_{tot'}}{q"_{tot}}\right]_{1\text{-sided cos}} = \frac{\sqrt{3}}{2} = 0.866$$

for the ONB and OSNVG equations.

If we were not to ignore the end heating portions of the heating profile, then the adjustment factors for the ONB and OSNVG equations would be exactly the same as for the P1 heating profile case. The above factor is applied to these equations in order to account for the ignored end heating yielding the appropriate reduction factors for the P2 profile.

P2: $n_2 = 0.866$ vs. 1.0 for P1

$n_3 = 0.866$ vs. 1.0 for P1

In a similar way, some amount of vapor at the ends is also ignored because of the cooling effect assumption. The unwrapped attached wall bubble layer would look like(for a unit tube radius)

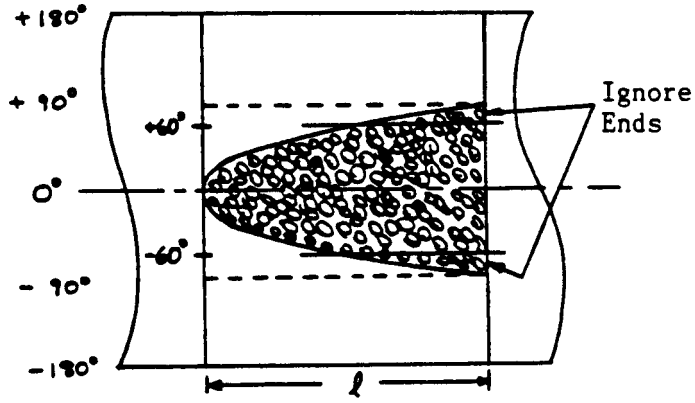

Thus the reduction in vapor formation and flow blockage is calculated as(asumming unit tube radius)

$$A_{\text{uniform heating}} = 2\pi \ell$$

$$A_{\text{cos less ends}} = \int_{-\pi/3}^{+\pi/3} \ell \cos(\theta)\, d\theta$$

$$= \sqrt{3}\, \ell$$

$$n_4 = n_5 = \frac{A_{\text{cos less ends}}}{A_{\text{uniform heating}}} = \frac{\sqrt{3}}{2\pi} = 0.28 \text{ for P2 .}$$

Summarizing the reduction factors for the one-sided cosine heating profile P2,

P2: $n_2 = 0.866$

$n_3 = 0.866$

$n_4 = 0.28$

$n_5 = 0.28$

The reader is reminded that these adjustments to the full heating equations are meant only as rough estimates for the two one-sided heating cases.

Appendix F

Review of Gambill Critical

Heat Flux Correlation

A general equation predicting the critical heat flux(CHF) for forced-convective flows of wetting liquids was proposed by Gambill[30]. This equation is based on the premise that the critical heat flux can be characterized as consisting of two contributions, (1) the boiling contribution in absense of forced convection, and (2) the equivalent forced convection contribution in absense of boiling. These terms are independently formulated and added to yield the total heat flux at burnout. The equation is given as

$$\phi_{bo} = (\phi_{bo})_{boil} + (\phi_{bo})_{nb}$$

$$= K\, i_{fg}\, \rho_v \left[\frac{\sigma\ (9.81)\ \Delta\rho}{\rho_v^2}\right]^{0.25} x \left[1 + \left(\frac{\rho_f}{\rho_v}\right)^{0.923} \frac{c_p\ \Delta T_{sub}}{25\ i_{fg}}\right] +$$

$$h_{nb}(T_w - T_b)_{bo}$$

The boiling contribution is found by

$$(\phi_{bo})_{boil} = (\phi_{bo})_{poolsat} \left[\frac{(\phi_{bo})_{sub}}{(\phi_{bo})_{sat}}\right]_{pool} = (\phi_{bo})_{poolsat}\ F_{sub}$$

where

$$(\phi_{bo})_{poolsat} = K\, i_{fg}\, \rho_v \left[\frac{\sigma\ \Delta\rho}{\rho_v^2}\right]^{0.25} \quad \text{from Kutateladze[32]}$$

and

$$F_{sub} = 1 + \left(\frac{\rho_f}{\rho_v}\right)^{0.923} \left(\frac{c_p\ \Delta T_{sub}}{25\ i_{fg}}\right) \quad \text{from Bonilla[33]}$$

and K is normally taken to be within the range of 0.12 to 0.17, with the exact value finalized from comparison to relevant forced-convection CHF data. The convective contribution is found by

$$(\phi_{bo})_{boil} = h_{nb}\ (T_w - T_b)_{bo}$$

where $h_{nb} = 0.26(\frac{k}{D})Re^{0.8}Pr^{0.333}$.

Gambill's burnout heat flux equation has been compared with a large quantity of experimental data(1326 points) over a broad range of flow conditions.

Flow Velocities:	0.0152 - 53 m/s (0.05 - 174 ft/s)
Pressures:	0.29×10^5 - 206.8×10^5 Pa (4.2 - 3000 psia)
Inlet Subcoolings:	0 - 281.11 °C (0 - 506 °F)
Critical Heat Fluxes:	0.315×10^6 - 117×10^6 W/m^2 (0.1×10^6 - 37.4×10^6 Btu/hrft^2)

For 96% of the representative CHF experimental data, the predictions using the Gambill formula agree with the experimental data with a maximum deviation of 40%.

Gambill states that the additive nature of his correlation results in less shortcomings than most broad-range burnout correlations.

Professor Hoffman compared the Gambill correlation to CHF data for small diameter tubes and found that the Gambill correlation should be modified in order to yield better predictions for tubes less than 8 mm. This modification follows the adjustment used in the USSR Academy of Sciences CHF Table(see Collier[24] p. 261). The modification is given as

$$\phi_{crit} = \phi_{crit(Gambill)} \left[\frac{0.008}{D(m)}\right]^{0.5} \qquad (D \leq 8 \text{ mm})$$

The Gambill correlation was found to be the best, conservative, broadest-range correlation for design use.

Appendix G

Steam Data Output from the Code

	TSAT (K)	PSAT (PA)	VAPOR DENSITY (KG/M3)	SAT LIQUID ENTHALPY (J/KG)	SAT VAPOR ENTHALPY (J/KG)
1	273.1600	611.2203	.00485055	.6978	2501613.00
2	274.8167	688.8552	.00543349	6982.6520	2504637.00
3	277.5945	838.6093	.00654938	18670.8000	2509754.00
4	280.3722	1016.5630	.00786067	30340.3400	2514871.00
5	283.1500	1226.9910	.00939609	41993.6100	2519989.00
6	285.9278	1474.9270	.01118638	53635.2300	2525106.00
7	288.7055	1765.8160	.01326471	65267.5600	2529990.00
8	291.4833	2106.0040	.01567211	76890.5800	2535108.00
9	294.2611	2502.2450	.01844595	88508.9500	2540225.00
10	297.0389	2962.2630	.02163780	100122.7000	2545342.00
11	299.8167	3494.6700	.025293e4	111734.1000	2550227.00
12	302.5945	4108.1040	.02946737	123340.8000	2555344.00
13	305.3722	4813.4170	.03422017	134949.9000	2560461.00
14	308.1500	5621.5710	.03961045	146556.6000	2565346.00
15	310.9278	6544.7800	.04571479	158165.7000	2570463.00
16	313.7056	7596.2300	.05260579	169774.7000	2575347.00
17	316.4833	8790.8150	.06035820	181381.5000	2580232.00
18	319.2611	10142.9800	.06906296	192988.2000	2585349.00
19	322.0389	11670.7600	.07880775	204618.2000	2590234.00
20	324.8167	13392.3800	.08968904	216225.0000	2595118.00
21	327.5945	15327.0500	.10181440	227855.0000	2600003.00
22	330.3722	17495.4500	.11529050	239461.7000	2604888.00
23	333.1500	19920.3300	.13023140	251091.7000	2609772.00
24	335.9278	22625.8400	.14676990	262721.7000	2614424.00
25	338.7056	25637.4600	.16501970	274351.7000	2619309.00
26	341.4833	28982.8000	.18514170	285981.7000	2624193.00
27	344.2611	32690.8000	.20725140	297635.0000	2628845.00
28	347.0389	36791.1200	.23154760	309265.0000	2633497.00
29	349.8167	41317.5200	.25811250	320918.2000	2638149.00
30	352.5945	46304.5000	.28722360	332594.8000	2642801.00
31	355.3722	51786.5200	.31896580	344248.0000	2647453.00
32	358.1500	57805.6400	.35358700	355924.5000	2652105.00
33	360.9278	64397.0400	.39110440	367601.0000	2656525.00
34	363.7056	71602.0500	.43192750	379277.6000	2660944.00
35	366.4833	79468.9800	.47618730	390977.3000	2665596.00
36	369.2611	88046.0500	.52409580	402677.1000	2670016.00
37	372.0389	97374.6600	.57587230	414376.9000	2674202.00
38	374.8167	107503.1000	.63176750	426099.9000	2678622.00
39	377.5945	118493.3000	.69200210	437823.0000	2682809.00
40	380.3722	130393.7000	.75680160	449569.3000	2687228.00
41	383.1500	143266.2000	.82650340	461315.6000	2691415.00
42	384.2611	148699.2000	.85577860	466014.1000	2693043.00
43	386.4833	160068.7000	.91686010	475434.4000	2696299.00
44	388.7056	172148.3000	.98146340	484854.7000	2699556.00
45	389.8167	178457.0000	1.01511200	489576.5000	2701184.00
46	392.0389	191653.6000	1.08518000	498996.8000	2704440.00
47	394.2611	205636.1000	1.15916200	508440.3000	2707464.00
48	395.3722	212930.8000	1.19764200	513162.1000	2709092.00
49	397.5945	228154.4000	1.27759300	522628.9000	2712349.00
50	399.8167	244260.6000	1.36188300	532095.8000	2715373.00

51	400.9278	252251.5000	1.40574500	536817.5000	2716768.00
52	403.1500	270129.7000	1.49663300	546307.6000	2719792.00
53	405.3722	288587.0000	1.59229300	555797.7000	2722816.00
54	406.4833	298191.4000	1.64207700	560542.8000	2724444.00
55	408.7056	318172.4000	1.74493100	570056.1000	2727235.00
56	410.9278	339222.1000	1.85313100	579569.4000	2730259.00
57	412.0389	350157.2000	1.90918700	584291.2000	2731655.00
58	414.2611	372889.2000	2.02537200	593827.8000	2734446.00
59	416.4833	396793.3000	2.14716100	603364.4000	2737237.00
60	417.5945	409203.8000	2.21020500	608249.0000	2738633.00
61	419.8167	434948.9000	2.34075100	617785.6000	2741424.00
62	422.0389	461983.2000	2.47741400	627322.3000	2743982.00
63	423.1500	476000.3000	2.54811400	632206.8000	2745378.00
64	425.3722	505047.9000	2.69435200	641743.4000	2747937.00
65	427.5945	535495.1000	2.84722100	651280.0000	2750495.00
66	428.7056	551256.6000	2.92617500	656164.6000	2751891.00
67	430.9278	583903.3000	3.08944500	665933.8000	2754217.00
68	433.1500	618066.7000	3.25989300	675470.4000	2756775.00
69	434.2611	635731.1000	3.34792100	680355.0000	2757938.00
70	436.4833	672280.2000	3.52969600	689891.6000	2760264.00
71	438.7056	710470.3000	3.71925600	699660.8000	2762590.00
72	439.8167	730203.1000	3.81701000	704545.4000	2763753.00
73	442.0389	770971.8000	4.01878200	714314.6000	2765847.00
74	444.2611	813526.2000	4.22896200	724083.8000	2768173.00
75	445.3722	835486.0000	4.33740300	728968.4000	2769103.00
76	447.5945	880812.1000	4.56080600	738737.6000	2771197.00
77	449.8167	928061.9000	4.79336400	748506.8000	2773290.00
78	450.9278	952428.0000	4.91318700	753391.4000	2774220.00
79	453.1500	1002663.0000	5.15992300	763160.6000	2776314.00
80	455.3722	1054967.0000	5.41658400	772929.8000	2778175.00
81	456.4833	1081905.0000	5.54886500	777814.4000	2779105.00
82	458.7056	1137414.0000	5.82087400	787816.3000	2780966.00
83	460.9278	1195130.0000	6.10366700	797585.4000	2782594.00
84	462.0389	1224840.0000	6.24915700	802470.9000	2783524.00
85	464.2611	1285990.0000	6.54830500	812471.8000	2785153.00
86	466.4833	1349504.0000	6.85927400	822473.6000	2786548.00
87	467.5945	1382171.0000	7.01917700	827358.3000	2787479.00
88	469.8167	1449354.0000	7.34758200	837360.0000	2788874.00
89	472.0389	1519060.0000	7.68898500	847361.8000	2790270.00
90	473.1500	1554870.0000	7.86413800	852479.0000	2790968.00
91	475.3722	1628493.0000	8.22429700	862480.8000	2792131.00
92	477.5945	1704791.0000	8.59820800	872482.6000	2793526.00
93	478.7056	1743974.0000	8.79024500	877599.8000	2793991.00
94	480.9278	1824429.0000	9.18437300	887601.6000	2795154.00
95	483.1500	1907738.0000	9.59361700	897836.0000	2796085.00
96	484.2611	1950486.0000	9.80322200	902720.6000	2796783.00
97	486.4833	2038208.0000	10.23479000	912955.0000	2797713.00
98	488.7056	2128963.0000	10.68111000	923189.4000	2798411.00
99	489.8167	2175496.0000	10.91027000	928306.6000	2798876.00
100	492.0389	2270919.0000	11.38079000	938541.0000	2799574.00
101	494.2611	2369549.0000	11.86905000	948775.4000	2800272.00
102	495.3722	2420060.0000	12.11877000	953892.6000	2800504.00
103	497.5945	2523688.0000	12.63226000	964359.6000	2800969.00
104	499.8167	2630626.0000	13.16366000	974594.8000	2801435.00
105	500.9278	2685439.0000	13.43639000	979943.8000	2801667.00
106	503.1500	2797617.0000	13.99579000	990178.3000	2801900.00
107	505.3722	2913380.0000	14.57483000	1000645.0000	2802132.00
108	506.4833	2972606.0000	14.87171000	1005995.0000	2802365.00
109	508.7056	3093885.0000	15.48097000	1016462.0000	2802365.00
110	510.9278	3218955.0000	16.11127000	1026929.0000	2802365.00
111	512.0389	3282870.0000	16.43442000	1032279.0000	2802365.00
112	514.2611	3413732.0000	17.09749000	1042978.0000	2802132.00
113	516.4833	3548525.0000	17.78328000	1053445.0000	2801900.00
114	517.5945	3617472.0000	18.13500000	1058795.0000	2801667.00
115	519.8167	3758401.0000	18.85634000	1069727.0000	2801202.00
116	522.0389	3903467.0000	19.60236000	1080427.0000	2800737.00

117	523.1500	3977386.0000	19.96511000	1085777.0000	2800504.00
118	525.3723	4129063.0000	20.76975000	1096709.0000	2799806.00
119	527.5945	4284954.0000	21.58124000	1107409.0000	2798876.00
120	529.7056	4364589.0000	21.99734000	1112991.0000	2798411.00
121	530.9278	4527167.0000	22.85068000	1123923.0000	2797480.00
122	533.1500	4694365.0000	23.73387000	1134855.0000	2796317.00
123	534.2611	4779653.0000	24.18684000	1140438.0000	2795852.00
124	536.4833	4953883.0000	25.11550000	1151603.0000	2794457.00
125	538.7056	5132940.0000	26.07639000	1162767.0000	2793061.00
126	539.8167	5224296.0000	26.56946000	1168350.0000	2792363.00
127	542.0389	5410730.0000	27.58047000	1179515.0000	2790735.00
128	544.2611	5602198.0000	28.62689000	1190912.0000	2788874.00
129	545.3723	5699827.0000	29.16372000	1196495.0000	2787944.00
130	547.5945	5899017.0000	30.26578000	1207892.0000	2786083.00
131	549.8167	6103446.0000	31.40629000	1219522.0000	2783990.00
132	550.9278	6207626.0000	31.99214000	1225337.0000	2782827.00
133	553.1500	6420191.0000	33.19407000	1236734.0000	2780501.00
134	555.3723	6638204.0000	34.43868000	1248597.0000	2777942.00
135	556.4833	6749278.0000	35.07821000	1254412.0000	2776546.00
136	558.7056	6975771.0000	36.39071000	1266275.0000	2773755.00
137	560.9278	7207987.0000	37.75090000	1278137.0000	2770731.00
138	562.0389	7326300.0000	38.45046000	1283952.0000	2769336.00
139	564.2611	7567341.0000	39.88661000	1296047.0000	2766079.00
140	566.4833	7814386.0000	41.37641000	1308143.0000	2762590.00
141	567.5945	7940210.0000	42.14165000	1314190.0000	2760730.00
142	569.8167	8196488.0000	43.71613000	1326518.0000	2757008.00
143	572.0389	8459040.0000	45.35110000	1338846.0000	2753054.00
144	573.1500	8592660.0000	46.19201000	1345126.0000	2750960.00
145	575.3723	8864865.0000	47.92217000	1357686.0000	2746774.00
146	577.5945	9143621.0000	49.72207000	1370247.0000	2742354.00
147	578.7056	9285169.0000	50.64806000	1376527.0000	2740028.00
148	580.9278	9574060.0000	52.55746000	1389320.0000	2735144.00
149	583.1500	9869845.0000	54.54393000	1402346.0000	2730026.00
150	584.2611	10020150.0000	55.56757000	1408858.0000	2727468.00
151	586.4833	10326970.0000	57.68262000	1422117.0000	2721885.00
152	588.7056	10639990.0000	59.88882000	1435375.0000	2716070.00
153	589.8167	10799260.0000	61.02737000	1442120.0000	2713047.00
154	592.0389	11124000.0000	63.38173000	1455844.0000	2706999.00
155	594.2611	11456330.0000	65.84644000	1469567.0000	2700254.00
156	595.3723	11625250.0000	67.12115000	1476545.0000	2696997.00
157	597.5945	11968610.0000	69.76683000	1490501.0000	2689787.00
158	599.8167	12320240.0000	72.54411000	1504690.0000	2682343.00
159	600.9278	12498820.0000	73.98829000	1511900.0000	2678389.00
160	603.1500	12862860.0000	76.98594000	1526554.0000	2670248.00
161	605.3723	13234490.0000	80.14842000	1541440.0000	2661409.00
162	606.4833	13424090.0000	81.79780000	1548884.0000	2656757.00
163	608.7056	13808820.0000	85.24086000	1564003.0000	2647221.00
164	610.9278	14202510.0000	88.88776000	1579587.0000	2636986.00
165	612.0389	14402460.0000	90.79210000	1587495.0000	2631637.00
166	614.2611	14809940.0000	94.78942000	1603545.0000	2620472.00
167	616.4833	15226380.0000	99.04447000	1619827.0000	2608377.00
168	617.5945	15438740.0000	101.28010000	1628200.0000	2602096.00
169	619.8167	15869660.0000	105.97730000	1645413.0000	2589071.00
170	622.0389	16310930.0000	111.00040000	1662858.0000	2574882.00
171	623.1500	16535010.0000	113.64640000	1671929.0000	2567672.00
172	625.3723	16991440.0000	119.35370000	1691235.0000	2551855.00
173	627.5945	17458900.0000	125.50570000	1711471.0000	2534875.00
174	628.7056	17696080.0000	128.93160000	1721705.0000	2525804.00
175	630.9278	18180100.0000	136.10730000	1742639.0000	2506498.00
176	633.1500	18675140.0000	144.00900000	1764271.0000	2485331.00
177	634.2611	18926800.0000	148.45660000	1775436.0000	2473934.00
178	636.4833	19439770.0000	158.00210000	1798929.0000	2449046.00
179	638.7056	19965150.0000	169.34630000	1824747.0000	2420436.00
180	639.8167	20232670.0000	175.83580000	1838703.0000	2404154.00
181	642.0389	20776660.0000	191.35660000	1871035.0000	2366007.00
182	644.2611	21334450.0000	213.03980000	1912903.0000	2314835.00

	TSAT (K)	SAT LIQUID SP HEAT (J/KG-K)
1	273.16000	4217.40000
2	283.15000	4192.80000
3	293.15000	4182.20000
4	303.15000	4178.70000
5	313.15000	4178.90000
6	323.15000	4181.20000
7	333.15000	4184.80000
8	343.15000	4189.90000
9	353.15000	4196.50000
10	363.15000	4205.00000
11	373.15000	4215.60000
12	383.15000	4228.80000
13	393.15000	4244.60000
14	403.15000	4263.30000
15	413.15000	4285.00000
16	423.15000	4310.00000
17	433.15000	4338.50000
18	443.15000	4370.90000
19	453.15000	4407.60000
20	463.15000	4449.20000
21	473.15000	4496.60000
22	483.15000	4550.80000
23	493.15000	4613.10000
24	503.15000	4685.00000
25	513.15000	4768.70000
26	523.15000	4866.70000
27	533.15000	4982.70000
28	543.15000	5121.60000
29	553.15000	5290.20000
30	563.15000	5498.60000
31	573.15000	5761.90000
32	583.15000	6104.00000
33	586.59440	6246.71000
34	593.15000	6564.90000
35	603.15000	7219.40000
36	608.59440	7707.90000
37	613.15000	8232.70000
38	623.15000	10104.70000
39	633.15000	14579.00000
40	641.66670	32012.27000
41	643.15000	43167.00000

Appendix H

Other Original Data

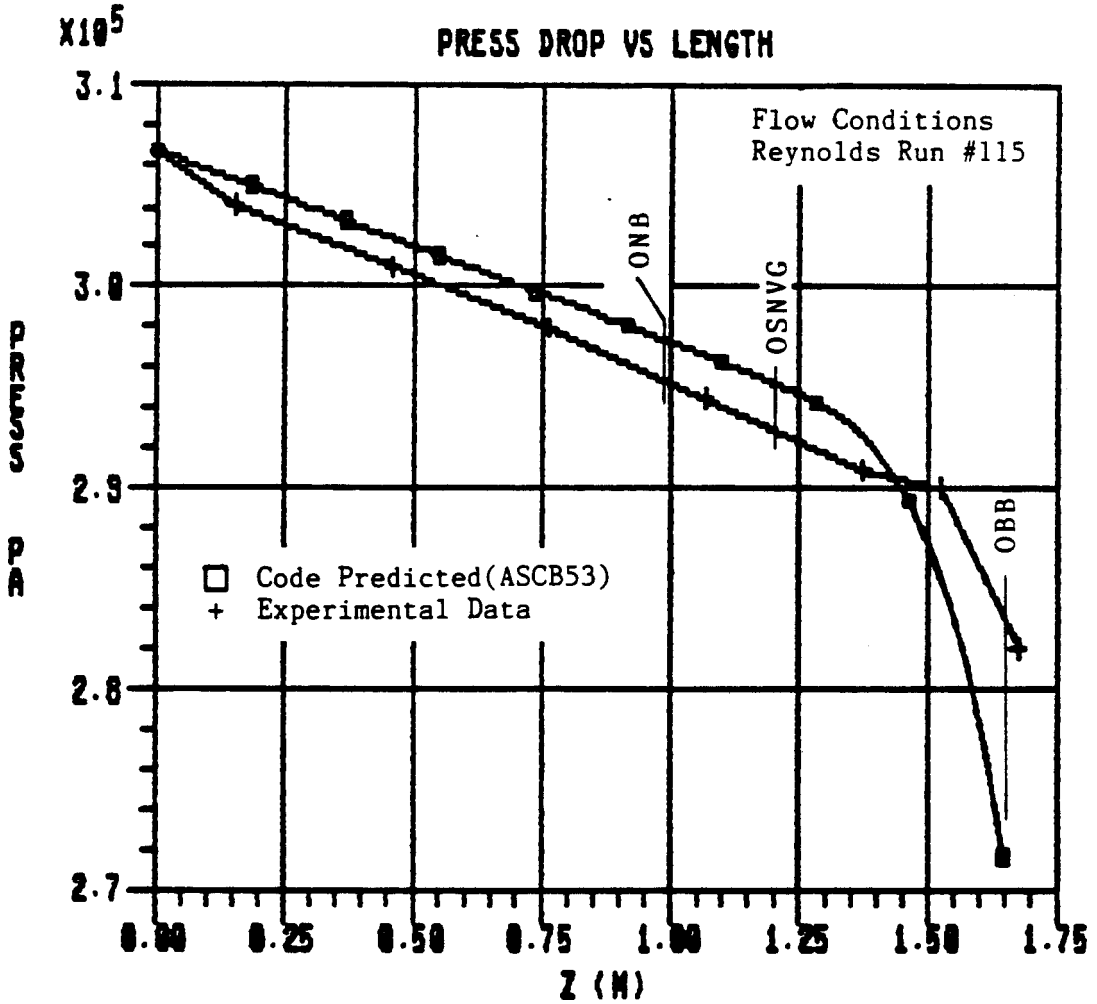

Comparison of Experimental and Code Predicted Pressure Drop Along Tube for Final Code Version ASCB53

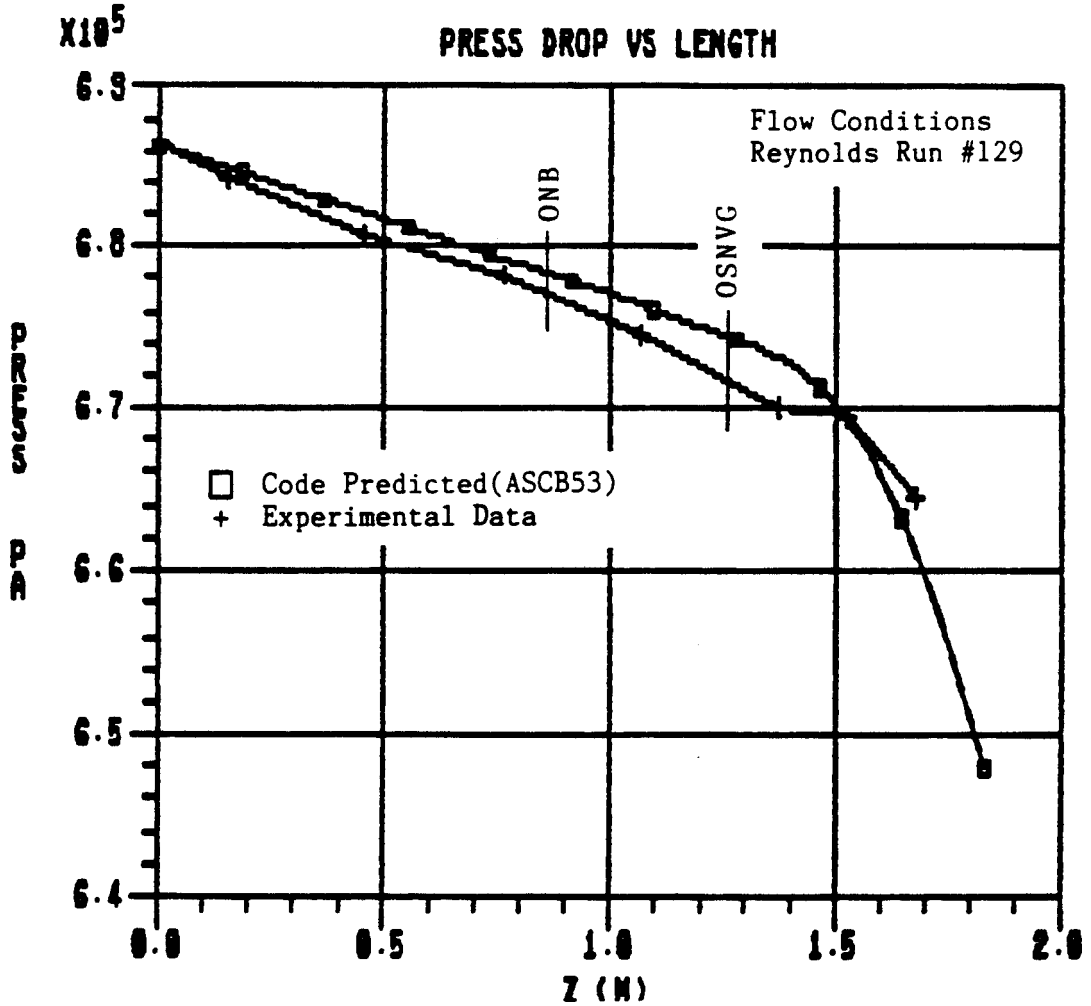

Comparison of Experimental and Code Predicted Pressure Drop Along Tube for Final Code Version ASCB53

Appendix I

Code Version Log

CODE LOG

PARAMETER

	OWB DEBG ROMS	OFDB	A/D	PDB FRIC EAME NOME	J/S	PLB BUBL NOME	RUUN	LEVY	AUUH	MUD OFDB	PDB I PFL LINE	S/Z	BD SHAM	MOD S/Z	PDB FRIC TP=1	MNUS	M/N	M/N CHSL	FDB CO CONS	NAME C2=C	C2=V	FLB UGJ COLL	DIF	FDB BUBL NOME	GAUN	CONS	LIN1	LIN2	LIN3	RHOH RUN AI TSAT	Tw1	F/F ISO PETR	0.4	0.3	COMMENTS
ASCB1		0		0			0			0		0				0			1.13			0			0				0		0			EQUIV KLINE CODE DELETED ALL STRESS CALCS
ASCB2		0		0			0			0		0				0			1.13			0			0				0		0			SAME AS ASCB1 DELETED STRESS INFO IN INPUT. ADDED PRESS DROP IN UNHEATED SECTION
ASCB3	0			0			0			0		0				0			1.13			0			0				0		0			ALSO CORRECTED SHAM NOBL BUT STILL COMMENTED OUT
ASCB3A	0			0			0				0	0				0			1.13			0			0				0		0			Linear Tw1 in PDB
ASCB4		0		0			0			0		0				0			1.13			0			0				0		0			CORRECTED D IN RE OF SUBRTN HOMOGFF & HTCOEFF
ASCB4A		0		0			0			0		0				0			1.13			0			0					0	0			RUN evaluated at Tw1
ASCB4B		0		0			0			0		0				0			1.13			0			0					0	0			USED 1/2 NVOID & NO NVOID in PDB
ASCB5		0		0			0			0		0				0			1.13			0			0				0		0			CHGD BK TO KLIN SR-2F & ADDED CNPTR COMPAR PGRM
ASCB5A		0		0			0			0		0				0			1.13			0			0				0		0			CORRECTED G TO BECOME GO IN RE IN SUBRTN HOMOGFF
ASCB5B		0		0			0			0		0				0			1.13			0			0				0		0			INCREASED STEPS TO 2000
ASCB6		0		0		0				0		0				0			1.13			0		0					0		0			EQUIV TO KLINE S-2F
ASCB7	0			0			0				0	0				0			1.13			0			0				0		0			SAME AS ASCB3A BUT REMM FOR CNPTR CMPRSON
ASCB8		0		0			0			0		0				0			1.13				0		0				0		0			CHG TO SUBRTN ZUBSF2 ONLY
ASCB9		0		0			0			0		0			0				1.13				0		0				0		0			EQUIV TO KLINE SR-2 EXCPT UGJ TERM
ASCB10		0		0		0				0		0			0				1.13				0	0					0		0			EQUIV TO KLINE S-2 EXCPT FOR UGJ TERM
ASCB11		0		0			0			0		0					0		1.13				0		0				0		0			CHG IN SUBRTN ZUBSF2 ONLY
ASCB11A		0		0			0			0		0						0	1.13				0		0				0		0			CHG IN SUBRTN ZUBSF2 ONLY
ASCB12		0		0		0				0		0					0		1.13				0	0					0		0			CHG IN SUBRTN ZUBSF2 ONLY
ASCB12A		0		0		0				0		0						0	1.13				0	0					0		0			CHG IN SUBRTN ZUBSF2 ONLY
ASCB13		0		0			0			0		0						0	1.13				0		0				0		0			USES 0.7 I NN TPFF W/CHISHOLM CHG IN SUBRTN ZUBSF2 ONLY
ASCB14		0		0		0				0		0						0	1.13				0	0					0		0			USES 0.7 I NN TPFF W/CHISHOLM CHG IN SUBRTN ZUBSF2 ONLY

PARAMETER

	DAB DERG RONS	UFDB	A/D	FDB FRIC ENHC NONE	J/S	PDB BUBL NONE	ROUN	LEVY	ROUG ROUN	FDB I PFL UFDB	LINE	WD S/Z	ROD SHAH	S/Z	FDB FRIC TP=1	HAGS	N/N	N/N CHSL	FDB CO CONS	HANC C2=C	C2=V	FDB UGJ CULL	DIT	FDB BUBL NONE	GROW	CONS	LIN1	LIN2	LIN3	RHOW MUW AT TSAT	TW1	F/F ISO PETR	0.4	0.3	COMMENTS
ASCB15		•		•		•				•		•				•					•		•	•						•		•			SET VOID TO 1.0E-06 INITL
ASCB16		•		•		•				•		•				•					•		•	•						•		•			ADDED ITER LOOP BTWN WVD & CO. ADDED CO & PE TO PRINTOUT
ASCB16A		•		•		•				•		•				•				•			•	•						•		•			HELD CO2 CONST IN ITERAT LOOP
ASCB16B		•		•		•				•		•				•					•		•	•						•		•			CORRECTED CO2 EQUATION IN ITERAT LOOP
ASCB17	•				•			•			•	•				•			1.13				•	•						•		•			EQUIV TO J/S EXCP FOR CO CONST, PETR F/FISO, & HAG TPFF NEW SUBRTN ZUBSF3
ASCB17A	•				•			•			•	•				•			1.13				•	•						•		•			USED FISO FROM BLASIUS W/ EXP=0.25
ASCB17B	•				•			•			•	•				•			1.13				•	•						•			0.14		F/FISO EXP=0.14
ASCB18	•				•			•			•	•				•			1.13				•	•						•			•		EQUIV TO J/S EXCP FOR CO CONST & HAG TPFF
ASCB18A	•				•			•			•	•				•			1.13				•	•						•			•		RAN WITH THETA=0 FOR NO GRAV TERMS
ASCB18B	•				•			•			•	•				•			1.13				•	•							•		•		CORRECT RHOW & MUW TERMS
ASCB19	•				•			•			•	•				•				•			•	•							•		•		
ASCB20	•				•			•			•	•				•			1.13				•	•							•		•		USED 500 STEPS
ASCB21	•				•		•				•	•				•			1.13				•	•							•		•		Rouhani wall void but J/S enhanced f
ASCB22	•			•				•			•	•				•			1.13				•	•							•		•		Levy wall void, no enhanced f
ASCB23	•			•			•				•	•				•			1.13				•	•							•		•		Rouhani wall void but no J/S enhanced f
ASCB24	•			•			•				•	•					•		1.13			•		•							•		•		REFERENCE CODE VERSION 02
ASCB24A	•			•			•				•	•					•		1.2			•		•							•		•		
ASCB24B	•			•			•				•	•					•		1.13			•		•							•		•		TW=1-EXP(-Z+) CHG IN SUBRTN ZUBSF3 ONLY
ASCB25	•			•			•				•	•					•		1.13			•		•							•		•		X'=f(XEQ,XEQBD) INSTEAD NEW SUBRTN ZUBSF4
ASCB26	•			•			•				•	•					•		1.13			•					•				•		•		FDB BLKG LINEAR DECREASE TO DBB FROM BB

PARAMETER

	DNB BENG ROWS	OFDB	A/B	PDB FRIC ENHC NONE	J/S	FDB BUBL NONE	ROUH	LEVY	MOD ROUH	FDB T PFL DFDB	LINE	BD S/Z	SHAH	MOD S/Z	FDB FRIC TP=1	MAGS	M/N	M N CHSL	FDB CO CONS	HANC C2=C	C2=V	FDB UGJ COLL	DIT	FDB BUBL NONE	GROW	CONS	LIN1	LIN2	LIN3	HHOW NUM AT TSAT	TWI	F/F ISO PETR	0.4	0.3	COMMENTS
ASCD27	*			*			*				*	*					*		1.13			*						*			*		*		FDB BLKG LINEAR DECREASE TO 1/2 BTWN DNB & BD
ASCD28	*			*			*				*	-10%					*		1.13			*		*							*		*		S/Z BD CRITERION REDUCED BY 10%
ASCD29	*			*			*				*	*					*		1.13			*				*					*		*		HVD CONST AT BD VALUE IN FDB REGION
ASCD30	*			*			*				*	*					*		1.13			*							*		*		*		FDB BLKG LINEAR DECREASE TO 1/4 OF (2000-200)
ASCD31	*			*			*				*	-20%					*		1.13			*		*							*		*		S/Z BD CRITERION REDUCED BY 20%
ASCD32	*			*			*				*	*					*		1.3			*					*				*		*		MATCH SLP IN FDB REGION BY COMBINED CO AND FDB BUBL LAYER EFFORT
ASCD32A	*			*			*				*	*					*		1.3			*					*		*		*		*		SAME AS ASCD32 EXCEPT FOR 1/4 FDB BLKG MODEL FOR D<0.002m
ASCD33	*			*			*				*			MOD1			*		1.25			*					*		*		*		*		1/4 BLKG MODL FOR D<0.002 1st MODF OF S/Z FOR HIGH PE NUMBERS
ASCD34	*			*			*				*		*				*		1.25			*					*		*		*		*		1/4 BLKG MODL FOR D<0.002 SHAH BD ONLY. NO SHAH h IN PDB OR FDB
ASCD35	*			*			*				*			MOD2			*		1.25			*					*		*		*		*		1/4 BLKG MODL FOR D<0.002 2nd MODF OF S/Z FOR HIGH PE NUM. NO DIAM DEPEND FIT #1
ASCD36	*			*			*				*			MOD3			*		1.25			*					*		*		*		*		1/4 BLKG MODL FOR D<0.002 3rd MODF OF S/Z FOR HIGH PE NUM. FIT #2
ASCD36A	*			*			*				*			MOD4			*		1.25			*					*		*		*		*		1/4 BLKG MODL FOR D<0.002 4th MODF OF S/Z FOR HIGH PE NUM. FIT #3
ASCD37	*			*			*				*			MOD4			*		1.25			*							*		*		*		SWITCHED BACK TO 1/4 BLKG MODL FOR ALL D
ASCD37A	*			*			*				*			MOD4			*		1.25			*							*		*		*		N=2000 STEPS
ASCD38	*			*			*				*			MOD4			*		1.25			*							*		*			*	EXPNT=0.3 FOR HEATING
ASCD39	*			*				*			*			MOD4			*		1.25			*							*		*			*	LEVY HVOID TO SOLVE JUMP FIG 28
ASCD40	*			*					0.5		*			MOD4			*		1.25			*							*		*			*	1/2 ROUH HVOID IN PDB

PARAMETER

	JHB BERG NONE	OFDB	A/D	PDB FRIC ENHC NONE	J/S	PDB SUBL NONE	ROUH	LEVI	MOD ROUH	FDB T PFL OFDB	LINE	BD S/Z	SHAH	MOD S/Z	FSB FRIC IP=1	HNGS	M/N	M/N CHSL	FCB CO CONS	HANE C2=C	C2=V	FDB UGJ COLL	GIE	FDB SUBL NONE	GROW	CONS	LIN1	LIN2	LIN3	RHOW NUM AT TSAT	INT	F/F ISO PETK	0.4	0.3	COMMENTS
ASCB41	•			•					0.75		•			MOD4			•		1.25			•							•		•			•	3/4 ROUH HVOID IN PDB
ASCB42	•			•					VAR		•			MOD4			•		1.25			•							•		•			•	REDUCED ROUH HVOID FOR D<0.00339
ASCB43	•			•					VAR		•			MOD4			•		1.25			•							•		•			•	REDUCED ROUH HVOID FOR D<0.0046
ASCB44	•			•					VAR		•			MOD4			•		1.25			•							•		•			•	REDUCED ROUH HVOID FOR D<0.00339. St NUM CUT-OFF -40% FOR S/Z MOD4.
ASCB45	•			•					VAR		•			MOD4			•		1.25			•							•		•			•	REDUCED ROUH HVOID FOR D<0.00339. St NUM CUT-OFF -50% FOR S/Z MOD4. SAME RESULT AS ASCB44
ASCB44A	•			•					VAR		•			MOD4			•		1.25				•						•		•			•	REDUCED ROUH HVOID FOR D<0.00339. St NUM CUT-OFF -40% FOR S/Z MOD4. DIX Ugj INSTEAD OF COLLIER
ASCB46	•			•					VAR		•			MOD4			•		1.25			•							•		•			•	ADDED METHOD FOR CHGING NUMBER OF INTEGRATION STEPS
ASCB47			Rcrit	•					VAR		•			MOD4			•		1.25			•							•		•			•	USED A/D ONB WITH R H/A =R CRIT(TANGENCY PT)
ASCB47A			R=1um	•					VAR		•			MOD4			•		1.25			•							•		•			•	USED A/D ONB WITH USERS CHOICE OF R H/A
ASCB47B			R=5um	•					VAR		•			MOD4			•		1.25			•							•		•			•	USED A/D ONB WITH USERS CHOICE OF R H/A
ASCB47C			Rcrit	•					VAR		•			MOD4			•		1.25			•							•		•			•	CHGED S/Z MODF TO ONLY D<7mm
ASCB48			Rcrit	•					VAR		•			MOD4			•			•		•							•		•			•	HANCOX Co AGAIN TO SEE EFFECT
ASCB49			Rcrit	•					VAR		•			MOD4			•		1.25				0						•		•			•	SET Ugj=0 TO SEE EFFECT OF CORRECTING KLINE
ASCB50			Rcrit	•					VAR		•			MOD4			•		1.25			•							•	•				•	RHOW AND NUM AT TSAT AGN TO SEE EFFECT
ASCB51		•		•					VAR		•			MOD4			•		1.25			•							•		•			•	USED OFDB INSTEAD OF ONB TO SEE EFFECT
ASCB52			Rcrit	•					VAR				•	MOD4			•		1.25			•							•		•			•	CODED SHAH BD AS WELL AS SHAH & PDB & FDB CORRELS TO SEE EFFECT
ASCB53			Rcrit	•					VAR		•			MOD4			•		1.25			•							•		•			•	Final code version - same as ASCB47